PEACE RIVER INTEGRATED MODELING PROJECT 2 (PRIM 2)

DRAFT REPORT

Prepared by:

HydroGeoLogic, Inc.
11107 Sunset Hills Road, Suite 400
Reston, Virginia 20190

Prepared for:

Southwest Florida Water Management District

November 2022

TABLE OF CONTENTS

Page

1.0 INTRODUCTION 1-1
1.1 BACKGROUND AND OBJECTIVES 1-1
1.2 STRUCTURE AND CONTENT OF THE REPORT 1-1

2.0 BACKGROUND INFORMATION AND AVAILABLE DATA 2-1
2.1 PROJECT AREA DESCRIPTION 2-1
2.2 CLIMATE 2-1
2.3 PHYSIOGRAPHY AND SOILS 2-2
2.4 HYDROLOGY AND HYDROGEOLOGY 2-3
2.4.1 Hydrography 2-3
2.4.2 Lakes 2-4
2.4.3 Karst Features 2-4
2.5 HYDROGEOLOGY 2-4
2.6 LAND USE 2-6
2.7 WATER USE 2-7

3.0 MODEL DEVELOPMENT 3-1
3.1 OVERVIEW OF MODEL DEVELOPMENT APPROACH 3-1
3.2 DISCRETIZATION 3-1
3.2.1 Spatial Discretization 3-1
3.2.2 Temporal Discretization 3-3
3.3 MODEL PARAMETERIZATION 3-3
3.3.1 Overland Flow Domain 3-4
3.3.2 Channel Flow Domain 3-6
3.3.3 Subsurface Flow Domain 3-7
3.4 MODEL STRESSES 3-8
3.4.1 Precipitation 3-8
3.4.2 Evapotranspiration 3-9
3.4.3 Groundwater and Surface Water Withdrawals 3-10
3.4.4 Return Flows and Surface Water Discharges 3-10
3.5 BOUNDARY CONDITIONS 3-11
3.5.1 Aquifer Bottom Boundaries 3-12
3.5.2 Lateral Subsurface Boundaries 3-12

4.0 MODEL CALIBRATION AND VERIFICATION 4-1
4.1 CALIBRATION APPROACH 4-1
4.1.1 Streamflows 4-1
4.1.2 Lake Levels 4-1
4.1.3 Groundwater Heads 4-2
4.2 CALIBRATION TARGETS AND GOALS 4-2
4.3 STREAMFLOW CALIBRATION RESULTS 4-3
4.3.1 Peace River Streamgages 4-3
4.3.1.1 Peace River at Bartow 4-3

TABLE OF CONTENTS (continued)

Page

4.3.1.2 Peace River at Fort Meade 4-4
4.3.1.3 Peace River at Zolfo 4-5
4.3.1.4 Peace River at Arcadia 4-5
4.3.2 Tributary Sub-Basin Streamflow Results 4-6
4.3.2.1 Saddle Creek at P-11 4-6
4.3.2.2 Peace Creek Canal Near Wahneta 4-7
4.3.2.3 Payne Creek at Bowling Green 4-8
4.3.2.4 Charlie Creek at Gardner 4-8
4.3.2.5 Horse Creek at Arcadia 4-9
4.3.2.6 Joshua Creek at Nocatee 4-9
4.4 LAKE CALIBRATION RESULTS 4-9
4.5 GROUNDWATER CALIBRATION RESULTS 4-10
4.6 CALIBRATED MODEL PARAMETERS 4-12
4.6.1 OLF Leakance 4-12
4.6.2 SA Hydraulic Conductivity and Leakance 4-13
4.6.3 IAS Transmissivity and Leakance 4-13
4.6.4 UFA Transmissivity and Leakance 4-13
4.7 WATER BUDGETS 4-13

5.0 SUMMARY AND DISCUSSION 5-1

6.0 REFERENCES 6-1

APPENDIX A Definition of Calibration Metrics
APPENDIX B Streamflow Calibration Results
APPENDIX C Lake Level Calibration Statistics and Lake Level Plots
APPENDIX D Groundwater Calibration Results
APPENDIX E PRIM Water Budgets by Individual Sub-Basins
APPENDIX F P-11 Discharge

LIST OF FIGURES

Figure 2.1	Peace River Basin
Figure 2.2	Annual Rainfall Amounts during PRIM2 Modeling Period
Figure 2.3	Drainage Features and Basin Delineations of the Peace River Basin
Figure 2.4	Hydrogeological North-South Cross Section
Figure 2.5	Generalized Hydrostratigraphy (from Spechler and Kroening, 2006)
Figure 2.6	Annual Groundwater and Surface Water Use
Figure 3.1	Schematic Representation of the GW-SW System in the PRIM Model
Figure 3.2	PRIM Model Grid, Plan View
Figure 3.3	Correspondence between SD Model, DWRM Model, and the PRIM Subsurface Model Layers
Figure 3.4	Model Cross Section (West–East)
Figure 3.5	Model Cross Section (North–South)
Figure 3.6	PRIM Channel Network
Figure 3.7	Schematic Relationship Between Input Data Sources and MODHMS Simulation Packages
Figure 3.8	Inactive Mining OLD Cells
Figure 3.9	Schematic Representation of Karst Features
Figure 3.10	Thickness of Model Layer 1 (SA) in the PRIM
Figure 3.11(a)	Thickness of Model Layer 2 (IAS-PZ2) in the PRIM
Figure 3.11(b)	Thickness of Model Layer 3 (IAS-PZ3) in the PRIM
Figure 3.12(a)	Thickness of Model Layer 4 (UFA-UPZ) in the PRIM
Figure 3.12(b)	Thickness of Model Layer 5 (UFA-LPZ) in the PRIM
Figure 3.13	Comparison of daily rainfall data recorded by rain gauge station Winter Haven Gilbert Airport NWS (SWFWMD Site ID 844099) and NEXRAD pixel from year 2003 to 2018
Figure 3.14	Comparison of monthly rainfall data recorded by rain gauge station Winter Haven Gilbert Airport NWS (SWFWMD Site ID 844099) and NEXRAD pixel from year 2003 to 2018
Figure 3.15	Comparison of daily rainfall data recorded by rain gauge station Bartow 1 SE NWS (SWFWMD Site ID 25164) and NEXRAD pixel from year 2003 to 2018
Figure 3.16	Comparison of monthly rainfall data recorded by rain gauge station Bartow 1 SE NWS (SWFWMD Site ID 25164) and NEXRAD pixel from year 2003 to 2018
Figure 3.17	Comparison of daily rainfall data recorded by rain gauge station Wauchula NWS (SWFWMD Site ID 24537) and NEXRAD data from year 2003 to 2018
Figure 3.18	Comparison of monthly rainfall data recorded by rain gauge station Wauchula NWS (SWFWMD Site ID 24537) and NEXRAD data from year 2003 to 2018
Figure 3.19	Comparison of daily rainfall data recorded by rain gauge station Arcadia NWS (SWFWMD Site ID 24570) and NEXRAD pixel from year 2003 to 2018
Figure 3.20	Comparison of monthly rainfall data recorded by rain gauge station Arcadia NWS (SWFWMD Site ID 24570) and NEXRAD pixel from year 2003 to 2018

LIST OF FIGURES (continued)

Figure 3.21	NPDES Discharge Locations
Figure 4.1	Hydrography and Stream Gaging Stations of the Peace River Basin
Figure 4.2	Observed vs. Simulated Annual Streamflows (Peace River at Bartow)
Figure 4.3	Observed vs. Simulated Streamflow Hydrographs (Peace River at Bartow) (a) Linear Scale (b) Logarithmic Scale
Figure 4.4	Observed vs. Simulated Flow Exceedance Curves (Peace River at Bartow)
Figure 4.5	Observed vs. Simulated Annual Streamflows (Peace River at Fort Meade)
Figure 4.6	Observed vs. Simulated Streamflow Hydrographs (Peace River at Fort Meade) (a) Linear Scale (b) Logarithmic Scale
Figure 4.7	Observed vs. Simulated Flow Exceedance Curves (Peace River at Fort Meade)
Figure 4.8	Observed vs. Simulated Annual Streamflows (Peace River at Zolfo Springs)
Figure 4.9	Observed vs. Simulated Streamflow Hydrographs (Peace River at Zolfo Springs) (a) Linear Scale (b) Logarithmic Scale
Figure 4.10	Observed vs. Simulated Flow Exceedance Curves (Peace River at Zolfo Springs)
Figure 4.11	Observed vs. Simulated Annual Streamflows (Peace River at Arcadia)
Figure 4.12	Observed vs. Simulated Streamflow Hydrographs (Peace River at Arcadia) (a) Linear Scale (b) Logarithmic Scale
Figure 4.13	Observed vs. Simulated Flow Exceedance Curves (Peace River at Arcadia)
Figure 4.14	Observed vs. Simulated Annual Streamflows (Saddle Creek at P-11 Near Bartow)
Figure 4.15	Observed vs. Simulated Streamflow Hydrographs (Saddle Creek at P-11 Near Bartow) (a) Linear Scale (b) Logarithmic Scale
Figure 4.16	Observed vs. Simulated Flow Exceedance Curves (Saddle Creek at P-11 Near Bartow)
Figure 4.17	Observed vs. Simulated Annual Streamflows (Peace Creek Near Wahneta)
Figure 4.18	Observed vs. Simulated Streamflow Hydrographs (Peace Creek Near Wahneta) (a) Linear Scale (b) Logarithmic Scale
Figure 4.19	Observed vs. Simulated Flow Exceedance Curves (Peace Creek Near Wahneta)
Figure 4.20	Observed vs. Simulated Annual Streamflows (Payne Creek Near Bowling Green)
Figure 4.21	Observed vs. Simulated Streamflow Hydrographs (Payne Creek Near Bowling Green) (a) Linear Scale (b) Logarithmic Scale
Figure 4.22	Observed vs. Simulated Flow Exceedance Curves (Payne Creek Near Bowling Green)
Figure 4.23	Observed vs. Simulated Annual Streamflows (Charlie Creek Near Gardner)
Figure 4.24	Observed vs. Simulated Streamflow Hydrographs (Charlie Creek Near Gardner) (a) Linear Scale (b) Logarithmic Scale
Figure 4.25	Observed vs. Simulated Flow Exceedance Curves (Charlie Creek Near Gardner)
Figure 4.26	Observed vs. Simulated Annual Streamflows (Horse Creek Near Arcadia)
Figure 4.27	Observed vs. Simulated Streamflow Hydrographs (Horse Creek Near Arcadia) (a) Linear Scale (b) Logarithmic Scale

LIST OF FIGURES (continued)

Figure 4.28	Observed vs. Simulated Flow Exceedance Curves (Horse Creek Near Arcadia)
Figure 4.29	Observed vs. Simulated Annual Streamflows (Joshua Creek at Nocatee)
Figure 4.30	Observed vs. Simulated Streamflow Hydrographs (Joshua Creek at Nocatee) (a) Linear Scale (b) Logarithmic Scale
Figure 4.31	Observed vs. Simulated Flow Exceedance Curves (Joshua Creek at Nocatee)
Figure 4.32	Spatial Bias of AE in Lake Levels for the Calibration Period
Figure 4.33	Minimum Flows and Levels Lakes: Group 1
Figure 4.34	Minimum Flows and Levels Lakes: Group 2
Figure 4.35	Spatial Bias of AE in the SA for the Calibration Period
Figure 4.36	Spatial Bias of AE in the IAS for the Calibration Period
Figure 4.37	Spatial Bias of AE in the UFA for the Calibration Period
Figure 4.38	Comparison of Simulated Potentiometric Surface in Layer 5 (UFA) in September 2005 with USGS Contours
Figure 4.39	Comparison of Simulated Potentiometric Surface in Layer 5 (UFA) in May 2007 with USGS Contours
Figure 4.40	Comparison of Simulated Potentiometric Surface in Layer 5 (UFA) in September 2014 with USGS Contours
Figure 4.41	Observed and Simulated Groundwater Heads at ROMP 45
Figure 4.42	Observed and Simulated Groundwater Heads at ROMP 30
Figure 4.43	Observed and Simulated Groundwater Heads at ROMP 26
Figure 4.44	Overland Flow Leakance Map
Figure 4.45	Calibrated Hydraulic Conductivity Distribution for Model Layer 1 in the PRIM 2
Figure 4.46	Calibrated Vertical Leakance Distribution for Model Layer 1 in the PRIM 2
Figure 4.47	Calibrated Transmissivity Distribution for Model Layers 2 and 3 (IAS) in the PRIM 2
Figure 4.48	Calibrated Vertical Leakance Distribution for Model Layers 2 and 3 in the PRIM 2
Figure 4.49	Calibrated Transmissivity Distribution for Model Layers 4 and 5 in the PRIM 2
Figure 4.50	Calibrated Vertical Leakance Distribution for Model Layers 1 to 4 in the PRIM 2

LIST OF TABLES

Table 2.1 Streamflow Summary for Long-Term Gauging Stations
Table 2.2 Land Use Types in PRIM Model
Table 3.1 Lakes Incorporated into the OLF Domain of the PRIM Model
Table 3.2 Summary of Active Model Cells in PRIM Model
Table 3.3 Land Use Dependent Overland Flow Parameters
Table 3.4 Land Use Dependent ET Parameters[1]
Table 3.5 Soil Hydraulic Properties[1]
Table 4.1 Primary Calibration Goals
Table 4.2 Calibration Statistics for Selected Streamgages
Table 4.3 Observed and Simulated Flow Percentiles for Main Peace River Gages from 2003 to 2018
Table 4.4 Observed and Simulated Flow Percentiles for Tributary Streamgages from 2003 to 2018
Table 4.5 Summary of Lake Level Calibration Results
Table 4.6 Summary of Groundwater Calibration Statistics
Table 4.7 Annual Water Budgets for the Calibrated PRIM Model

LIST OF ACRONYMS AND ABBREVIATIONS

AE	average error
ASCE	American Society of Civil Engineers
BCI	BCI Engineers and Scientists
CHF	Channel Flow Package of MODHMS
cfs	cubic feet per second
CSA	clay settling area
d^{-1}	per day
DHI	DHI Water & Environment, Inc.
DWRM	District Wide Regulation Model
DWRM2	District Wide Regulation Model, Version 2
E	Nash-Sutcliffe efficiency coefficient
ET	evapotranspiration
ET_{ref}	reference ET
ETS	Evapotranspiration Time Series Package of MODHMS
EVT	Evapotranspiration Package of MODHMS
FDEP	Florida Department of Environmental Protection
FLUCCS	Florida Land Use and Cover Classification System
ft/day	feet per day
ft^2/day	feet squared per day
GSVE	gravity-segregated vertical equilibrium
GW	groundwater
IAS	Intermediate Aquifer System
ICPR	Interconnected Pond Routing Model
in/yr	inches per year
IPT1	Interception Package of MODHMS
K	hydraulic conductivity
k_c	crop coefficient
km	kilometer
LFA	Lower Floridan Aquifer
LHSEW	Lake Hancock Single Event Watershed
LPZ	Lower Production Zone
LULC	Land Use and Land Cover
LUP	Land Use Package
MFL	minimum level of flow
Mgd	million gallons per day

MnE	minimum error
MODHMS	MODFLOW-based Hydrologic Modeling System
MxE	maximum error
NEXRAD	Next Generation Radar
NPDES	National Pollutant Discharge Elimination System
NRCS	National Resource Conservation Service
OLF	overland flow
PRIM	Peace River Integrated Modeling Project
PRMRWSA	Peace River Manasota Regional Water Supply Authority
PWS	public water supply
PZ	Permeable Zone
R^2	Coefficient of Determination
RMSE	Root Mean Square Error
RTS	Rainfall Time Series
SA	surficial aquifer
SCBIM	Saddle Creek Basin Integrated Model
SD	Southern District
SSURGO	Soil Survey Geographic Database
SW	surface water
SWFWMD	Southwest Florida Water Management District
SWMM	Storm Water Management Model
UFA	Upper Floridan Aquifer
UPZ	Upper Production Zone
USGS	U.S. Geological Survey
VCONT	vertical conductance
WSR-88D	Weather Surveillance Radar-88 Doppler
WUP	water use permit
WWTP	wastewater treatment plant

1.0 INTRODUCTION

1.1 BACKGROUND AND OBJECTIVES

The Peace River watershed, located in Polk, Hardee, and DeSoto counties, comprises the largest watershed in the Southwest Florida Water Management District (SWFWMD), with a total area of 2,350 square miles. The Peace River is an important ecological, water supply, and recreation resource. There has been extensive agricultural and industrial development in the watershed for many years with a heavy reliance on groundwater resources. Peace River flows have been in a long-term decline beginning in the 1930s. The impact has been most pronounced in the Upper Peace River, where sections of the river have lost all flow in recent dry seasons.

The factors affecting flows in the Peace River include natural phenomena as well as human impacts. Long-term natural variation in rainfall is understood to have a major influence on river flows in the Peace River and similar river systems in Florida. In addition, there are numerous human influences that impact the Peace River. These include lowering of the groundwater potentiometric surface due to groundwater pumping for industrial, agricultural, and domestic water use; structural alterations and regulation of surface water; land use and land cover (LULC) changes; and reduction of wastewater discharges to the Peace River and its tributaries. Although numerous studies have been conducted to investigate and understand the phenomena that have impacted flows in the Peace River, the relative importance and quantifiable impact of these phenomena are not thoroughly understood.

The Peace River Integrated Modeling Project 1 (PRIM 1) began in 2008. The objectives of the project were to gain a better understanding of the hydrologic processes and interactions that affect the Peace River basin and flows in the river itself. The principal goal was to develop a numerical model of the Peace River basin that can test water resource management options. The model integrated simulated surface water and groundwater flows and was designed to assist in identifying the effects of previous development in the watershed and ways of meeting SWFWMD-identified recovery goals in the Peace River basin. The model, based on the data from 1994 to 2002, was completed in 2011 (HGL, 2011). PRIM 2 was initiated in 2020 by SWFWMD to update the PRIM 1 model using data from 2003 to 2018. This report documents the update and calibration of the PRIM 2 model.

1.2 STRUCTURE AND CONTENT OF THE REPORT

This report is organized as follows:

Section 1: Describes project background and objectives;

Section 2: Describes the Peace River basin, including pertinent climatic, land use, and hydrologic/hydrogeologic characteristics of the Peace River watershed;

Section 3: Describes the model development of the integrated PRIM model;

Section 4: Describes the calibration and verification of the PRIM model;

Section 5: Provides a discussion of the PRIM model calibration; and

Section 6: Lists the references cited in the report.

This page was intentionally left blank.

2.0 BACKGROUND INFORMATION AND AVAILABLE DATA

This section of the report presents a summary description of the Peace River basin, including hydrological and hydrogeological conditions during the PRIM model simulation period of 2003 to 2018. Descriptions of the Peace River characteristics are presented below. Additional details are also provided in the PRIM 1 reports (HGL, 2009; HGL, 2011; and HGL, 2012).

2.1 PROJECT AREA DESCRIPTION

The Peace River Basin is the SWFWMD's largest watershed, encompassing approximately 2,350 square miles. The watershed boundaries and principal sub-basins are shown in Figure 2.1. The headwaters of the Peace River originate in the northernmost group of lakes of the Saddle Creek and Peace Creek sub-basins. Surface water from the headwaters region flows to Saddle Creek and Peace Creek, which form the beginning of the Peace River channel at their confluence near Bartow, south of Lake Hancock. From the confluence, the river flows south approximately 85 miles and ultimately discharges into the Charlotte Harbor estuary. The Peace River basin encompasses the following sub-basins: Saddle Creek, Peace Creek, Peace at Zolfo Springs, Payne Creek, Charlie Creek, Horse Creek, Joshua Creek, and Peace at Arcadia. Two other sub-basins, Shell Creek and Coastal, are not part of this project since they drain into the Peace River below the location of the Peace River Manasota Regional Water Supply Authority (PRMRWSA) surface water intake point near Fort Ogden. Their intake represents the downstream boundary for the PRIM model.

2.2 CLIMATE

The climate of the area is subtropical, with an average annual temperature of about 73 degrees Fahrenheit. Rainfall and evapotranspiration (ET) represent the largest sources and sinks of water in the Peace River basin. Average annual rainfall in the Peace River drainage basin is typically reported as 50+ inches per year (in/yr), while ET is given as 37 to 38 in/yr. Some 60% of the rainfall occurs from June through September; ET is highest in May and June. Streamflows are typically the lowest at the end of the dry seasons, in April and May. It is common for portions of the river between Bartow and Fort Meade to be completely dry during this period. Tropical storms and hurricanes can produce extremely high amounts of rainfall in short durations, and their impacts are registered on streamflow hydrographs. For example, on September 11, 2017, Hurricane Irma brought over 8 to 10 inches of daily rainfall throughout the watershed, which resulted in extraordinarily high water flow of the Peace River.

Rainfall data used in the PRIM model, provided by the SWFWMD, were obtained from the national network of Weather Surveillance Radar-88 Doppler (WSR-88D), commonly known as Next Generation Radar (NEXRAD). The NEXRAD data have a 15-minute temporal and 2×2 kilometers (km) (1.6 square miles [mi^2]) spatial resolution.

Figure 2.2 summarizes the basin-wide annual rainfall amounts obtained from the NEXRAD data for the period from 2003 to 2018, which represents the PRIM 2 modeling period. The figure shows that, 2005 was a wet year, and 2007 was a dry year. Of the 16 years, 8 years (the first 3 years and the last 5 years) were above average rainfall years, and the intervening 8 years were below average rainfall years.

2.3 PHYSIOGRAPHY AND SOILS

The Peace River begins in the Polk Uplands physiographic province, flows through the DeSoto Plain, and discharges into Charlotte Harbor in the Gulf Coastal Lowlands.

The Upper Peace River watershed is bounded by the Lakeland Ridge to the west, and by the Lake Wales Ridge to the east. The Winter Haven Ridge lies between the Lakeland and Lake Wales Ridges. Its limits separate Saddle Creek, located north of Lake Hancock, from the Peace Creek Canal, which begins near Lake Hamilton in the northeast area of the watershed. These areas converge south of Lake Hancock, marking the beginning of the Peace River.

The central area of the Peace River watershed is located in southern Hardee and DeSoto counties and lies in the DeSoto Plain physiographic province. This region is particularly flat, with elevation drops of only 20 to 30 feet over distances of 25 to 40 miles. The Gulf Coastal Lowlands, located in Charlotte and southeastern DeSoto counties, encompass the southernmost portion of the Peace River watershed before it connects to Charlotte Harbor and the Gulf of Mexico.

The majority of natural soils in the Peace River basin area are described as Flatwoods soils. These sandy soils are generally nearly level, with 0 to 2 percent slopes. These soils have good permeability, but they are considered poorly drained because of generally shallow water table conditions. The dominant soil series and their percentage of the Peace River basin area are as shown below.

Smyrna	32%
Pomona	25%
Candler	8%
Arents	7%
Wabasso	7%
Felda	5%

Collectively, these soil types account for 84 percent of the basin area. The remaining basin area is occupied by soil types that each account for less than 5 percent of the area.

The northern section of the watershed is dominated by Candler soils on the ridges, Smyrna soils in the lowlands, and Arents soils in the areas that have been impacted by phosphate mining. Candler soils are characteristic of uplands and are moderately sloping, excessively to moderately well drained, sandy, and underlain by loamy or clay material. Flatwoods soils, represented by the Smyrna and Pomona soil series, are the most extensive natural soil types in the Peace River watershed. These soils formed from sandy marine sediments and are found in broad areas of flatwoods throughout the basin. Felda soils are poorly drained sandy soils found in sloughs, depressions, or floodplains. They are found along most of the Peace River and its tributaries from north of Lake Hancock in Polk County to the confluence with Horse Creek in DeSoto County. The Wabasso soils consist of deep, poorly drained, and slowly permeable soils on flatwoods, floodplains, and depressions in the southern portion of the Peace River basin.

Extensive phosphate mining in the upper part of the Peace River watershed has resulted in large areas mapped as Arents and Hydraquents soils. Arents are soils that have been disturbed and deeply

mixed as a result of human earthmoving activities. In areas affected by phosphate mining, Arents soils correspond to overburden and sand tailings.

2.4 HYDROLOGY AND HYDROGEOLOGY

2.4.1 Hydrography

The Peace River originates in the lakes and wetlands of the northern region of the watershed, south of Interstate Highway 4 in Polk County. The Peace River begins just north of Bartow at the confluence of Peace Creek and Saddle Creek. From there the Peace River flows south to its mouth in Charlotte Harbor. Between Bartow and the mouth of the river, several tributaries discharge into the Peace River. The major tributaries in the model domain, such as Bowlegs, Payne, Charlie, Joshua, and Horse Creeks, are shown on Figure 2.3. The river is 113 miles long from its mouth at Charlotte Harbor to the U.S. Geological Survey (USGS) gauging station 02293987 on the Peace Creek Drainage Canal near Wahneta. The Peace River and its tributaries are currently gaged at 19 locations by the USGS. A number of these gages had no or only a very short observation record during the period of interest for the PRIM 2 model from 2003 to 2018. The streamgages located on the Peace River or at the outlets of the main sub-basins were used in calibrating the PRIM model (see Section 4.0 of this report).

The Peace River has four long-term streamgages.

- Peace River at Bartow (USGS 02994650)
- Peace River at Fort Meade (USGS 02294898)
- Peace River at Zolfo Springs (USGS 02295637)
- Peace River at Arcadia (USGS 02296750)

The primary tributary streamgages are listed below.

- Saddle Creek at Structure P-11 near Bartow (USGS 02294491)
- Peace Creek near Wahneta (USGS 02293987)
- Payne Creek near Bowling Green (USGS 02295420)
- Charlie Creek near Gardner (USGS 02296500)
- Joshua Creek at Nocatee (USGS 02297100)
- Horse Creek near Arcadia (USGS 02297310)

Table 2.1 summarizes the streamflow characteristics of these gages, which are shown in Figure 2.3. The upper portion of the Peace River basin, represented by Saddle Creek, Peace Creek, Peace River at Bartow, and Peace River at Fort Meade, is characterized by distinctly lower unit discharge values as compared to the lower portion of the basin. The factors that contribute to this behavior likely include greater lake storage and associated evaporation losses in Saddle Creek and Peace Creek, disruption of surface drainage patterns caused by phosphate mining activities, and greater groundwater recharge in the upper portion of the basin. The very low value for the Fort Meade gage can be attributed in part to flow losses to Karst features in and adjacent to the Peace River stream channel between Bartow and Fort Meade.

2.4.2 Lakes

The Peace River basin is endowed with a large number of lakes, with most located in the Saddle Creek and Peace Creek sub-basins in Polk County. The majority of the lakes are the result of sinkhole activity and are classified as either seepage lakes or drainage lakes. Seepage lakes have no surface water outflow; the water level in these lakes is controlled by groundwater level. Drainage lakes are lakes that lose water through surface outflows. Many of the larger lakes in the Peace River basin are drainage lakes and are hydraulically connected, often as a result of human drainage improvements.

Lake Hancock is the principal lake in the Saddle Creek sub-basin, and most of the sub-basin drains into Lake Hancock. Outflow from Lake Hancock is controlled by the P-11 structure. The SWFWMD has recently completed the Lake Hancock Lake-Level Modification and Ecosystem Restoration Project for meeting minimum flows established for the Upper Peace River (UPR) and improving water quality within the Peace River to protect the Charlotte Harbor Estuary.

In the Peace Creek sub-basin, the Winter Haven Chain of Lakes consists of 21 interconnected lakes within and around the city of Winter Haven. Flows between the lakes are regulated by hydraulic control structures. The lakes in the Winter Haven chain drain into the Peace Creek Drainage Canal, which in turn discharges into the Peace River near Bartow.

2.4.3 Karst Features

Portions of the upper Peace River, especially the section between Bartow and Homeland, are characterized by numerous Karst features in or near the river channel. Historically, the upper Peace River basin exhibited artesian flow from the underlying confined aquifers. Kissengen Spring, located 4 miles southeast of Bartow, discharged 20 million gallons per day (Mgd) between the 1880s and 1930s, when flow began to decline and ultimately stopped in 1950. Cessation of flow from the springs is generally attributed to the decline in the potentiometric head in the Intermediate and Upper Florida Aquifers. Associated with this decline, Karst features now act as sinks for flow in the Peace River. During dry periods, Karst features can capture much or even all of the flow in the Peace River above Fort Meade, and sections of the river can be completely dry due to complete interception of all streamflow. The average flow loss is 17 cubic feet per second (cfs) (11 Mgd), with a maximum recorded flow loss of 50 cfs (Metz and Lewelling, 2010). The Karst features provide a direct hydraulic connection between the Peace River and the Intermediate Aquifer. At Dover Sink, which is one of the largest Karst features, a direct conduit exists between the Peace River and both the Intermediate and Floridan aquifers (Metz and Lewelling, 2010).

2.5 HYDROGEOLOGY

The Peace River basin is underlain by three aquifer systems. The uppermost system is the unconfined Surficial Aquifer (SA). The depth of the SA varies from a few feet to over one hundred feet in the sand hill ridges. The aquifer material consists of unconsolidated quartz sand, silt, and clayey sand. The typical stratigraphy has sandy materials at the surface, with an increasing percentage of clay with depth. The transmissivity of the SA is extremely variable. Hydraulic conductivity ranges in the SA from 0.1 feet per day (ft/day) to 1,493 ft/day (SWFWMD, 2000) throughout the SWFWMD area. In the southern areas of the Peace River basin, the SA hydraulic

conductivities range from 20 to 50 ft/day (SWFWMD, 2000). Lewelling and Wylie (1993) cite hydraulic conductivities of 0.1 to 17.9 ft/day, obtained from nine slug tests in unmined areas of the phosphate mining region of Hillsborough, Hardee and Polk counties. In the upper sandy zones, 10 to 25 ft/day is a typical range for much of the area.

Typically, the water table is at or near the land surface near the river, wetlands, tributary streams, and natural lakes in the northern portion of the basin. Areas of higher elevation typically exhibit a water table of about 5 to 10 feet below the land surface, which fluctuates a few feet seasonally. The depth of the water table can be as much as 50 to 100 feet on the Lake Wales Ridge.

Underlying the SA is the confined Hawthorn Aquifer System (HAS), also commonly referred to as the Intermediate Aquifer System (IAS), which consists of thin, inter-bedded limestones, sands, and phosphatic clays of generally low permeability. The IAS is relatively thin in the upper reaches of the Peace River basin and thickens to the south. The IAS in the Peace River basin is located within the Hawthorn Group of formations (Figure 2.5). In the extreme northern reaches of the basin, the uppermost confining bed below the SA may be absent, and the water producing zone of the IAS is often missing. Spechler and Kroening (2006) depict the IAS as being absent in Saddle Creek and Peace Creek north of the Lakeland-Winter Haven line. The top of the IAS ranges in elevation from greater than 100 feet above sea level in the central Polk County to more than 100 feet below sea level in Highlands County (Duerr and Enos, 1990). Progressing southward in the basin, the section thickens. The IAS includes both water-bearing and confining units.

The IAS as a whole, where present, is characterized by a substantially lower permeability (2 to 3 orders of magnitude) than the underlying Upper Floridan Aquifer (UFA) and is often classified as a (semi-) confining unit. The IAS generally includes an upper confining unit of clayey sand, shell, and marl, and a lower confining unit of sandy clay and clayey sand. Lying between these confining units are one or two permeable zones, which are also separated by another confining unit. The upper permeable zone is designated as PZ2 (Barr, 1996) or Zone 2 (Knochenmuss, 2006; Spechler and Kroening, 2006). The second zone is designated as PZ3 or Zone 3. Within the Peace River basin, the IAS transmissivity ranges from 1 to 8,800 (square feet per day (ft^2/day) for Zone 2 and from 200 to 43,000 ft^2/day for Zone 3 (Knochenmus, 2006).

Underlying the IAS, the confined Floridan aquifer consists of limestone and dolostone formations. The Floridan aquifer is subdivided into the UFA and Lower Floridan aquifer (LFA), which are separated by the Middle Confining Unit (MCU). The UFA is separated from the IAS by a confining unit consisting of clays and dolomitic limestones of the lower Acadia Formation of the Hawthorn Group. The top of the UFA dips to the south from approximately sea level elevation in Central Polk County to more than 1,000 feet below North American Vertical Datum of 1988 (NAVD88) in Southern Charlotte County (Knochenmus, 2006). The hydrogeologic units of the UFA are the Upper Production Zone (UPZ) (Basso, 2002), which corresponds to the Suwanee Limestone, the semi-confining Ocala Limestone, and the Lower Production Zone (LPZ) of the Avon Park Formation. The UFA is extremely permeable along some horizons. This is the principal water supply source for the basin. About 85 to 90 percent of all groundwater is derived from the UFA. Based on aquifer testing data compiled by the SWFWMD (SWFWMD, 2000), transmissivity values for the UFA in the Peace River basin range from 30,000-300,000 ft^2/day and reported leakance values are in the range of 10^{-3} to 10^{-5} per day (d^{-1}). The UFA is bounded below by the MCU.

Figure 2.4 shows a general north-south hydrogeological cross section along the Peace River, from Lakeland in the north to Arcadia in the south. The hydrostratigraphy underlying the Peace River is depicted in Figure 2.5.

2.6 LAND USE

The primary land uses in the basin are agricultural, wetlands, urban, and phosphate mining. The majority of agriculture in the Peace River watershed is located in Hardee and DeSoto counties. Cropland and pastureland account for approximately 71% of the agricultural land use. Citrus and other tree crops are the other dominant agriculture land use types at 27%.

Urban and suburban areas exist primarily in the Saddle Creek and Peace Creek sub-basins, and include the towns of Lakeland, Winter Haven, Auburndale, and Bartow. The other large area of urban land cover is located at Charlotte Harbor and includes the cities of Port Charlotte and Punta Gorda. A significant portion of the upper basin near Lakeland and Bartow has been mined, reclaimed, and incorporated into the urban landscape. Citrus groves, once dominant on the sandy soils on the Lakeland and Winter Haven ridges, continue to be converted to residential subdivisions.

The dominant landcover types in the middle portion of the Peace River basin are related to phosphate mining. This area of southern Polk and northern Hardee counties is a disturbed area with active, reclaimed, and unreclaimed mining land. Other land uses in this portion of the basin include a variety of agricultural categories (row crops, citrus, and pasture) and wetlands.

The Florida Land Use and Cover Classification System (FLUCCS), which was used to develop the basin-wide PRIM model, includes a total of 39 categories—a combination of Level II and Level III categories. In the PRIM 2 model, land use affects a number of hydrologic characteristics. The primary characteristic is ET, which is determined by land use-dependent crop coefficients (k_c) and root zone depths. Land use also affects surface runoff and infiltration characteristics. For instance, paved surfaces associated with urban, commercial, and industrial areas have increased surface runoff and reduced infiltration as compared to natural forest and range land. These differences are expressed via land surface roughness coefficients and soil surface leakance coefficients in the PRIM 2 model. Based on the variation and uniqueness of the model parameters, principally k_c, which is associated with the different land use categories, the 39 different FLUCCS categories were assembled into a total of 13 different land use types in the PRIM model, as presented in Table 2.2. In the table, the land use type 12, "Extractive," is an aggregate category for operational and former mine areas for which no specific land use information is available. Identified lakes and ponds, including active clay settling areas (CSAs) within mine areas, are assigned land use type 9, Open Water. Former mine lands, reclaimed and nonreclaimed, for which the current land use is known (for example, urban or pasture), are assigned to the corresponding land use type, leaving land use type 12 for those mine areas for which no specific information is available. Likewise, land use type 13, Other, is used for any remaining areas that are not included in any of the other types.

2.7 WATER USE

The annual rate of groundwater and surface water withdrawn from within the Peace River basin is 230 to 330 Mgd, with the majority of the water being provided by groundwater. Annual water use (groundwater and surface water) from 2003 to 2018 is shown in Figure 2.6. Surface water use is relatively small compared to that of groundwater, and surface water use has been fairly consistent over time.

Agricultural use accounts for more than half of the total water use within the basin. Public supply is the next biggest water use. Mining and other commercial/industrial uses account for approximately one fifth of the total water use. During the year, water use is highest during the spring months, which represent the peak growing season as well as the driest period of the year, thereby driving agricultural irrigation demand.

A large portion of the industrial and mining consumption in the Peace River basin is related to phosphate mining. Polk County was the largest user of water in this category, with over 90% of the total industrial and mining usage in the three-county area that makes up the Peace River basin.

This page was intentionally left blank.

FIGURES

This page was intentionally left blank.

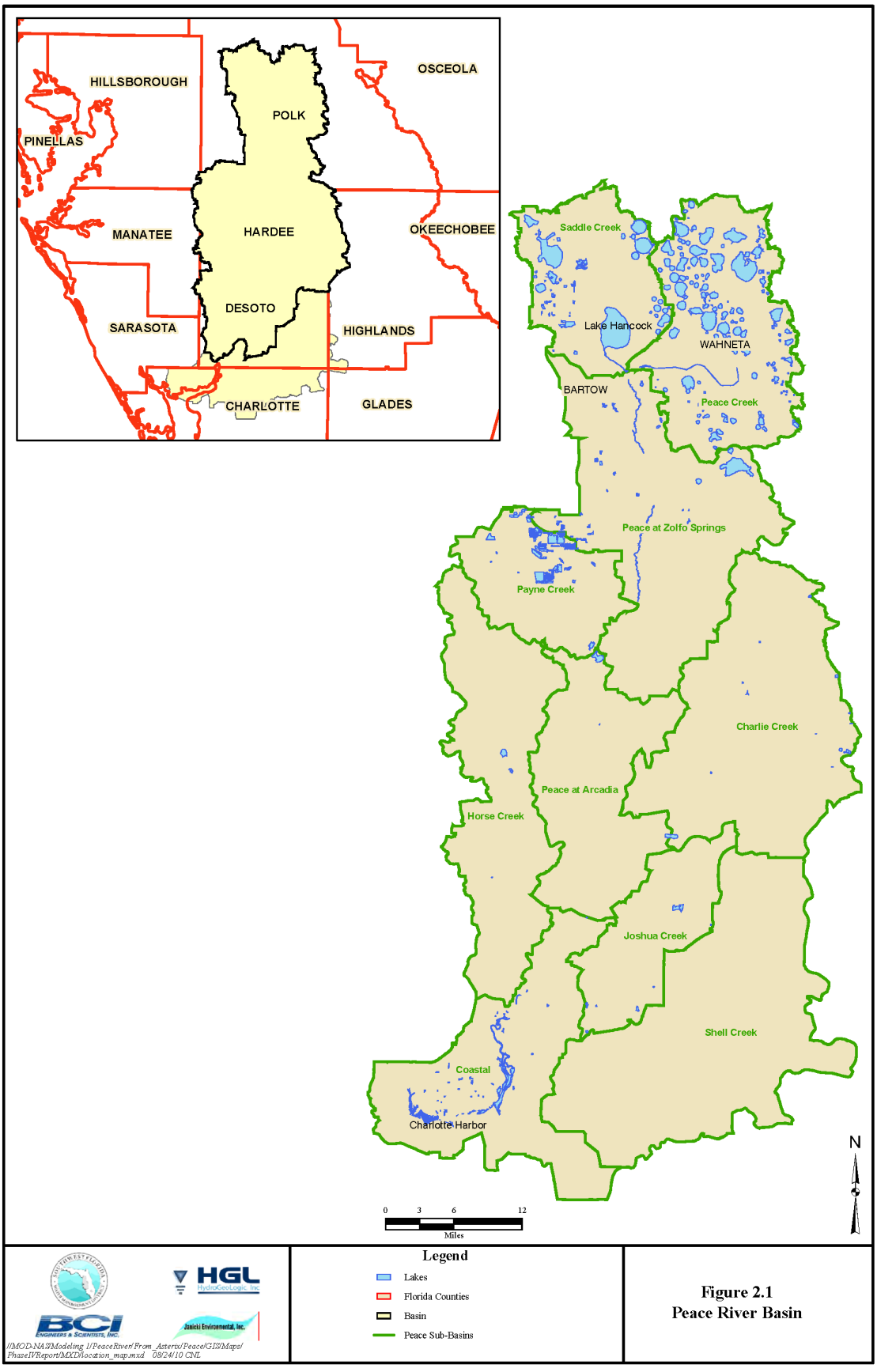

Figure 2.1
Peace River Basin

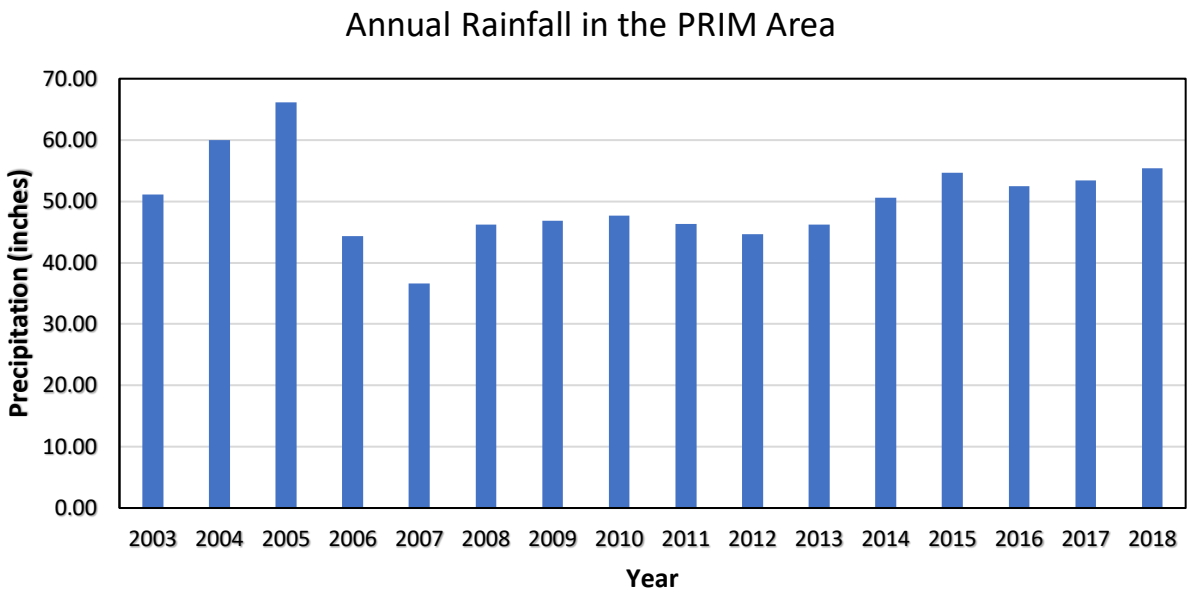

Figure 2.2 Annual Rainfall Amounts during PRIM2 Modeling Period

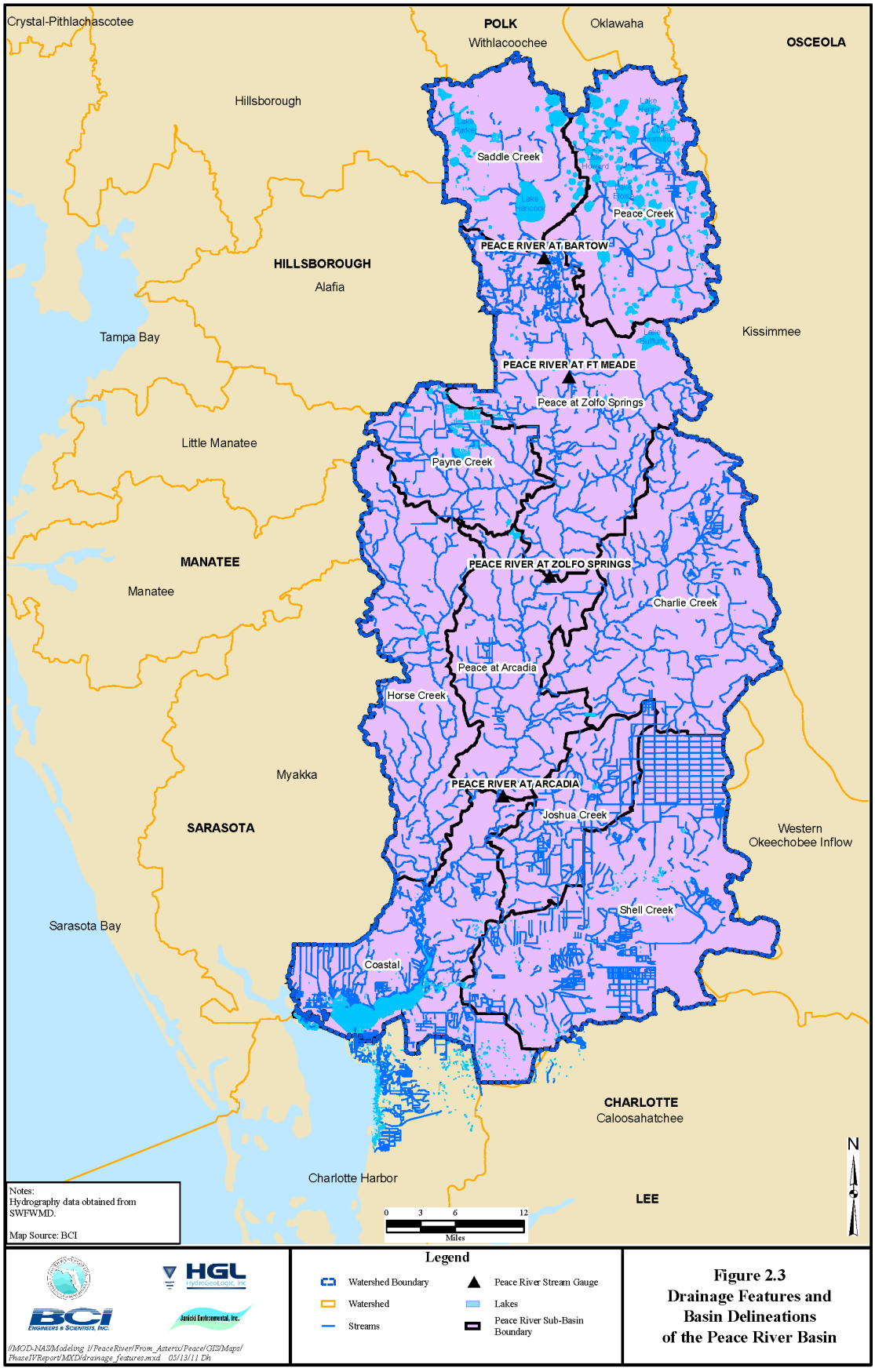

Figure 2.3
Drainage Features and Basin Delineations of the Peace River Basin

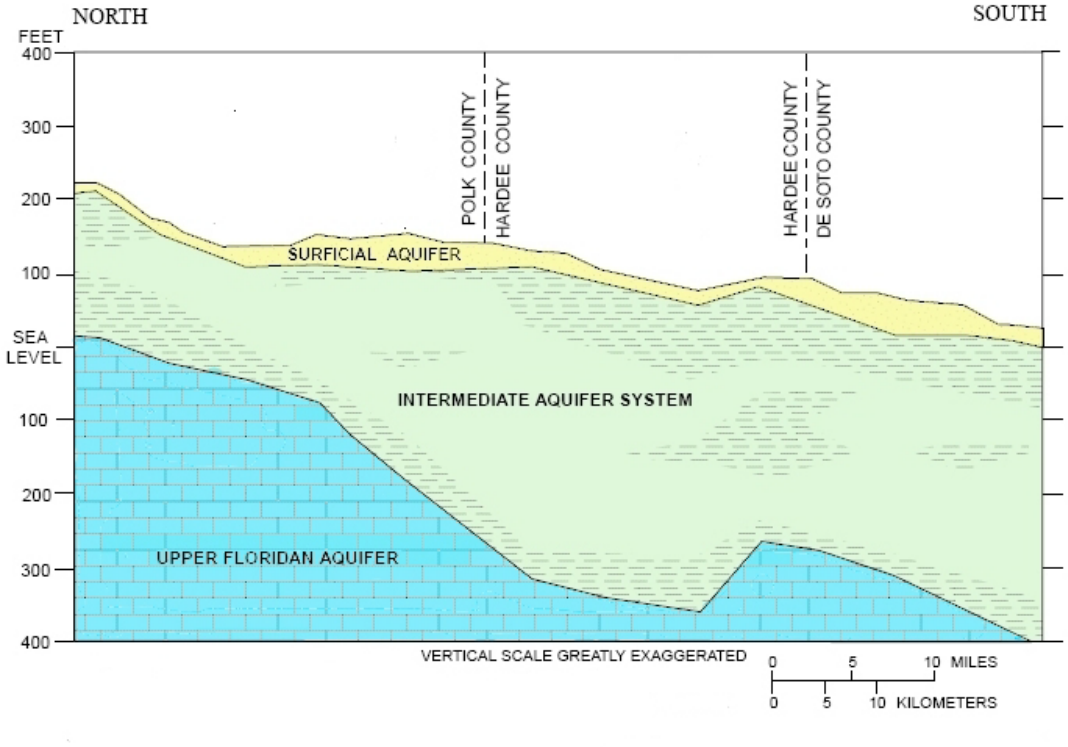

Figure 2.4 Hydrogeological North-South Cross Section

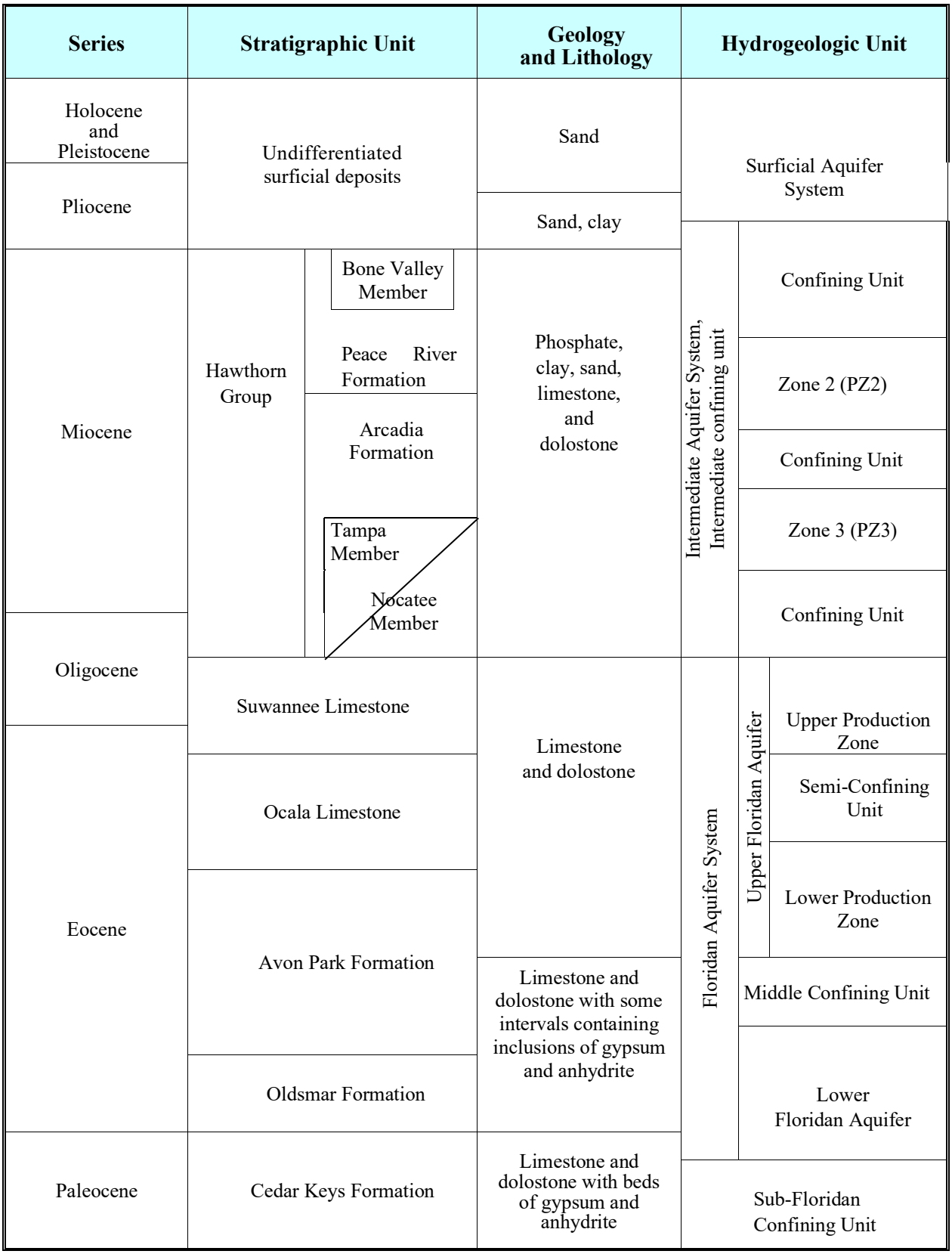

Figure 2.5 Generalized Hydrostratigraphy (from Spechler and Kroening, 2006)

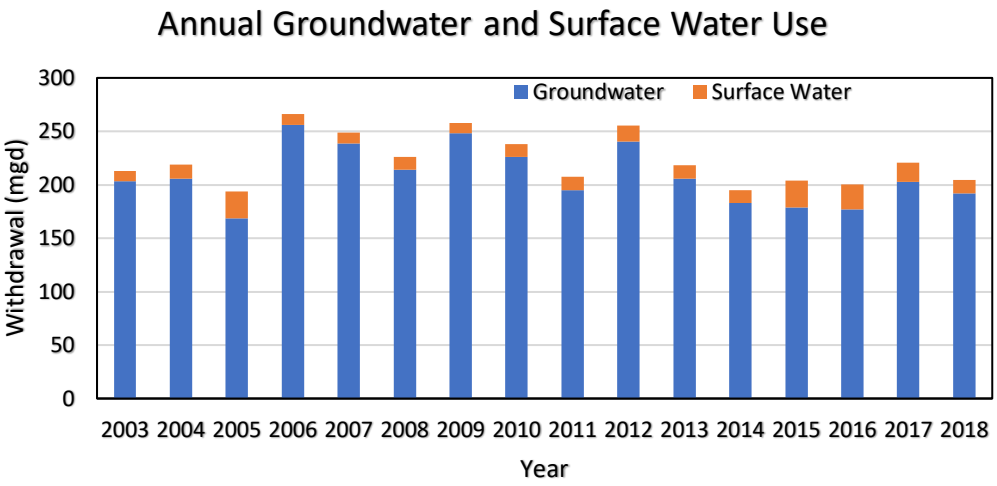

Figure 2.6 Annual Groundwater and Surface Water Use

TABLES

This page was intentionally left blank.

Table 2.1
Streamflow Summary for Long-Term Gauging Stations

Gauging Station	Period of Record	Drainage Area (Sq. Mile)	Discharge (cfs)				Unit Discharge (cfs/square mile)
			Mean	10th	50th	90th	
Saddle Creek at P11	1963-2018	135	65	0	0	244	0.482
Peace Creek near Wahneta	1992-2018	162	94	7	33	277	0.579
Payne Creek near Bowling Green	1979-2018	121	124	12	64	499	1.023
Charlie Creek near Gardner	1980-2018	330	272	6	51	525	0.826
Joshua Creek at Nocatee	1950-2018	132	114	7	38	317	0.863
Horse Creek near Arcadia	1950-2018	218	193	7	42	482	0.887
Peace River at Bartow	1939-2018	390	221	9	55	532	0.566
Peace River at Fort Meade	1974-2018	480	208	6	75	624	0.433
Peace River at Zolfo	1933-2018	826	612	59	247	1291	0.740
Peace River at Arcadia	1931-2018	1,367	1065	87	388	2420	0.779

Table 2.2
Land Use Types in PRIM Model

Type	FLUCCS Categories	Percentage of Basin Area
1	Low Density Urban, Recreational	5.0
2	Medium Density Urban, Institutional	4.7
3	High Density Urban, Industrial, Transportation	3.7
4	Cropland and Pasture	28.7
5	Row Crops	0.6
6	Tree Crops, Citrus	11.1
7	Shrub Land	4.1[1]
8	Upland Forest	5.0
9	Open Water	4.7
10	Forested Wetlands	11.3
11	Non-Forested Wetlands, Marshland	8.0
12	Extractive	13.0
13	Other	0.1

[1]Does not include lakes and ponds on mined lands.

3.0 MODEL DEVELOPMENT

3.1 OVERVIEW OF MODEL DEVELOPMENT APPROACH

The PRIM 1 and PRIM 2 models were developed using the MODFLOW-based Hydrologic Modeling System (MODHMS) integrated GW-SW modeling software (HGL, 2007). The basis for selecting MODHMS has been discussed in Appendix F of HGL (2009).

Figure 3.1 provides a schematic representation of the GW-SW hydrologic system simulated in MODHMS. The integrated system comprises a surface layer that represents the land surface and its associated hydrologic processes (for example, rainfall and runoff); a surface water component (for example, ponds, streams, canals, and hydraulic structures); and a subsurface component, which comprises the unsaturated zone and underlying groundwater layers. In MODHMS the land surface layer is represented using 2-D planar grid cells that are oriented to represent surface topography. Streams and lakes are represented as a network of 1-D channel segments and storage nodes overlain on the land surface. Subsurface layers are represented using 3-D grid blocks. The surface and subsurface layers in the model are linked via flux terms that represent infiltration, ET, and overland flow (OLF)-stream and groundwater-stream interactions.

The original PRIM 1 model was constructed by extending the Saddle Creek Basin Integrated Model (SCBIM) developed by HGL (2008). The PRIM 1 model utilized the same horizontal and vertical spatial grid discretization as well as the same temporal discretization as the SCBIM model. Calibrated ET, soil, and land use parameters from the SCBIM model provided the initial values for the PRIM 1 model. Several other existing groundwater, surface water, and integrated models covering all or part of the Peace River basin were also utilized in developing the PRIM model. The Southern District (SD) groundwater model (Beach, 2006) and the District Wide Regulation Model 2 (DWRM2) (ESI, 2007) were used to build the subsurface component of the PRIM model and to provide initial values for hydraulic conductivities and leakances of aquifer and aquitard units, respectively. The Lake Hancock Single Event Watershed (LHSEW) model (BCI Engineers and Scientists [BCI], 2006), the Peace Creek Storm Water Management Model (SWMM) surface water model (PBS&J, 2004), and the Mike-SHE integrated model of the Horse Creek sub-basin (SDI, 2003) were used to develop the surface water channel network for the Saddle Creek, Peace Creek, and Horse Creek sub-basins, respectively. HEC-RAS models of the Peace River, developed in support of the District Minimum Flow and Levels Program (SWFWMD, 2002), were used to obtain Peace River channel cross sections. Spatial discretization and stream cross sections remain the same for the current PRIM 2 model.

3.2 DISCRETIZATION

3.2.1 Spatial Discretization

The lateral grid dimensions for the OLF and subsurface grid were set to 2,500×2,500 feet. The areal size of the grid was 196 rows by 102 columns (Figure 3.2). Grid cells in the rectangular grid outside the Peace River basin boundary (including cells located outside the downstream model boundary near Arcadia) were inactivated during the PRIM 2 simulations. The active model cells are outlined in blue in Figure 3.2; inactive cells are shown in red.

The PRIM 1 grid comprised five subsurface layers, from top to bottom: the SA is represented by model layer 1, the permeable zones (PZ2 and PZ3) of the IAS are represented by model layers 2 and 3, and the upper and lower permeable zones of the UFA are represented by layers 4 and 5. The PRIM 1 model adopted the same hydrostratigraphic layers as the regional SD groundwater model. Spatial discretization remained unchanged for the PRIM 2 model.

The SD model is a quasi-3D model in that actual layer elevations and thicknesses are not explicitly represented in the model; rather, the hydraulic characteristics of each layer are defined in terms of transmissivities. Bottom elevations of the SA and IAS within the PRIM model domain were, therefore, obtained from the DWRM2 model. The DWRM2 model encompasses the entire SWFWMD jurisdiction and was developed to support SWFWMD's review of water use permits (WUP). The DWRM2 model is a five-layer model comprising the SA (Layer 1), IAS-PZ2 (Layer 2), IAS-PZ3 (Layer 3), UFA (Layer 4), and LFA (Layer 5). Because the DWRM2 model uses a single layer to represent the UFA, the thicknesses of the upper and lower permeable zones within the UFA of the PRIM models were assigned based on top and bottom elevation maps of the Suwannee (upper permeable zone) and the Avon Park (lower permeable zone) Formations of the UFA developed by the SWFWMD. The relationship of layers between the SD and the PRIM 1 and 2 models is depicted in Figure 3.3.

Figure 3.4 shows a west-east vertical cross sectional view of the grid along A-AN, and Figure 3.5 shows an analogous north-south cross sectional view of the grid along B-BN, where A-AN and B-BN are shown in Figure 3.2. The north-south cross section displays the thickening and downward dip of the IAS and UFA toward the south. Areas shown in white in Figures 3.4 and 3.5 represent aquitard layers that were represented indirectly in the model, in terms of the vertical leakance between adjacent aquifer units. In these zones the tops and bottoms of the vertically adjacent aquifer units do not match up. The separation between aquifer units shown in Figure 3.2 does not necessarily provide an accurate picture of the actual thickness of confining layers owing to uncertainties and inconsistencies in the elevation data that were used to construct the model layers. However, errors and uncertainties in the exact thickness and elevation of model layers do not affect the accuracy of the groundwater flow model, which is calibrated in terms of transmissivity and vertical leakance.

Stream Channel Network

The channel flow domain comprises streams, canals, lakes, ponds, man-made flow structures, and sinkholes. The latter are significant as hydraulic conduits between the Peace River and the underlying aquifers along sections of the Peace River between Bartow and Fort Meade. Except for the larger lakes in the Saddle Creek and Peace Creek sub-basins, all components of the channel network were represented by channel segments and flow structures of the MODHMS Channel Flow (CHF) Package (HGL, 2008).

Owing to the availability of detailed stormwater drainage models for the Saddle Creek and Peace Creek sub-basins, the channel network in Saddle Creek and Peace Creek basins was defined by a node-link structure consisting of 1,394 single-segment nodes representing small to mid-size lakes and ponds connected via 2,362 direct links (channel and streams) and 520 weir and culvert structures. The Saddle Creek channel network was developed from the Interconnected Pond Routing Model (ICPR)-based LHSEW model (BCI, 2006), as described in HGL (2008). The

channel network for the Peace Creek sub-basin was developed in a similar manner from an existing SWMM-based stormwater model (PBS&J, 2004).

The stream network in the remainder of the PRIM model was represented by an inter-connected channel network consisting of 2,999 reaches. The channel network was developed using the USGS hydrography map in combination with a flow accumulation analysis of the land surface topography using the ArcHydro toolbox. The channel network generated from these sources was then processed by hand to ensure continuity of the reaches and consistency of streambed elevations with real-world streamflow directions. Information on channel cross sections for the Peace River was obtained from various sources, as discussed in HGL (2008).

The final model stream channel network comprised 9,807 channel segments and is shown in Figure 3.6. Smaller lakes and ponds were represented as storage nodes in the network. For these features, the lake or pond bathymetry is represented in terms of a stage-volume relationship to describe the storage characteristics of the corresponding node in the channel network. The bathymetry of the larger lakes, which cover multiple grid cells, was incorporated directly into the elevation of the corresponding OLF grid cells. In other words, these lakes were directly represented as depressions in the land surface elevation. The lakes that were represented in this manner are listed in Table 3.1.

Table 3.2 summarizes the number of active cells in each component of the PRIM model domain. The number of active cells in the OLF layer is less than that in the subsurface model layers because OLF cells in areas of phosphate mining operations were set as inactive cells in the model simulations (see section 3.3.1).

3.2.2 Temporal Discretization

The model simulation period was a total of 192 months (January 2003 to December 2018). The time periods of the imposed stresses were as follows:

- Daily rainfall;
- Monthly reference ET (ET_{ref});
- Monthly lateral boundary heads; and
- Monthly pumping and National Pollutant Discharge Elimination System (NPDES) discharges.

The model was run on a variable time step using the adaptive time-stepping feature in MODHMS. At the beginning of rainfall events, the code would reduce the computational time step to a few seconds in order to resolve rapid changes in runoff and streamflow and automatically increase the time step as the effects of changes in stresses were propagated through the system. The maximum time step was constrained to 1 day to accommodate daily rainfall inputs. The total run-time was around 30 hours on a computer with a 3.6 GHz i9-9900K CPU and 64 gigabytes of RAM.

3.3 MODEL PARAMETERIZATION

This section discusses the model parameters and assignment of their values in the PRIM 2 model. The discussion is organized by the main components of the model: the OLF domain, the surface

water channel domain, and the subsurface domain, followed by a discussion of the model stresses (for example, rainfall, ET, pumping) and groundwater boundary conditions. Building and running the model involved nearly all of the simulation packages in MODHMS. The relationships between various sources of model inputs and the MODHMS model packages is depicted schematically in Figure 3.7 and is further discussed in this section.

3.3.1 Overland Flow Domain

Overland flow properties of the model control surface runoff and affect the vertical water flux between the land surface and the subsurface (for instance, infiltration and seepage). These properties are functions of topography, soil type, and land use. The specific MODHMS parameters are grid cell surface elevation, rill and obstruction storage height, Manning's roughness coefficient, and surface leakance.

The land surface elevations of the PRIM model were mainly provided by the USGS 1-foot contour data. Rill storage heights were set to 0.1 feet for most areas, except at certain areas where prominent flow barriers exist, such as at some of the clay setting areas or mining areas. Obstruction heights were assigned a constant value of 0.1 feet. Manning's surface roughness coefficient was treated as a land use-dependent calibration parameter, and land surface leakance, which controls infiltration, was determined based on land use and soil type. The land surface leakance parameter was calculated as the harmonic mean of the leakance of the soil type at each grid cell and the paved surface leakance of the land use type in the same grid cell. The soil leakance value was determined as the vertical conductivity of the upper subsurface grid layer (representing the SA) divided by half the thickness of the upper subsurface grid layer. The vertical soil hydraulic conductivity values were set to one-tenth the horizontal hydraulic conductivity values of the SA. The paved surface leakance represents low-permeability paved surfaces associated with urban land use types. It was incorporated to account for reduced infiltration and corresponding increased surface runoff in paved areas.

Land use information was obtained from the available FLUCCS land use maps of the Peace River basin between 2003 and 2018 (2004, 2005, 2006, 2007, 2010, 2014, and 2017 maps). Land use maps from 2004, 2005, 2006, 2007, 2010, and 2017 were used. Land use information in 2014 was not utilized due to the fact that different FLUCCS classifications were used in that year. The modeling period was divided into successive time intervals, during which each land use distribution was assumed to be unchanged. The 36 FLUCCS land use classifications and sub-classifications that are present in the Peace River basin were consolidated into 13 categories following the methodology discussed in HGL (2009). Initial assignments for a land use-dependent Manning's coefficient and a paved surface leakance were derived from the Saddle Creek sub-basin calibration (HGL, 2008) and are listed in Table 3.3. The soil type and land use-dependent parameters were mapped onto the PRIM grid as areally weighted averages of the values for each land use category present in the grid cell.

A paved surface leakance parameter was assigned to the first three (urban) land use types listed in Table 3.3, which are expected to have a significant proportion of paved land surface. Low leakance values limit the infiltration of rainfall and, thereby, promote surface runoff. For other land use types, leakance (infiltration) of rainfall was determined directly by the soil hydraulic conductivity,

which in turn was obtained from National Resource Conservation Service (NRCS) soil maps and is discussed in Section 3.3.2.

Phosphate Mining Areas

Phosphate mining represents a significant land use in the upper portions of the Peace River basin, between Bartow and Zolfo Springs. The primary sub-watersheds impacted by mining are the Peace River at Zolfo and Payne Creek sub-basins. Numerous studies have been conducted to evaluate the impacts of these mining activities on surface and subsurface hydrology of the Peace River and other impacted basins (HGL, 2009).

In both the PRIM 1 and 2 models, reclaimed and unreclaimed areas of mining operations were treated separately, using different surficial properties. In the model, operating mines refer to the specific areas of ongoing mining operations in which surface runoff is being actively captured for use in the mine circulation system. Conceptually, these are the areas within the perimeter trench system that surround the actual mines. These areas are hydrologically isolated from the rest of the watershed by the perimeter trench and other runoff control systems. Precipitation that falls on these areas enters the watershed hydrologic system only through vertical infiltration and groundwater recharge, and via point discharges of excess water regulated under NPDES permits. In the PRIM 1 and 2 models, the hydraulic isolation of operating mine areas was simulated by inactivating the corresponding OLF grid cells. Interactions between the inactive cells and the rest of the PRIM model occurred via prescribed fluxes, including recharge to the SA grid blocks directly underlying the inactive OLF cells, prescribed surface water discharges at the NPDES outfall locations for each mine, and extraction of groundwater from the subsurface. Recharge to the SA was assigned a constant and uniform rate of approximately 2 in/yr. This value is representative of recharge rates for phosphate mining areas estimated from mine water budget analyses (for example, Garlanger, 2002). For the PRIM model period of 2003 to 2018, surface water discharges from operating mine areas were set equal to reported phosphate mining NPDES discharge data obtained from the Florida Department of Environmental Protection (FDEP). Mining-related groundwater pumping was simulated by incorporating mining water supply wells that were included in the pumping data set supplied by the SWFWMD. Historical mining areas (reclaimed and unreclaimed lands) were simulated using OLF cells with different surficial properties. The former was simulated as cropland and pasture areas, and the latter was simulated as extractive areas (see Table 2.2).

The assignment of inactive OLF cells that represent the operating mines in the Peace River basin was based on detailed aerial imagery of the mined portion of the Peace River basin taken in 2017 and LULC information between 2003 and 2018. Some adjustments in the positions of inactive grid cells were made to align them with locations of NPDES outfalls.

Figure 3.8 shows the locations of the inactive OLF cells representing operating mine areas in the PRIM 2 model. In total, there were 204 inactive cells, representing a total area of 29,270 acres. As stated above, this conceptually represents the total area that is under active surface runoff control. There is no easy way to independently verify the reliability of this area estimate. As it should be, the area is less than the total permitted area of phosphate mines operating during the PRIM project period of 2003 to 2018 but greater than the approximately 400 acres per year that are actually being mined in each operating mine. In the model, the inactive mining cells were not varied during the simulation. In reality, this is a dynamic process, where the areas being mined and associated areas

that are under drainage and runoff control shift over time. The simulated inactive mine areas should therefore be interpreted as being representative of mining impacts over a larger area, not less than the sub-basin scale, rather than as accurate representations of the actual local mine boundaries.

3.3.2 Channel Flow Domain

The parameters required for the channel segments include bank elevation, riverbed elevation, channel cross sectional geometry (conveyance), bed leakance, and Manning's roughness coefficient. The riverbank elevation equals the land surface of the grid-block at the channel segment's midpoint. The bed elevation was assumed to be 10 to 15 feet below the bank elevation. Channel cross sections were developed from available stream cross section data for the Peace River and tributaries. The channel bed leakance was assigned a uniform value of 0.01 d^{-1}. Based on literature data for stable channels (Chow, 1959; Barnes, 1967) Manning's roughness coefficient (n) was assumed to be 0.02 for the Peace River and main tributaries, and 0.04 for smaller tributaries. These values were consistent with channel roughness coefficients used in the Mike-SHE Horse Creek model (SDI, 2003).

The majority of lakes and ponds in the model were simulated as storage nodes in the CHF domain. The parameters required include the depth versus surface-area relationships for the lakes, the perimeter dimensions, and the bottom leakance of the lake or pond bed. For the lakes and ponds in the Saddle Creek sub-basins, information on geometric characteristic of these surface water bodies was extracted from the available ICPR and SWMM stormwater models. A number of lakes had separate bathymetry data available. For these lakes, the depth-surface area characteristics used in the PRIM 1 model were developed based on measured bathymetry. For these same lakes, the measured bathymetry was also compared to the depth-storage relationships obtained from the existing ICPR and SWMM models in order to evaluate the accuracy of the data in these models. It was judged that the agreement was generally reasonable to good and that using lake storages from the ICPR and SWMM models would not be a significant source of error in the model. During the model calibration process, the modeled storage characteristics for a number of the lakes in Peace Creek that did not have measured bathymetries were adjusted to improve agreement between measured and simulated lake levels. Data on leakance values for lakes were not available; this parameter was therefore used as a calibration parameter, with values ranging from 10^{-4} d^{-1} to 1,000 d^{-1}. The PRIM 2 model is based on the same set of bathymetric data.

Hydraulic control structures, which regulate outflows from a number of the lakes, were simulated as static features. Structure operations were not actively simulated in the model. Tabulated flow curves (F-tables in surface water flow literature) were created that relate the upstream and downstream heads to the flux across the structure. These F-tables were used to initially parameterize the hydraulic structures, with some adjustments to structure outflow elevation settings made during model calibration.

<u>Karst Features</u>

Flow losses from the Peace River through Karst features in the section of the river between Bartow and Fort Meade were simulated using the node-link feature of MODHMS for modeling channel flow. Direct hydraulic links between CHF channel segments, representing the Peace River, and the underlying grid blocks of subsurface Layer 2, representing PZ2 of the IAS, were incorporated

in the model. The USGS, in a study of Karst features in the Upper Peace River basin (Metz and Lewelling, 2010), distinguished four reaches along the river for the purpose of quantifying Karst flow losses. The PRIM 1 and 2 models incorporated Karst "links" of each of these four reaches. Conceptually, Karst features provide a direct hydraulic conduit between the river channel and the underlying aquifer. If the river stage exceeds the groundwater potentiometric head, the river will lose water; if the head in the aquifer is higher than river stage, the same Karst links will allow the model to simulate upward discharge of groundwater into the river, in effect simulating spring conditions that historically existed in this area of the basin.

The node-link features of MODHMS do not provide a direct way to account for the storage of water associated with Karst cavities. This storage was incorporated indirectly in the PRIM 1 and PRIM 2 models by lowering the bottom elevation of the channel segments that contained Karst flow "links." This modification allowed the model to simulate the physical process of streamflow losses in Karst features. First, the cavity of the Karst feature is filled. This is simulated by the storage associated with the streambed depression. After the storage capacity of the Karst feature has been satisfied, flow losses continue at a reduced rate that is controlled by the head difference with the groundwater and the ability of the aquifer to absorb Karst flows, as a function of the aquifer's transmissivity. This second state is simulated in the model by inserting vertical hydraulic links between stream channel segments and underlying IAS and UFA model cells. Figure 3.9 shows a simple schematic conceptualization of Karst features in the PRIM model.

3.3.3 Subsurface Flow Domain

Subsurface hydrologic properties required by the PRIM 1 and 2 models include the top and bottom elevations of each model layer, as well as horizontal hydraulic conductivity and storage parameters. Vertical hydraulic conductivity is expressed as the leakance between model layers.

The PRIM models included five subsurface layers representing the SA, IAS-PZ2, IAS-PZ3, UFA upper zone, and UFA lower zone. The bottom of an aquifer layer does not necessarily correspond to the top of the layer underneath, owing to the presence of confining units. These were represented by vertical conductance (VCONT). The top of the SA was the land surface elevation (see previous section). The bottom elevations of model Layers 1 through 5 were obtained from the hydrostratigraphic elevations in the SD model and the DWRM2 (Environmental Simulations, Inc., 2006), as described in Section 3.2.1. Plan view maps of the thicknesses of the aquifer model layers in the PRIM model are provided in Figures 3.10, 3.11, and 3.12 for the SA, IAS, and UFA, respectively.

Initial hydraulic conductivity values for the SA were determined as area weighted averages of the hydraulic conductivities of the soil types appearing in each model grid block. The soil hydraulic conductivities were obtained from the Soil Survey Geographic Database (SSURGO).

The horizontal hydraulic conductivity values for the IAS-PZ2, IAS-PZ3, and upper and lower zones of the UFA were obtained by dividing the transmissivities from the SD model by the layer thicknesses from the DWRM model. The transmissivity values were also adjusted based on the pump test data provided by the SWFWMD (SWFWMD, 2006). The horizontal hydraulic conductivities were further calibrated with head data, lake stages, and streamflow data.

In the MODHMS PRIM model, all subsurface layers were allowed to switch between confined and unconfined depending on local aquifer conditions by setting the LAYCON variable to a value of 43. In practice, flow in Layers 3, 4, and 5 was always confined, and flow in Layer 2 was confined in most of the model domain, except locally in the northernmost portion of the PRIM model domain. Flow in Layer 1 of the model (SA) was unconfined. Variable saturated flow in the unsaturated zone of the SA was simulated using the gravity-segregated vertical equilibrium (GSVE) option of MODHMS, which provides a linearized and computationally simple approximation to the Richards equation for unsaturated flow (HGL, 2006; Panday and Huyakorn, 2008). The parameters needed for flow in unconfined layers are the lateral and vertical hydraulic conductivity, and specific yield. The specific yield is conceptually equivalent to the difference between water content at full saturation (porosity) and the soil residual water content. In the model it was treated as a soil type-specific calibration parameter.

The specific yield values were mapped onto the model grid based on the basin-wide soils map (HGL, 2011). CSAs associated with phosphate mining were assigned the properties of Hydraquents and Haplaquents. While the parameter values associated with the various soil types may change during calibration, the areal soil group distributions remained as the original. The soil properties for prominent soil types are shown in Table 3.4.

A specific storage coefficient (storativity) value of 10^{-4} was used in all confined model layers representing the compressible storage of the aquifer matrix. The leakance between model layers was defined by VCONT, similar to the MODFLOW convention. The VCONT value of a model layer represents an aggregate leakage effect of this layer, the layer below, and any confining layers in between. For instance, the VCONT of Layer 1 is a combined leakage effect of Layer 1, Layer 2, and the aquitard between Layer 1 and Layer 2. Initial values for the VCONTs of Layers 1 through 4 were obtained from the SD model and ranged from 10^{-7} to 10^{-2} d^{-1}. These VCONT values were adjusted during the calibration process. Layer 5 of the model (UFA-LPZ) did not have a VCONT value because the bottom of this layer was assigned a no-flow boundary condition.

3.4 MODEL STRESSES

This section discusses development of natural and man-made stresses of the PRIM. These include rainfall, ET, groundwater and surface water extraction, and return flows.

3.4.1 Precipitation

NEXRAD weather data provided the rainfall inputs to the model. The 15-minute NEXRAD data were consolidated into daily rainfall amounts data and then input via the Rainfall Time Series (RTS) package of MODHMS. Average annual rainfall for the calibration period of 2003 to 2018 was around 48 inches. During the recalibration period, 2003 and 2004 were wet years, whereas 2011, 2012, and 2013 were dry.

To evaluate the quality of the NEXRAD data, the daily and monthly precipitation data were compared with that of the long-term rain gauges available in the watershed. Figures 3.13 through 3.20 show the comparisons between the NEXRAD data and rain gauges at Winter Haven, Bartow, Wauchula, and Arcadia. The visualized comparison includes a time series plot, a correlation plot, a cumulative plot, exceedance curves, and histogram of residuals. The comprehensive comparison

revealed that the NEXRAD provided a reasonably accurate representation of the spatial and temporal pattern of precipitation in the watershed. Discrepancies exist mainly during high rainfall events. Annual rainfall pattern shows that NEXRAD tends to overestimate before 2005 and underestimate after 2010.

3.4.2 Evapotranspiration

The ET processes simulated in the PRIM model included canopy interception, unsaturated zone ET, and saturated zone (groundwater) ET. The MODHMS Interception (IPT1) and Evapotranspiration (EVT) packages were used to simulate these ET processes. The IPT1 package simulated interception and unsaturated zone ET, and saturated zone ET was simulated using the EVT package.

Interception is the retention of precipitation on the canopy, the understory, the bottom vegetation, the litter layer, and the land surface. In the PRIM model, root zone storage was included in the interception storage, and all the interception terms were combined into a single, land use-dependent interception capacity. Any rainfall that exceeds the interception capacity results in runoff and infiltration to the saturated zone. Root zone storage was determined as the product of the root zone depth and available plant water (defined as field capacity moisture content minus wilting point moisture content). In the conceptualization used in the PRIM model, root zone storage was the largest component of interception. The root zone depth was assigned as a function of land use type (Table 3.4). The field capacity and wilting point moisture contents are functions of the soil type and are listed in Table 3.5.

Saturated zone ET was represented using the ET surface and extinction depth concepts employed in the EVT module of MODFLOW. In this framework, the saturated zone ET is zero when the water table is below the extinction depth, and it increases linearly to a maximum saturated zone ET as the water table rises from the extinction depth to the ET surface. If the water table is above the ET surface, maximum ET will be achieved. The ET surface in the PRIM was set as 2 feet below the land surface for areas without significant open water. For areas covered by open water, the ET surface was set to be equal to the bed elevation of the water body. An extinction depth of 6 feet was used in the PRIM model. This value was established during calibration of the Saddle Creek sub-basin model (HGL, 2008).

Additional ET inputs were the ET_{ref} and land use-dependent k_c (crop coefficient). A daily reference ET time series for the Peace River basin was developed from climate stations located in the Peace River basin as described in the PRIM Phase I report. The ET_{ref} time series was entered via the ETS package of MODHMS. The potential ET at any location is obtained by multiplying ET_{ref} by the k_c at that location. The k_c parameter is a function of the land use and varied monthly to reflect seasonal variations. Grid block values of k_c were determined as area-weighted averages of the values for the land use types present in that grid block. The k_cs were entered in the Land Use Package (LUP) of MODHMS. Values for k_c were obtained from a review of the literature (HGL, 2009), with a number of adjustments made during calibration of the Saddle Creek sub-basin (HGL, 2008). These calibrated values were adopted for the basin-wide model and were not further modified during the calibration. The values for k_c used in the model are listed in Table 3.4.

3.4.3 Groundwater and Surface Water Withdrawals

The PRIM model accounted for groundwater and surface water withdrawals located inside the model domain. The influence of groundwater withdrawals from wells located outside the PRIM model boundaries was incorporated via the boundary conditions assigned to the lateral boundaries of the model, which are discussed in Section 3.6 below.

The PRIM 2 model included withdrawals from permitted groundwater wells and surface water diversions. Well locations and pumping rates were provided by the SWFWMD. Groundwater is the major water supply source; surface water use accounts for less than 10 percent of total water use and is concentrated in the Saddle Creek and Peace Creek sub-basins. Phosphate mining operations account for a significant portion of industrial water use. Groundwater extractions associated with mining operations are directly accounted for in the model. Captured surface water runoff is a significant source of water for mining operations (see Section 2.5.2 in the PRIM Phase I report), but that portion of surface water use is not directly simulated in the PRIM model. Rather, the model accounts for operating mines in terms of their net contributions to basin water budget via groundwater pumping, groundwater recharge, and surface water discharges. Groundwater pumping was assigned to the appropriate model grid cells and layers based on well locations and screen depths. Monthly varying pumping rates were specified via the MODHMS FWL5 and WEL packages.

The surface water diversions included in the PRIM model vicinity were primarily withdrawals from irrigation ponds, which are often maintained by groundwater pumping during dry periods. This water use was included in the SWFWMD water uses database provided by SWFWMD. The largest surface water uses in the Peace River are the water supply withdrawals for the PRMRWSA intake near Ogden and the surface water diversions from Lake Parker in Saddle Creek to provide cooling water for the Larsen and McIntosh power plants in Lakeland. These diversions were not in the PRIM 1 and 2 models. The PRMRWSA intake is outside the PRIM model boundary, which ends at Arcadia. The power plant cooling water is discharged back into Lake Parker. Neither the withdrawals nor the discharges were included in the models on the assumptions that cooling water losses are small and that the withdrawals and discharges will balance out.

3.4.4 Return Flows and Surface Water Discharges

In order to approximate as closely as possible a closed hydrologic system in the PRIM models, groundwater and surface water extracted within the model boundaries were also returned to the model as areally distributed groundwater return flows and surface water discharges.

Extracted water was returned to the integrated SW/GW system through the LUP (land use) and CHF (channel flow) packages as well as by injection to the SA through the WEL package. The methodology to determine return flows was a function of the water use category, as specified in the SWFWMD water use database. Water extracted from public supply, agricultural, landscaping, recreational, and industrial/commercial wells was applied as rainfall additions to service areas or permit areas or both.

It was assumed that public water supply (PWS) service areas correspond to areas that are also on public sewer systems. In those areas, return water through lawn irrigation and reclaimed water

from wastewater treatment plants were applied as rainfall additions. It is assumed that the water not used in lawn irrigation is routed to a wastewater treatment system and eventually returned to the watershed as either surface-applied reclaimed water or as an NPDES discharge. For public supply withdrawals, the amount of water discharged from municipal wastewater treatment plants (WWTPs) was first subtracted from the withdrawal amount, then the remaining water was evenly distributed over the public supply service area excluding any WUP areas. For domestic supply withdrawals, 50% of the withdrawn water (CFWI, 2020) was returned to the Surficial Aquifer model cells corresponding to the well locations.

Part of industrial/commercial water use was discharged via NPDES. The fraction of industrial/commercial water use that was not discharged via NPDES was counted toward the rainfall additions. For industrial/commercial (excluding phosphate mining) withdrawals, the corresponding WWTP surface water discharges were subtracted from the withdrawal amount, and the remaining water was evenly applied over the OLF model cell corresponding to the well location. Service areas that overlap with permit areas were excluded to avoid duplicate applications. If the withdrawal location supply well was not located in either a service or permit area, the water was applied to either the same model cell where the well is located or distributed among the four nearest cells.

In the case of agricultural, landscaping and recreational withdrawals, the entire withdrawal amounts were returned as rainfall additions. The additional rainfall was evenly applied over the surface of the WUP area.

Groundwater withdrawals for phosphate mining operations were treated in accordance with the approach for simulating mining operations discussed in Section 3.3.1. Groundwater pumped for mining operations becomes part of the mine circulation system. The water that is not lost in the mining process, including groundwater recharge and ET losses, is eventually discharged to the watershed via monitored NPDES surface water outfalls. Groundwater extraction by mining water supply wells were directly simulated in the model. Surface water return flows were accounted for in terms of NPDES point discharges. Groundwater recharge in operational mine areas (i.e., inactive OLF cells) was set to a uniform value of 2 in/yr. Surface water discharges were incorporated into the models as point sources in the MODHMS CHF package. Discharge locations and rates were obtained from NPDES permit information maintained by the FDEP. NPDES discharge locations are shown in Figure 3.21.

3.5 BOUNDARY CONDITIONS

Boundary conditions along the PRIM model perimeter were set to no-flow conditions for the OLF plane and for the SA subsurface layer, consistent with the conceptualization that the watershed boundaries also represent no-flow boundaries for the shallow groundwater. The outflow boundary for the CHF domain at the Peace River outlet (the location of the PRMRWSA surface water intake near Arcadia) was set to a zero depth-gradient condition. The same boundary condition was also applied to the OLF cell at the outlet location. Boundaries between sub-basins in the model were defined only in terms of topographic elevations, as translated into elevations of adjacent OLF model cells and stream channel hydrograph; the model did not enforce internal no-flow boundaries between sub-basins.

3.5.1 Aquifer Bottom Boundaries

The lower boundary of the model was the bottom of the LPZ of the UFA. This boundary was set as a no-flow boundary in the model. This was consistent with most previous groundwater models developed within the SWFWMD.

3.5.2 Lateral Subsurface Boundaries

Lateral groundwater boundaries for the IAS and UFA aquifer units were assigned prescribed head values, which varied monthly. The boundary conditions accounted for regional head fluctuations in aquifer heads due to both natural variations and groundwater pumping. In order to develop the boundary heads, the East-Central Florida Transient Expanded (ECFTX) model (CFWI, 2020) was used. The ECFTX model was developed by the Central Florida Water Initiative (CFWI), which undertook a robust and cooperative effort to identify the extent of the groundwater system in central Florida, support regional water supply planning, and understand groundwater resource limitations for sustainable water supplies while protecting natural systems. A primary tool for the groundwater assessment is the ECFTX groundwater flow model, which was used to generate groundwater heads along the PRIM model boundaries. The model was used to generate monthly heads between 2004 and 2015. Monthly groundwater heads in 2003 and between 2016 and 2018 were found by correlating observed data and simulated heads between 2004 and 2014 and using the correlations to extrapolate backward to January 2003 and forward to December 2018.

FIGURES

This page was intentionally left blank.

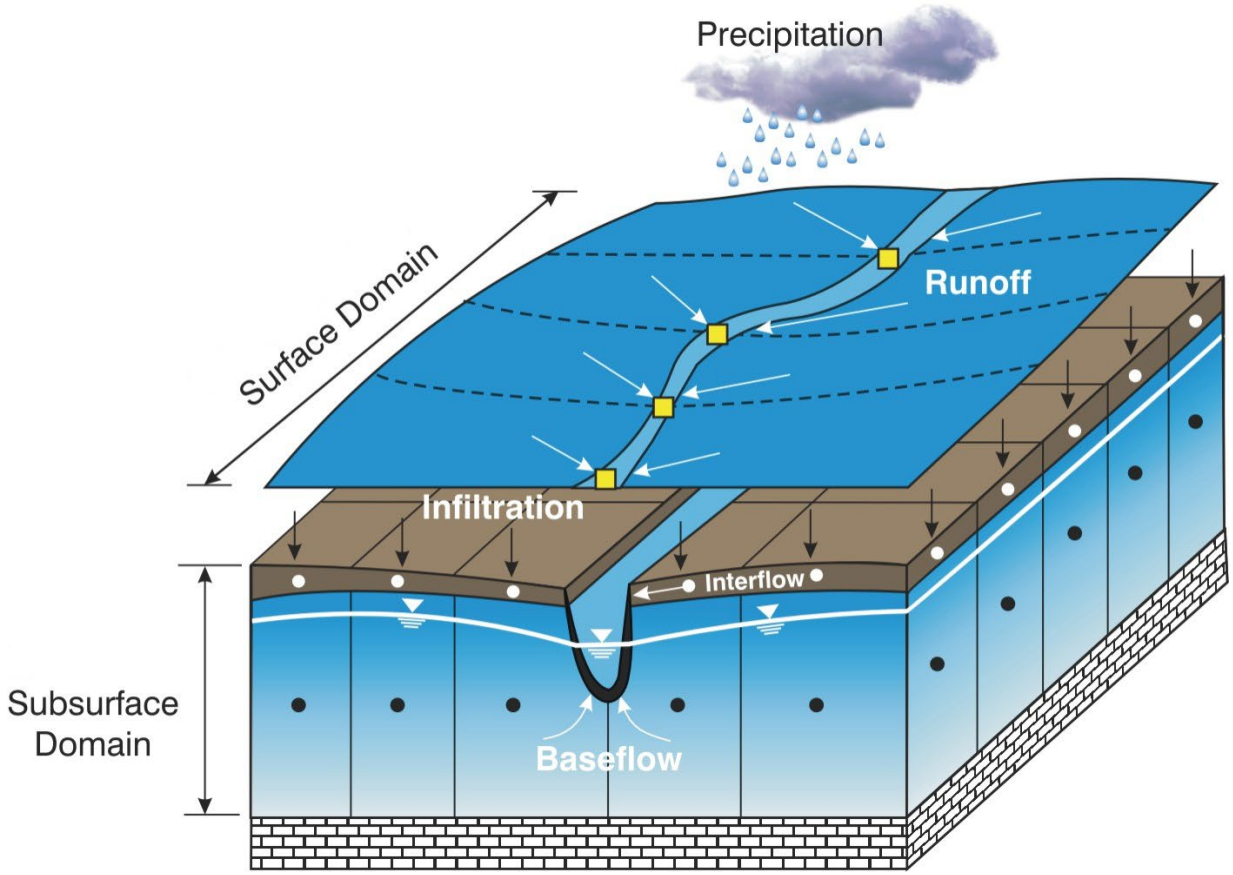

Figure 3.1 Schematic Representation of the GW-SW System in the PRIM Model

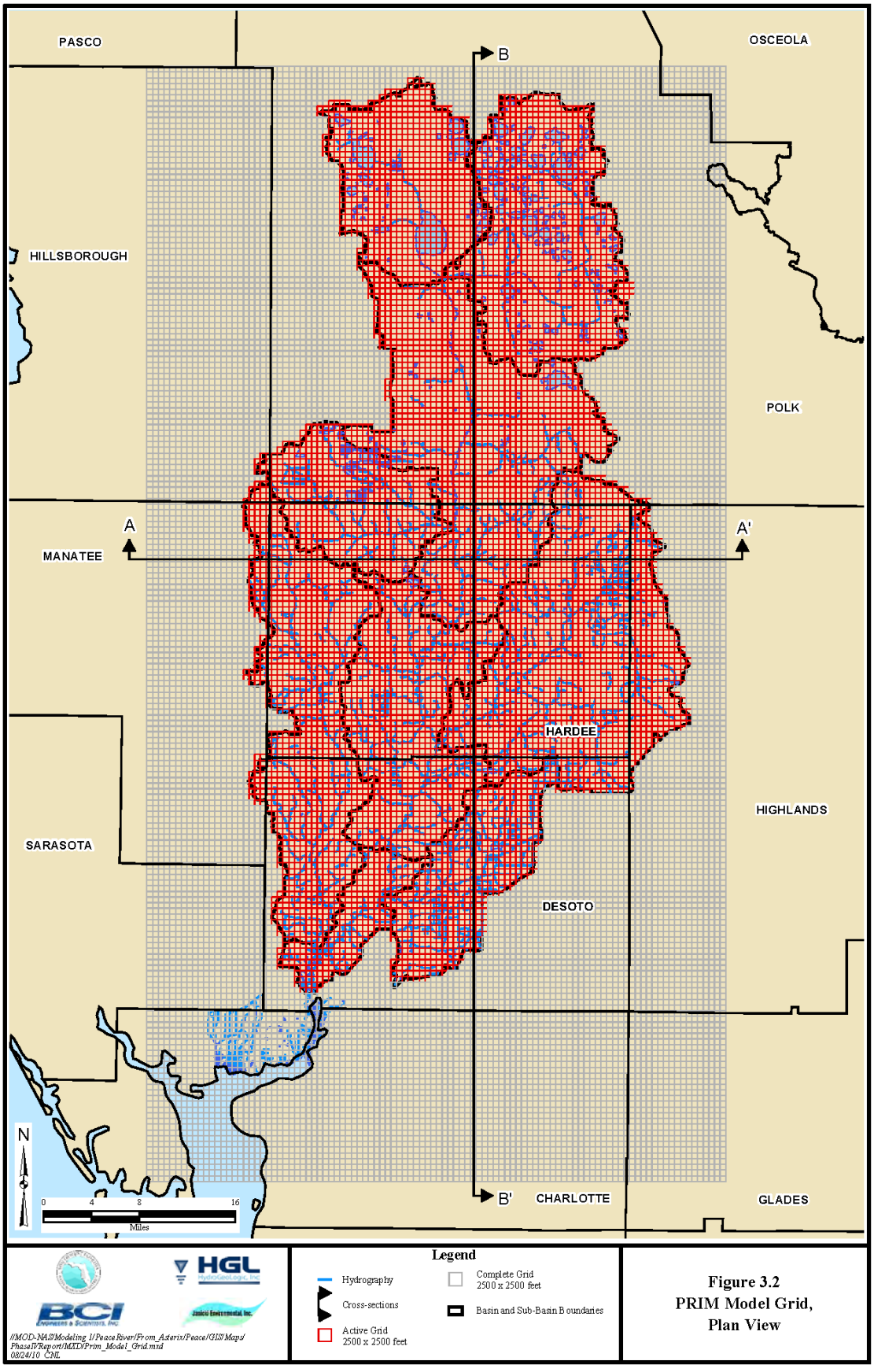

Figure 3.2
PRIM Model Grid, Plan View

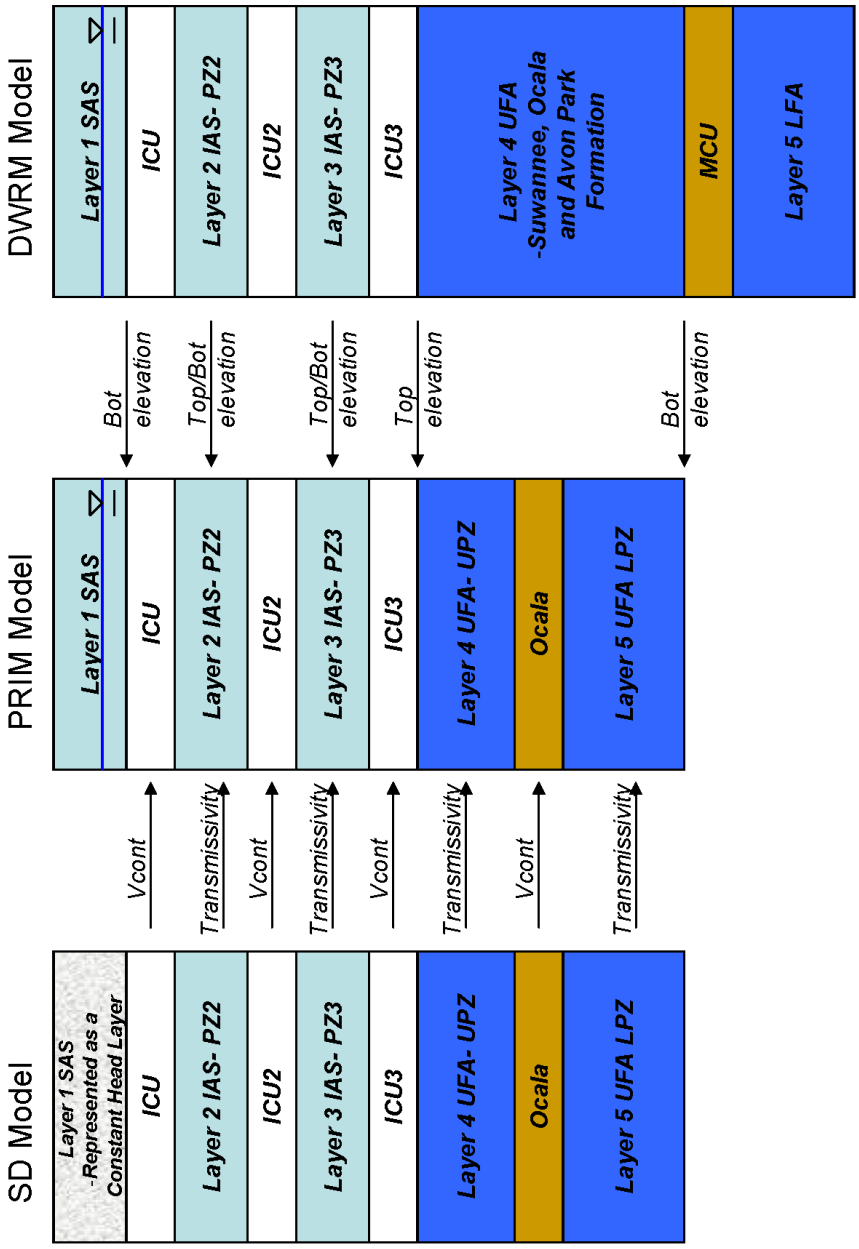

Figure 3.3 Correspondence between SD Model, DWRM Model, and the PRIM Subsurface Model Layers

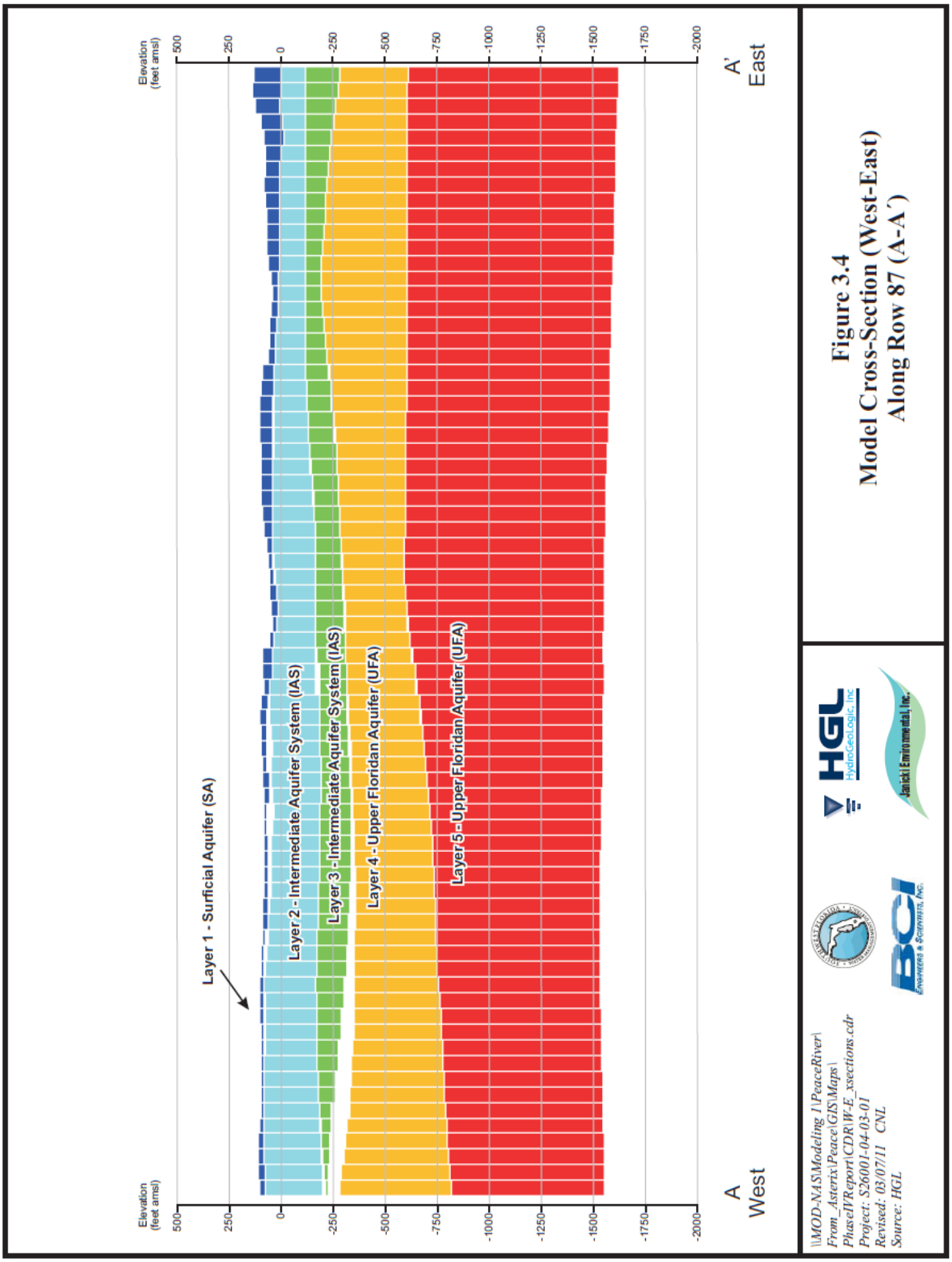

Figure 3.4
Model Cross-Section (West-East)
Along Row 87 (A-A')

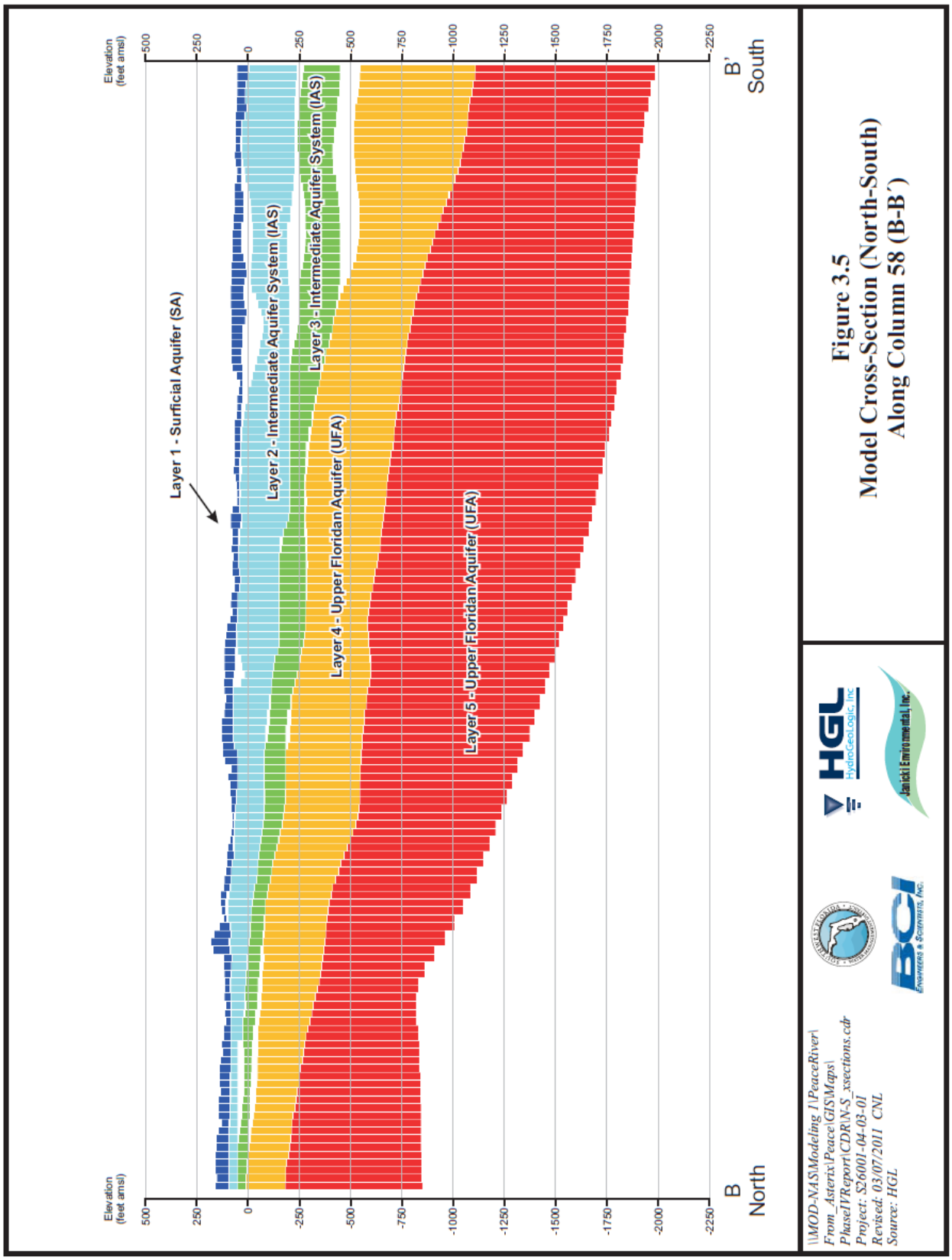

Figure 3.5
Model Cross-Section (North-South)
Along Column 58 (B-B´)

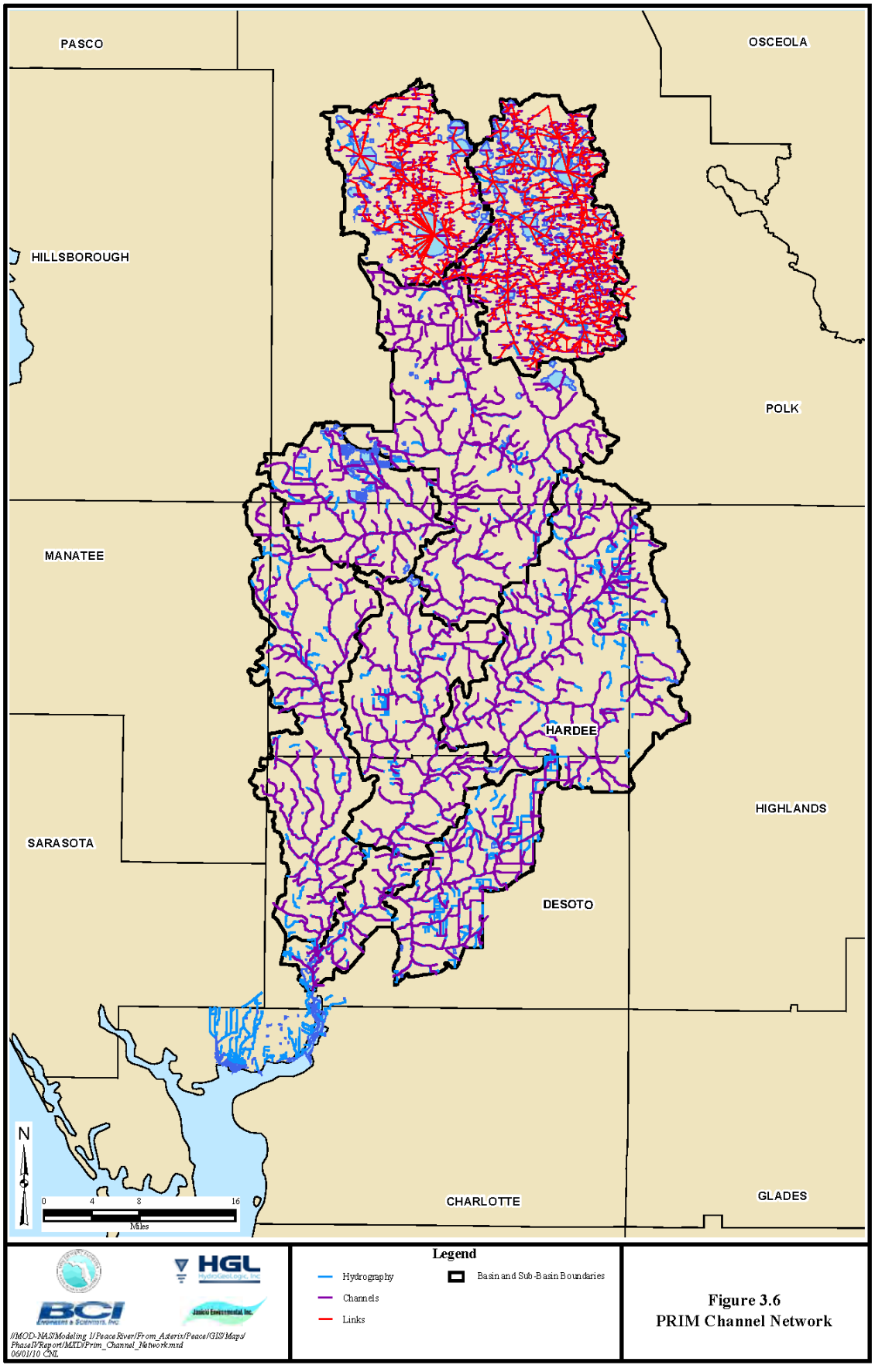

Figure 3.6
PRIM Channel Network

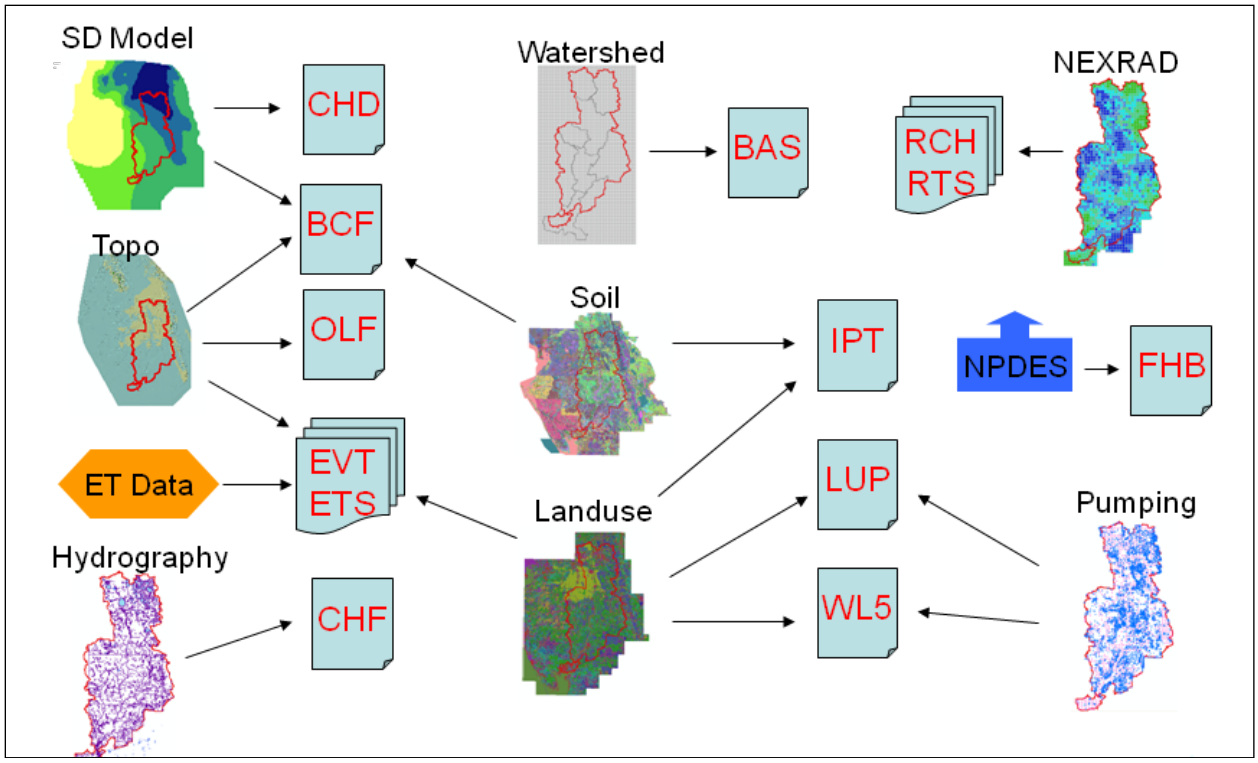

Figure 3.7 Schematic Relationship Between Input Data Sources and MODHMS Simulation Packages

HGL—Peace River Integrated Modeling 2

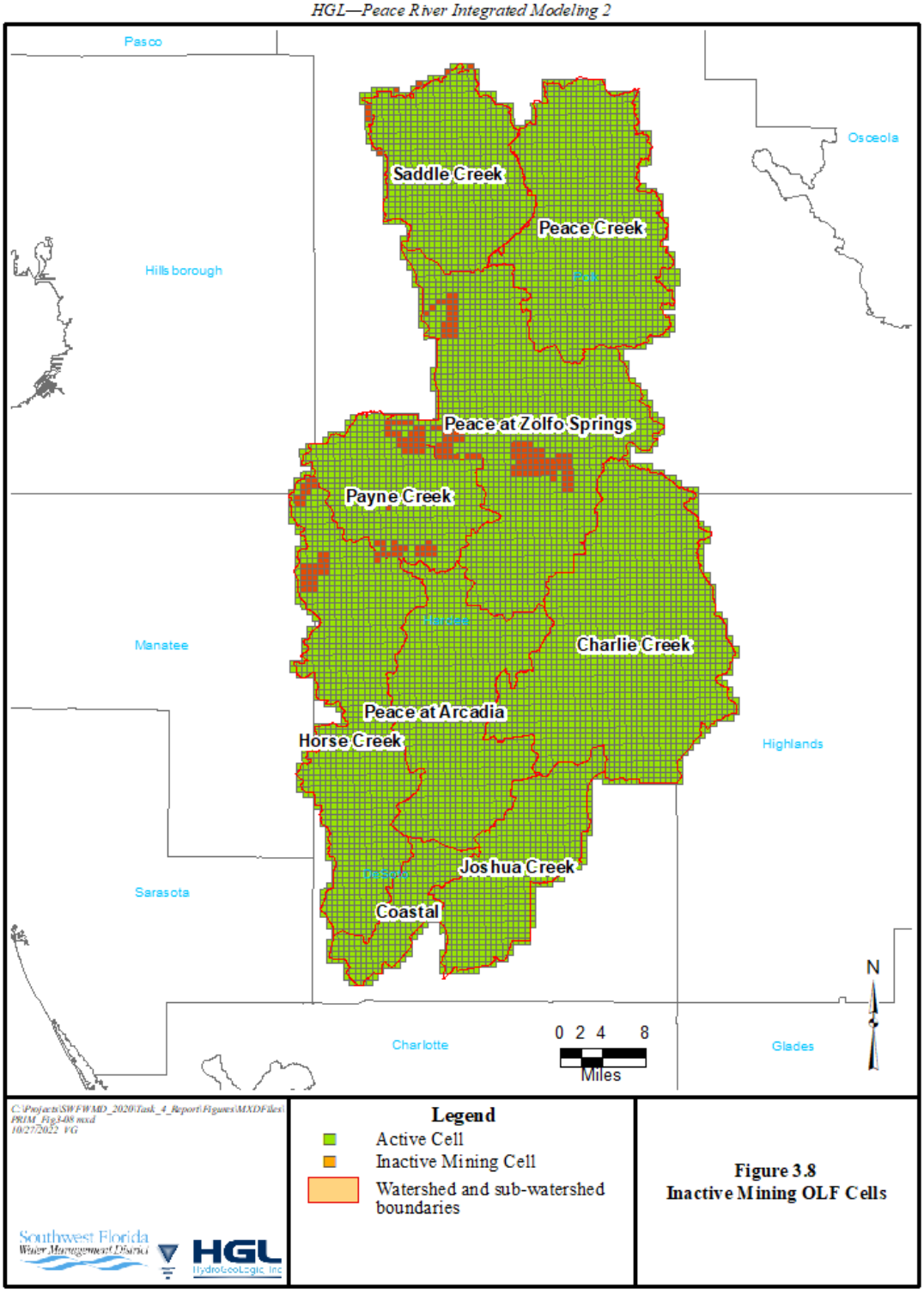

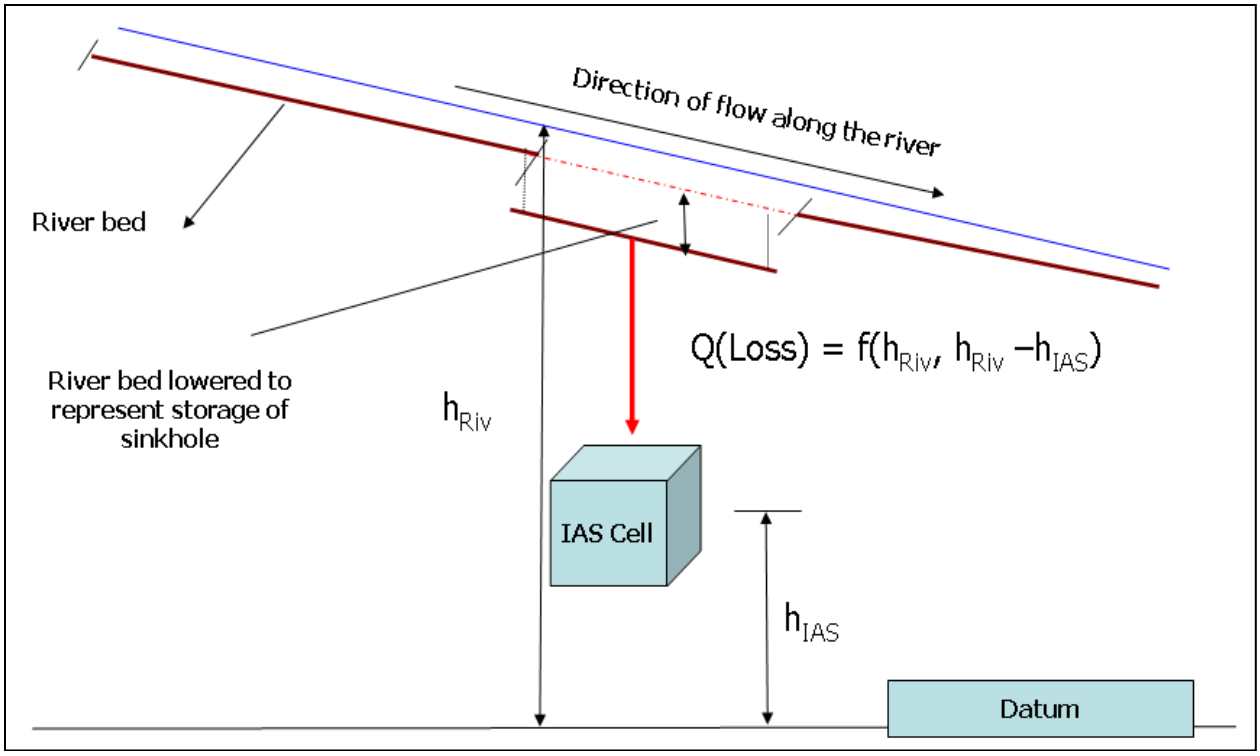

Figure 3.9 Schematic Representation of Karst Features

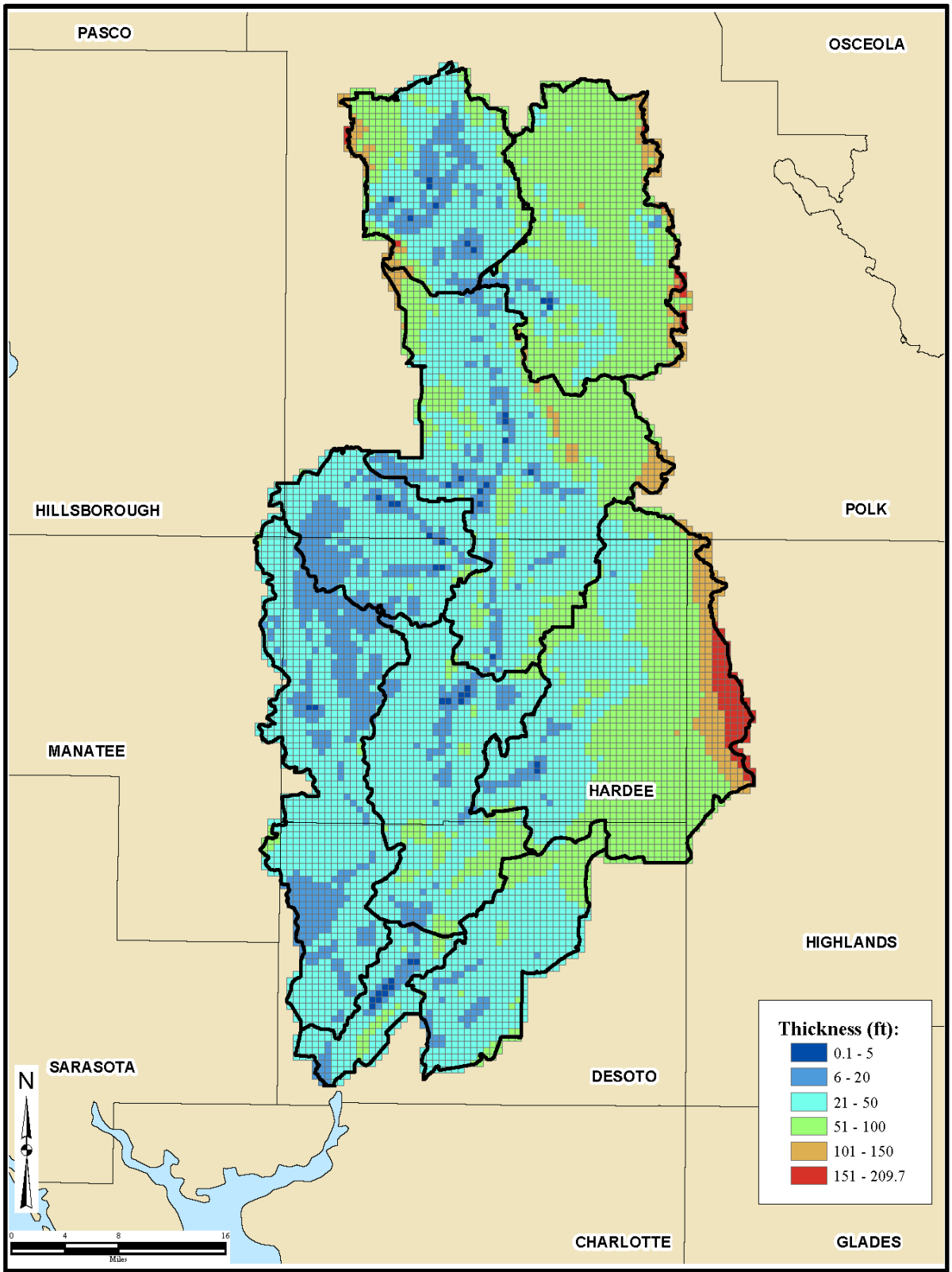
PASCO
OSCEOLA
HILLSBOROUGH
POLK
MANATEE
HARDEE
HIGHLANDS
SARASOTA
DESOTO
CHARLOTTE
GLADES
N
0 4 8 16
Miles
Thickness (ft):
0.1 - 5
6 - 20
21 - 50
51 - 100
101 - 150
151 - 209.7
Legend
Basin and Sub-Basin Boundaries
Figure 3.10
Thickness of
Model Layer 1 (SA)
in the PRIM

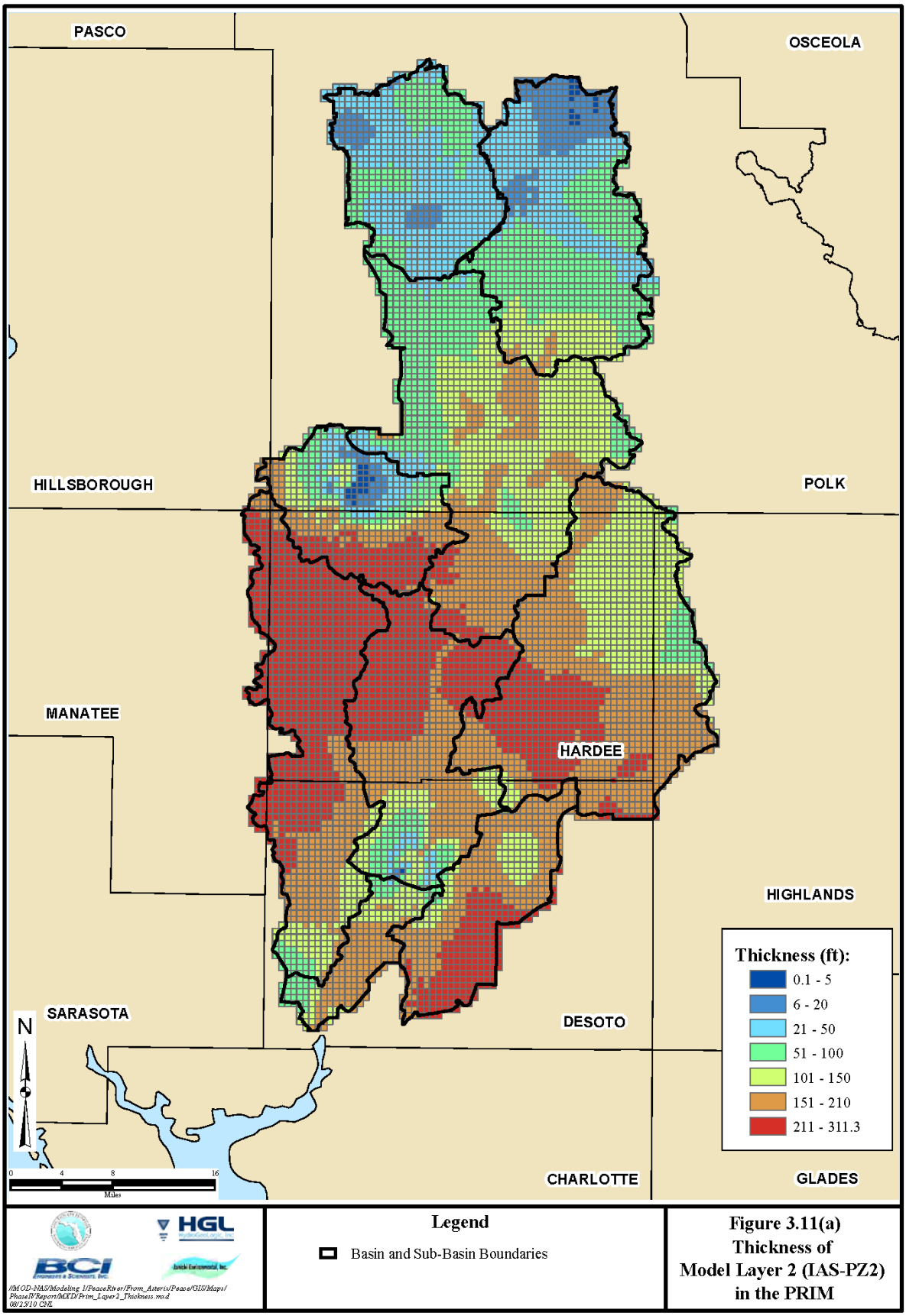
PASCO
OSCEOLA
HILLSBOROUGH
POLK
MANATEE
HARDEE
HIGHLANDS
SARASOTA
DESOTO
CHARLOTTE
GLADES
N
0 4 8 16
Miles
Thickness (ft):
0.1 - 5
6 - 20
21 - 50
51 - 100
101 - 150
151 - 210
211 - 311.3
HGL
BCI
Legend
Basin and Sub-Basin Boundaries
Figure 3.11(a)
Thickness of
Model Layer 2 (IAS-PZ2)
in the PRIM

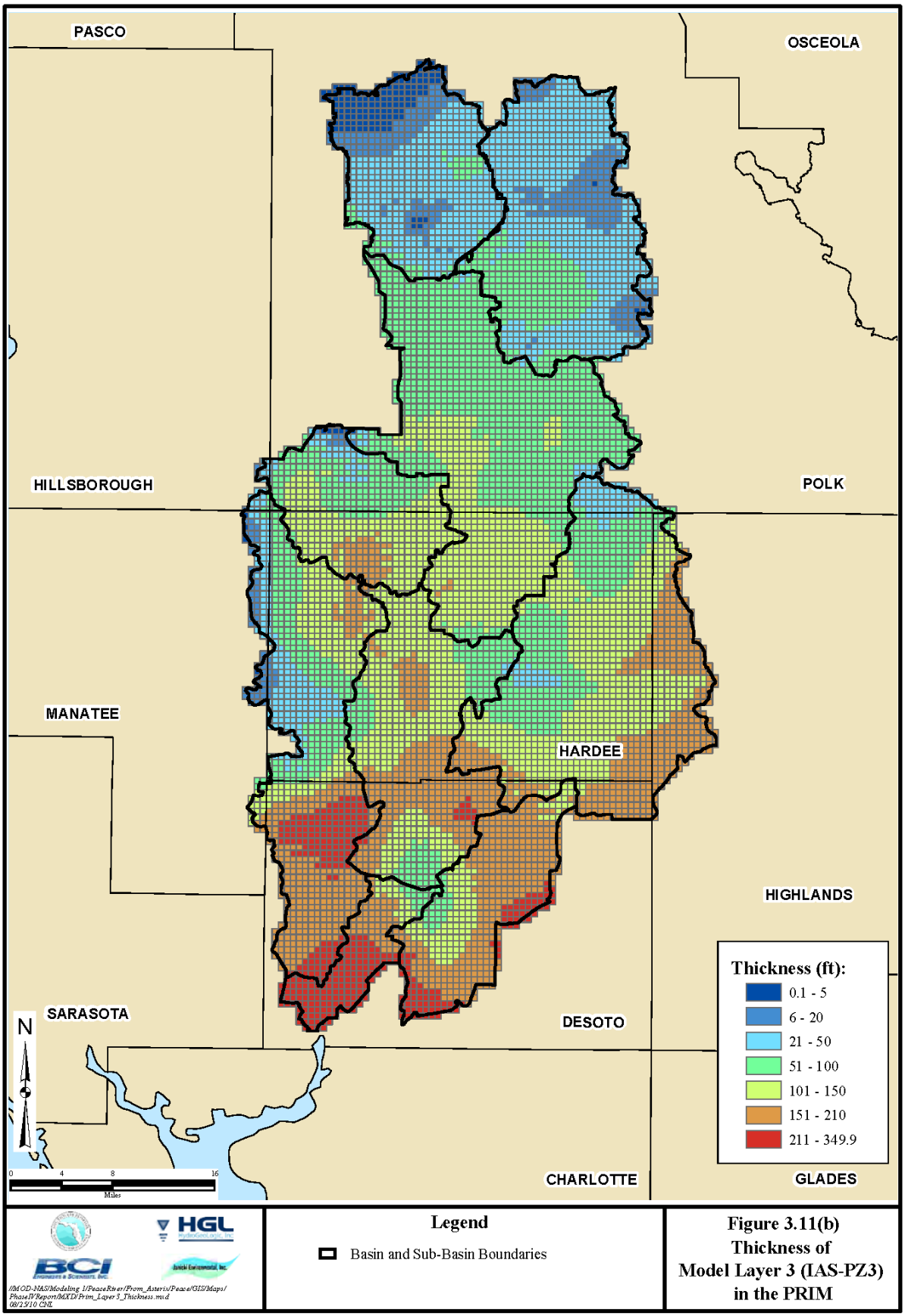
PASCO
OSCEOLA
HILLSBOROUGH
POLK
MANATEE
HARDEE
HIGHLANDS
SARASOTA
DESOTO
CHARLOTTE
GLADES
N
0 4 8 16
Miles
Thickness (ft):
0.1 - 5
6 - 20
21 - 50
51 - 100
101 - 150
151 - 210
211 - 349.9
Legend
Basin and Sub-Basin Boundaries
Figure 3.11(b)
Thickness of
Model Layer 3 (IAS-PZ3)
in the PRIM

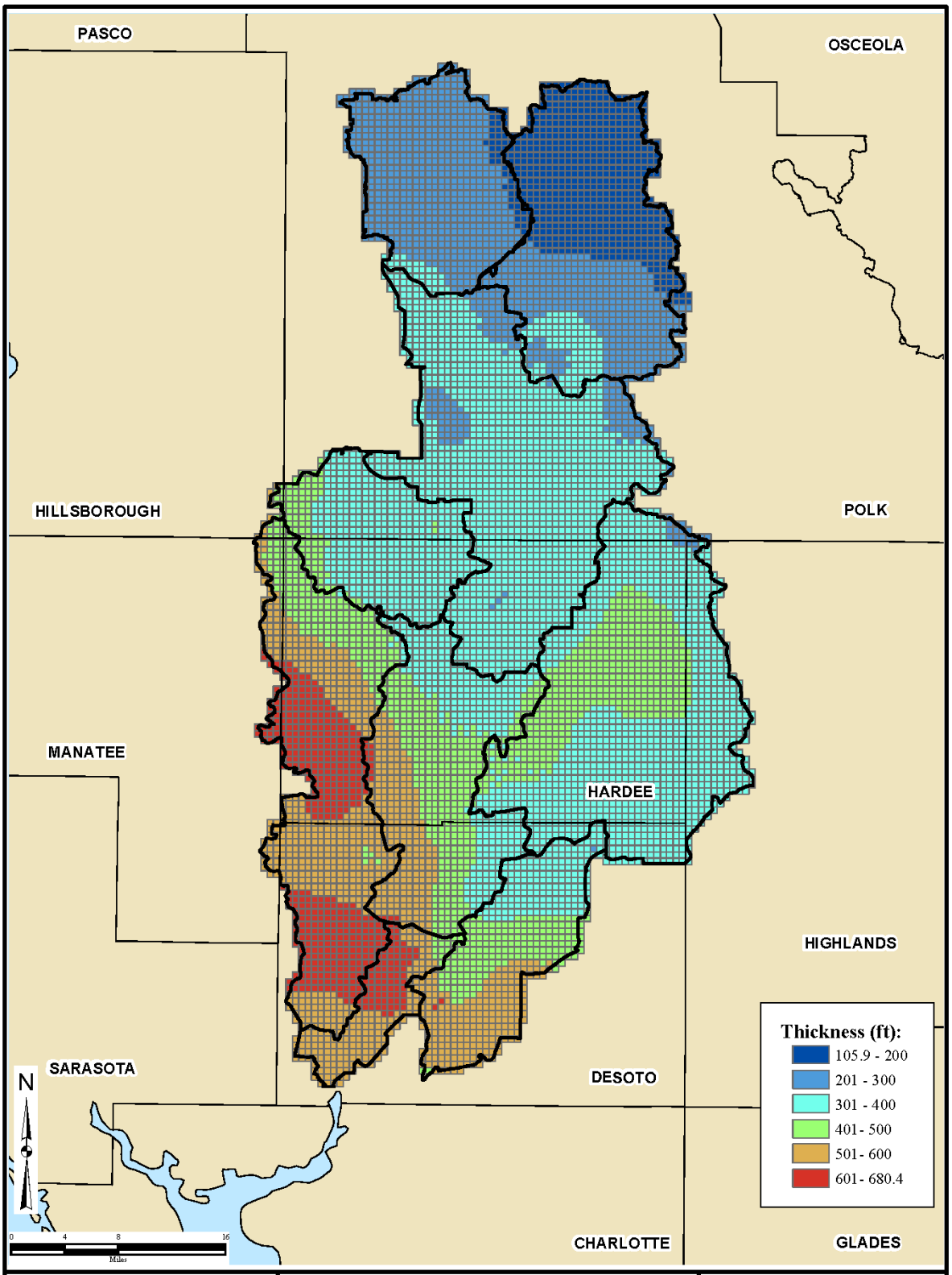
PASCO
OSCEOLA
HILLSBOROUGH
POLK
MANATEE
HARDEE
HIGHLANDS
SARASOTA
DESOTO
CHARLOTTE
GLADES
N
0 4 8 16
Miles
Thickness (ft):
105.9 - 200
201 - 300
301 - 400
401 - 500
501 - 600
601 - 680.4
HGL
BCI
//MOD-NAS/Modeling 1/PeaceRiver/Prim_Asteris/Peace/GIS/Maps/PhaseIVReport/MXD/Prim_Layer4_Thickness.mxd
08/25/10 CNL
Legend
Basin and Sub-Basin Boundaries
Figure 3.12(a)
Thickness of
Model Layer 4 (UFA-UPZ)
in the PRIM

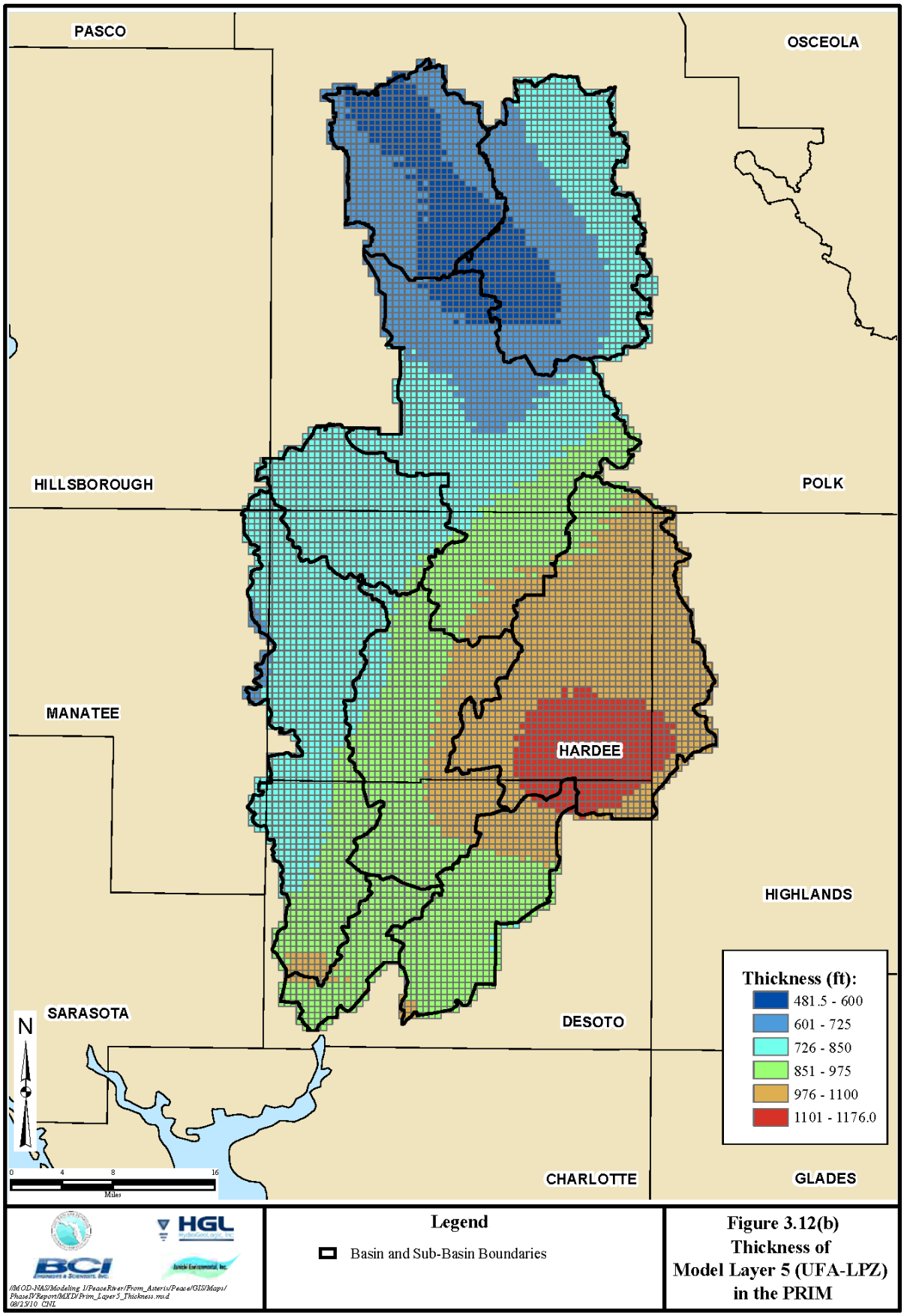
PASCO
OSCEOLA
HILLSBOROUGH
POLK
MANATEE
HARDEE
HIGHLANDS
SARASOTA
DESOTO
CHARLOTTE
GLADES
N
0 4 8 16
Miles
Thickness (ft):
481.5 - 600
601 - 725
726 - 850
851 - 975
976 - 1100
1101 - 1176.0
HGL
BCI
//MOD-NAS/Modeling 1/PeaceRiver/From_Asterix/Peace/GIS/Maps/PhaseIVReport/MXD/Prim_Layer5_Thickness.mxd
08/23/10 CNL
Legend
Basin and Sub-Basin Boundaries
Figure 3.12(b)
Thickness of
Model Layer 5 (UFA-LPZ)
in the PRIM

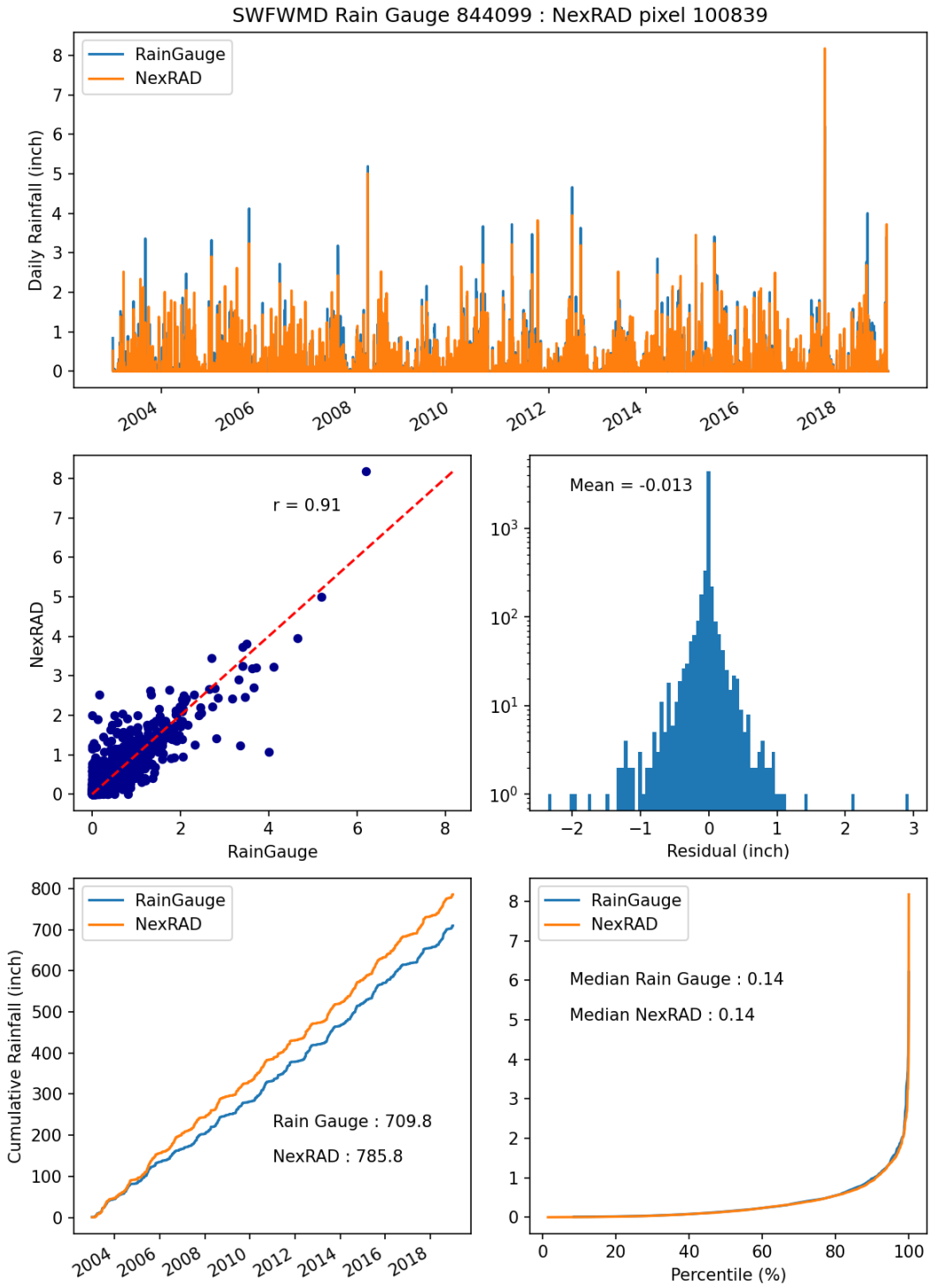

Figure 3.13 Comparison of daily rainfall data recorded by rain gauge station Winter Haven Gilbert Airport NWS (SWFWMD Site ID 844099) and NEXRAD pixel from year 2003 to 2018

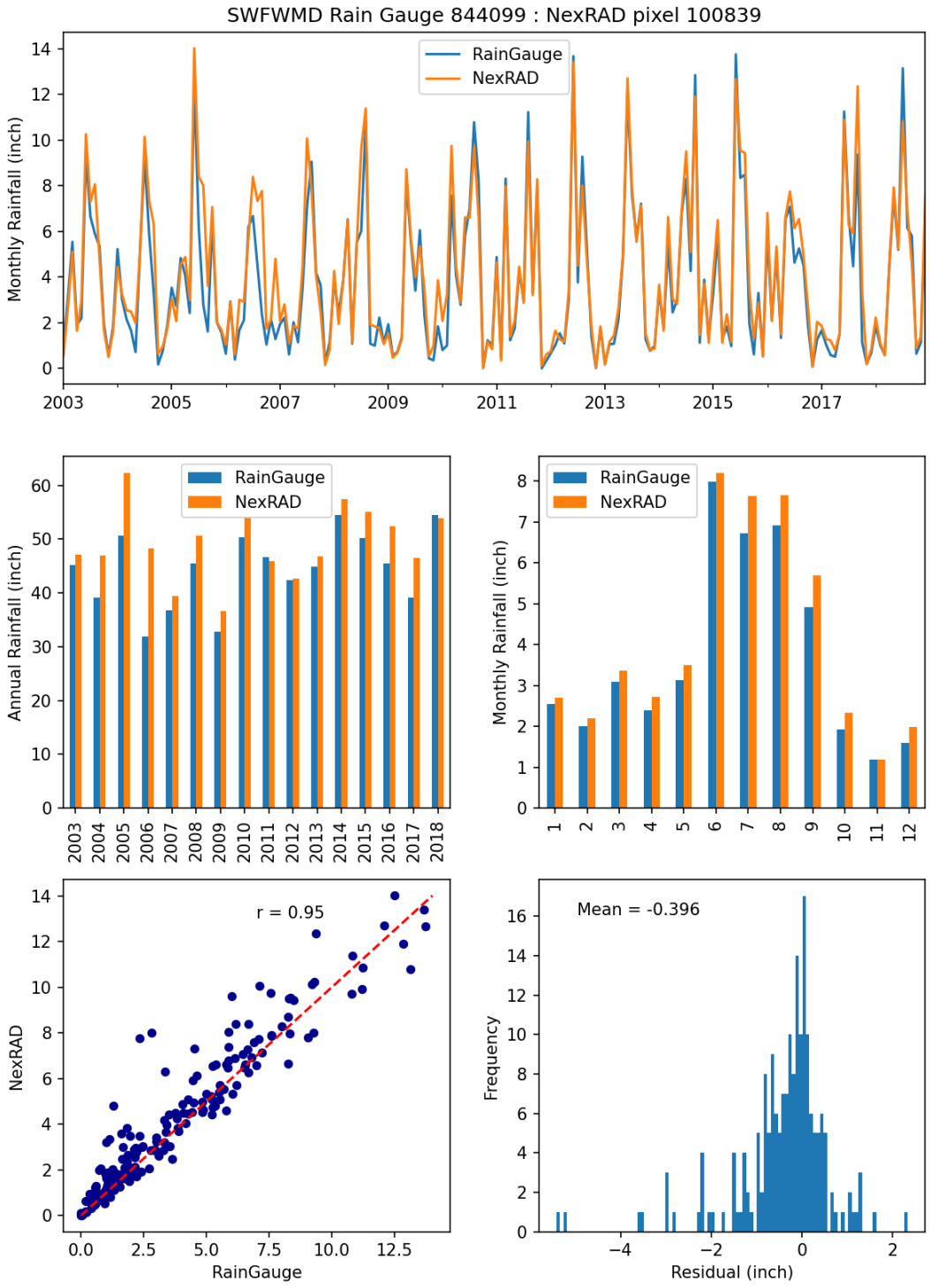

Figure 3.14 Comparison of monthly rainfall data recorded by rain gauge station Winter Haven Gilbert Airport NWS (SWFWMD Site ID 844099) and NEXRAD pixel from year 2003 to 2018

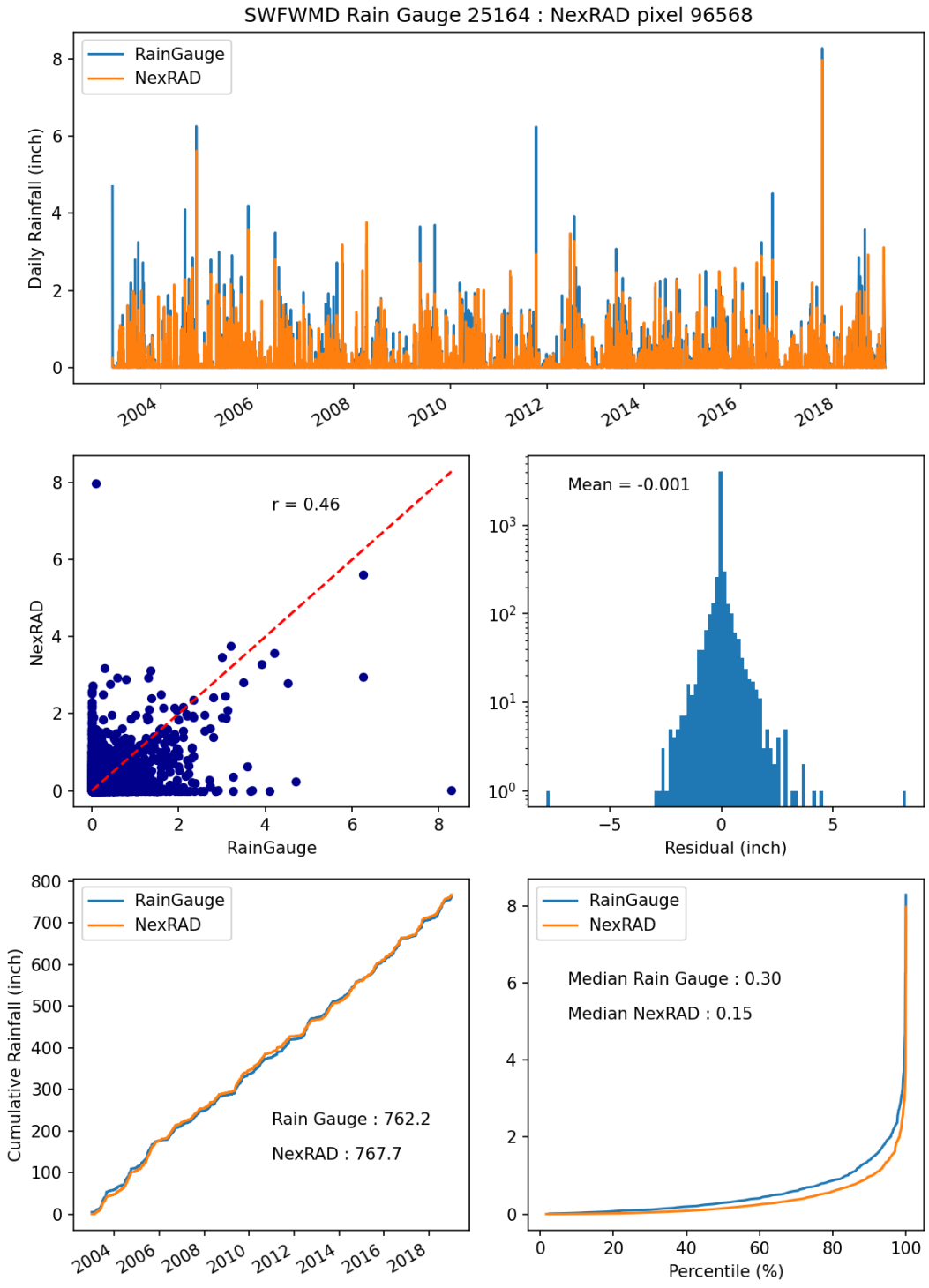

Figure 3.15 Comparison of daily rainfall data recorded by rain gauge station Bartow 1 SE NWS (SWFWMD Site ID 25164) and NEXRAD pixel from year 2003 to 2018

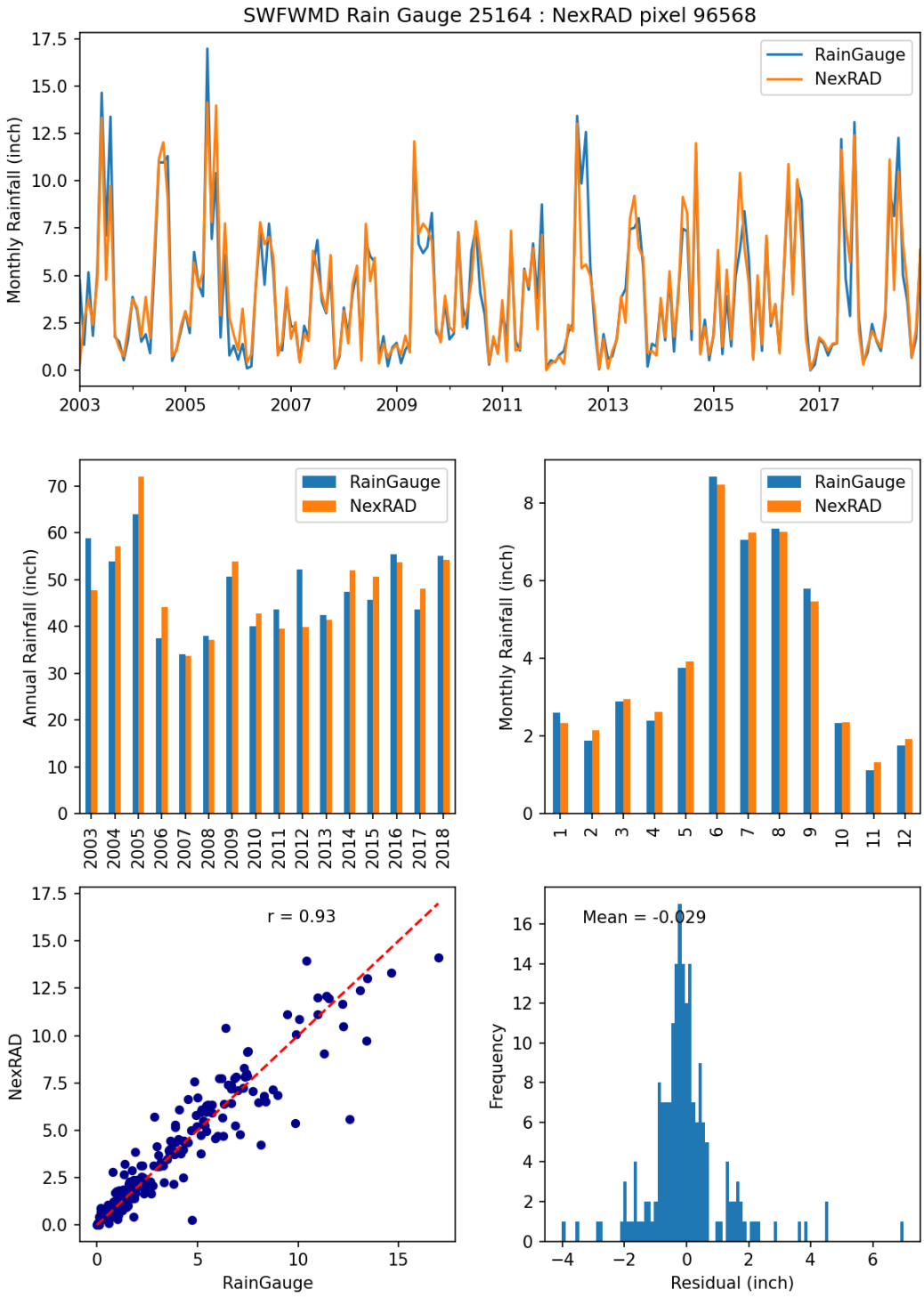

Figure 3.16 Comparison of monthly rainfall data recorded by rain gauge station Bartow 1 SE NWS (SWFWMD Site ID 25164) and NEXRAD pixel from year 2003 to 2018

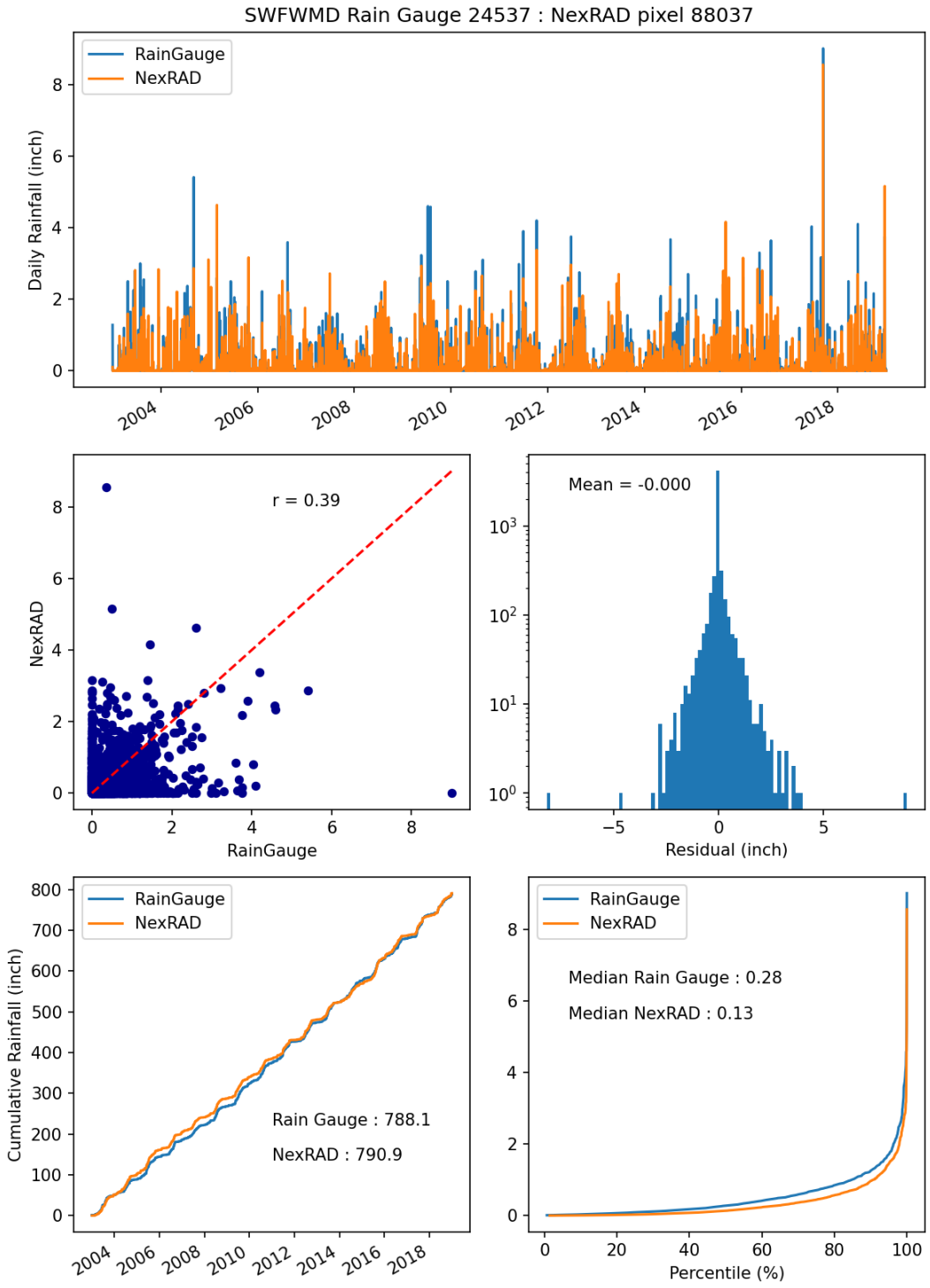

Figure 3.17 Comparison of daily rainfall data recorded by rain gauge station Wauchula NWS (SWFWMD Site ID 24537) and NEXRAD data from year 2003 to 2018

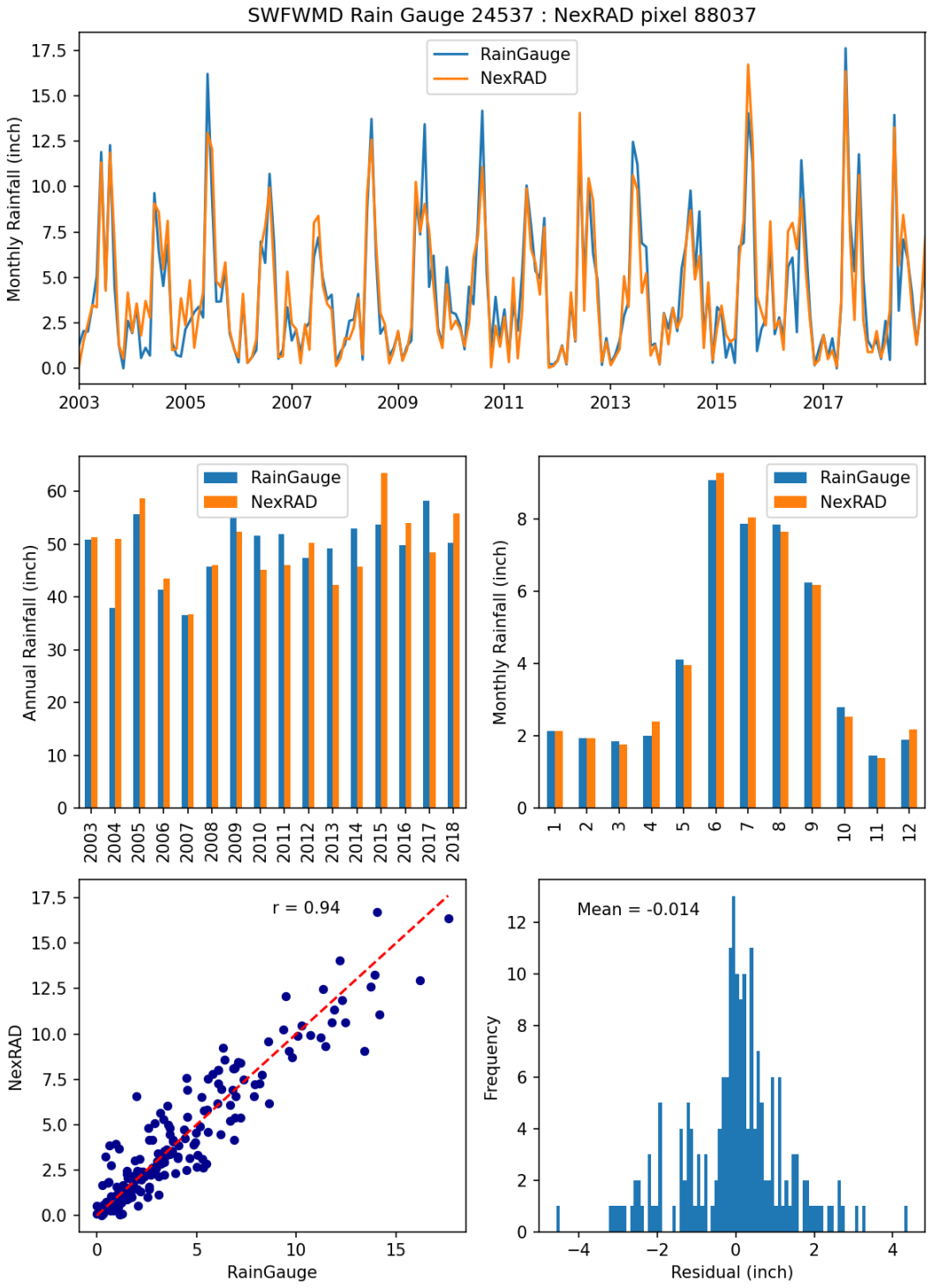

Figure 3.18 Comparison of monthly rainfall data recorded by rain gauge station Wauchula NWS (SWFWMD Site ID 24537) and NEXRAD data from year 2003 to 2018

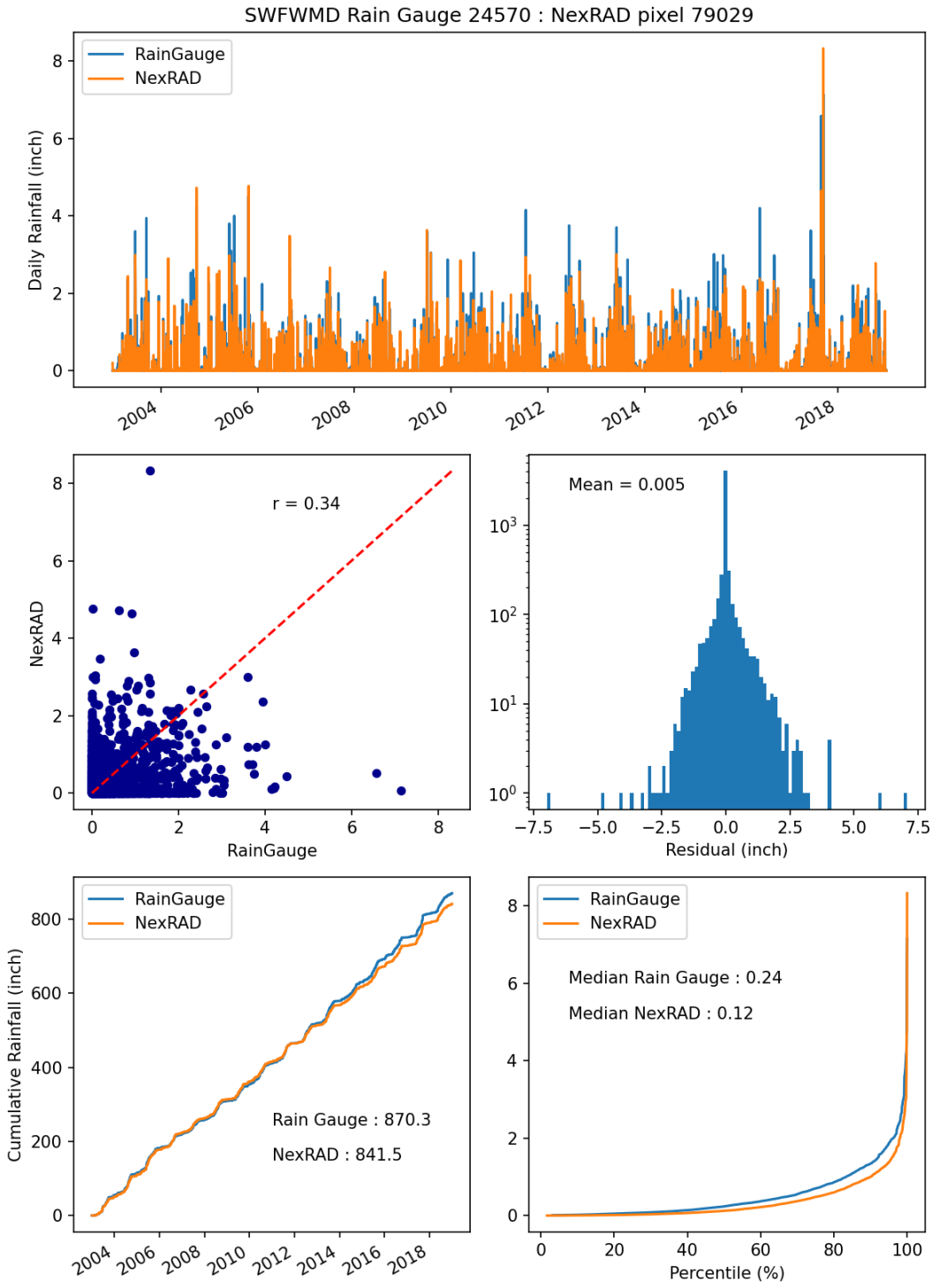

Figure 3.19 Comparison of daily rainfall data recorded by rain gauge station Arcadia NWS (SWFWMD Site ID 24570) and NEXRAD pixel from year 2003 to 2018

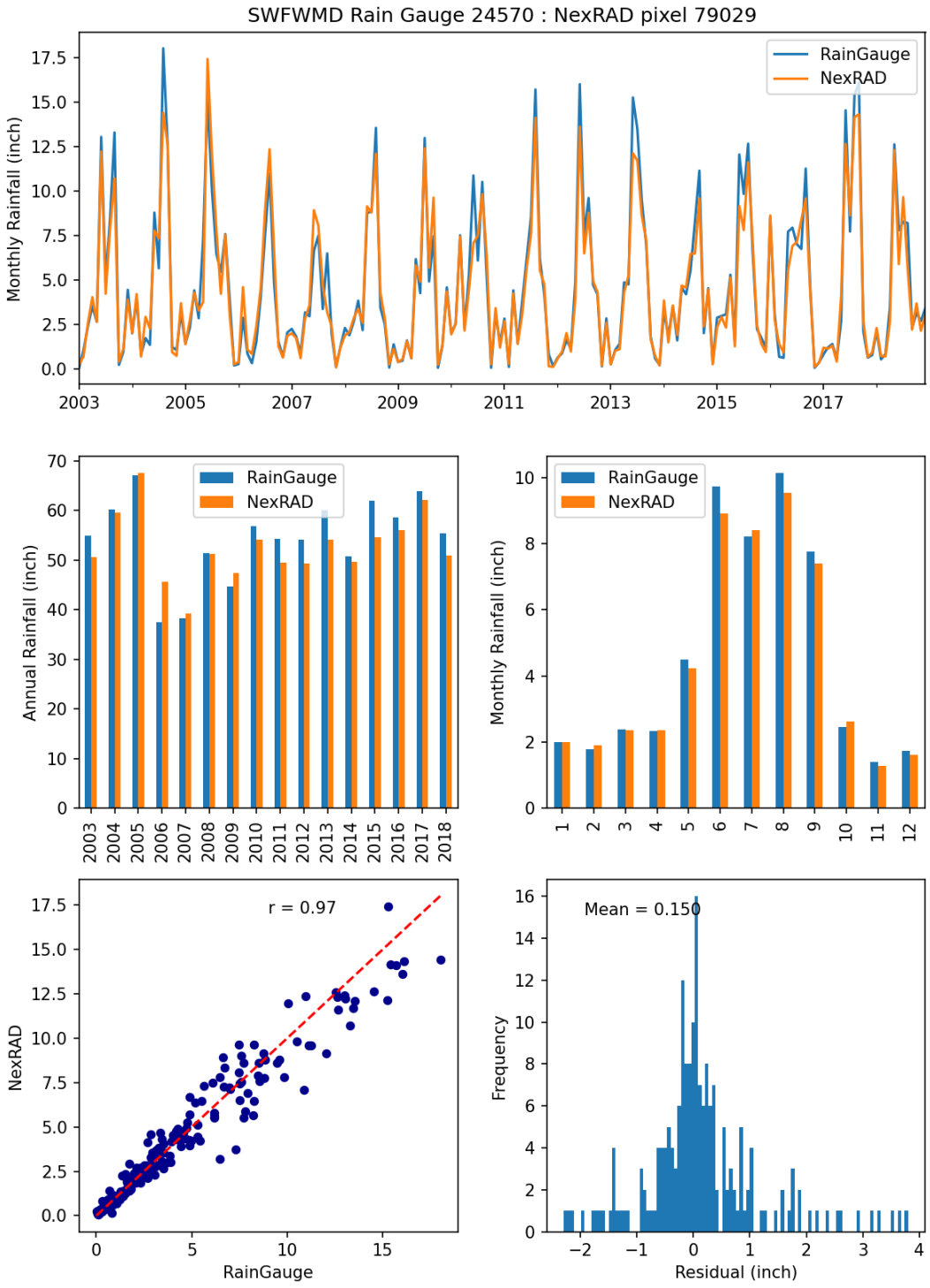

Figure 3.20 Comparison of monthly rainfall data recorded by rain gauge station Arcadia NWS (SWFWMD Site ID 24570) and NEXRAD pixel from year 2003 to 2018

HGL—Peace River Integrated Modeling 2

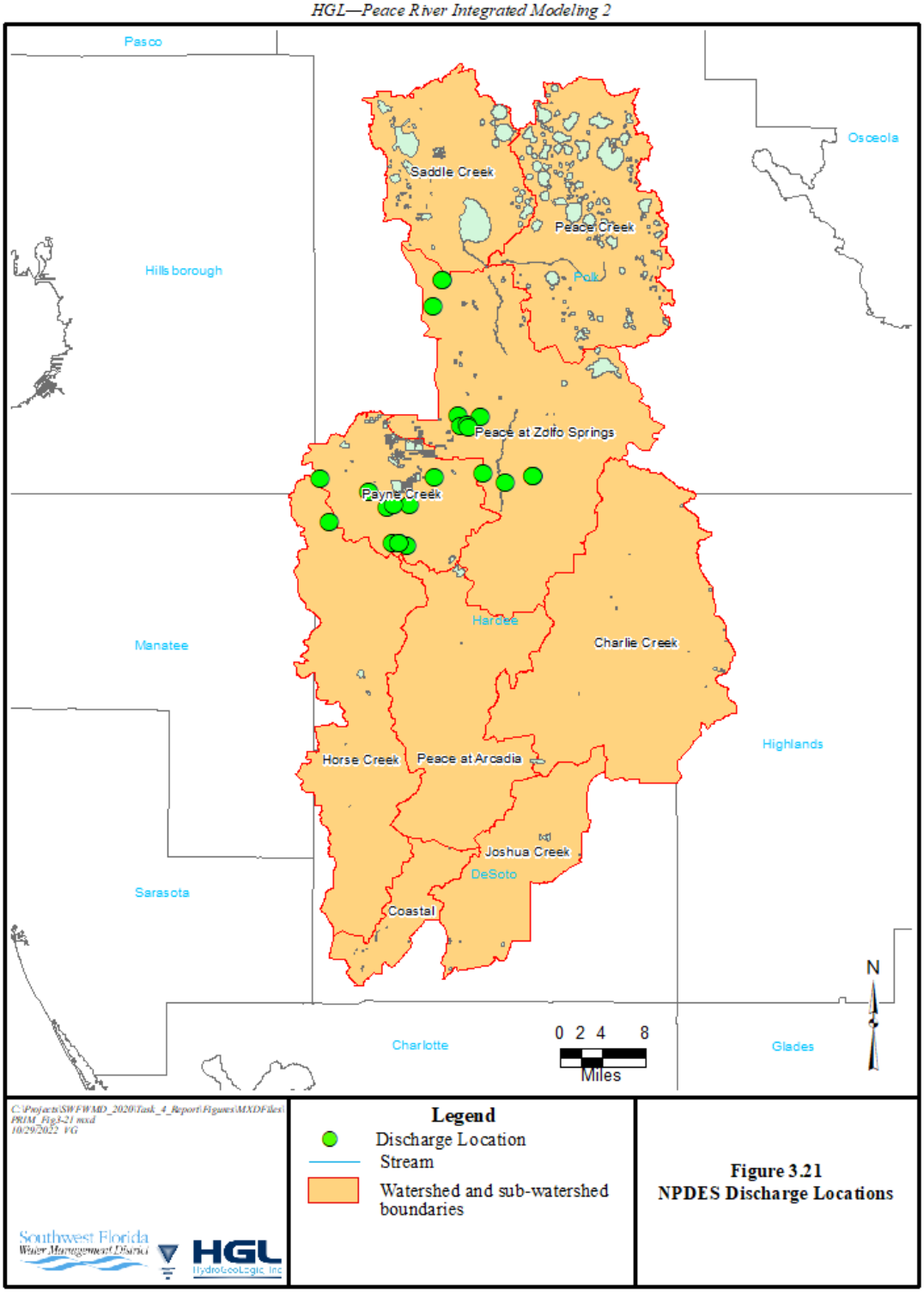

This page was intentionally left blank.

TABLES

This page was intentionally left blank.

Table 3.1
Lakes Incorporated into the OLF Domain of the PRIM Model

Saddle Creek Sub-Basin	Peace Creek Sub-Basin
Lake Hancock	Lake Hamilton
Lake Parker	Lake Annie
	Lake Starr
	Lake Howard
	Lake Shipp
	Lake Lulu
	Lake Eloise
	Lake Winterset
	Lake Garfield

Table 3.2
Summary of Active Model Cells in PRIM Model

Model Component	Number of Active Cells
Channel Domain (CHF)	9807[1]
Overland Flow Domain (OLF)	7997
Groundwater Layers 1 - 5[2]	8367

[1]Number of channel segments.
[2]Number of cells per layer.

Table 3.3
Land Use Dependent Overland Flow Parameters

Land Use Category	FLUCCS Classifications	Manning's Roughness Coefficient (-)[1]	Paved Surface Leakance (day^{-1})
1	Low Density Urban, Recreational	0.080	0.001
2	Medium Density Urban, Institutional	0.065	0.001
3	High Density Urban, Industrial, and Transportation	0.035	10^{-6}
4	Cropland and Pasture	0.075	N/A
5	Row Crops	0.075	N/A
6	Tree Crops, Citrus	0.150	N/A
7	Shrubland	0.150	N/A
8	Upland Forest	0.225	N/A
9	Open Water	N/A	N/A
10	Forested Wetlands	0.175	N/A
11	Non-Forested Wetlands, Marshland	0.030	N/A
12	Extractive (mining)	0.150	N/A
13	Other	0.100	N/A

[1]Manning's coefficient was taken to be isotropic, i.e., the same values were applied in the x- and the y-directions.

Table 3.4
Land Use Dependent ET Parameters[1]

Type	Land Use	Root Zone (feet)	Crop Coefficient											
			Jan	Feb	Mar	Apr	May	Jun	Jul	Aug	Sep	Oct	Nov	Dec
1	Low Density Urban, Recreational	2.0	0.55	0.44	0.44	0.66	0.88	0.99	0.92	0.79	0.72	0.72	0.72	0.72
2	Medium Density Urban, Institutional	1.5	0.55	0.33	0.33	0.55	0.66	0.66	0.66	0.66	0.55	0.55	0.55	0.55
3	High Density Urban, Industrial and Transportation	1.0	0.33	0.28	0.28	0.33	0.39	0.55	0.55	0.55	0.55	0.39	0.33	0.33
4	Cropland and Pasture	2.5	0.51	0.37	0.4	0.59	0.88	0.99	0.92	0.79	0.75	0.68	0.76	0.72
5	Row Crops	2.5	0.97	0.7	0.76	0.96	1.05	0.95	0.73	0.67	0.73	0.78	0.96	1.02
6	Tree Crops, Citrus	2.5	0.88	0.77	0.77	0.77	0.88	0.97	1.07	1.16	1.16	1.16	1.16	1.16
7	Shrubland	4	0.44	0.44	0.44	0.66	0.83	0.94	0.94	0.94	0.88	0.66	0.44	0.44
8	Upland Forest	6	0.55	0.55	0.55	0.72	0.88	0.94	0.94	0.94	0.88	0.77	0.66	0.66
9	Open Water	N/A	1.3	1.3	1.3	1.3	1.3	1.3	1.3	1.3	1.3	1.3	1.3	1.3
10	Forested Wetlands	3.5	0.96	0.96	0.96	1.08	1.15	1.2	1.2	1.15	1.15	1.03	0.96	0.96
11	Non-forested wetlands	2	1.1	1.1	1.1	1.1	1.1	1.1	1.1	1.1	1.1	1.1	1.1	1.1
12	Extractive	1.5	0.6	0.55	0.55	0.6	0.72	0.84	0.84	0.84	0.84	0.78	0.78	0.78
13	Other	2.5	0.73	0.66	0.67	0.78	0.89	0.95	0.94	0.91	0.9	0.84	0.8	0.8

[1]The methodology and data sources are presented in Section 2.2.2 and Appendix C of the PRIM Phase I report (HGL, 2009).

Table 3.5
Soil Hydraulic Properties[1]

Soil Series	Hydraulic Conductivity (ft/day)[2]	Porosity	Specific Yield[2]	Wilting Point	Field Capacity	Hydrologic Soil Group
Adamsville	26.08	0.45	0.11	0.04	0.09	C
Ancolte	26.08	0.44	0.11	0.07	0.13	D
Apopka	18.24	0.45	0.11	0.06	0.09	A
Arents	59.53	0.57	0.14	0.02	0.05	C
Basinger	15.87	0.44	0.11	0.05	0.10	B/D
Bradenton	14.30	0.44	0.11	0.07	0.14	B/D
Candler	48.38	0.44	0.11	0.03	0.06	A
Chobee	15.38	0.45	0.11	0.09	0.16	D
Felda	16.21	0.49	0.12	0.06	0.10	B/D
Floridana	20.94	0.45	0.11	0.07	0.12	D
Haplaquents/Clayey	0.02	0.57	0.14	0.15	0.20	D
Hydraquents/Clayey	0.02	0.57	0.14	0.15	0.20	D
Immokalee	20.20	0.45	0.11	0.05	0.11	B/D
Kaliga Muck	13.74	0.45	0.11	0.13	0.19	B/D
Myakka	21.19	0.42	0.10	0.04	0.08	B/D
Oldsmar	15.39	0.45	0.11	0.06	0.12	B/D
Ona	18.24	0.45	0.11	0.08	0.13	B/D
Pomello	38.27	0.45	0.11	0.04	0.08	C
Pomona	15.53	0.45	0.11	0.07	0.12	B/D
Samsula	26.08	0.44	0.11	0.08	0.12	B/D
Smyrna	18.26	0.42	0.10	0.05	0.09	B/D
Tavares	47.94	0.82	0.20	0.03	0.08	A
Wabasso	16.85	0.78	0.19	0.05	0.11	B/D
Wauchula	17.77	0.45	0.11	0.07	0.13	B/D
Zolfo	18.24	0.45	0.11	0.08	0.17	C

[1]Original data from the U.S. Department of Agriculture SSURGO soil database. http://www.ncgc.nrcs.usda.gov/products/datasets/ssurgo.
[2]These parameters were calibrated.

This page was intentionally left blank.

4.0 MODEL CALIBRATION AND VERIFICATION

During the calibration, model parameters were adjusted to match observed calibration targets within acceptable ranges. In this section, the calibration approach is first discussed to provide a framework for the calibration process. This is followed by the discussions of calibration targets and results.

4.1 CALIBRATION APPROACH

The general calibration approach for PRIM 2 is based on that of PRIM 1. Insights on the sensitivity of the model to various parameters gained in the PRIM 1 calibration enabled the calibration to be focused on a relatively parsimonious group of calibration parameters. This provided a number of advantages. First, it increased the efficiency of the calibration process. Second, and more important, it helped to ensure consistency of the calibration and made it easier to verify that the calibrated model remained physically plausible. The primary calibration parameters, by the main categories of calibration targets, were as detailed in sections 4.1.1 through 4.1.3.

4.1.1 Streamflows

- Channel leakance and Manning's roughness coefficients had strong effects on simulated streamflows. Channel bed leakances influenced the volume of simulated streamflow, and the Manning coefficient influenced height and duration of peak flow events. Higher values for Manning's coefficient in stream channels reduced simulated flow peaks and increased peak durations.
- Land surface rill heights were used to hold back surface runoff, thereby reducing the volume and magnitude of peak flows but increasing baseflow. Higher rill heights were used to approximate the effect of disconnected surface drainage, especially in reclaimed mine areas.
- ET was a dominant factor controlling streamflow in dry periods. Because plausible ranges of ET are well established (HGL, 2009; HGL, 2011), only relatively minor adjustments to ET parameters were made. For cells that had channels or lakes, the ET surface was set to the bottoms of the water bodies to ensure that all water was available for evaporation during dry periods.
- Land surface roughness coefficients and leakances were adjusted to calibrate streamflows. Surface roughness coefficients affected streamflow peaks, while surface leakance values affected streamflow volumes.

4.1.2 Lake Levels

- Lakebed leakances and leakances of underlying aquifers were adjusted to influence lake levels by increasing or decreasing lake-groundwater interactions.
- Elevations of hydraulic structures were adjusted within their reported operating range to control high water levels in lakes that have outflow control structures.

4.1.3 Groundwater Heads

- The groundwater (subsurface) components of the model were calibrated by adjusting transmissivities of aquifer units and vertical leakances between units. For the SA, specific yield was also adjusted.

4.2 CALIBRATION TARGETS AND GOALS

The model was calibrated against measurements of daily streamflows, monthly lake levels, and monthly groundwater levels.

The calibration targets included the following:

- 19 streamflow target locations,
- 89 lake level target locations,
- 42 groundwater head target locations in the SA,
- 28 groundwater head targets in the IAS, and
- 36 groundwater head targets in the UFA.

Multiple calibration metrics were used to evaluate the performance of the model calibration. The statistical metrics were as follows:

- Root mean square error (RMSE),
- Average error (AE),
- Mean absolute error (MAE)
- Maximum error (MxE) and minimum error (MnE),
- Coefficient of determination (R^2), and
- Nash-Sutcliffe efficiency coefficient (E).

Appendix A lists the formulae for calculating each of these metrics. In this report, residuals (calibration errors) are defined as simulated minus observed values.

The calibration statistics include both residuals between observed and simulated values and the overall correlation between observed and simulated values. The RMSE, AE, MAE, MxE, and MnE metrics measure the residuals in terms of average and maximum/minimum differences, whereas R^2 and E represent the overall correlation between observed and simulated quantities. Table 4.1 summarizes the primary calibration goals. These calibration goals were established in consultation with the SWFWMD and reflect experience from similar modeling projects regarding reasonable and attainable goals.

The degree of calibration cannot be fully deduced from statistical performance metrics alone. Graphical comparisons of observed values to simulated values are also important. Visual inspection of these graphical comparisons was useful in identifying overall spatial and temporal biases and provided a measure of the overall model performance. The visual evaluations included the following:

- Observed versus simulated flow exceedance curves,
- General groundwater flow directions,
- Semiannual USGS potentiometric maps for the UFA versus simulated head contours,
- Observed versus simulated cumulative stream discharge,
- General magnitudes of fluctuations in streamflow and groundwater levels, and
- Long-term temporal trend in streamflow and groundwater levels.

Calibration results for streamflow, lake levels, and groundwater levels are presented in the following sections.

4.3 STREAMFLOW CALIBRATION RESULTS

Locations of streamgages used in the model calibration are shown in Figure 4.1. Streamflow calibration results for selected streamgages on the Peace River and for the gages of principal sub-basins are discussed in this section. Table 4.2 presents a summary of the calibration statistics for these gages. The calibration goals for the various metrics are listed in parentheses. AE and RMSE are both listed as the actual values (units of cfs) and as a percentage of the difference between the highest and lowest observed streamflows. Detailed streamflow calibration results are provided in Appendix B.

4.3.1 Peace River Streamgages

The major streamgage stations along the Peace River are Bartow, Fort Meade, Zolfo Springs, and Arcadia in the order of upstream to downstream. The Arcadia station is the last major gage station of the river. It is regarded as the streamflow control point for the whole basin, except for the Horse Creek and Joshua sub-basins, as these tributaries join the Peace River downstream of the Arcadia station.

Streamflow calibration results are presented graphically in three types of plots in the ensuing subsections: annual streamflow bar charts, streamflow hydrographs, and flow exceedance curves. These types of plots are useful for visual inspections in terms of overall matching, magnitudes of fluctuations, and long-term temporal trends. For further statistical and detailed measures of calibration results, tables of calibration statistics, and flow percentiles are also presented.

4.3.1.1 Peace River at Bartow

Streamflow results for the Bartow gage are presented in Figures 4.2 through 4.4. Figure 4.2 shows observed and simulated annual flows; Figure 4.3 shows the streamflow hydrographs. Figures 4.3a and 4.3b show the same data but using a linear versus a logarithmic streamflow axis. The use of a logarithmic scale in Figure 4.3b highlights low flow events. Figure 4.4 compares observed and simulated streamflow exceedance plots. Note that annual flows (Figure 4.2) are shown in inches. They represent the cumulative flow amount divided by the gage drainage area to facilitate comparison of flows among gages. Streamflow hydrographs (Figures 4.3 and 4.4) depict flows in units of cfs.

The streamflow results for the Bartow gage presented in these figures show a number of general patterns that were also exhibited in the streamflow results for the other gages:

- Simulated streamflows generally agreed well with observed flows with a tendency to overpredict flows in most years (Figure 4.2);
- Over the entire simulation period of 2003-2018, the model closely matched the total observed streamflow, as illustrated in Figure 4.3a; and
- The model overpredicted peak flow events around 2006, as is evident for the departure of the simulated cumulative flow curve from the observed cumulative flow curve (Figure 4.3a). The difference between the two curves appears to be relatively unchanged from 2007 to 2018.

The streamflow exceedance plots presented in Figure 4.4 show good agreement between the model and observed streamflows, except for flows less than 9 cfs, where the model simulated higher flows than observed.

Calibration statistics for the Bartow gage, along with those of the other streamflow gages discussed in this section, are presented in Table 4.2. The calibrated PRIM model met the calibration goal for AE, R^2 and the Nash-Sutcliffe E-statistic. The model also met the RMSE goal of no more than 5% of the difference between maximum and minimum flows.

Observed and simulated 10^{th}, $50^{th,}$ and 90^{th} flow percentiles for the Bartow gage, along with the Fort Meade, Zolfo, and Arcadia gages, are summarized in Table 4.3. These percentiles were calculated over the 16-year model calibration period, from 2003 through 2018. In comparing the tabulated flow percentiles with the flow exceedance plots for each gage, it should be kept in mind that the flow exceedance graphs display the probability that a given flow rate is exceeded. In other words, the 10^{th} percentile flow is exceeded 90% of the time; in the exceedance plots, the flow rates at each gage are ordered from high (never exceeded) to low (exceeded 100% of the time).

Table 4.3 indicates that the 10^{th} and the 50^{th} percentile flows were overpredicted by the model at all gages. The 90^{th} percentile flows were also overpredicted at most gages except at Arcadia. The absolute magnitude of the differences between observed and simulated flows is clearly the most significant at the 10^{th} percentile flows and reflects the consistent overprediction of low flow events.

4.3.1.2 Peace River at Fort Meade

Simulated annual streamflows at Fort Meade (Figure 4.5) were generally in good agreement with observed flow. Likewise, the streamflow hydrographs (Figures 4.6a,b) show good agreement between simulated and observed flow, with an R^2 value of 0.80 and an E value of 0.77. The RMSE was 171 cfs (6.99%) and did not meet the RMSE goal of no more than 5% of the difference between maximum and minimum flows.

Over the entire simulation period, the model overpredicted streamflow as shown by the cumulative hydrograph plot of Figure 4.6a. Similar to the results for Bartow, this was primarily a result of overpredicted streamflows in wet periods before year 2007. In the years 2007 to 2018, simulated and observed cumulative flows were similar in trend with an almost constant difference as a result

of overpredicted high flows in 2003 and 2006. Low flows during the dry period of 2007 and 2013 were accurately simulated, although the model tended to overpredict peak flows in the period 2006 to 2018.

Figure 4.7 shows the flow exceedance plots for the Fort Meade gage. The model overpredicted flows between the 30th (50 cfs) to 1st (0.01 cfs) percentile range. At other percentiles, the simulated exceedance curve follows the observed curve well. Figure 4.6b indicates that during very dry conditions, as occurred during 2007 to 2013, the model performs quite well and slightly overpredicts the very lowest flows (note the logarithmic scale in Figure 4.6b accentuates very low flows).

4.3.1.3 Peace River at Zolfo

Streamflow results for the Peace River at Zolfo are presented in Figures 4.8 through 4.10 and Table 4.3. The annual cumulative streamflow plots for Zolfo show similar patterns as the results for Bartow and Fort Meade except that the overprediction of streamflows is less pronounced. The model overpredicted annual flows in 2004 through 2006 and 2018. Except for these peak flow events, the observed and simulated hydrographs were in good agreement, with an R^2 value of 0.82 and an E value of 0.82.

The simulated low flows followed the observed flows closely (Figures 4.9a,b), which is also reflected in the exceedance plot (Figure 4.10). In addition to deviations for extreme flow events, the flow exceedance plots show some slight overpredictions between the 30th and the 1st percentile range of flow frequencies, which represents flows between 8 cfs and 100 cfs.

Comparison of the streamflows at Zolfo against those of the contributing upstreamgages Fort Meade and Payne Creek at Bowling Green, indicates that the annual flows at Zolfo are controlled by surface water flows in wet years, but that the contribution from groundwater (baseflow) is more important in drier years. In 2005, a wet year, the flows at Fort Meade and Payne Creek at Bowling Green accounted for 76% of the annual flow at Zolfo, but only for 59% in 2007, which was a dry year. It is plausible that the contributions from other tributaries, such as Whidden Creek and Bowlegs Creek, follow the same pattern. The corollary is that the accuracy of simulated streamflows depends more strongly on the accuracy of the groundwater simulation, especially of the SA, in dry periods than in wet years. For 2010 and 2011 (two dry years), simulated annual streamflow matched observed annual streamflow quite closely (Figure 4.8). This indicates that GW-SW interactions were reproduced properly for this region.

4.3.1.4 Peace River at Arcadia

Streamflow results for the Peace River at Arcadia are presented in Figures 4.11 through 4.13, while flow exceedance percentiles are listed in Table 4.3. The pattern of observed and simulated annual flows is similar to that of the previously discussed gages. However, at this gage, except for years 2004 through 2006, the model underpredicted annual flows. The sub-basins contributing to flows at Peace at Arcadia are Peace at Zolfo and Charlie Creek. These sub-basins represent 60 percent and 24 percent, respectively, of the control area of the Peace at Arcadia gage. Streamflow patterns at these gages, therefore, exert significant influence on the streamflow behavior at the Arcadia gage.

The hydrograph plot for the Arcadia gage (Figures 4.12a and b) of observed and simulated flows shows an R^2 value of 0.77 and an E value of 0.76. The flow exceedance plots in Figure 4.13 indicate that the simulated and observed flow percentiles agree reasonably well at all percentiles. The gradual departure of the simulated cumulative flow curve from the observed is likely due to the slight overall underprediction of flow by the model. The effects of underprediction are evident in the underprediction of the simulated cumulative hydrograph in the figures.

4.3.2 Tributary Sub-Basin Streamflow Results

This section presents calibration results for the primary tributary sub-basins of the Peace River: Saddle Creek, Peace Creek, Payne Creek, Charlie Creek, Horse Creek, and Joshua Creek. A detailed discussion of the hydrologic characteristics of the Saddle Creek sub-basin have been documented in HGL (2008), and HGL (2011).

4.3.2.1 Saddle Creek at P-11

Streamflow calibration results for the P-11 gage are presented in Figures 4.14 through 4.16 and Tables 4.2 and 4.4. All calibration criteria were met. The portion of the model was found to be difficult to calibrate. The difficulty in calibrating this portion of the model was due to several factors. The streamflow behavior at this gage is controlled by the presence of Lake Hancock and the P-11 outflow control structure. The P-11 structure is a weir structure with a crest elevation of 97.6 feet (1988 NAVD). The structure has two radial gates, which can be manually opened or closed to regulate the outflow of water from Lake Hancock. The P-11 operation summary states that one gate is opened clear of the water when the Lake Hancock water level is above the maximum desirable water level. Conversely at low water levels, the gates are closed, except that one gate may be opened slightly to provide water downstream for cattle. The elevation of the crest of the weir was raised from 97.6 feet to 99.1 feet (1988 NAVD) in June 2015. Because all the hydraulic structures in the model are static, change in the P-11 structure configuration resulted in separating the model run into two separate runs: pre-elevation change and post elevation change. Observed historical discharge through the P-11 structure from 2003 to 2018 is shown in Appendix F.

Downstream from the P-11 structure, there is a wetland that receives water pumped from Lake Hancock. The water from Lake Hancock passes through the wetland. As the water traverses the wetland, a portion of water is lost through ET and groundwater recharge. The remaining amount of water is discharged to a channel downstream of P-11. Pumping from Lake Hancock occurred from January 2016 to December 2018. During the same period, water was released from the wetland to a channel downstream from P-11. Observed historical pumping from Lake Hancock and discharge from the wetland from 2003 to 2018 are shown in Appendix F.

To bypass the static limitation of P-11 (gate operation), an attempt was made to pump water from Lake Hancock to be released downstream of P-11 in order to mimic the gate operation. Such an attempt resulted in numerical divergence and was aborted. The adopted solution was to inject an amount of water equal to the difference between discharge from P-11 and observed discharge downstream of P-11 to simulate the total observed discharge from P-11.

An inspection of Figures 4.15a and 4.15b indicates that observed peak flows were very well matched; however, the model tended to slightly overestimate a few low flow episodes, perhaps due to the model's tendency to maintain minimum flow within streams. This observation is reflected by the slight overprediction of cumulative flow. The low flow overestimation did not impact the favorable agreement between observed and simulated discharge distributions in Figure 4.16. The observed and simulated 10^{th}, 50^{th}, and 90^{th} percentile flows for the P-11 gage are summarized in Table 4.4. As shown in the table, the differences between the observed and simulated flows at this gage are very small compared with the differences at other gages.

4.3.2.2 Peace Creek Canal Near Wahneta

Calibration results for the Wahneta streamgage are presented in Figures 4.17 through 4.19 and Tables 4.2 and 4.4. The Peace Creek Canal near Wahneta and P-11 are the contributing gages to Peace at Bartow. The Wahneta gage, however, is the control point for only about two-thirds of the Peace Creek sub-basin. It receives flow primarily from the northern part of the sub-basins, including the northern Winter Haven Chain of Lakes, which drains into the Peace Creek Canal at Lake Hamilton. The southern chain of lakes drain into the Wahneta Farms drainage canal via Lake Lulu. The Wahneta Farms drainage canal flows into the Peace Creek Canal downstream of the Wahneta gage. Discharge from Lake Garfield also flows into the Peace Creek Canal downstream of the Wahneta gage. These discharges are ungaged but do contribute to flow at Bartow. As discussed in HGL (2009), and HGL (2011), streamflow from the Peace Creek sub-basin accounts for most of the flow at the Bartow gage in dry years, with relatively little contribution from Saddle Creek, but in wet years Saddle Creek contributes a greater proportion of the flow.

In the Peace Creek sub-basin, low rainfall quantities, combined with relatively high groundwater recharge, resulted in a significant underprediction of observed streamflow at the Wahneta gage during initial model calibration runs of PRIM 2. Attempts to match observed streamflows required adjustments of land surface leakance and a Manning's roughness coefficient to values equivalent to simulating all of the Peace Creek sub-basin as having a low permeability and smooth land surface. This has the effect of increasing runoff for a given rainfall amount but was deemed not physically plausible for the entire sub-basin. To remedy this situation, the NEXRAD daily rainfall values for all model grid cells within Peace Creek were replaced by the gage data. As shown in Figures 3.13 and 3.14, the NEXRAD and gage data at Winter Haven (a gage in the sub-basin) are very similar; however, greater peak rainfalls are associated with the gage data. The use of gage data resulted in higher discharge from the sub-basin. A similar situation was found during the PRIM 1 calibration.

The PRIM model consistently underpredicted annual streamflows at the Wahneta gage in most years, except 2005, 2006, and 2007. The cumulative streamflow hydrograph shown in Figure 4.18a shows that cumulative streamflow in the model remained consistently lower than observed flows for the whole model period. The discrepancy increases during 2009 and 2018.

The occurrence of a streamflow deficit at the Wahneta gage, which occurred with the original NEXRAD data (see Section 3.4.1), is a consequence of the high effective leakance to the UFA in the upper part of the Peace River basin, which includes Peace Creek. This reflects the relatively unconfined nature of the UFA in this area and leads to a greater proportion of rainfall contributing to groundwater recharge rather than generating streamflow. A better match of observed

streamflows at the Wahneta gage could have been achieved by adjusting the effective leakance between the SA and UFA, but it was judged that a higher leakance, consistent with values used in the neighboring Saddle Creek sub-basin, were more physically defensible.

Flows from and between the lakes in the Winter Haven Chain of Lakes are regulated by a number of hydraulic control structures HGL (2009). The operational history of these structures is not well documented, but they are operated on the general principle that outflows are reduced in dry periods in order to maintain lake levels, and outflows are increased during, or in anticipation of, wet periods. In the model, all structures were simulated as static structures, with outflow levels set to their target operating levels, with some adjustment made during the calibration process to better match observed lake levels. The simplifications in the handling of control structures in the model are probably a contributing factor to the discrepancies between observed and simulated flows at the Wahneta gage, as it is at the Saddle Creek at P-11 gage.

Low and medium flows were captured reasonably well for the Wahneta gage. It is important to have good controls on low flows at this gage, as it affects the low flows at Bartow station significantly. The flow exceedance curves in Figure 4.19 show good agreement between observed and simulated results, except for a small discrepancy above the 75th percentile. Although the model underpredicted flows at the Wahneta gage, the calibrated model met the calibration goals, except for the relatively high (7%) error in the RMSE percentage metric (Table 4.2). The underprediction of high flows accentuates this metric because differences between observed and simulated flows are squared in the RMSE.

4.3.2.3 Payne Creek at Bowling Green

Streamflow results for the Payne Creek at Bowling Green gage are presented in Figures 4.20 through 4.22 and Tables 4.2 and 4.4. The model met all calibration goals at this gage, except for E, which is 0.33 as shown in Table 4.2. Figure 4.20 shows that the model generally overpredicted annual flows in high-flow years with the maximum discrepancy in 2018, while it closely matched observed annual flows for low-flow years. Figures 4.21a, and 4.21b show that the model reasonably captured the high-flow and low-flow events. The model did under-predict a small number of extremely high flow events in 2005, 2015, and 2017, but slightly overpredicted the rest of high flows. Table 4.4 shows that 90th percentile flows were overestimated by about 8.5%, whereas the model underpredicted high flows for all other tributary gages. The flow exceedance plot (Figure 4.22) shows a close agreement between the observed and simulated percentile exceedance curves.

4.3.2.4 Charlie Creek at Gardner

Streamflow results for the Gardner gage, which measures streamflows from the Charlie Creek sub-basin, are presented in Figures 4.23 through 4.25 and Tables 4.2 and 4.4. Calibration goals of AE and RMSE were met at this gage. R^2 was 0.56, slightly less than the goal of 0.60 or greater. Notably, E was 0.50, which is at the goal of 0.50. The simulated annual streamflows (Figure 4.23) showed a deficit compared to observed flows for most of the years in the project period except 2006. Over the entire period, the model has a significant deficit in cumulative streamflows (Figure 4.24a). This figure shows that the model underpredicted the magnitude of most major streamflow events. Peak flow at the Gardner gage occurred in 2017, producing flows in excess of 9,000 cfs.

In contrast, the highest simulated flows did not exceed 5,000 cfs. The underprediction of streamflows in Charlie Creek could be related to low rainfall estimates derived from NEXRAD data; however, no adjustments were made for Charlie Creek. Figure 4.24b shows that the model accurately simulated low flows in the period 2003 to 2018 but tended to under-predict extreme low flows. The flow exceedance curves in Figure 4.25 show that the model underpredicted flows above 100 cfs, and flows of 5 cfs or less. For intermediate flows, the simulated exceedance curve is in good agreement with the observed curve.

4.3.2.5 Horse Creek at Arcadia

Streamflow results for the Horse Creek at Arcadia gage are presented in Figures 4.26 through 4.28 and Tables 4.2 and 4.4. The model met all calibration goals at this gage except PBIAS, which is 43.3%, above the goal of 25%. The PRIM model overpredicted annual streamflows during 2003 and 2005, but underpredicted flows during the other years. The same observation is true in Figures 4.27a, and 4.27b. The model had an excess in cumulative flow from 2003 to 2012 and had a deficit in cumulative flow from 2012 to 2018. The excess in cumulative flow is partially due to lack of observed data from January to September 2003. The extreme high flow event in June 2003, observed in upstream gages in the Horse Creek, exacerbated the difference in cumulative flow. Figure 4.28 shows the model underpredicted at all percentiles. The underprediction of streamflows in Horse Creek could be related to low rainfall estimates derived from NEXRAD data; however, no adjustments were made for Horse Creek.

4.3.2.6 Joshua Creek at Nocatee

Streamflow results for the Joshua Creek at Nocatee gage are presented in Figures 4.29 through 4.31 and Tables 4.2 and 4.4. Calibration goals of AE and RMSE were met at this gage. R^2 was 0.52, slightly less than the goal of 0.60 or greater. E was 0.51, which is above the goal of 0.50. PBIAS was 26.91%, slightly higher than the goal of 25%. RMSE was 0.70, at the goal of 0.70. The pattern of annual streamflows was similar to that of Horse Creek: the model underpredicted annual streamflows in the years 2003 to 2018, except in 2006 during which the model overpredicted the annual flow.

Figures 4.30a and 4.30b show that the PRIM model tended to under-predict low flows throughout the modeling period. The flow exceedance plot (Figure 4.31) and streamflow percentiles (Table 4.4) for Joshua Creek illustrate the high baseflow behavior: streamflows are above 10 cfs more than 95% of the time. The simulated flow exceedance curve agrees well with the observed curve except for small differences under very low flow conditions, and underprediction of flow frequencies in the range of 100-300 cfs. The latter is especially evident in the comparison of observed and simulated 90th percentile flows. The model underpredicted observed flows by 52%. Due to the logarithmic scale in Figure 4.31, this discrepancy does not appear very pronounced in the flow exceedance plot, but the relative error in simulated 90th percentile flows was significant at the Joshua Creek gage.

4.4 LAKE CALIBRATION RESULTS

The PRIM model calibration included 89 lake level targets located in the Saddle Creek and Peace Creek sub-basins. The statistical metrics used for calibration were R^2, AE, and MxE and MnE.

Detailed lake calibration results are provided in Appendix C. A summary of the calibration results for R^2, RMSE, and AE is provided in Table 4.5.The R^2 was greater or equal to 0.7, the desired lower limit for lakes, for 33% (29 out of 89) of the lakes. Similarly, the RMSE was less than 2 feet for better than 60% (53 of 89) of the lakes. The AE was between -2 and +2 feet for better than 72% of the lakes. In general, the model performed reasonably well considering the absence of bathymetry data for many of the lakes and the lack of information on structure operations for lakes with hydraulic control structures.

Most of the PRIM 1 calibration effort was focused on a subset of the 89 lakes: 9 in Saddle Creek and 12 in Peace Creek. Early in the calibration effort it was found that the lake level calibration would typically involve adjustment to the lake storage (depth-area relation) and lakebed leakances on a lake-by-lake basis. The adjustment of parameters for individual lakes required considerable effort but had little impact on improving the streamflow predictions of the model. For PRIM 2, the calibration focused on 11 Minimum Flows and Water Levels (MFL) lakes. Five of the MFL lakes were part of the PRIM 1-focused lakes. The locations of these target lakes are shown in Figure 4.32. This figure includes the AE in the simulated lake levels of the calibrated PRIM model.

Observed and simulated lake level plots are shown in Figure 4.33 for 11 MFL lakes. The figure shows that the simulated trends in lake levels were generally consistent with observed data, and likewise simulated lake level fluctuations agreed with observed data in magnitude and timing. Lake levels were found to be sensitive to groundwater potentiometric levels, especially during the low-rainfall periods. During the lake calibration, lakebed leakances and vertical leakances between the SA and IAS in the lake vicinity were adjusted. Most of the MFL lakes, shown in Figure 4.34, met all or most of the calibration criteria. However, the deviation from the observed data was thought to be affected by the local NEXRAD data and by the resolution of lake storage information. Moreover, lake elevations of these lakes were found to be sensitive to leakance changes in the SA, which could also affect streamflows. The current lake properties were a compromise between the calibration of groundwater heads, streamflows, and lakes.

Most of the lakes in the Peace River basin have Karst origin and can represent zones of high groundwater recharge. During the calibration process the leakance of lakes was adjusted to match observed lake levels. Many of the lakes exhibited a drop in lake levels during the 2006 to 2012 low-rainfall period. During this period, inflows to lakes were reduced, and lake levels in the model were controlled primarily by evaporation and leakance losses (recharge to groundwater).

4.5 GROUNDWATER CALIBRATION RESULTS

The groundwater calibration involved 42 targets in the SA, 28 targets in the IAS, and 36 targets in the UFA. The locations of these targets are shown in Figures 4.35, 4.36, and 4.37, respectively. Tables 4.6a and 4.6b provide a summary of the groundwater calibration statistics. Detailed results for the groundwater transient calibration of each individual target wells are provided in Appendix D.

Table 4.6a presents separate statistics for the 2003-2018 average heads in the SA, the IAS, and the UFA. The R^2 criterion was set to be greater than 0.8, 0.7, and 0.6 for the SA, the IAS, and the UFA, respectively. R^2s as shown in Table 4.6 are all greater than 0.95. The RMSEs for all aquifers varied between 3.75 feet to 4.71 feet, all below 5 feet or 3.33 percent of the head variation within

the model area (approximately 150 feet). The AE varied between 0.34 feet for the UFA wells and -1.47 feet for the IAS wells. The numbers of wells within 2.5 feet in the calibrated PRIM model are all above 50 percent: 64%, 61%, and 61% for the SA, the IAS, and the UFA, respectively. The numbers of wells within 5 feet in the calibrated PRIM model are all above 80 percent: 86%, 82%, and 81% for the SA, the IAS, and the UFA, respectively. As shown in Table 4.6a, metrics are within the criteria, except for the AE of the IAS wells, and the Max Error of the SA and UFA. There is one well in the SA with the residual greater than 10 ft (21.71 ft). This well is in the mining area and is adjacent to a well where the residual is very small (2.57 ft). It is believed that the residual disparity is due the small-scale local heterogeneity. The Max Error in the UFA is at the well in the vicinity of the SA well with large Max Error. This well is the only well in the UFA where the maximum error exceeds 10 ft (11.28 ft). Between the three aquifers, the IAS in the model area has the least amount of information. The deviation in the IAS could also stem from the discretization disparity between PRIM 2 and the ECFTX model. The IAS boundary heads of PRIM 2 were extracted from the ECFTX model, which has one layer (layer 2) representing the IAS/Intermediate Confining Unit, whereas the IAS in PRIM 2 was simulated using two layers. The accuracy of the IAS may be improved in the future with additional information and vertical refinement of the ECFTX model.

Table 4.6b shows separate statistics for transient heads in individual wells from 2003 to 2018 in the SA, the IAS, and the UFA. The R^2 criterion was met by 7%, 61%, and 94% of the wells in the SA, the IAS, and UFA, respectively. The RMSE criterion was met by 83%, 75%, and 83% of the wells in the SA, the IAS, and UFA, respectively. The AE criterion was met by 24%, 25%, and 30% of the wells in the SA, the IAS, and UFA, respectively. The MAE first criterion (less than 2.5 feet) was met by 62%, 36%, and 33% of the wells in the SA, the IAS, and UFA, respectively, whereas the second criterion (less than 5 feet) was met by 83%, 79%, and 83% of the wells in the SA, the IAS, and UFA, respectively. The E criterion was met by 71%, 79%, and 94% of the wells in the SA, the IAS, and UFA, respectively. Based on the E values, it could be inferred that the simulated heads tracked the observed reasonably well in time. This inference may be confirmed by the reasonably high percentage of number of wells with R^2 above 0.60, as well as high percentage of wells with reasonable values of AE, MAE, and RMSE.

Another visual check on the model simulated heads is provided by the comparison against USGS-generated potentiometric surface maps for the UFA. The USGS generates these maps on a biannual basis, for May and September, which represent the seasonal low and high head conditions, respectively. For model evaluation purposes, these comparisons were made for September 2005 (Figure 4.38) and May 2007 (Figure 4.39), representing high potentiometric head and low head conditions, respectively, and for September 2014 (Figure 4.40), representing the mean potentiometric head conditions for the model period.

The September 2005 and September 2014 USGS potentiometric surface maps show similar head contours, although the 2007 potentiometric heads are 5 to10 feet higher in the middle and lower parts of the basin compared to the 2005 potentiometric map. The model simulated heads for September 2005 and September 2014 are very similar to each other, with the most obvious difference between the 50-foot head contour in the area between Joshua Creek and Charlie Creek, where the 2002 simulated potentiometric map shows higher head values compared to the 1998 map.

The May 2007 map shows, as expected, consistently lower head values than the 2005 and 2014 maps. May represents the seasonally low head condition, and 2007 was a dry year. The head values in the extreme northern portion of the basin were still around 120 feet. The head value along the southern boundary of Saddle Creek and Peace Creek is around 60 to70 feet, whereas it was 80 to 90 feet in September 2005 and 2014. The lowest head values underneath the western boundary of Horse Creek are 30 feet or more below the September 2005 and 2014 values. Overall, the PRIM model shows the same general head patterns as the USGS potentiometric maps. The calibrated PRIM head results were judged to be in reasonably good agreement with the USGS potentiometric maps.

The final visual comparisons presented in Figures 4.41 through 4.43 illustrate the PRIM groundwater calibration. These figures compare head plots for different aquifer units in multilevel monitoring wells. Figure 4.41 shows the observed and simulated head profiles in model Layer 2 (IAS-PZ2), Layer 3 (IAS-PZ3), Layer 4 (UFA-UPZ), and Layer 5 (UFA-LPZ) at the ROMP 45 well group near Fort Meade. Figure 4.42 shows the head profiles in Layer 1 (SA), Layer 3 (IAS-PZ3), and Layer 5 (UFA-LPZ) at ROMP 30 near Zolfo Springs, and Figure 4.43 shows the head profiles in Layer 1 (SA), Layer 2 (IAS-PZ2), Layer 3 (IAS-PZ3), and Layer 5 (UFA-LPZ) at ROMP 26 near Arcadia. Visually, the model-simulated heads track the observed heads better in the IAS and UFA than in the SA. This is consistent with the high R^2 calibration statistics. The model tracks the seasonal and pumping-induced head changes in the IAS and UFA very well but tends to under-predict the observed magnitude of head variations, especially with regard to the extremely low head values.

4.6 CALIBRATED MODEL PARAMETERS

The approach and identification of which parameters were adjusted in calibrating the integrated PRIM model have been discussed in Section 4.1. Values of calibrated soil, land use, and ET parameters are presented in Section 3.0. This section presents calibrated values of the OLF and subsurface layer leakances that affect SW–GW interactions, and of the aquifer transmissivities that affect groundwater head distributions.

4.6.1 OLF Leakance

Figure 4.44 shows the spatial distribution of calibrated leakance values. The blanked-out areas within the model boundaries represent areas where OLF cells were set as inactive to represent phosphate mining areas. As discussed in Section 3.0, initial leakance values were set based on soil type and land use conditions. The values were adjusted as part of the streamflow calibration. Low leakance values promote surface runoff and a rapid streamflow response during rainfall events. High OLF leakance values promote infiltration of rainfall into the soil and reduce the streamflow response to rainfall events.

OLF leakance values in most of the model were in the range of 0.01 to 15.0 d^{-1}. Low leakances (approximately 10^{-3} d^{-1} or lower) are associated with low permeability land surfaces including urban areas, and also CSAs in mining areas. High leakance values were associated with sand tailings in mining areas and locations of Karst features along the Peace River. OLF leakances were locally adjusted to achieve better calibration of lake levels. This adjustment was applicable to the larger lakes, the bathymetry of which was represented as depressions in the land surface, compared

to the majority of the lakes that were represented via depth-storage relationships without explicitly adjusting the OLF surface elevation. Figure 4.44 shows that these local lake adjustments generally kept the OLF leakances in the 0.01-15.0 d^{-1} range.

4.6.2 SA Hydraulic Conductivity and Leakance

Hydraulic conductivity (K) and leakance of the SA are presented in Figures 4.45 and 4.46, respectively. The leakance represents the vertical leakance between subsurface Layer 1 (SA) and Layer 2 (PZ2 of the IAS). Areas that have been impacted by mining in the Upper Peace river basin show the most contrast in hydraulic conductivity, with high and low K values occurring in proximity to one another. High K values are associated with areas of mine tailings and other reworked soils; low K values are associated with CSAs. Vertical leakance values are highest in the northern part of the basin, consistent with the more nearly unconfined nature of the IAS in this part of the basin and in the Lake Wales Ridge area along the eastern boundary of Charlie Creek.

4.6.3 IAS Transmissivity and Leakance

Transmissivity and leakance maps for the IAS are presented in Figures 4.47 and 4.48, respectively. The transmissivity is a combined transmissivity for PZ2 and PZ3 of the IAS (Layers 2 and 3 of the PRIM model). The transmissivity map shows values ranging from less than 100 ft^2/day in the northern part of the basin to values around 8,000 ft^2/day. The figure shows increasing transmissivity towards the south, which is consistent with the greater thickness of the IAS in the southern part of the basin. The vertical leakance of the IAS decreases in a southward direction, reflecting the greater confinement of the aquifers in this direction.

4.6.4 UFA Transmissivity and Leakance

Figure 4.49 shows the transmissivity distribution in the UFA (Layers 4 and 5 combined) in the calibrated PRIM 2 model. The pattern is similar to that of the PRIM 1 model with high transmissivity zones near the southern tip and the western portion of the Zolfo Springs watershed.

Figure 4.50 shows the effective vertical leakance between Layers 1 and 4 of the PRIM 2 model or the effective leakance between the SA and the UFA. In the upper portion of the Peace River basin, especially in the Peace Creek and Saddle Creek Sub-Basins, the leakance is an order of magnitude greater than that in the southern part of the Peace River Basin, consistent with the general conceptual model.

4.7 WATER BUDGETS

Water budgets, representing the inflow and outflow of water across the model boundaries, along with storage changes within the model, provide a useful way to assess overall performance of the PRIM model. A key requirement for model accuracy is a small mass balance error signifying that storage changes in the model are equal to the difference between total inflows and outflows. In addition, the magnitude of various water budget terms is a concise way to assess that the calibrated model is physically plausible.

This section presents simulated water budgets for the calibrated PRIM 2 model and compares the water budget results against other water budget analyses of the Peace River basin. Table 4.7

presents annual water budgets for the PRIM model. Sub-basin water budgets are provided in Appendix E.

The annual water budgets in Table 4.7 include the primary inflow and primary outflow components, as well as the storage gain/loss on a year-by-year basis. Groundwater pumping appears both as an inflow and as an outflow. This reflects that the model treats groundwater pumping as essentially a transfer of water from the subsurface to the surface. The return flow on the inflow side of the water budget reflects the addition of extracted groundwater to the OLF domain of the model as return flows. Groundwater pumping on the outflow side of the water budget is the removal of water from the subsurface domain of the model. The injection represents the injection downstream from P-11 structure described in Section 4.3.2.1, where the pumping from the Lake Hancock component of the outflows is also discussed.

The Lateral GW Inflow and Outflow terms in the water budget represent groundwater flows in the IAS and UFA across the lateral subsurface boundaries of the model. SW Outflow represents the Peace River discharge at the outlet boundary of the model, such as at the location of the Arcadia gage. The water budget table also provides total inflows and total outflows. Note that to facilitate comparison, the storage gains are included with Total Outflows. As shown in Table 4.7, the total inflows and outflows are in close agreement, with an average mass balance error in the annual water budgets in general of less than 0.5%. The annual storage gains show positive values in very wet years, such as 2004 and 2005, and negative values (losses) in very dry years, such as 2006 and 2007. This pattern is true for most sub-basins (Appendix E). The net storage loss during these years is probably related to the fact that high rainfall occurred only in the first part of the year, while the second half was dry, resulting in a net loss of the storage that had been built up prior. The table also shows that the net storage gain over the entire 2003 to 2018 period was very small.

An inspection of Tables E.1 to E.6 in Appendix E indicates that sub-basin precipitation patterns are generally similar but not identical. The same is true for their patterns of pumping, evapotranspiration, and storage gain. These sub-basins communicate with adjacent sub-basins through inflows and outflows. As in the case of the entire basin, the tables in Appendix E also show that the net storage gains for sub-basins over the entire 2003 to 2018 period were very small.

FIGURES

This page was intentionally left blank.

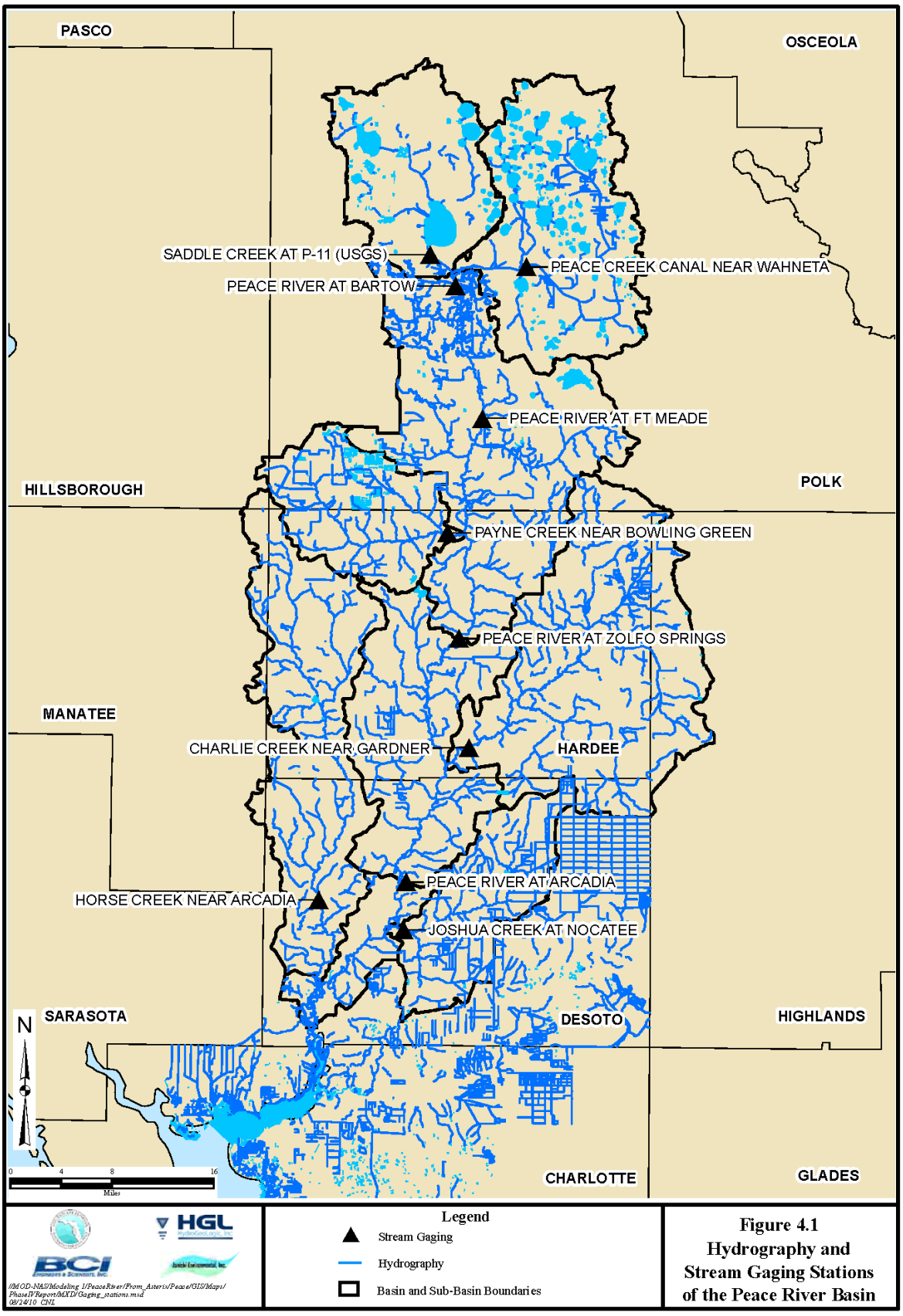
PASCO
OSCEOLA
SADDLE CREEK AT P-11 (USGS)
PEACE CREEK CANAL NEAR WAHNETA
PEACE RIVER AT BARTOW
PEACE RIVER AT FT MEADE
HILLSBOROUGH
POLK
PAYNE CREEK NEAR BOWLING GREEN
PEACE RIVER AT ZOLFO SPRINGS
MANATEE
CHARLIE CREEK NEAR GARDNER
HARDEE
PEACE RIVER AT ARCADIA
HORSE CREEK NEAR ARCADIA
JOSHUA CREEK AT NOCATEE
N
SARASOTA
DESOTO
HIGHLANDS
0 4 8 16
Miles
CHARLOTTE
GLADES
HGL
BCI
Legend
Stream Gaging
Hydrography
Basin and Sub-Basin Boundaries
Figure 4.1
Hydrography and
Stream Gaging Stations
of the Peace River Basin

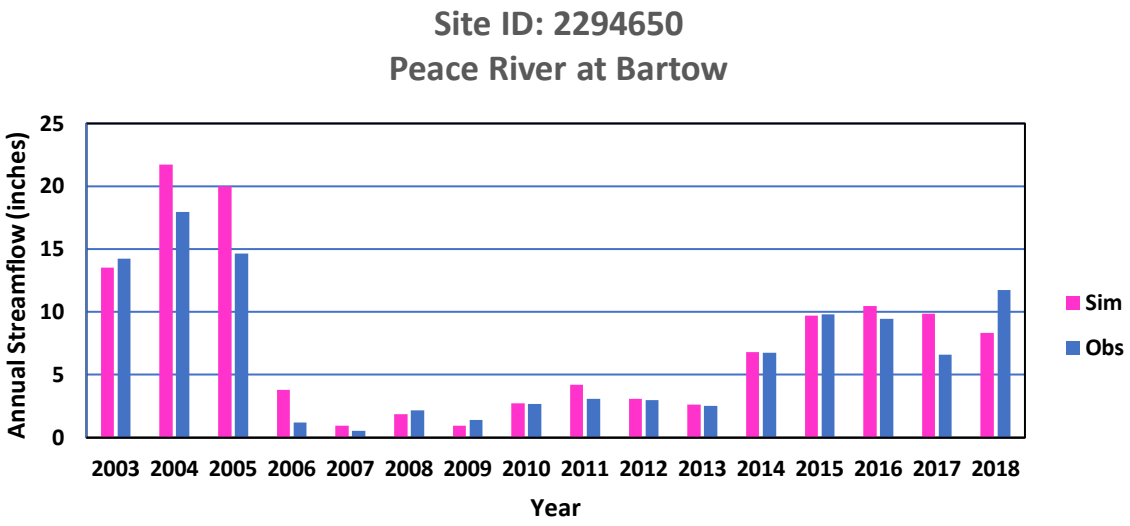

Figure 4.2 Observed vs. Simulated Annual Streamflows (Peace River at Bartow)

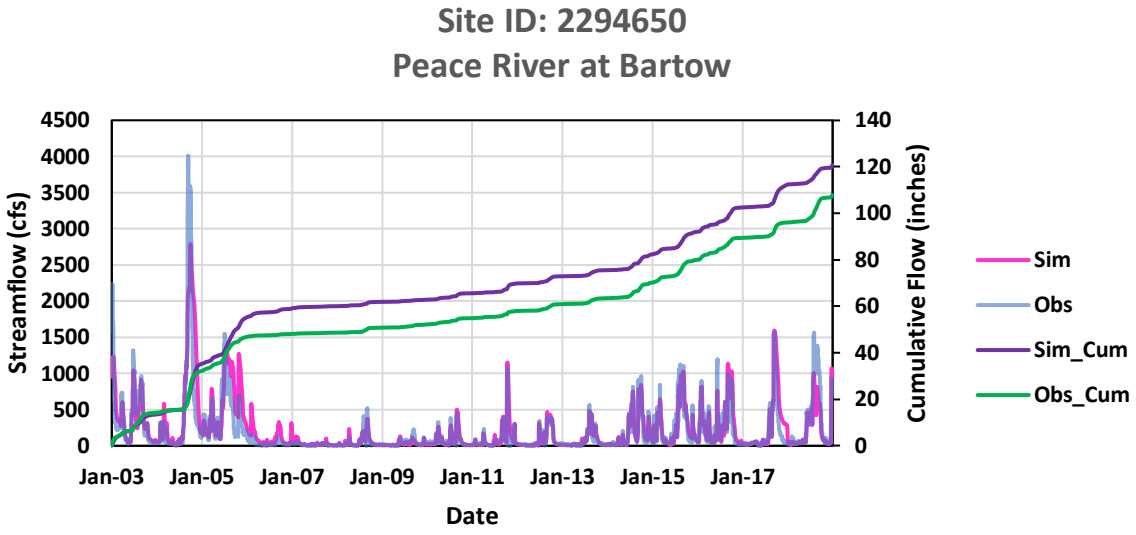

(a)

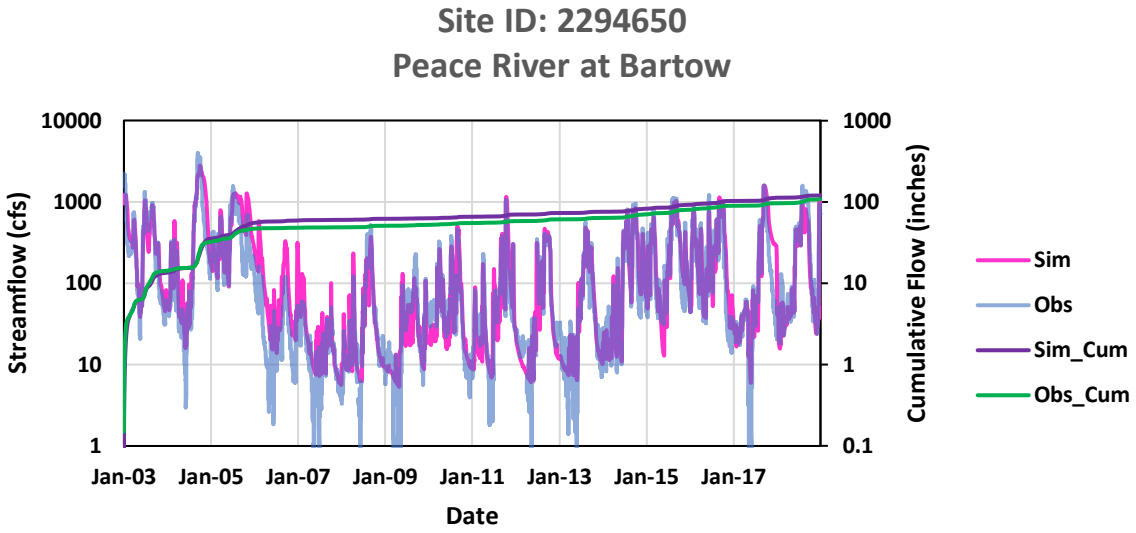

(b)

Figure 4.3 Observed vs. Simulated Streamflow Hydrographs (Peace River at Bartow) (a) Linear Scale (b) Logarithmic Scale

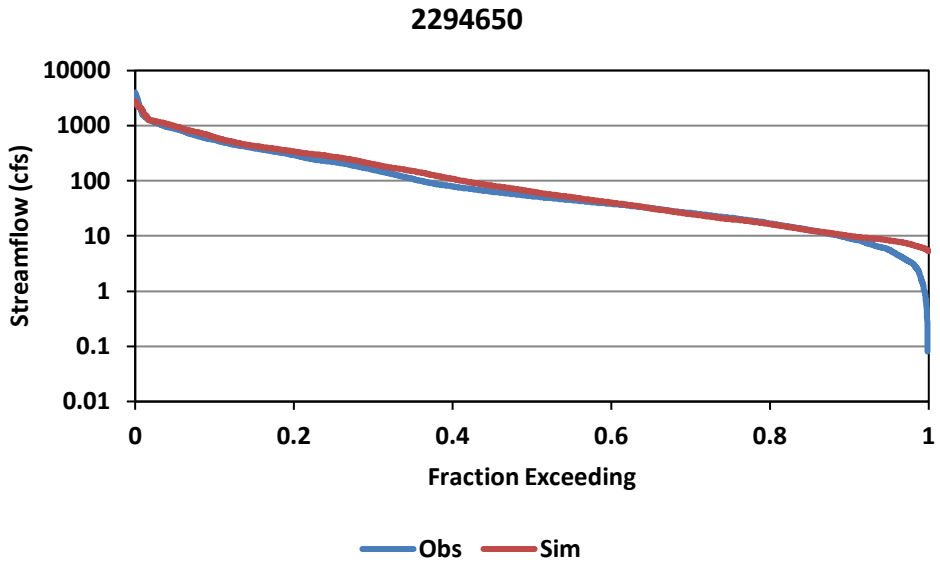

Figure 4.4 Observed vs. Simulated Flow Exceedance Curves (Peace River at Bartow)

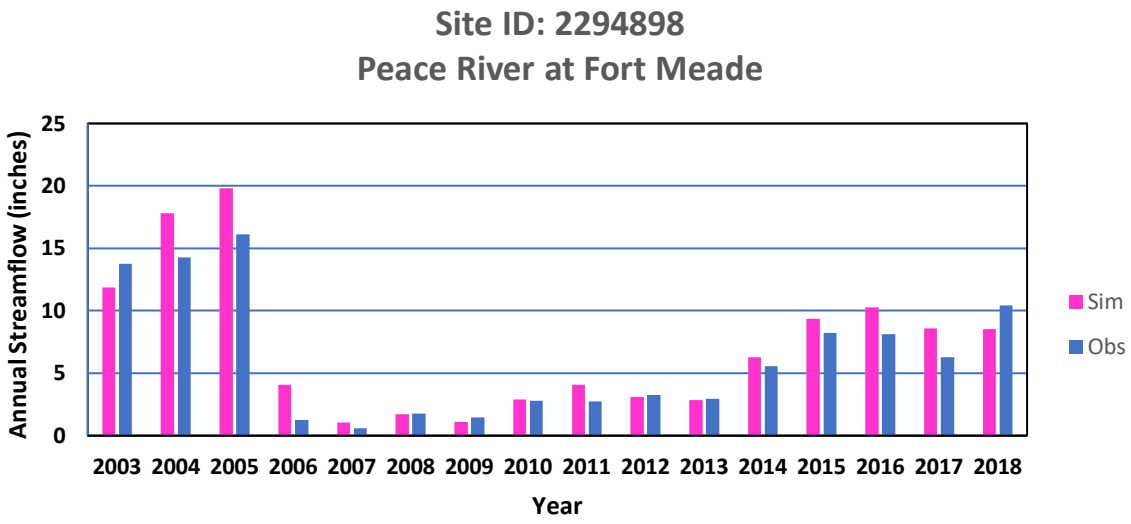

Figure 4.5 Observed vs. Simulated Annual Streamflows (Peace River at Fort Meade)

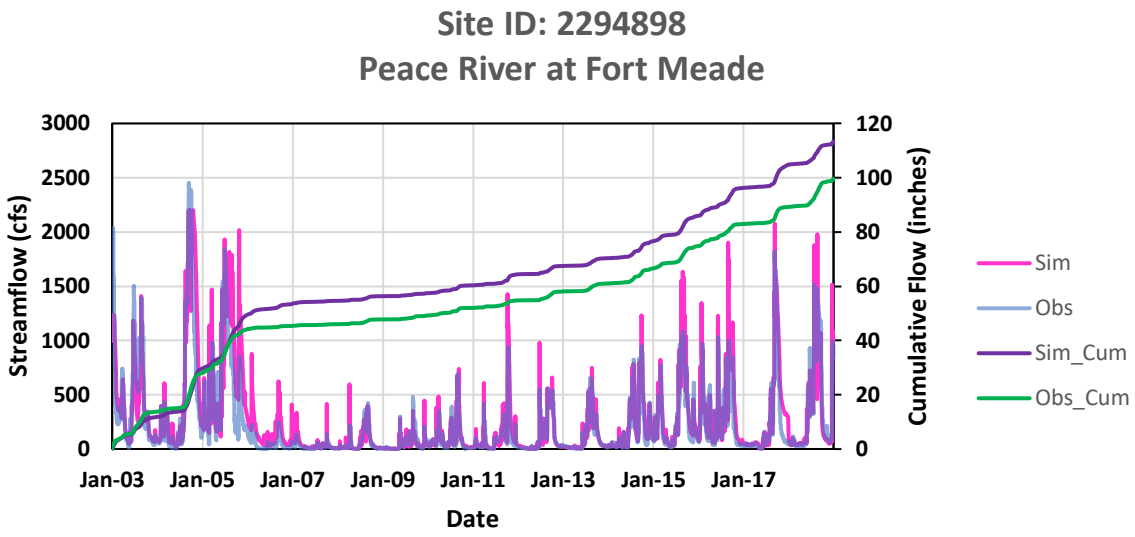

(a)

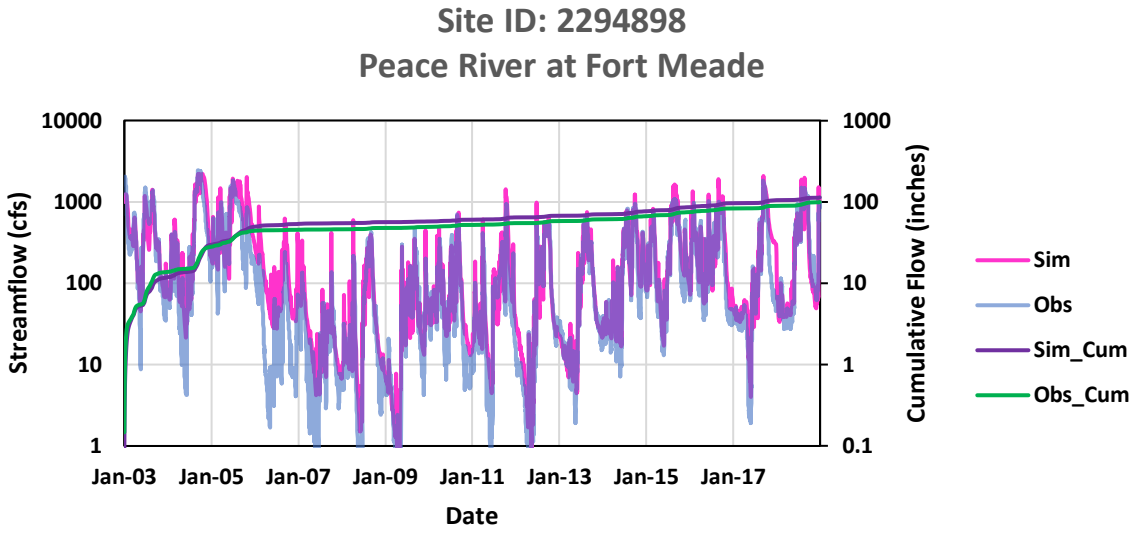

(b)

Figure 4.6 Observed vs. Simulated Streamflow Hydrographs (Peace River at Fort Meade) (a) Linear Scale (b) Logarithmic Scale

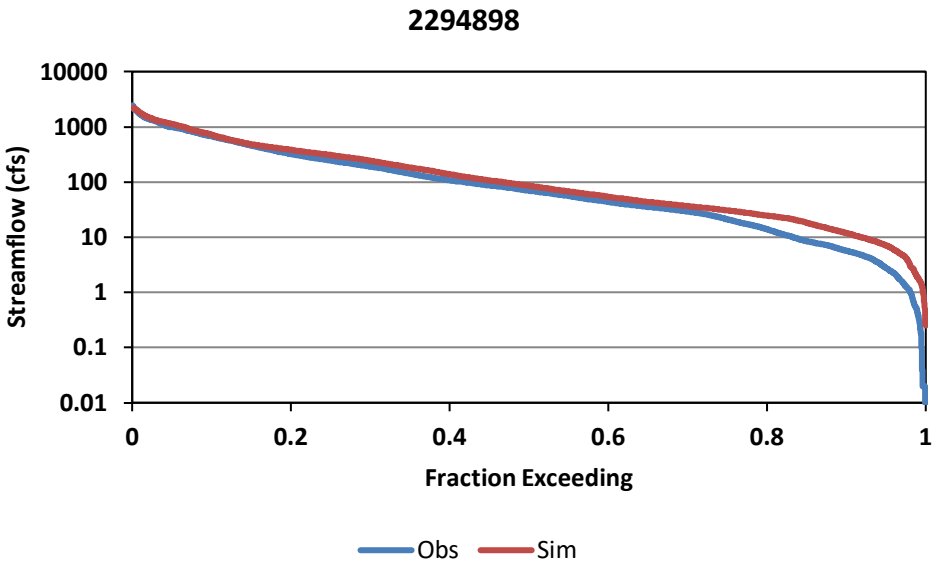

Figure 4.7 Observed vs. Simulated Flow Exceedance Curves (Peace River at Fort Meade)

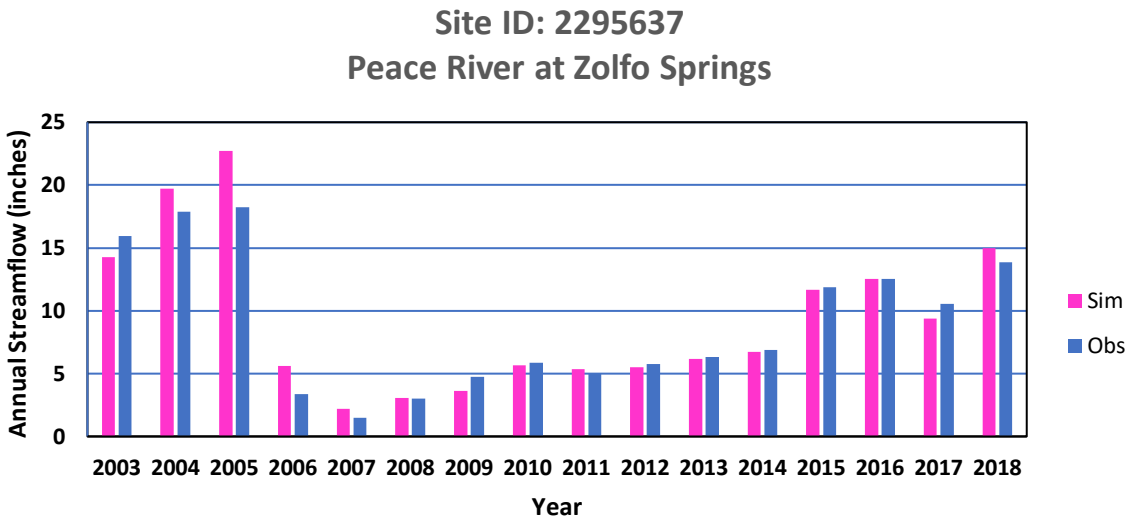

Figure 4.8 Observed vs. Simulated Annual Streamflows (Peace River at Zolfo Springs)

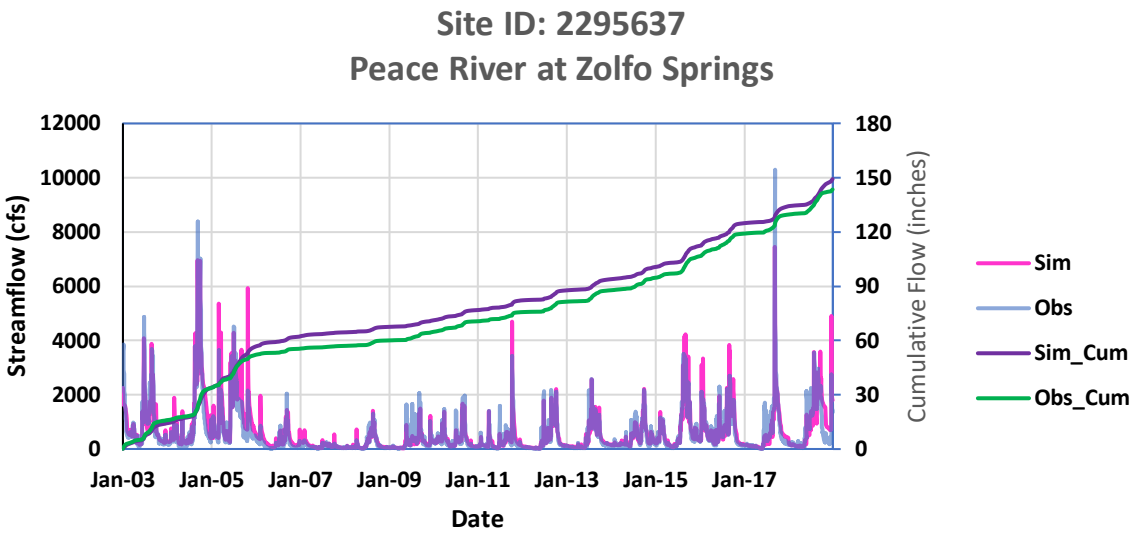

(a)

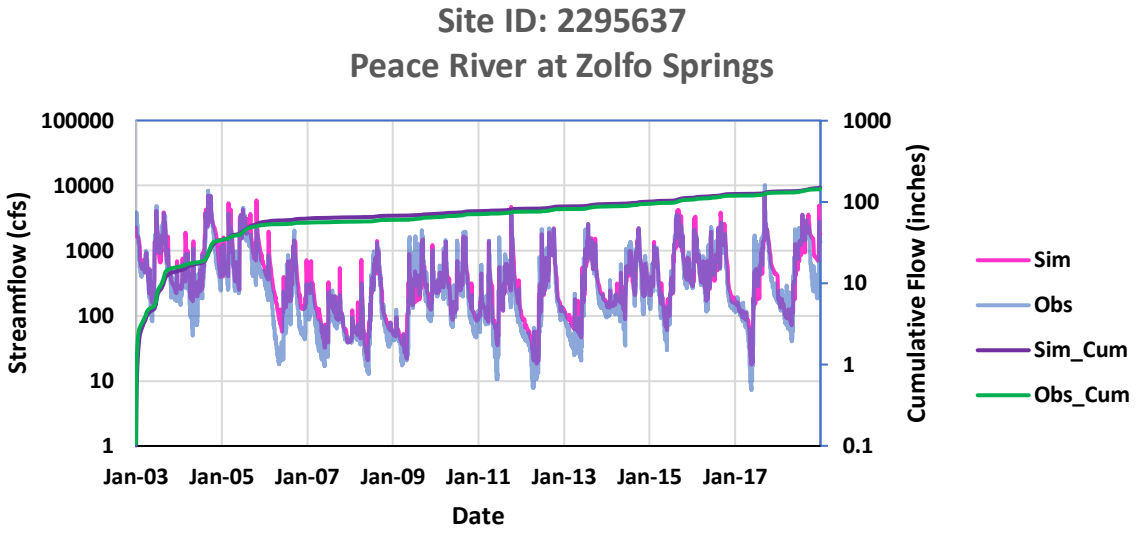

(b)

Figure 4.9 Observed vs. Simulated Streamflow Hydrographs (Peace River at Zolfo Springs) (a) Linear Scale (b) Logarithmic Scale

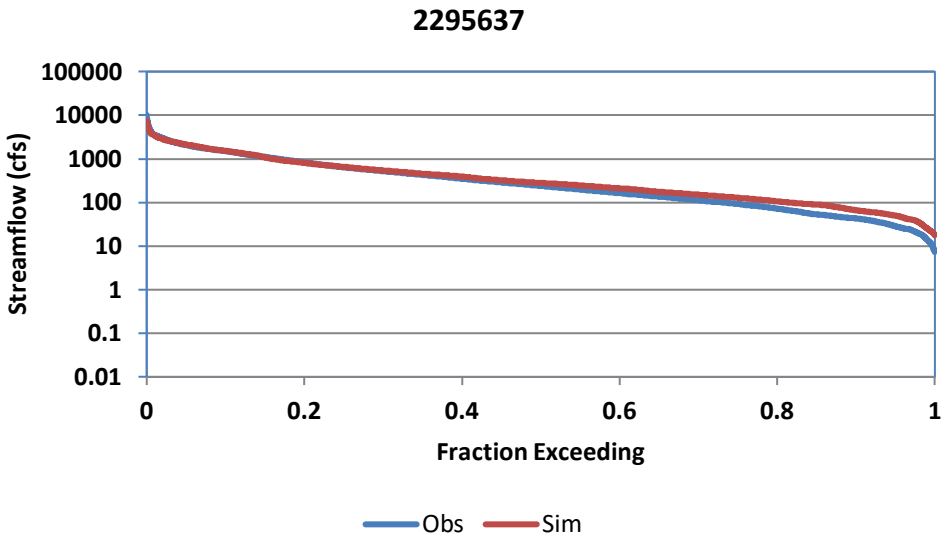

Figure 4.10 Observed vs. Simulated Flow Exceedance Curves (Peace River at Zolfo Springs)

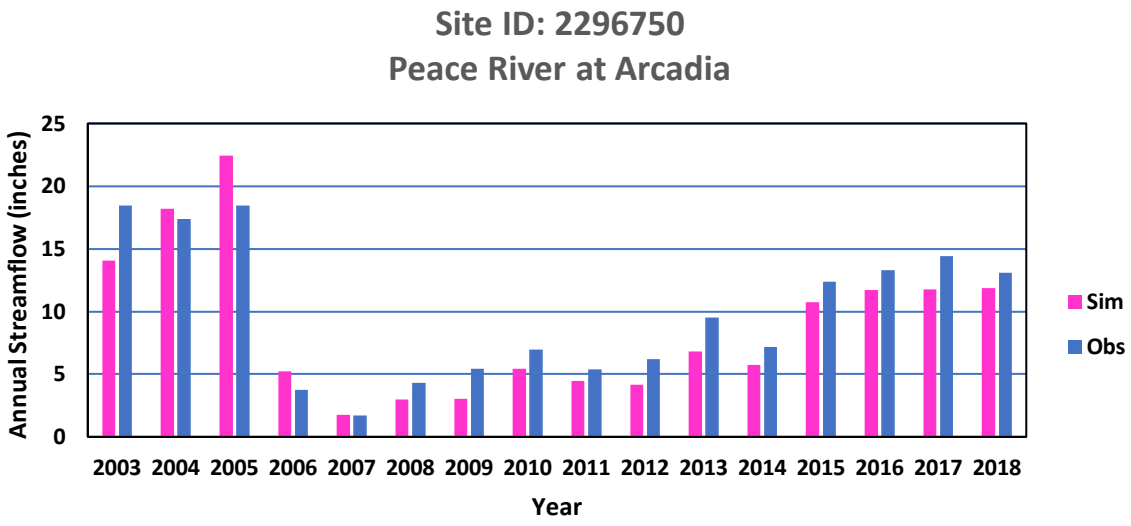

Figure 4.11 Observed vs. Simulated Annual Streamflows (Peace River at Arcadia)

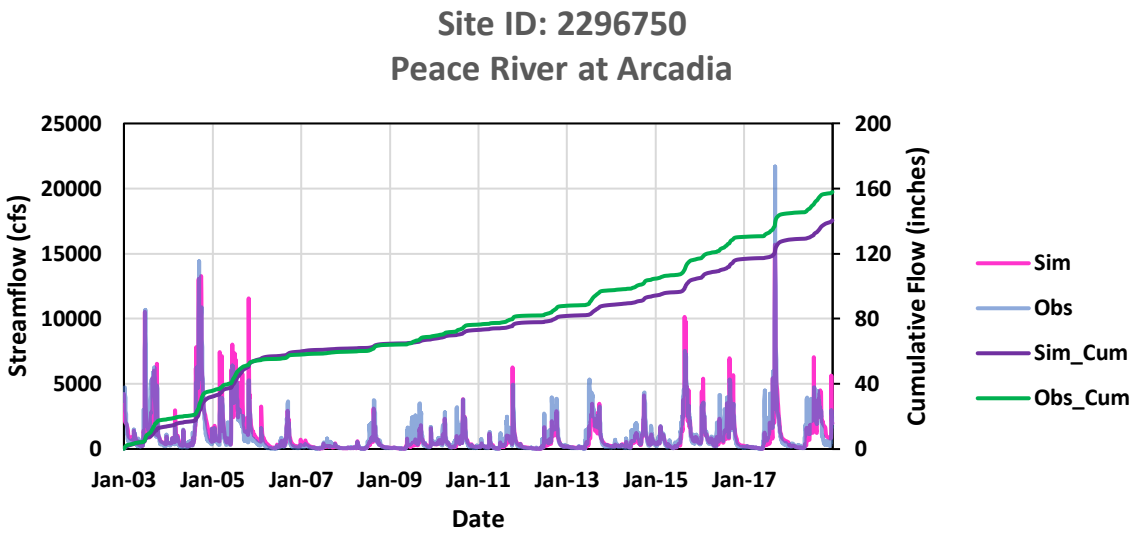

(a)

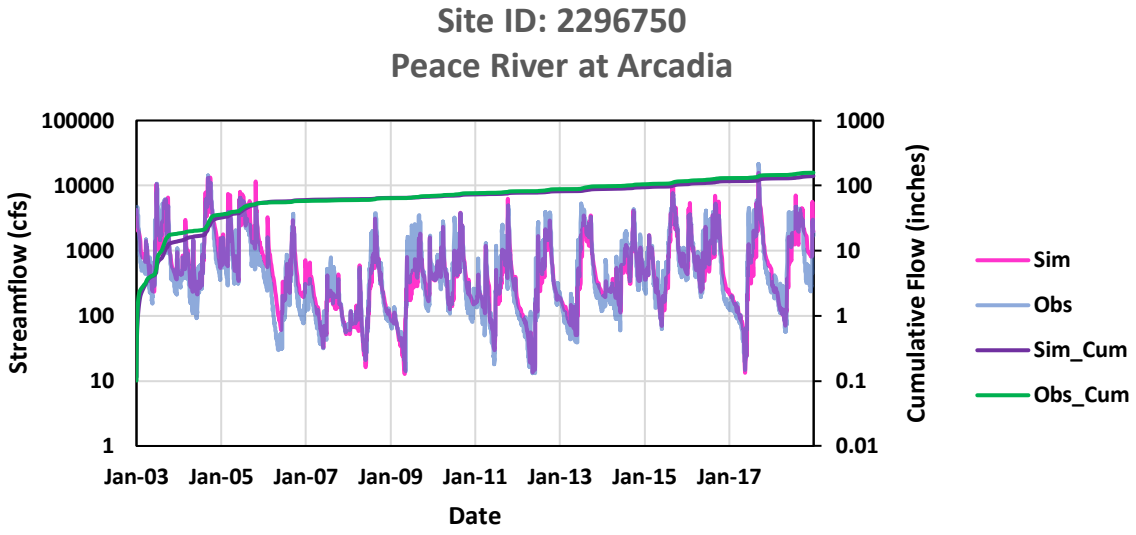

(b)

Figure 4.12 Observed vs. Simulated Streamflow Hydrographs (Peace River at Arcadia) (a) Linear Scale (b) Logarithmic Scale

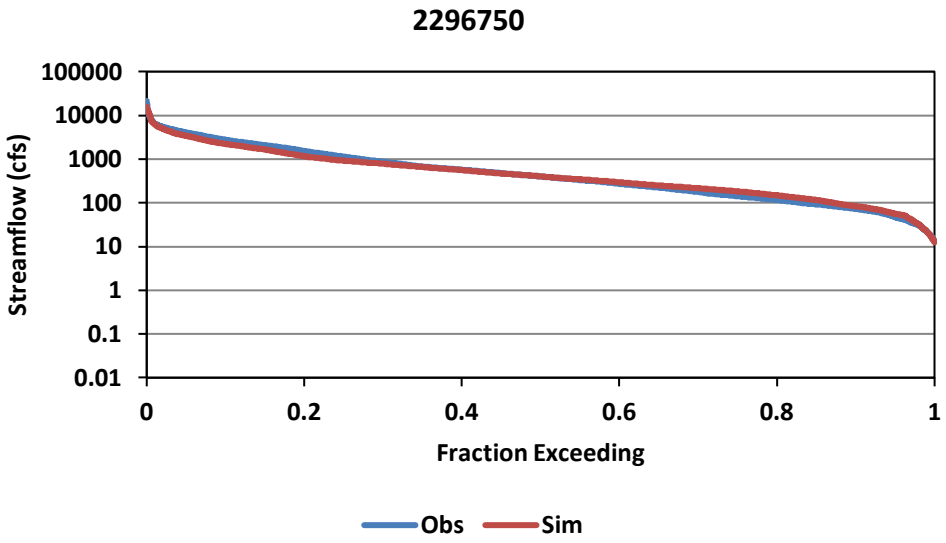

Figure 4.13 Observed vs. Simulated Flow Exceedance Curves (Peace River at Arcadia)

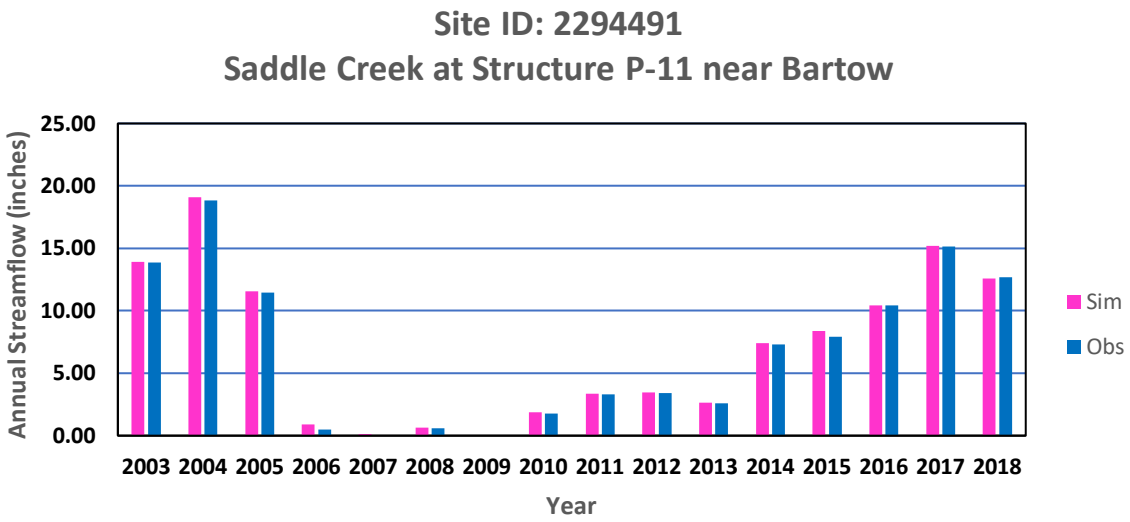

Figure 4.14 Observed vs. Simulated Annual Streamflows (Saddle Creek at P-11 Near Bartow)

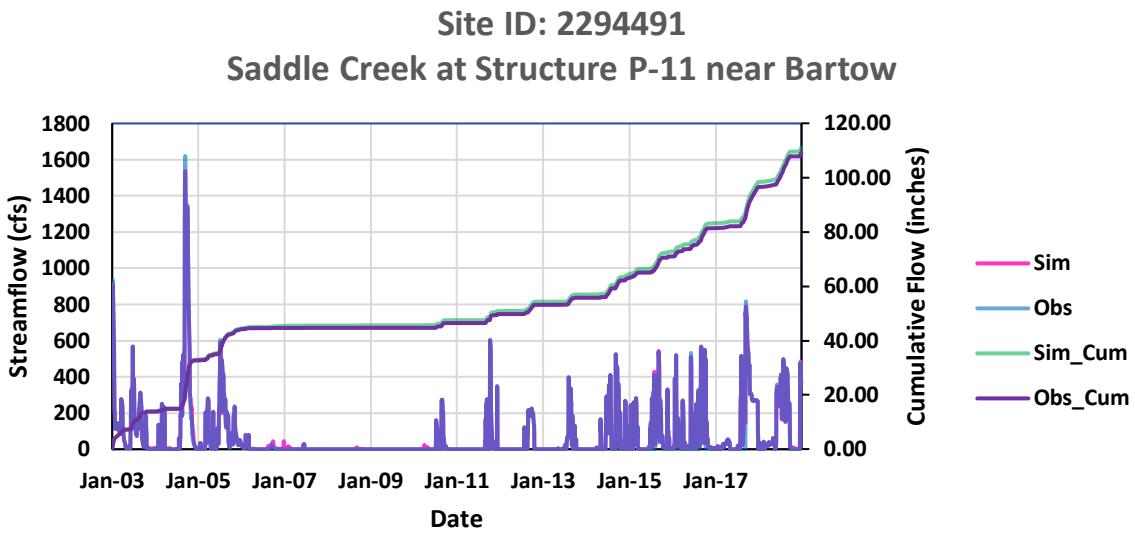

(a)

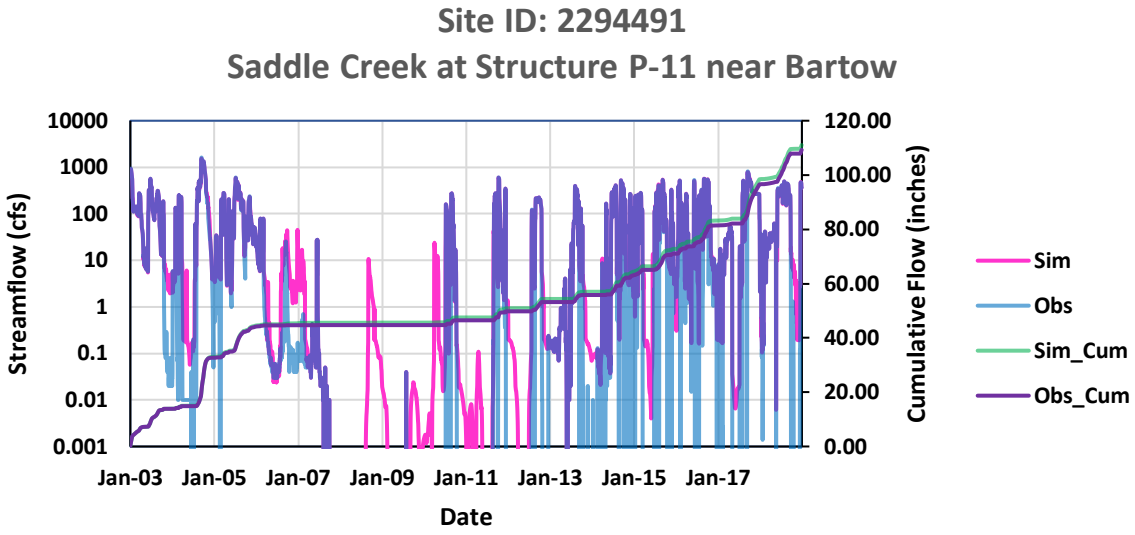

(b)

Figure 4.15 Observed vs. Simulated Streamflow Hydrographs (Saddle Creek at P-11 Near Bartow) (a) Linear Scale (b) Logarithmic Scale

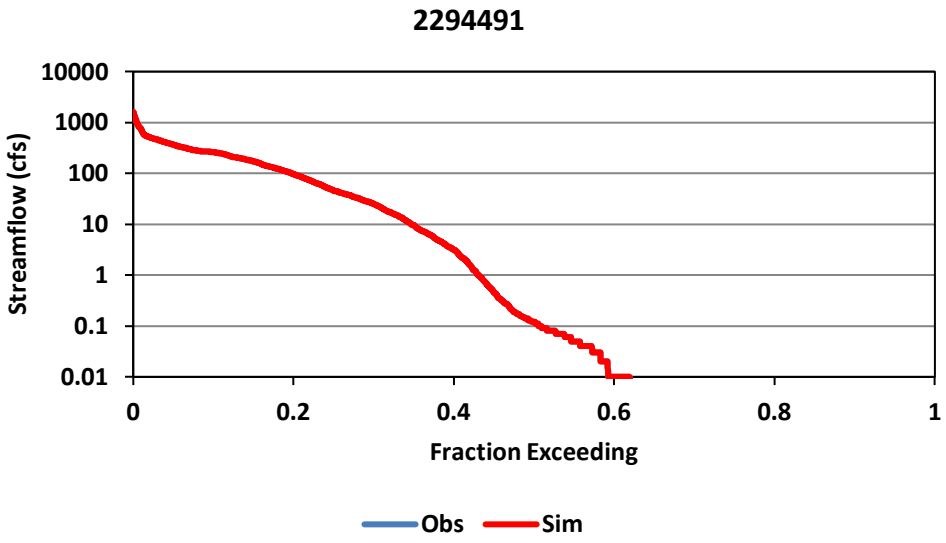

Figure 4.16 Observed vs. Simulated Flow Exceedance Curves (Saddle Creek at P-11 Near Bartow)

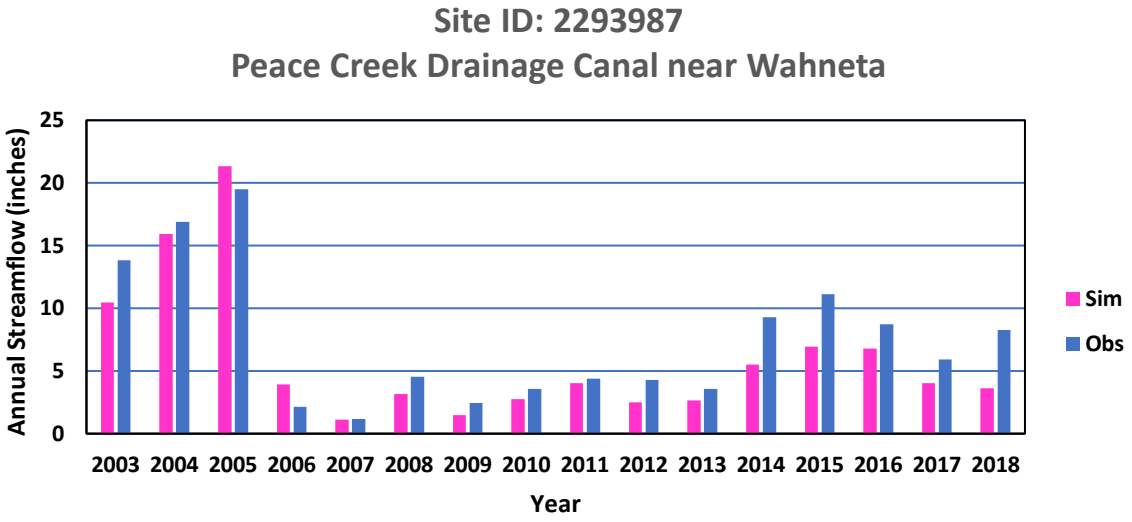

Figure 4.17 Observed vs. Simulated Annual Streamflows (Peace Creek Near Wahneta)

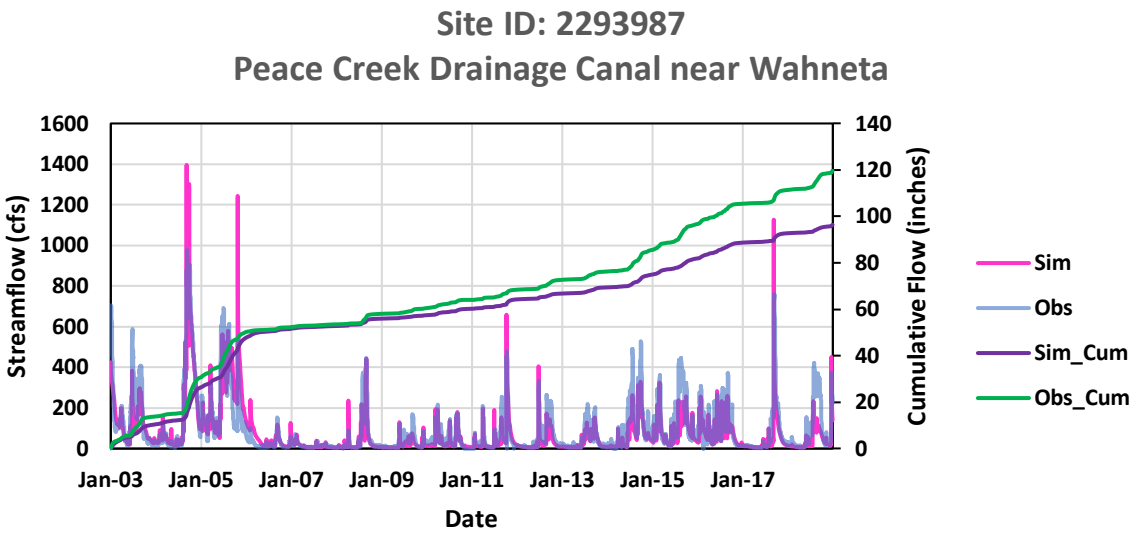

(a)

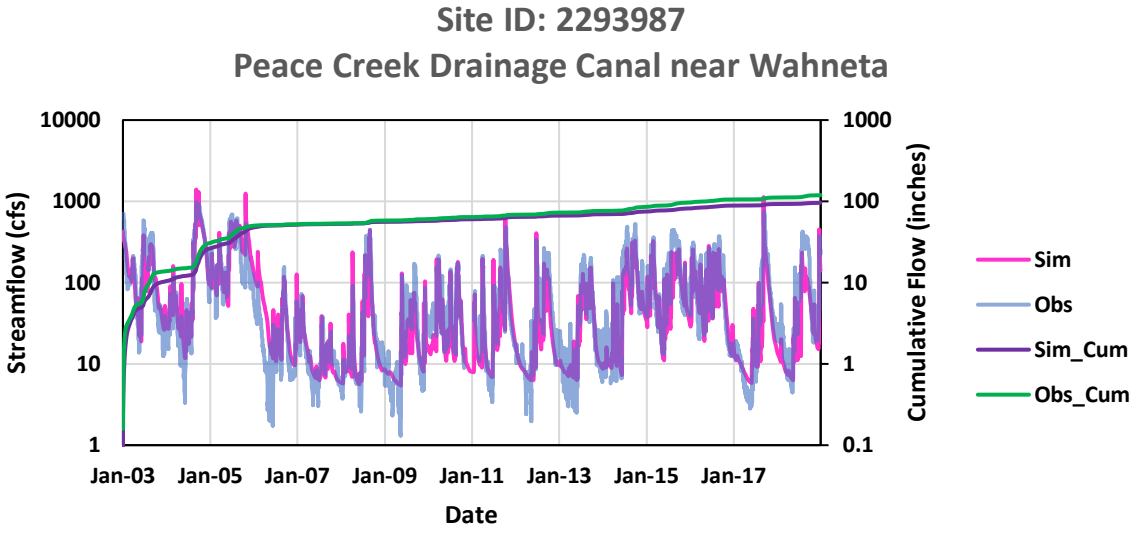

(b)

Figure 4.18 Observed vs. Simulated Streamflow Hydrographs (Peace Creek Near Wahneta) (a) Linear Scale (b) Logarithmic Scale

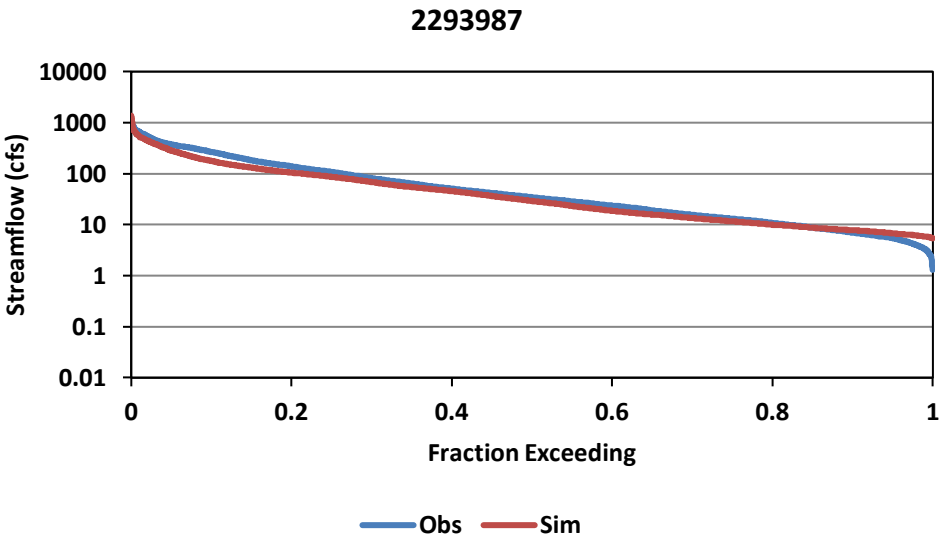

Figure 4.19 Observed vs. Simulated Flow Exceedance Curves (Peace Creek Near Wahneta)

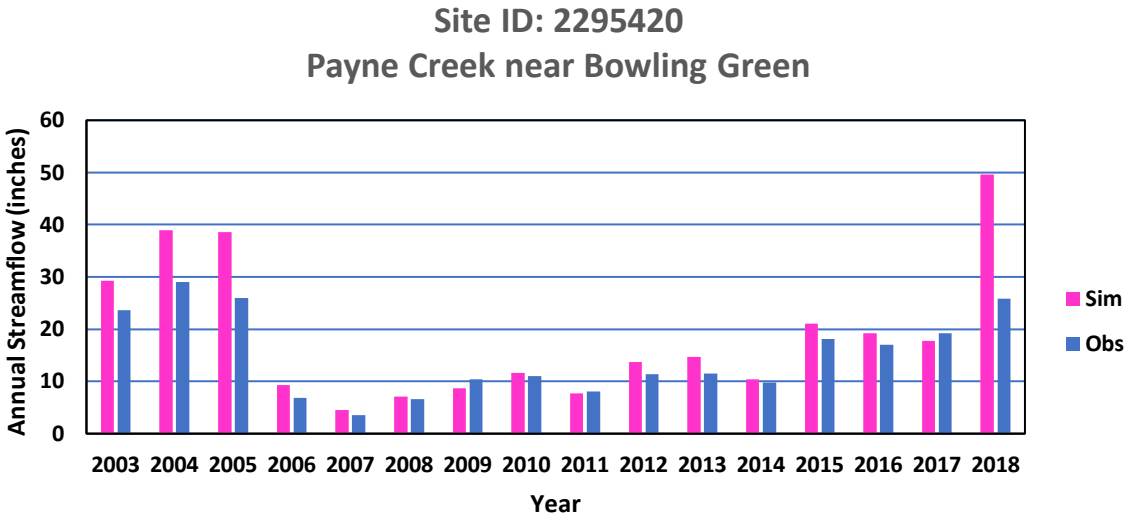

Figure 4.20 Observed vs. Simulated Annual Streamflows (Payne Creek Near Bowling Green)

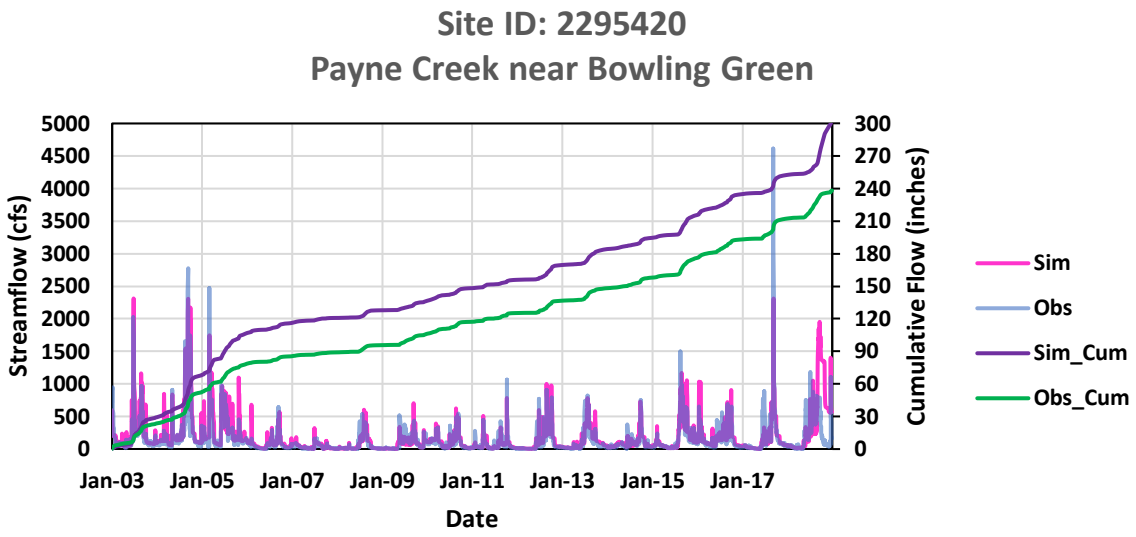

(a)

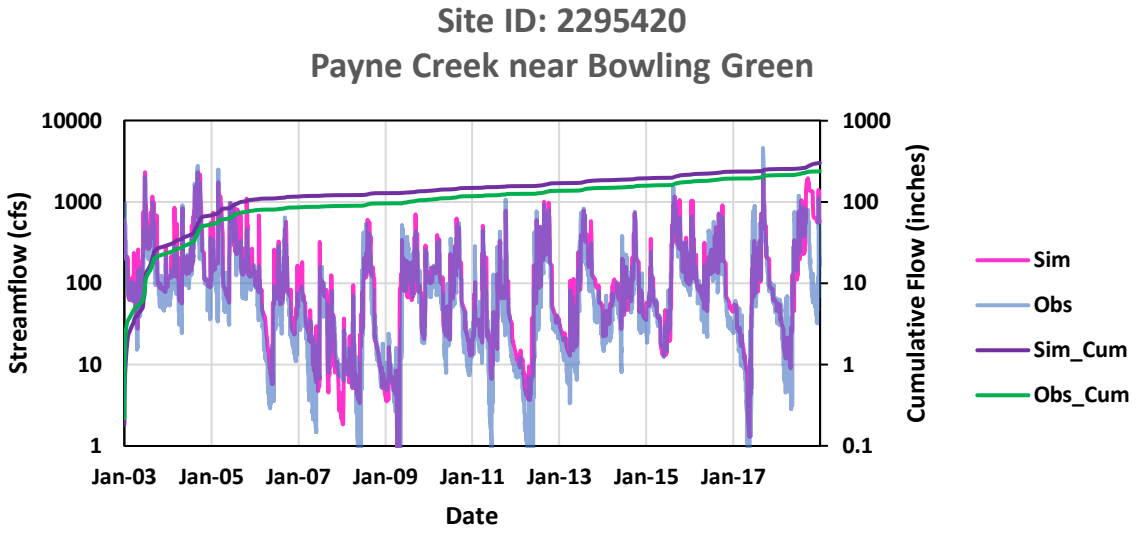

(b)

Figure 4.21 Observed vs. Simulated Streamflow Hydrographs (Payne Creek Near Bowling Green) (a) Linear Scale (b) Logarithmic Scale

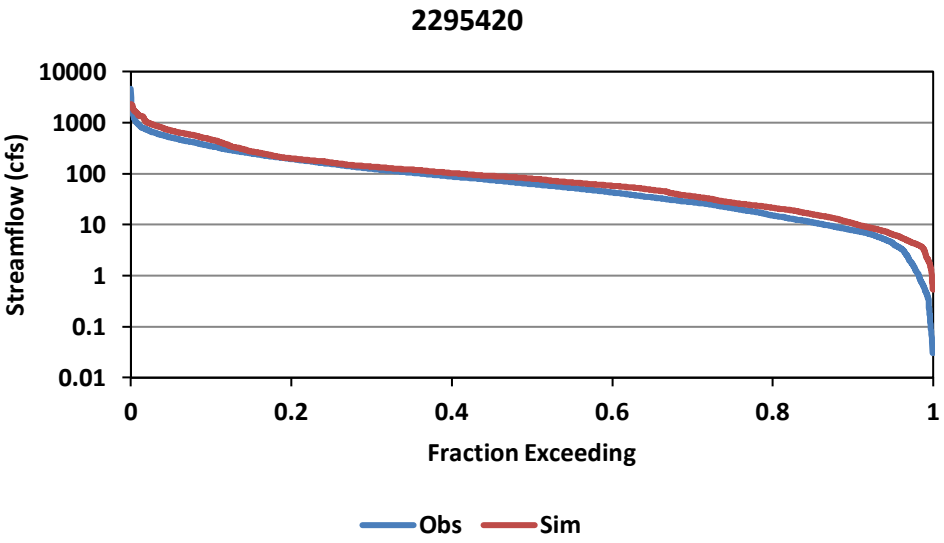

Figure 4.22 Observed vs. Simulated Flow Exceedance Curves (Payne Creek near Bowling Green)

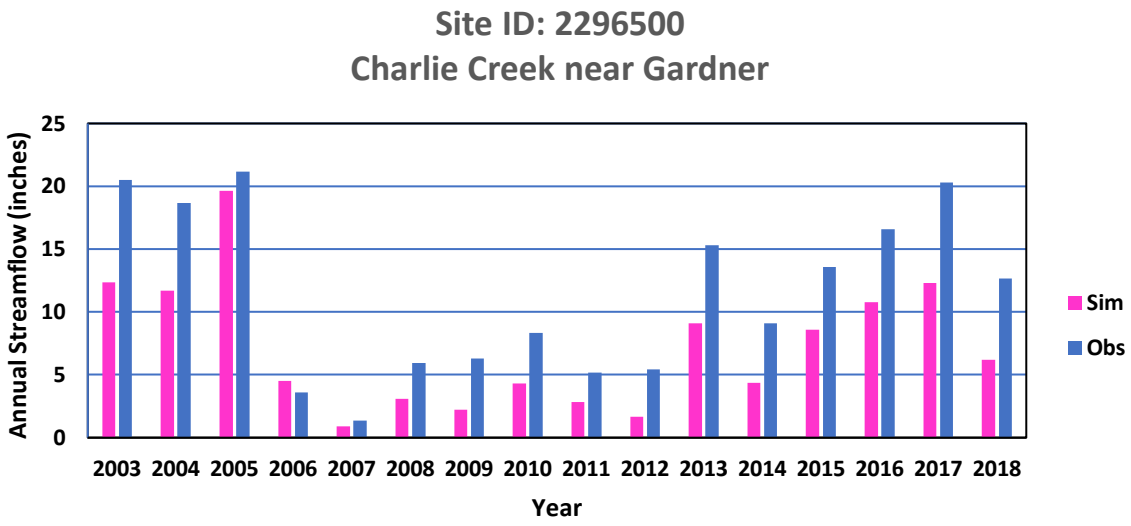

Figure 4.23 Observed vs. Simulated Annual Streamflows (Charlie Creek near Gardner)

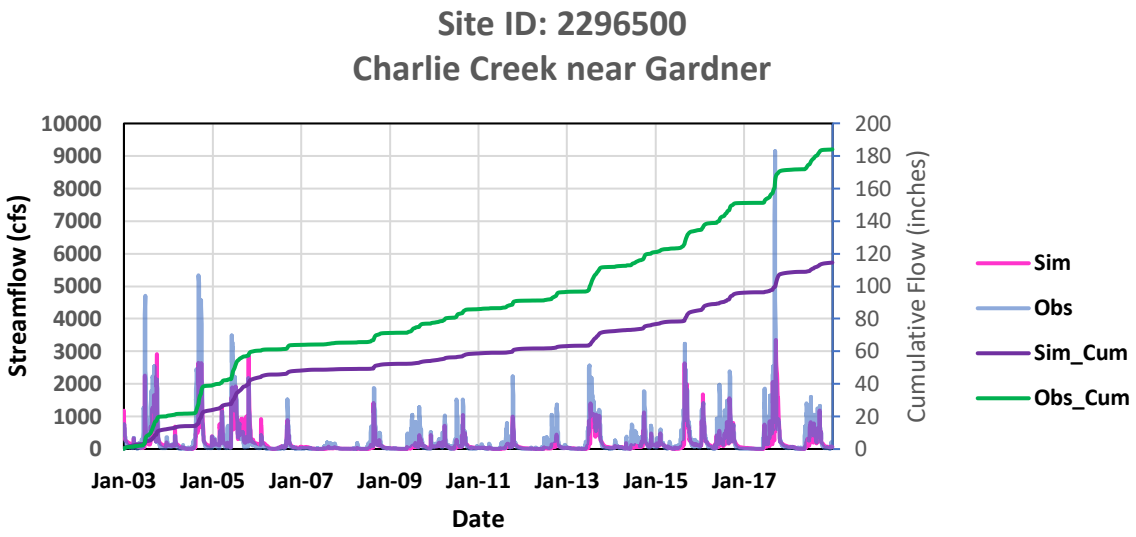

(a)

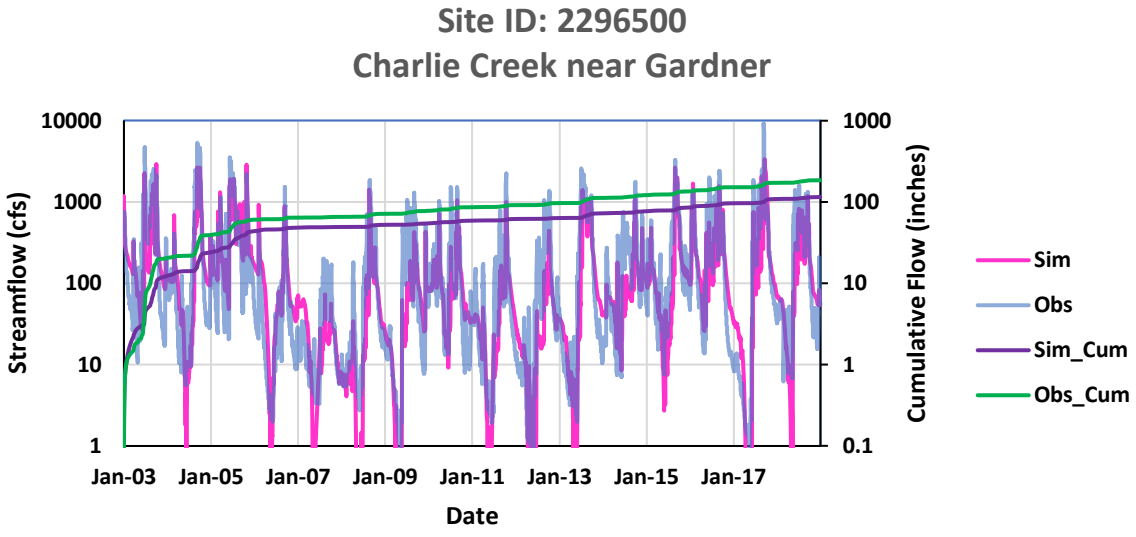

(b)

Figure 4.24 Observed vs. Simulated Streamflow Hydrographs (Charlie Creek near Gardner) (a) Linear Scale (b) Logarithmic Scale

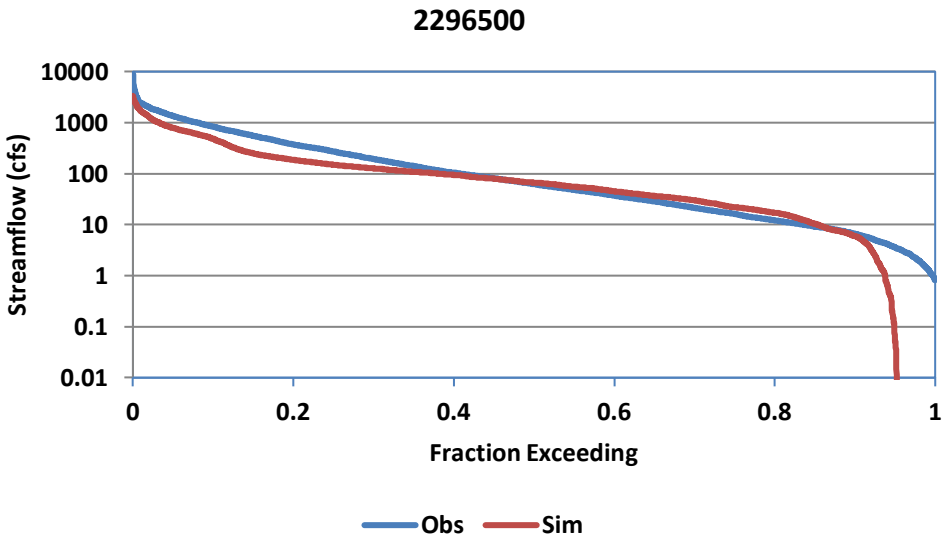

Figure 4.25 Observed vs. Simulated Flow Exceedance Curves (Charlie Creek near Gardner)

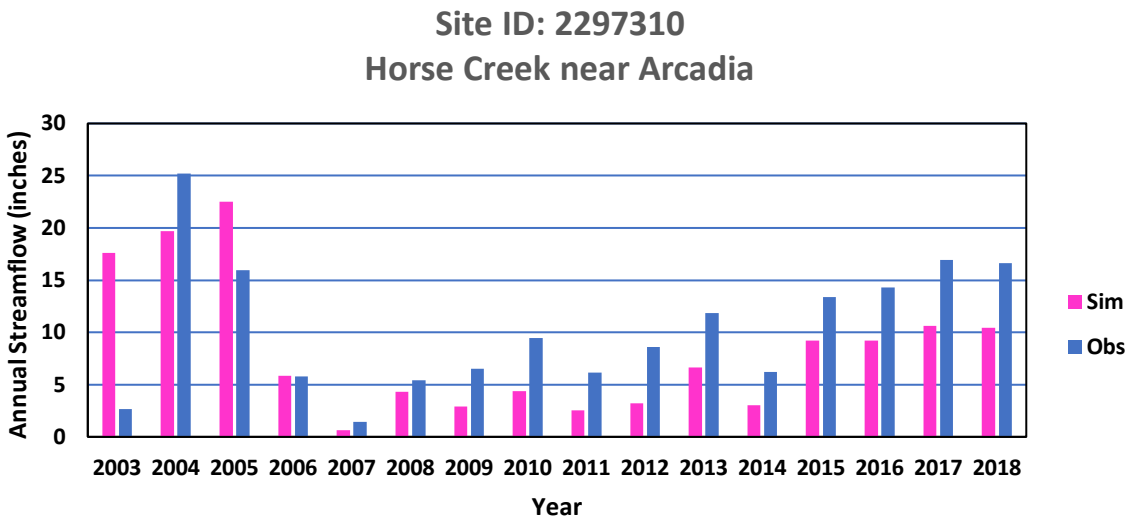

Figure 4.26 Observed vs. Simulated Annual Streamflows (Horse Creek near Arcadia)

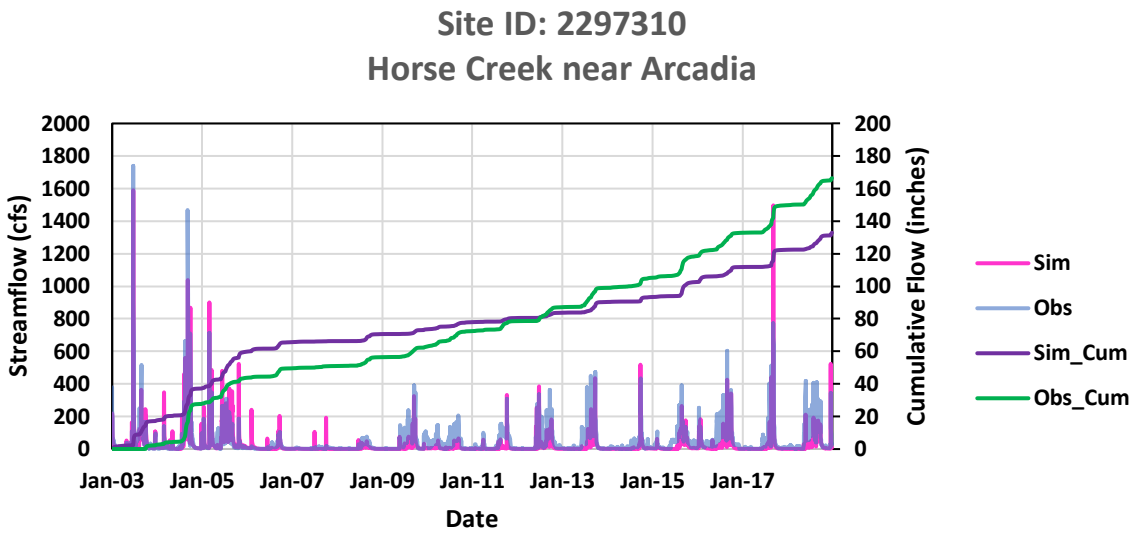

(a)

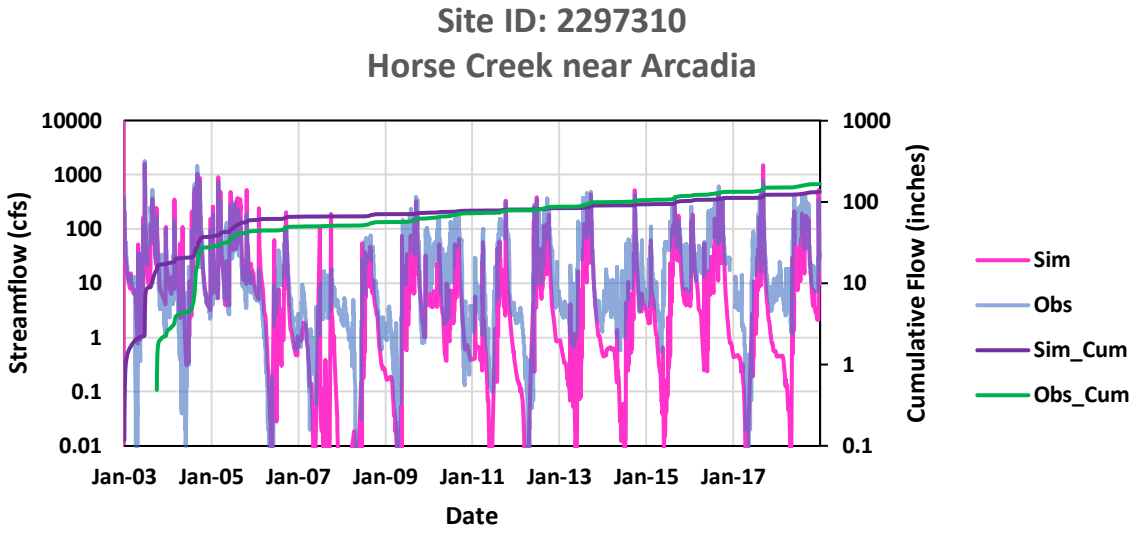

(b)

Figure 4.27 Observed vs. Simulated Streamflow Hydrographs (Horse Creek near Arcadia) (a) Linear Scale (b) Logarithmic Scale

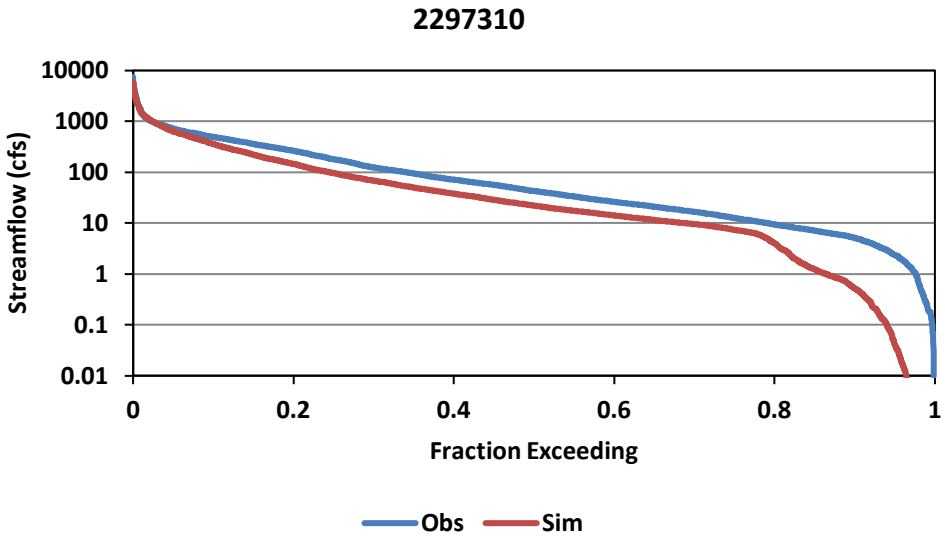

Figure 4.28 Observed vs. Simulated Flow Exceedance Curves (Horse Creek near Arcadia)

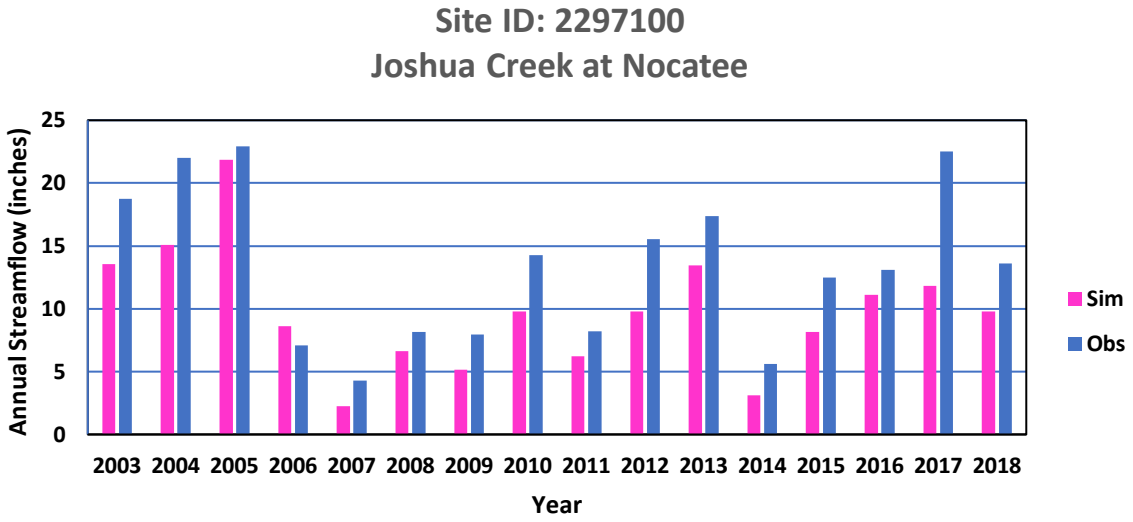

Figure 4.29 Observed vs. Simulated Annual Streamflows (Joshua Creek at Nocatee)

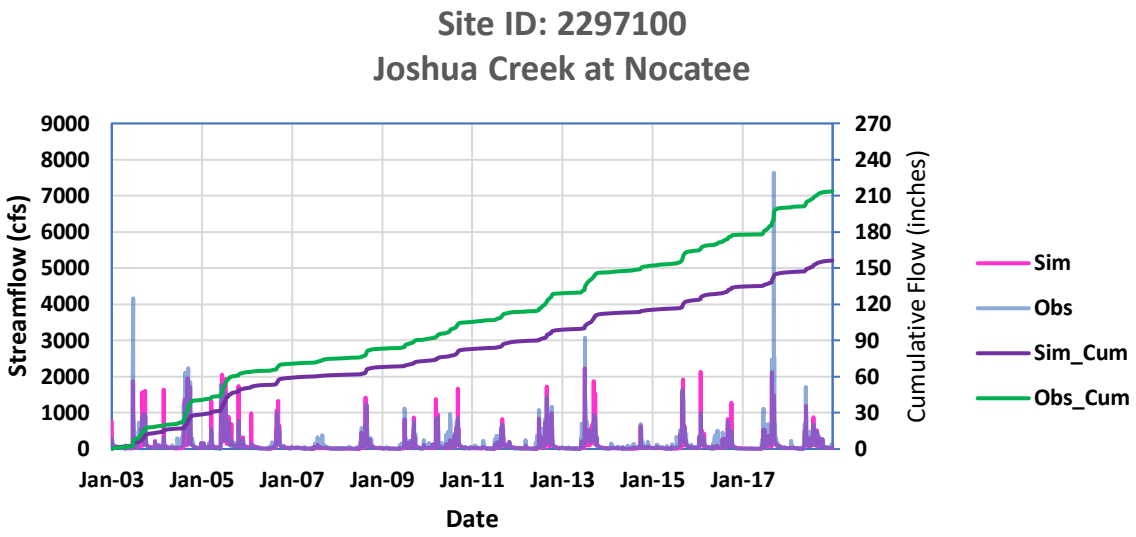

(a)

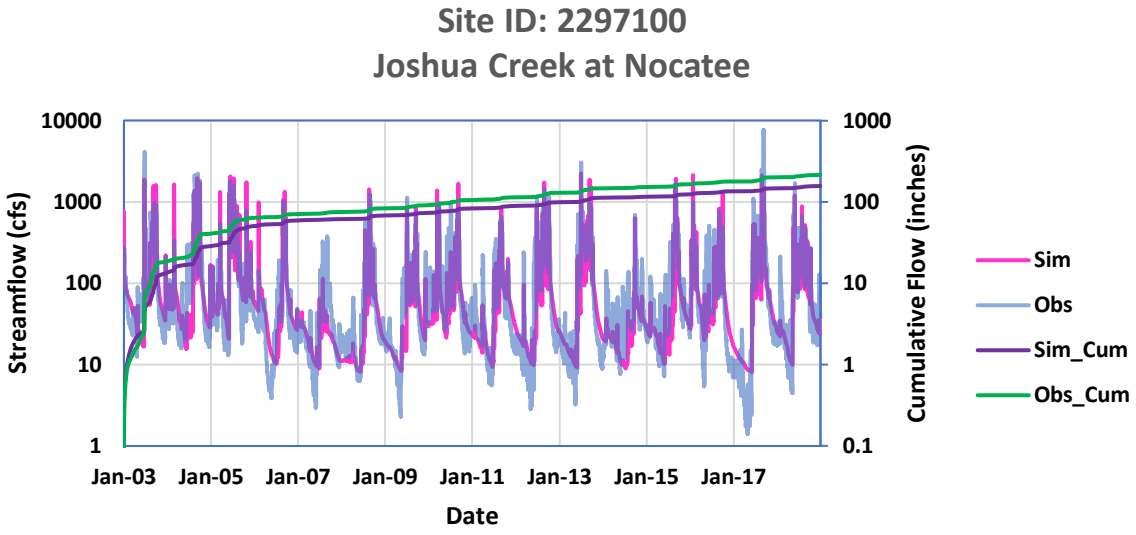

(b)

Figure 4.30 Observed vs. Simulated Streamflow Hydrographs (Joshua Creek at Nocatee) (a) Linear Scale (b) Logarithmic Scale

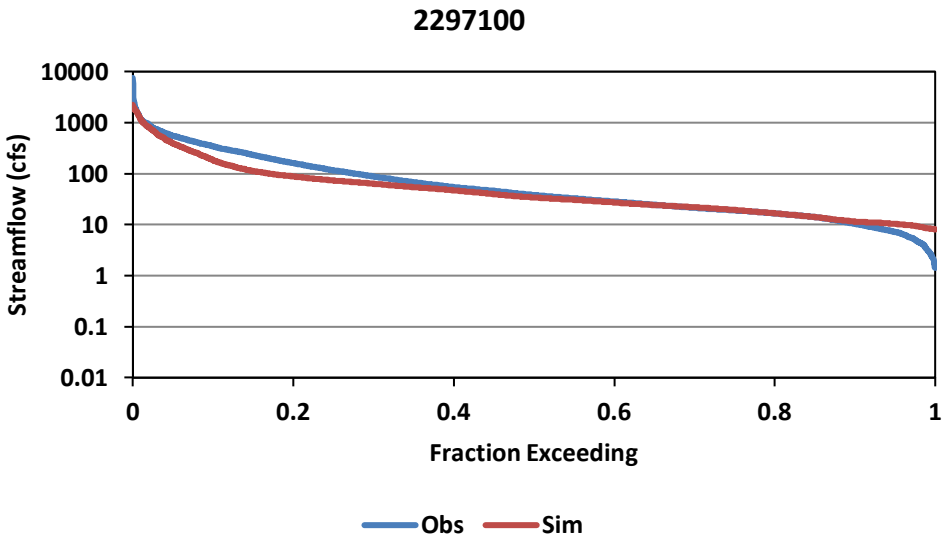

Figure 4.31 Observed vs. Simulated Flow Exceedance Curves (Joshua Creek at Nocatee)

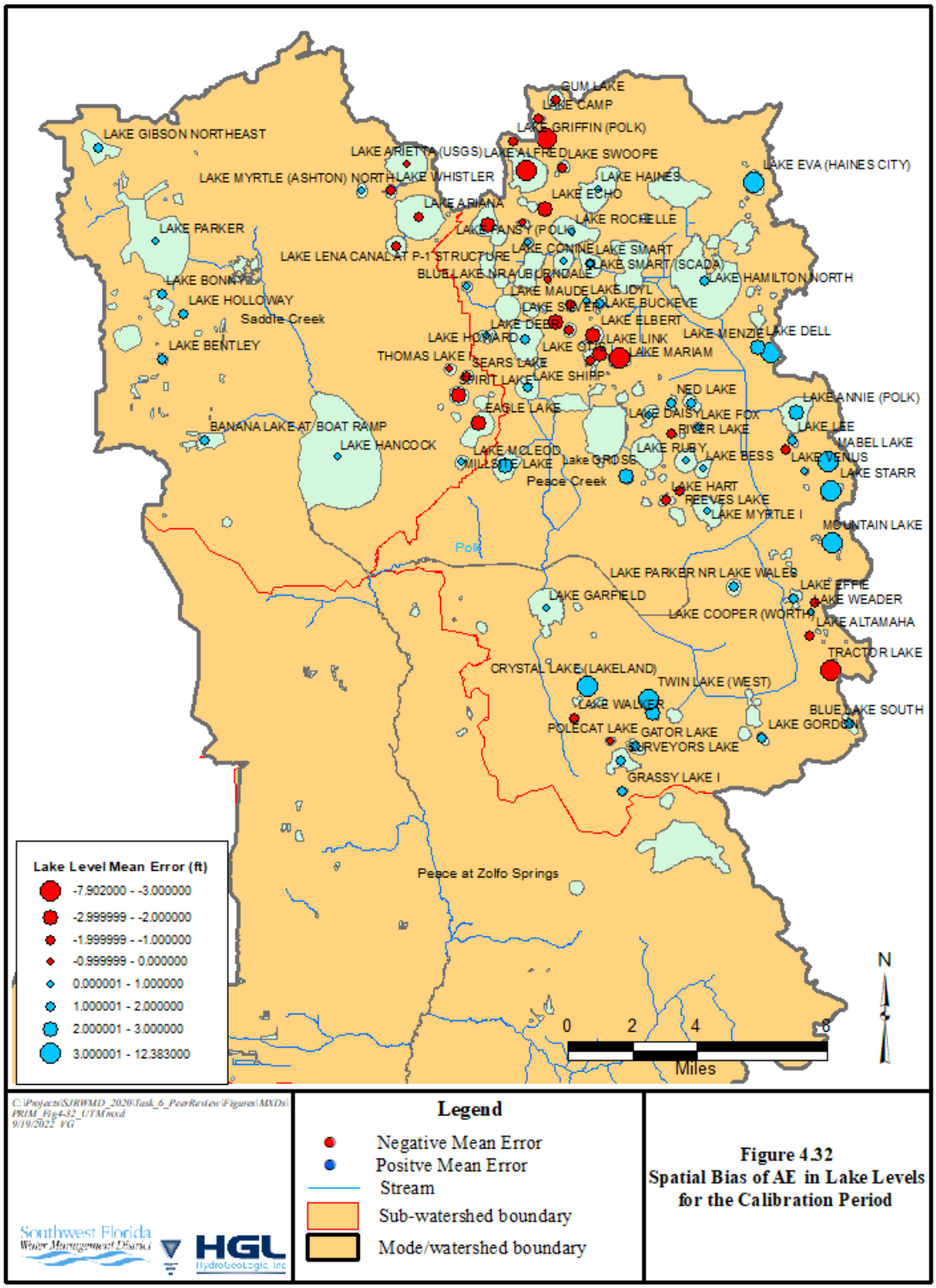

Figure 4.32
Spatial Bias of AE in Lake Levels for the Calibration Period

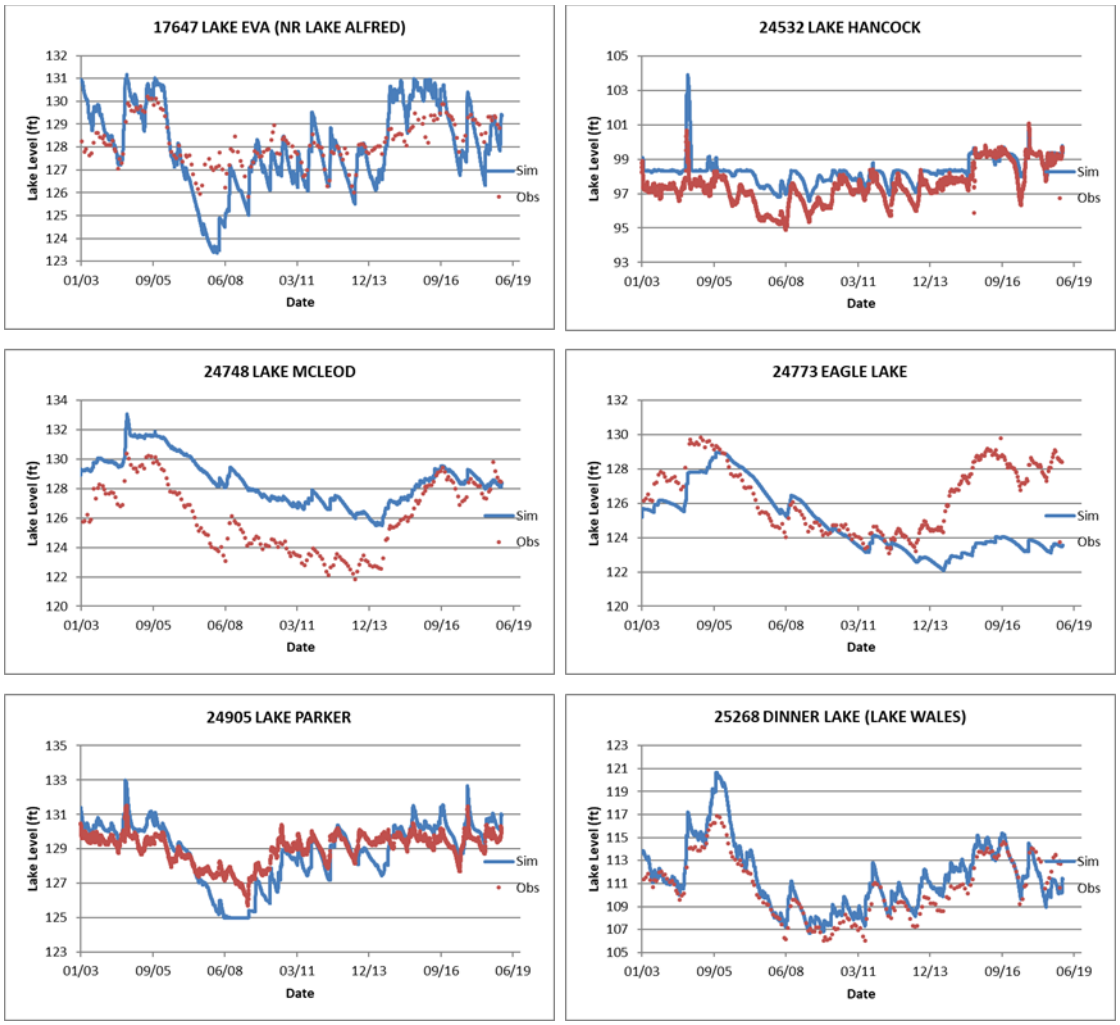

Figure 4.33 Minimum Flows and Levels Lakes: Group 1

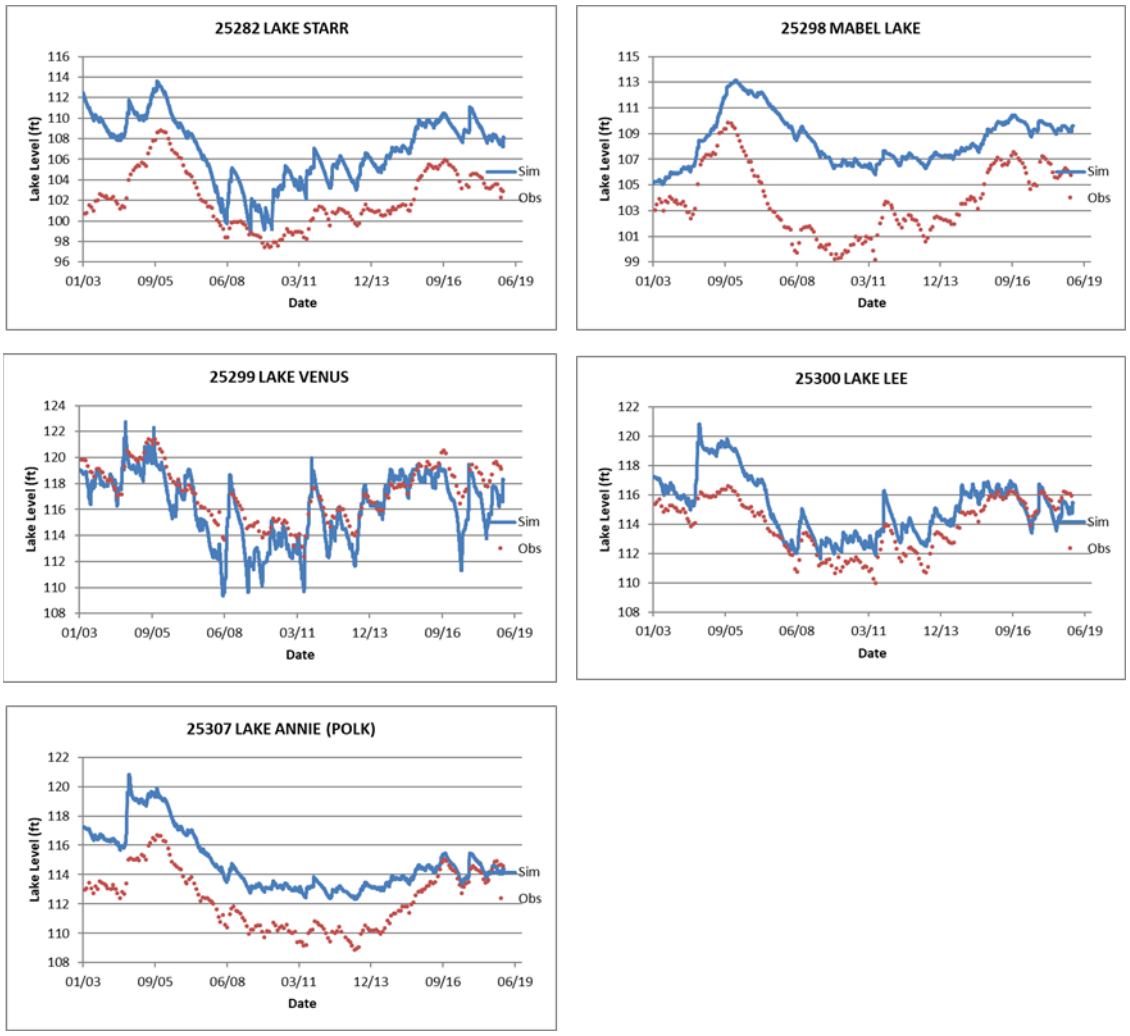

Figure 4.34 Minimum Flows and Levels Lakes: Group 2

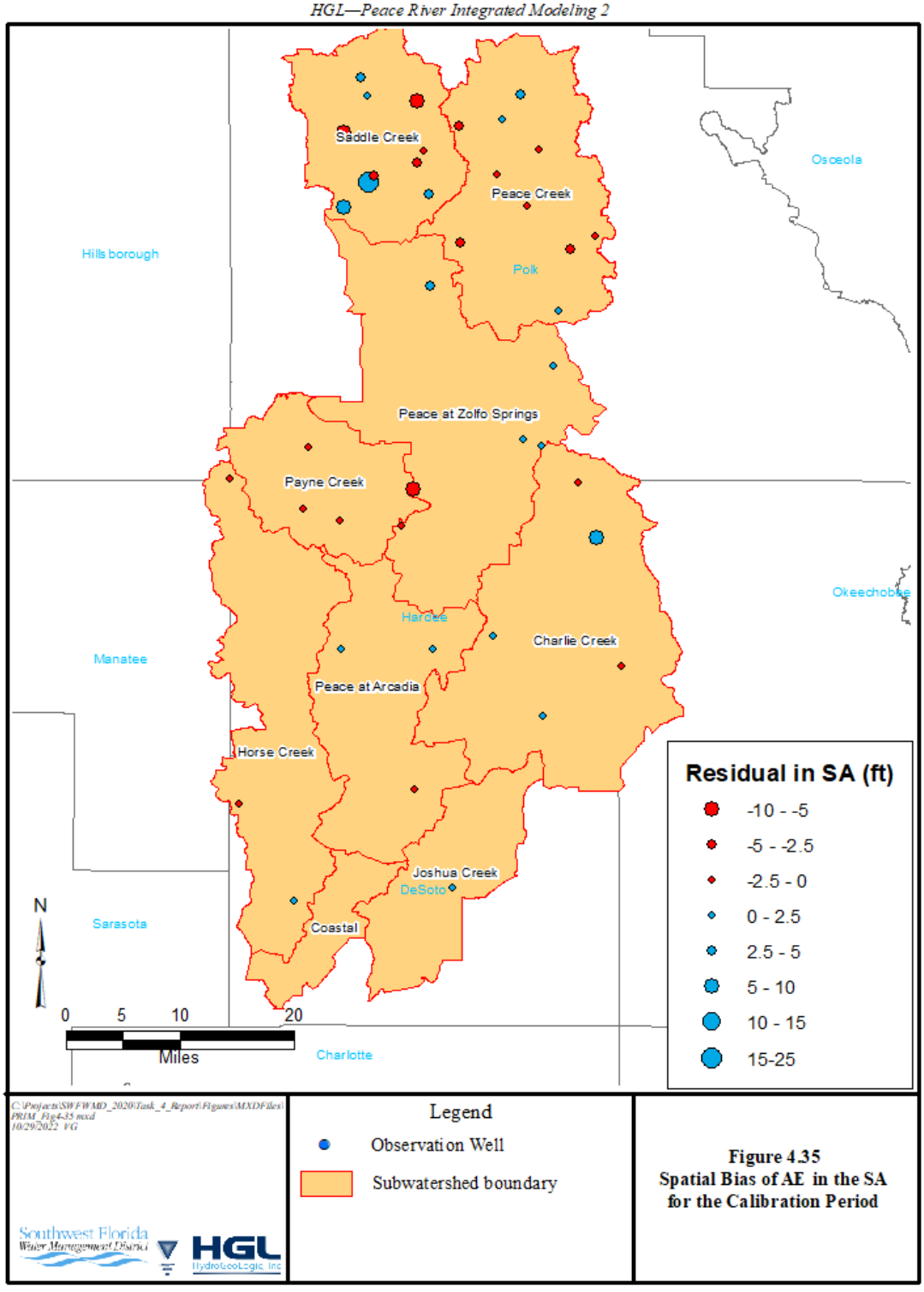

Figure 4.35
Spatial Bias of AE in the SA for the Calibration Period

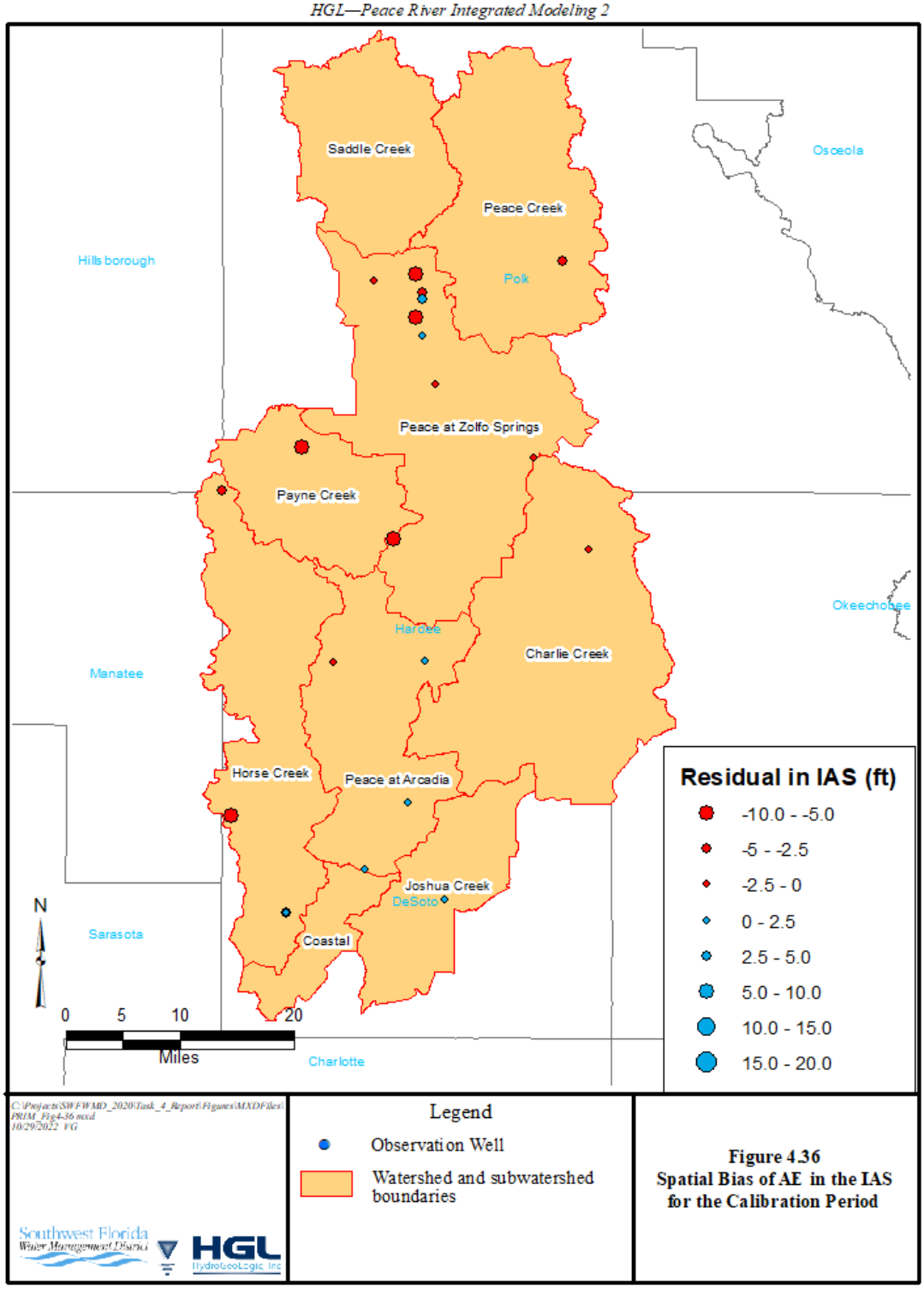

Figure 4.36
Spatial Bias of AE in the IAS for the Calibration Period

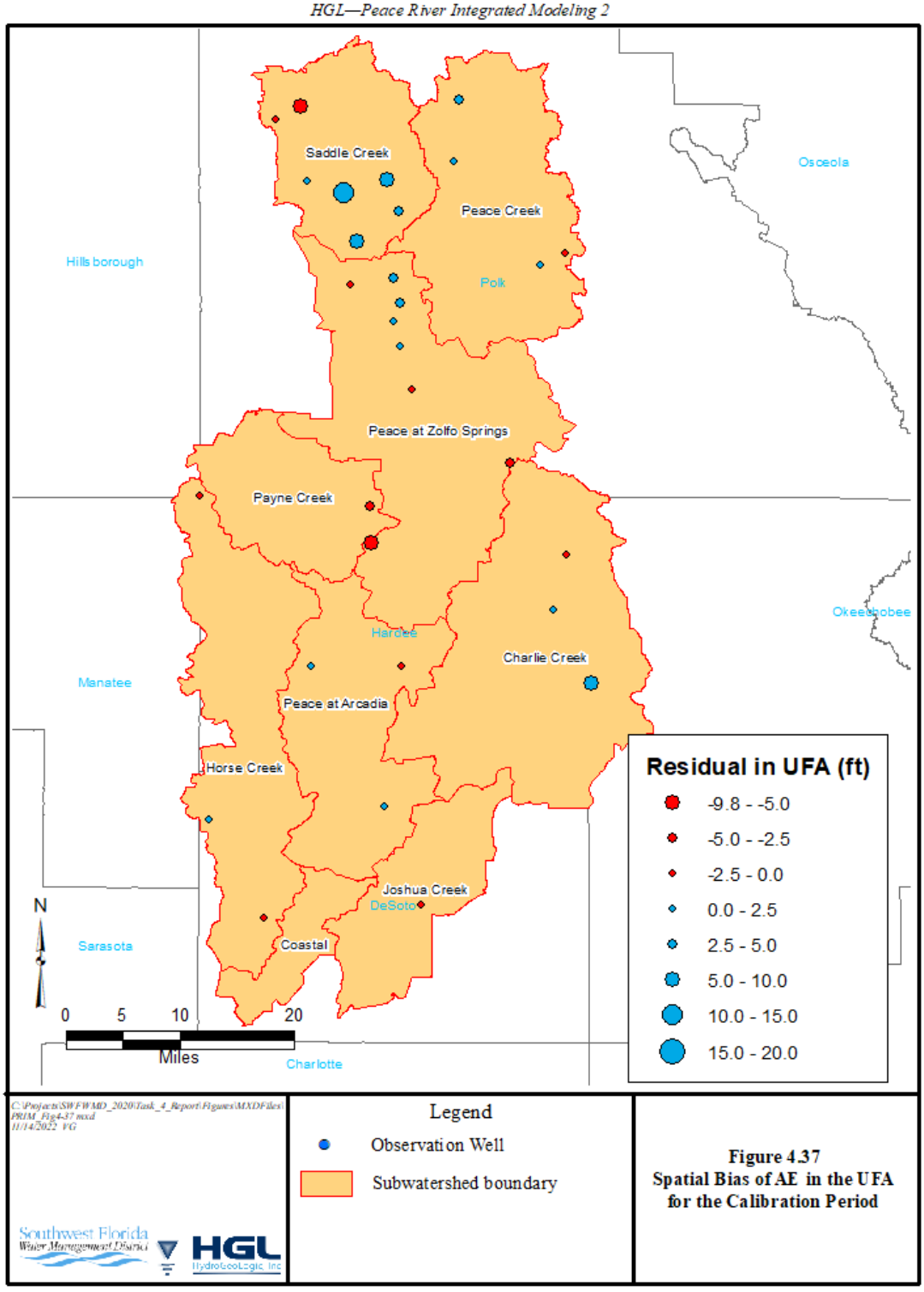

Figure 4.37
Spatial Bias of AE in the UFA for the Calibration Period

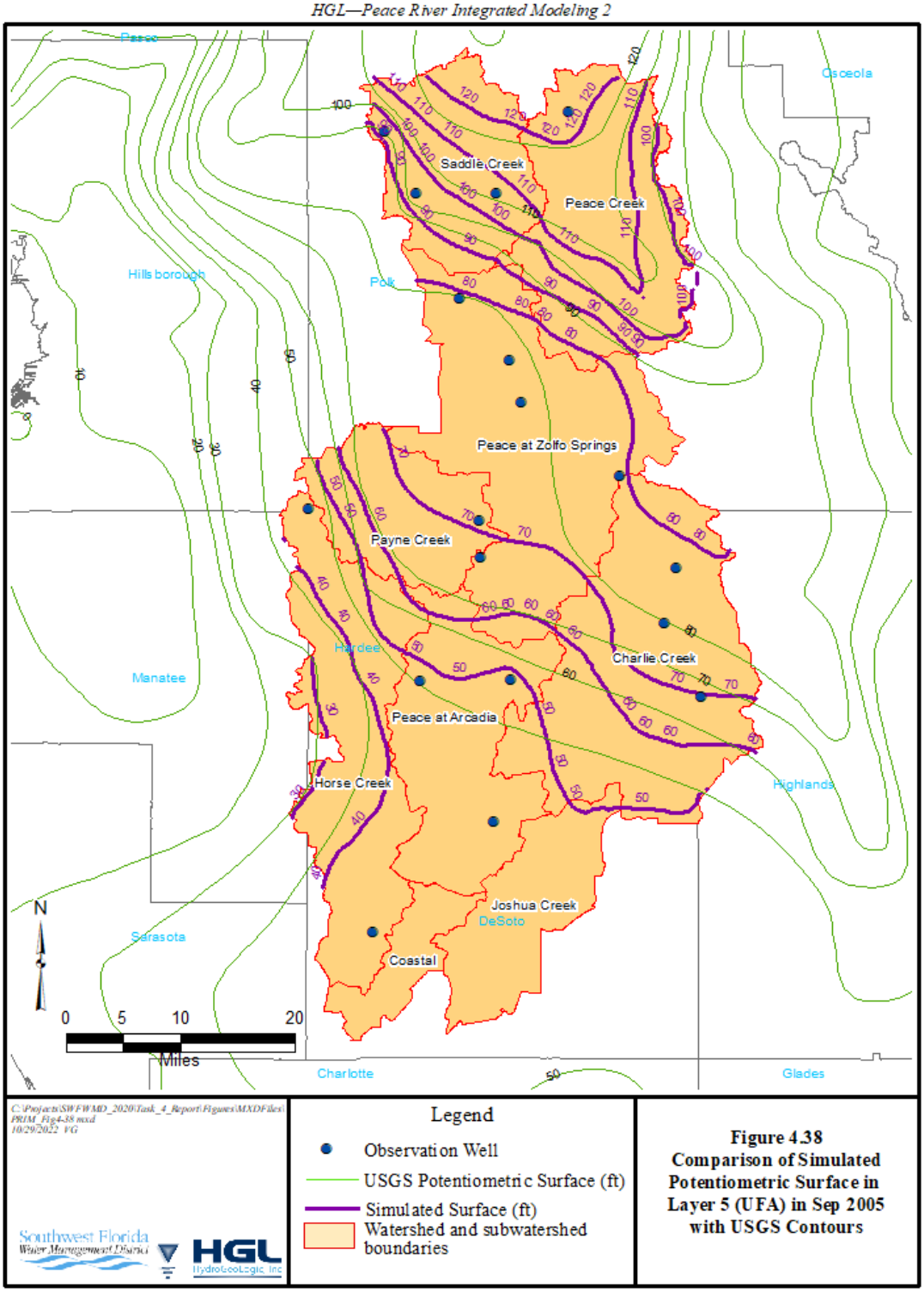

Figure 4.38
Comparison of Simulated Potentiometric Surface in Layer 5 (UFA) in Sep 2005 with USGS Contours

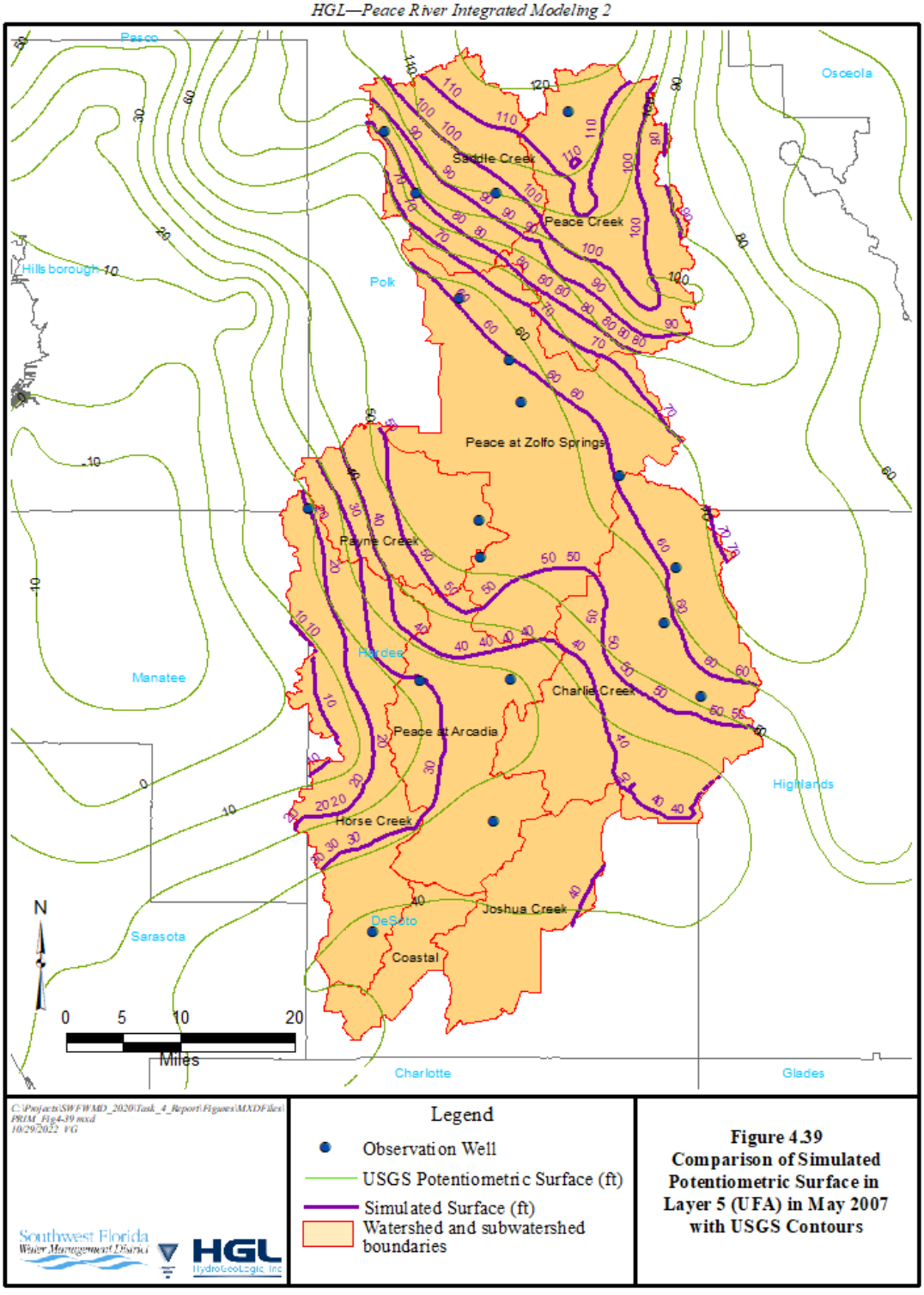

Figure 4.39
Comparison of Simulated Potentiometric Surface in Layer 5 (UFA) in May 2007 with USGS Contours

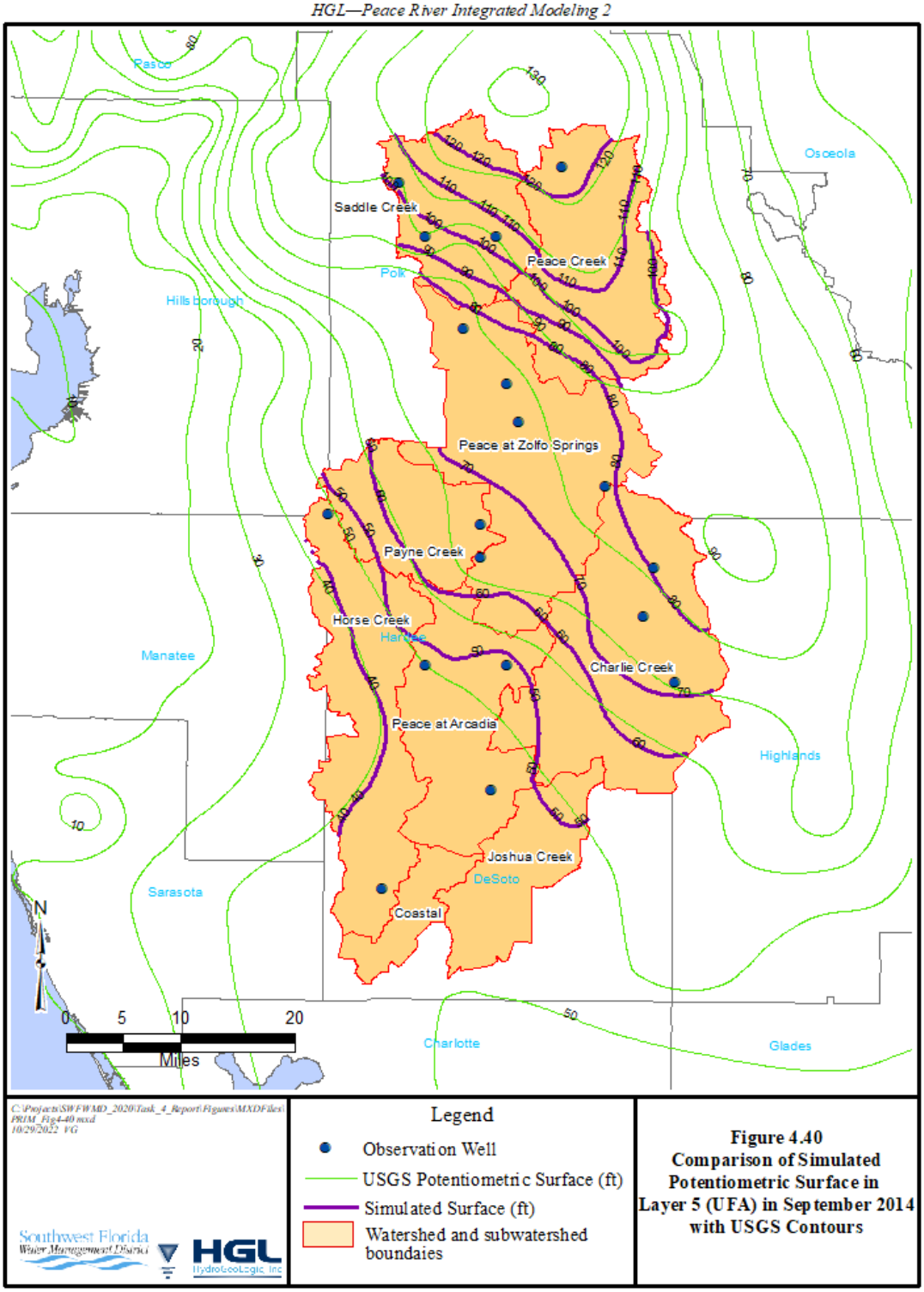

Figure 4.40
Comparison of Simulated Potentiometric Surface in Layer 5 (UFA) in September 2014 with USGS Contours

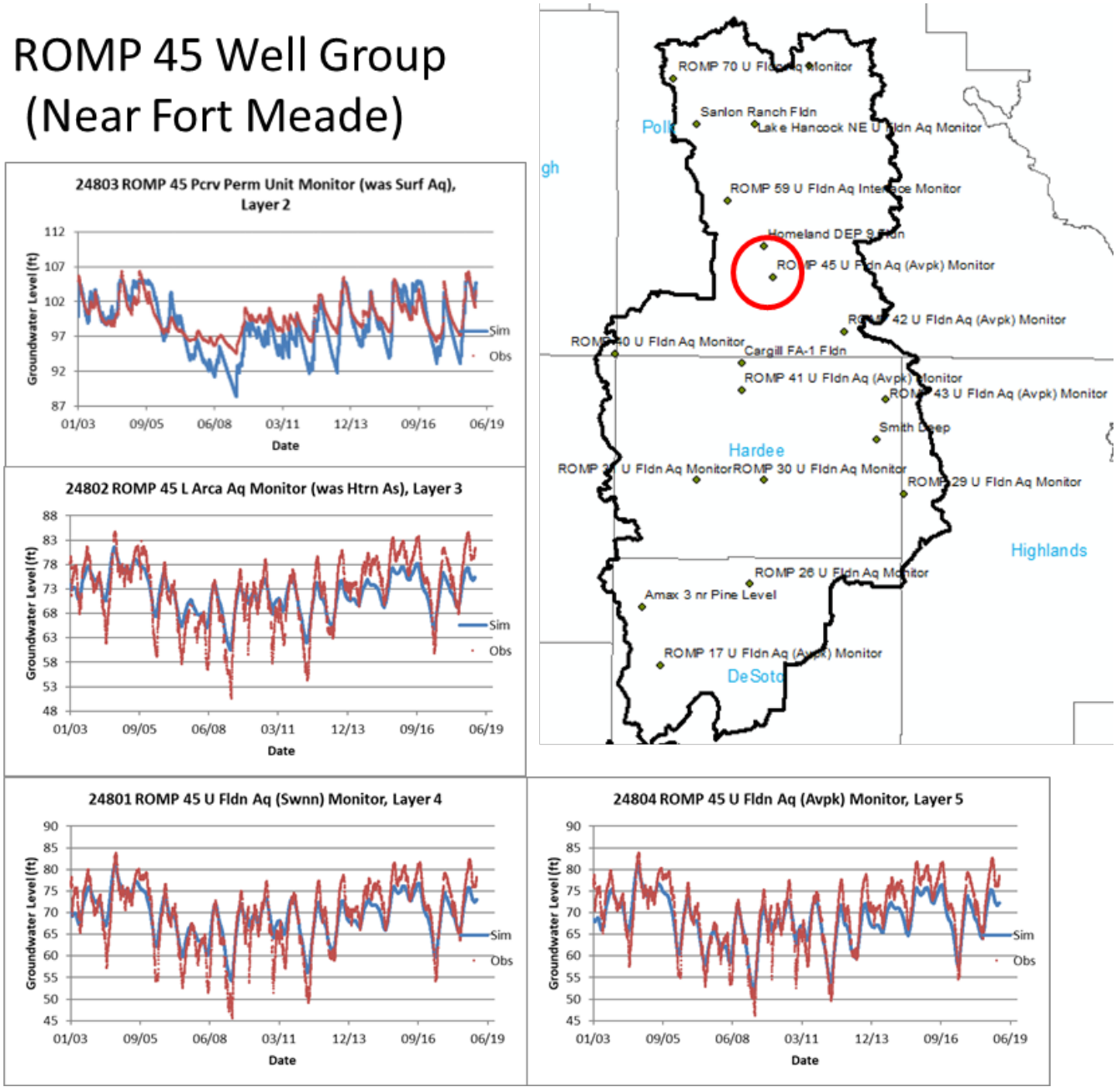

Figure 4.41 Observed and Simulated Groundwater Heads at ROMP 45

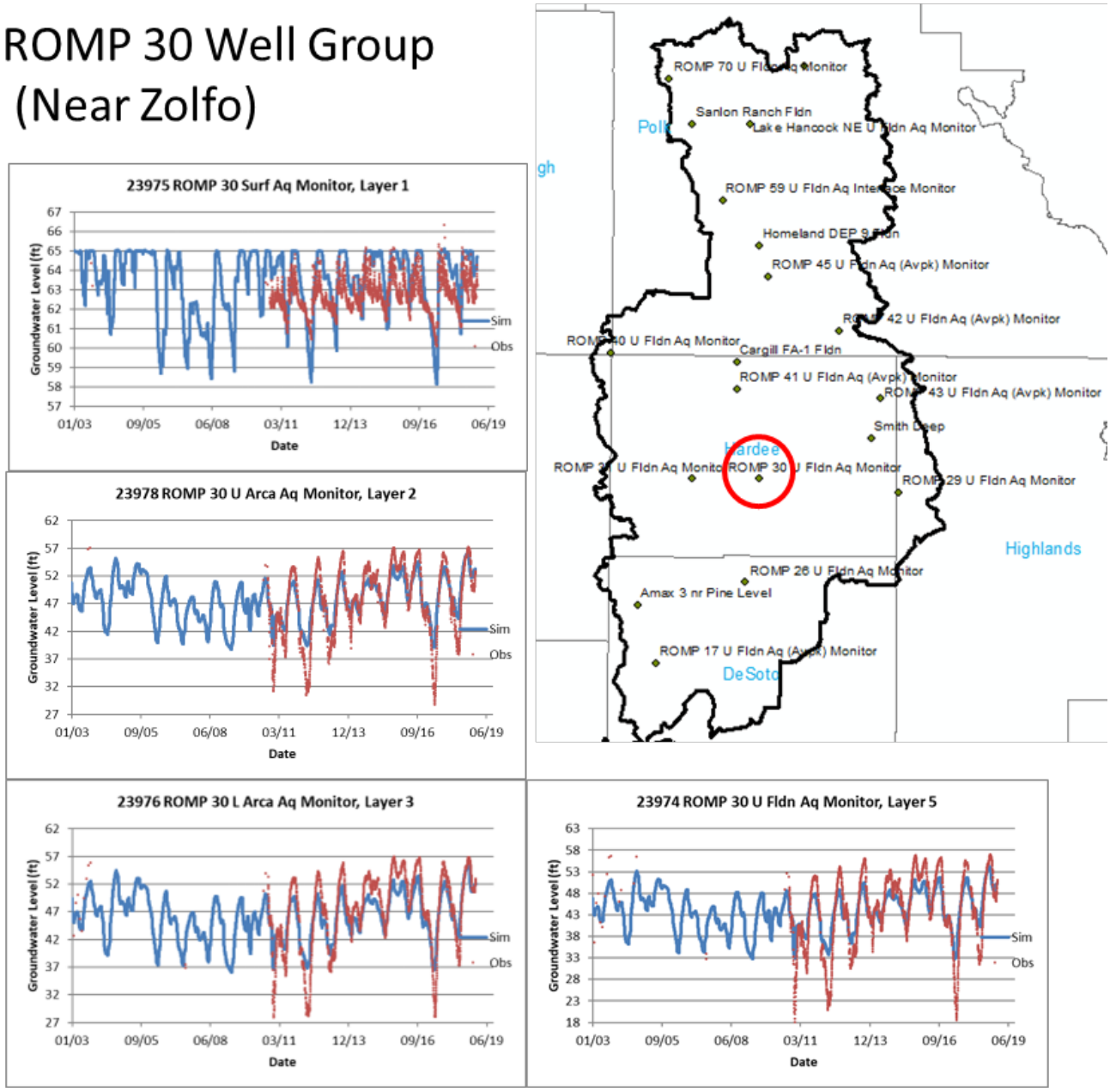

Figure 4.42 Observed and Simulated Groundwater Heads at ROMP 30

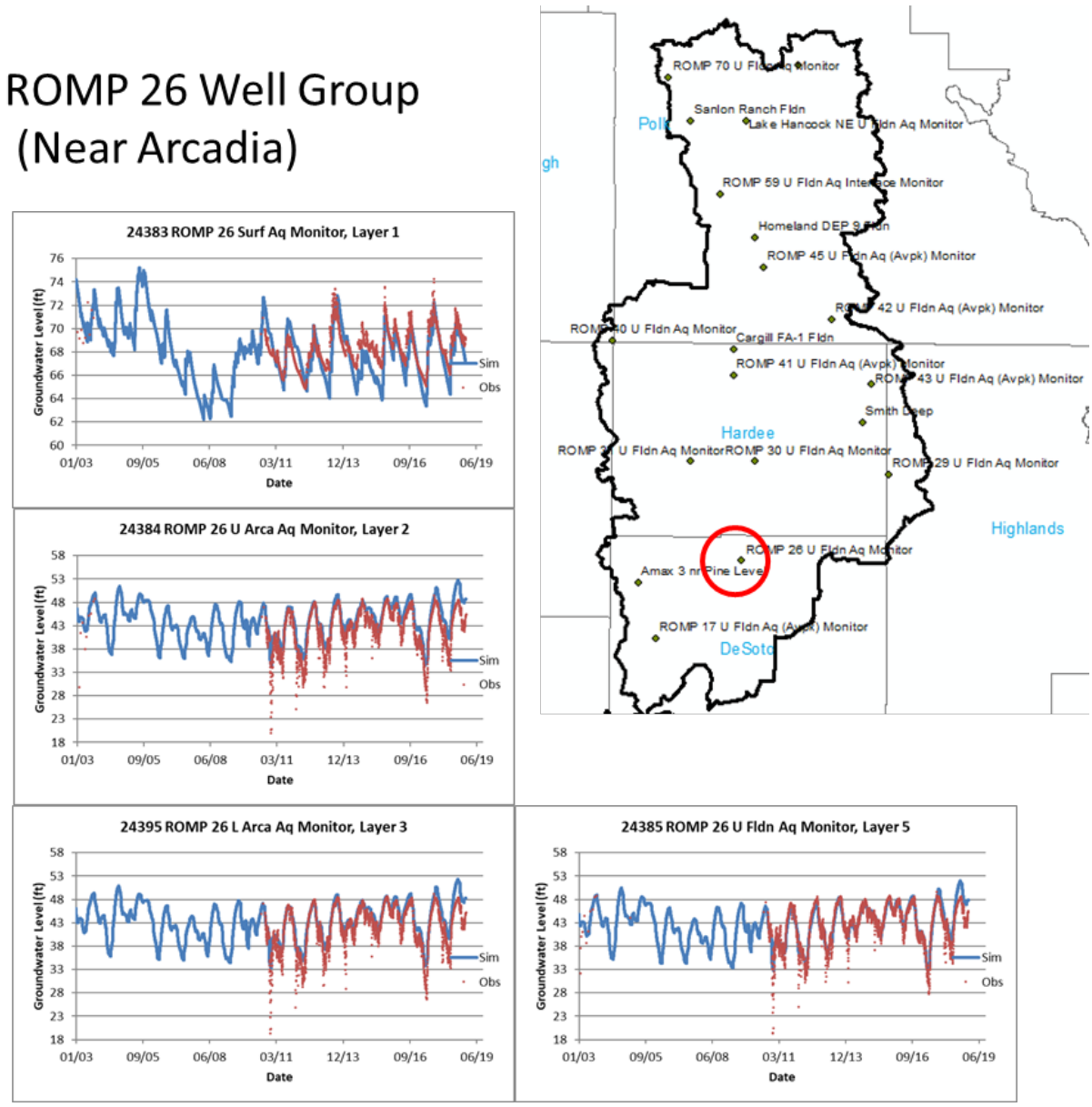

Figure 4.43 Observed and Simulated Groundwater Heads at ROMP 26

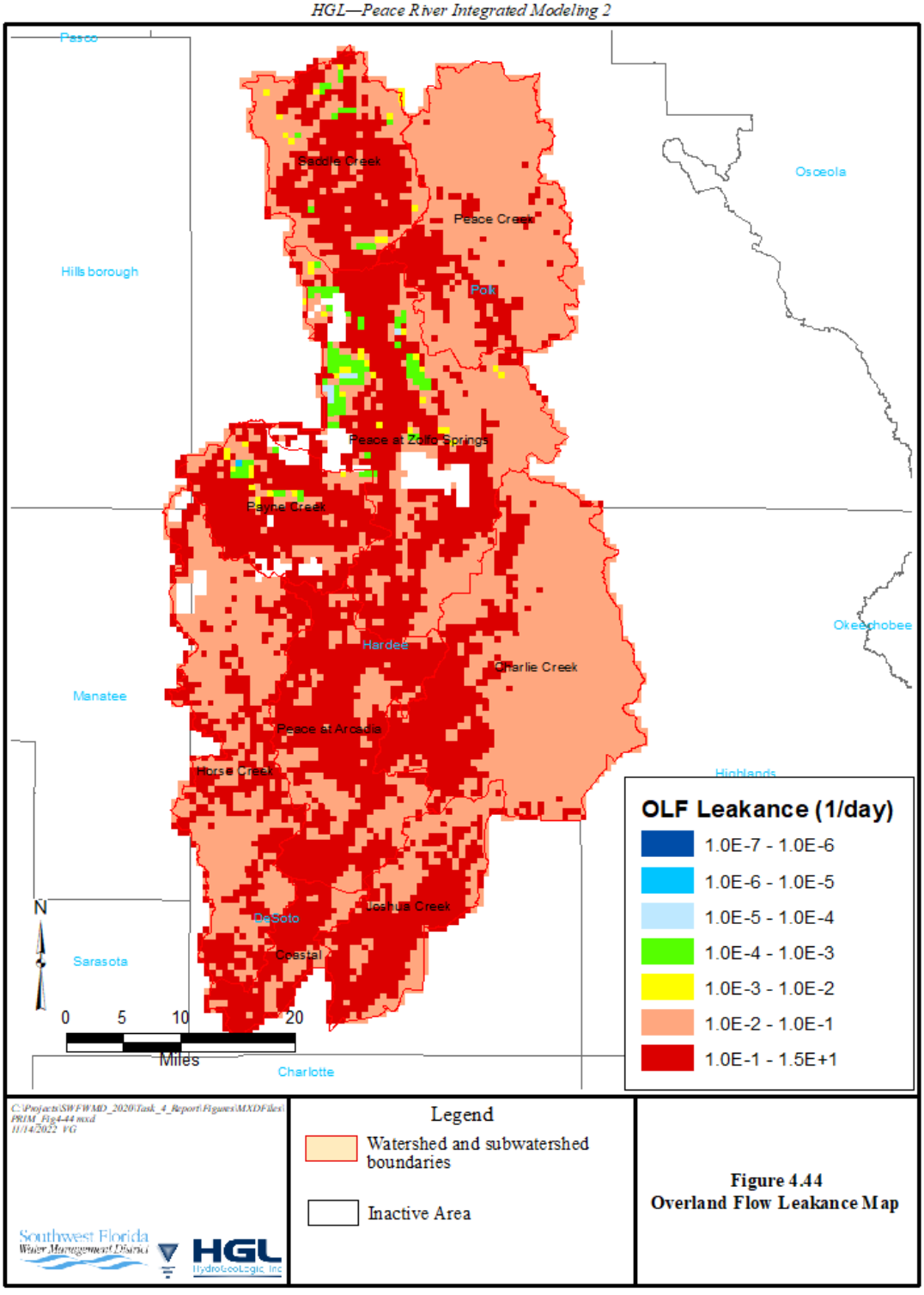

Figure 4.44
Overland Flow Leakance Map

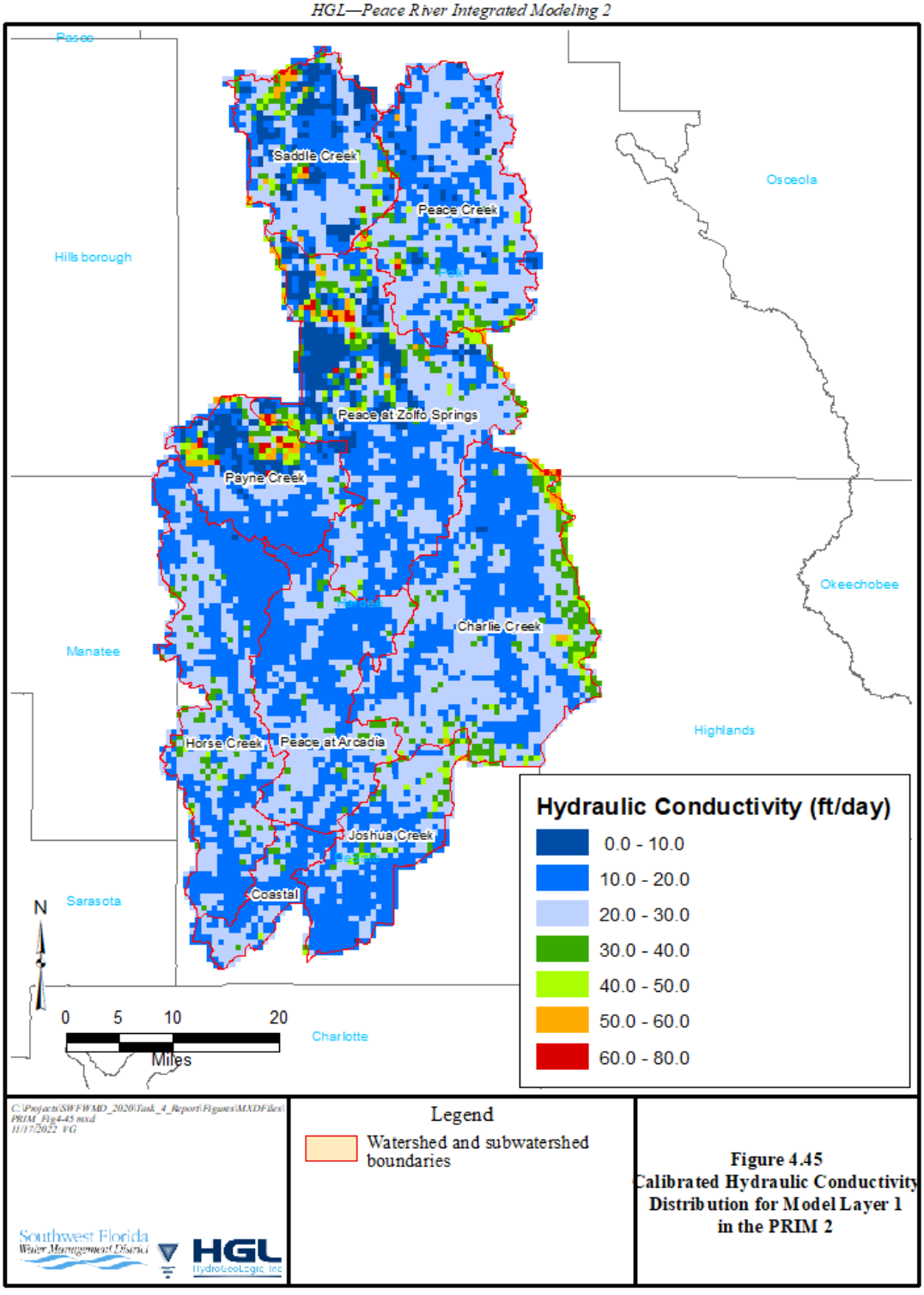

Figure 4.45
Calibrated Hydraulic Conductivity Distribution for Model Layer 1 in the PRIM 2

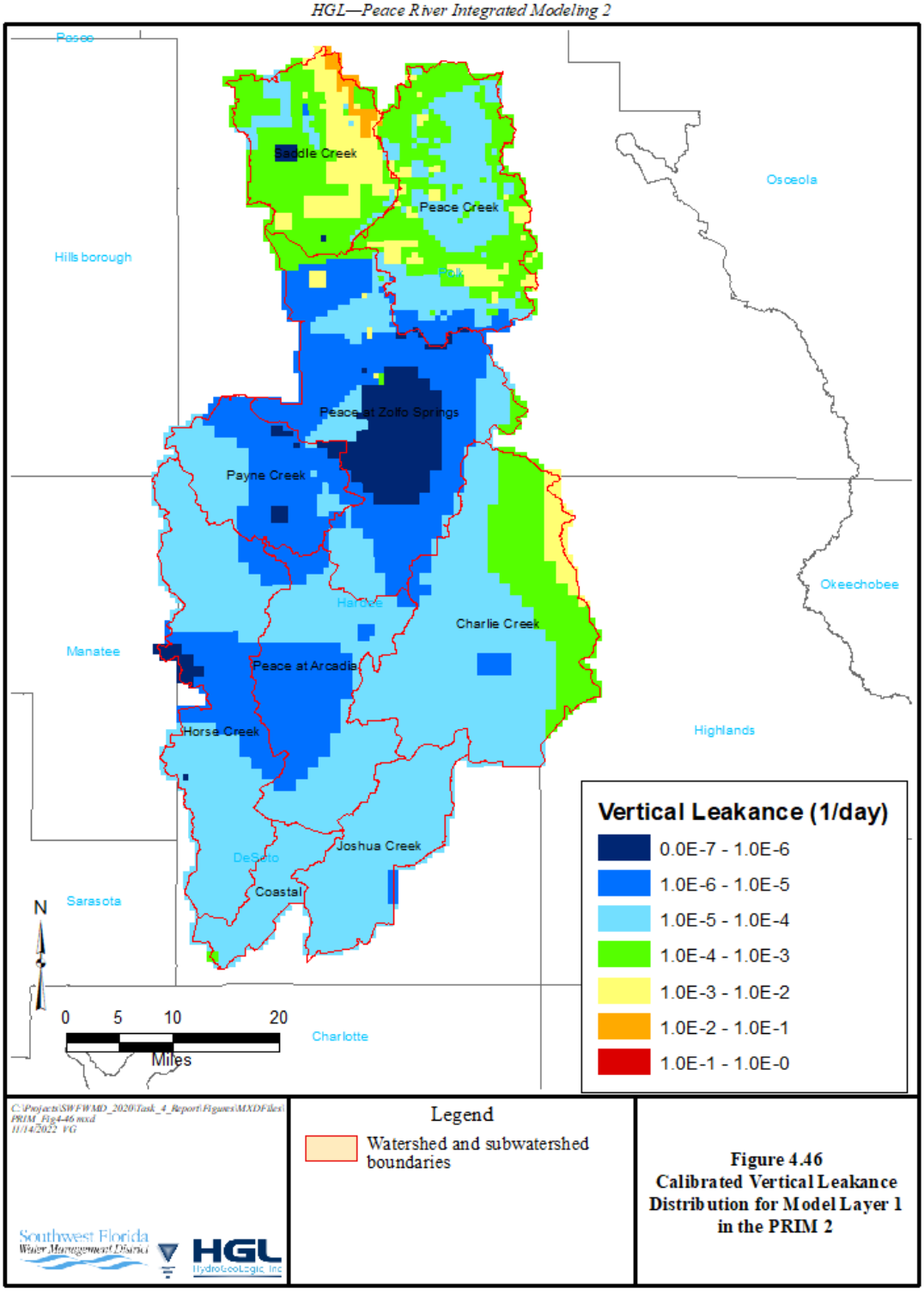

Figure 4.46
Calibrated Vertical Leakance Distribution for Model Layer 1 in the PRIM 2

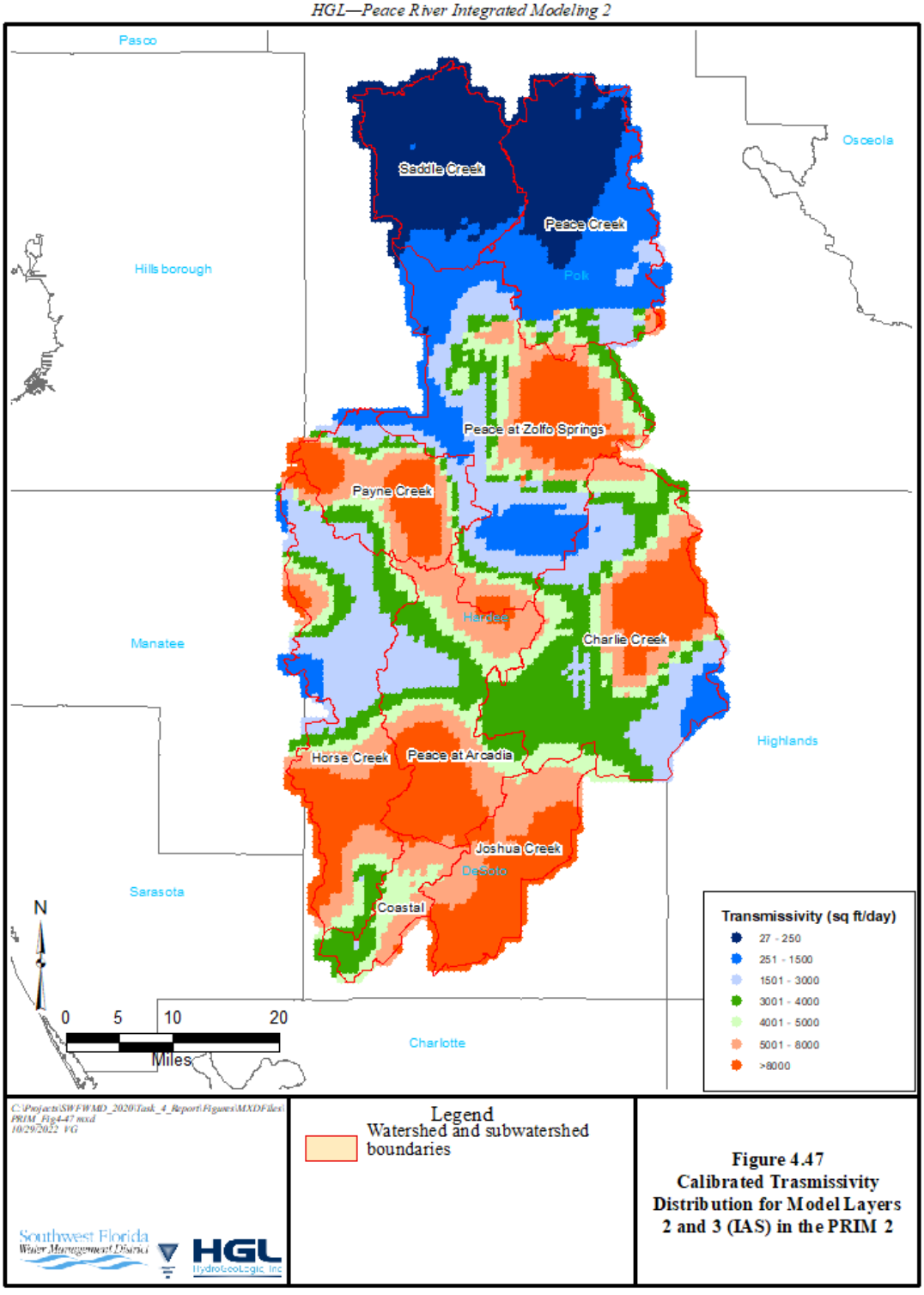

Figure 4.47
Calibrated Trasmissivity Distribution for Model Layers 2 and 3 (IAS) in the PRIM 2

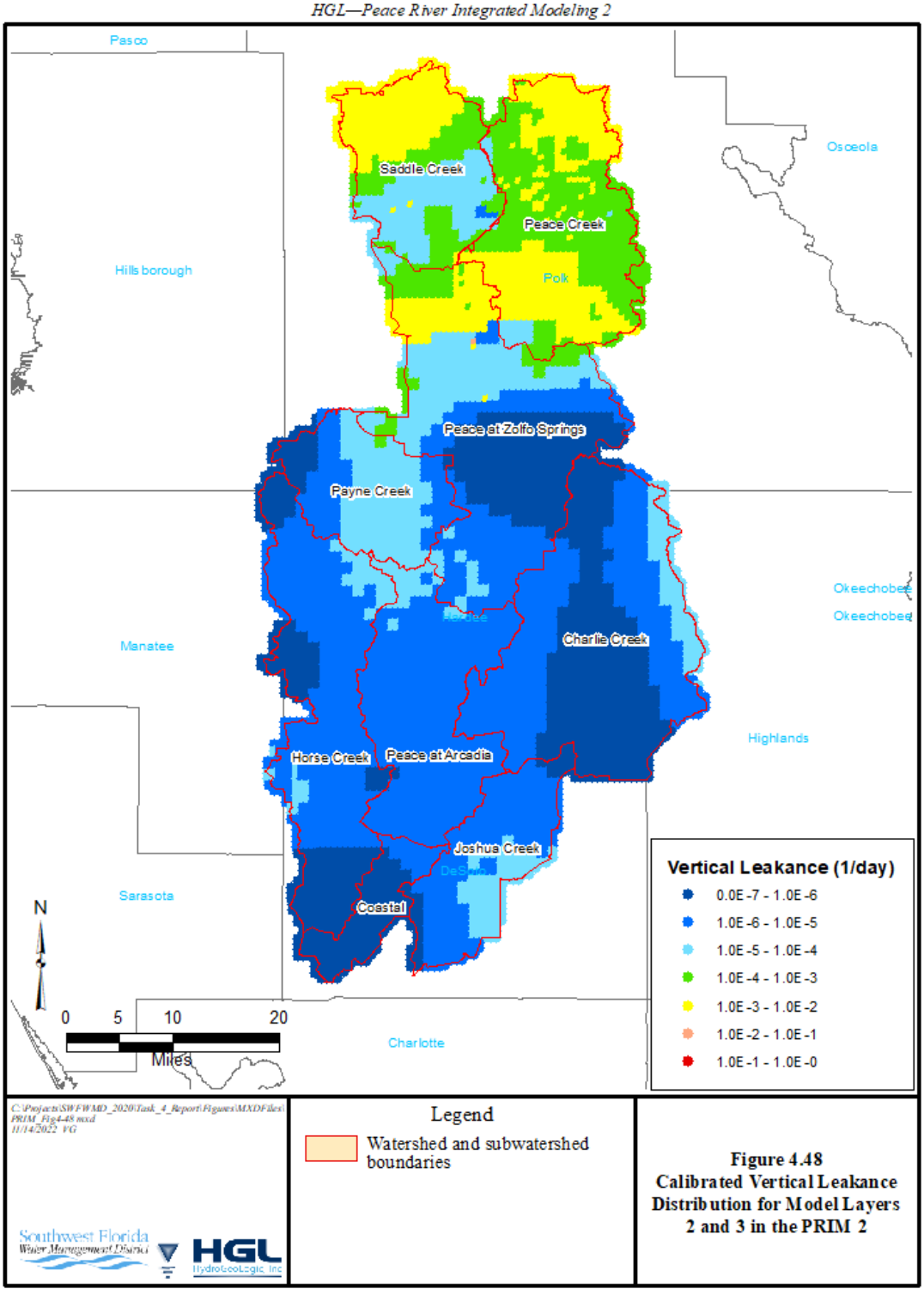

Figure 4.48
Calibrated Vertical Leakance Distribution for Model Layers 2 and 3 in the PRIM 2

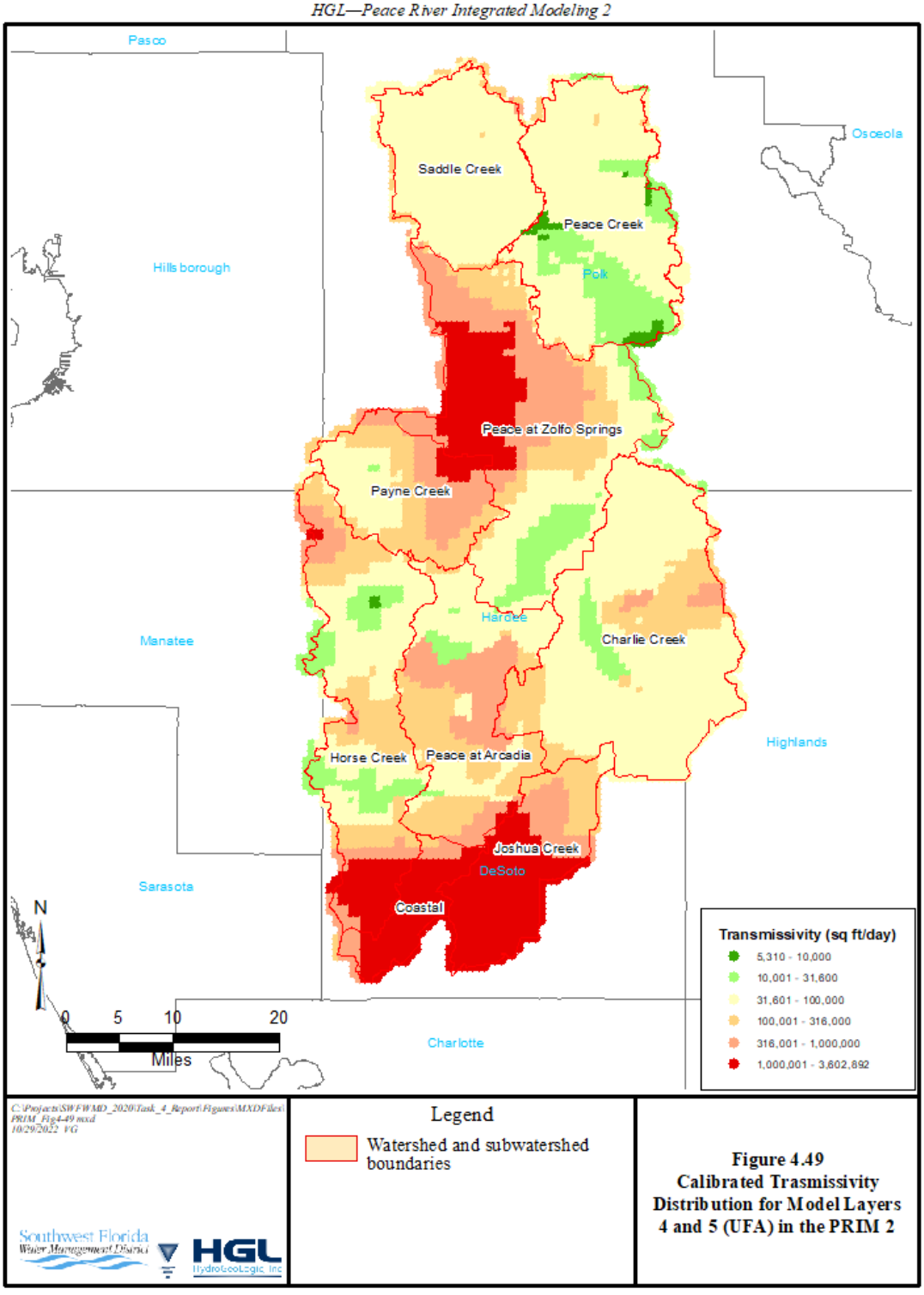

Figure 4.49
Calibrated Trasmissivity Distribution for Model Layers 4 and 5 (UFA) in the PRIM 2

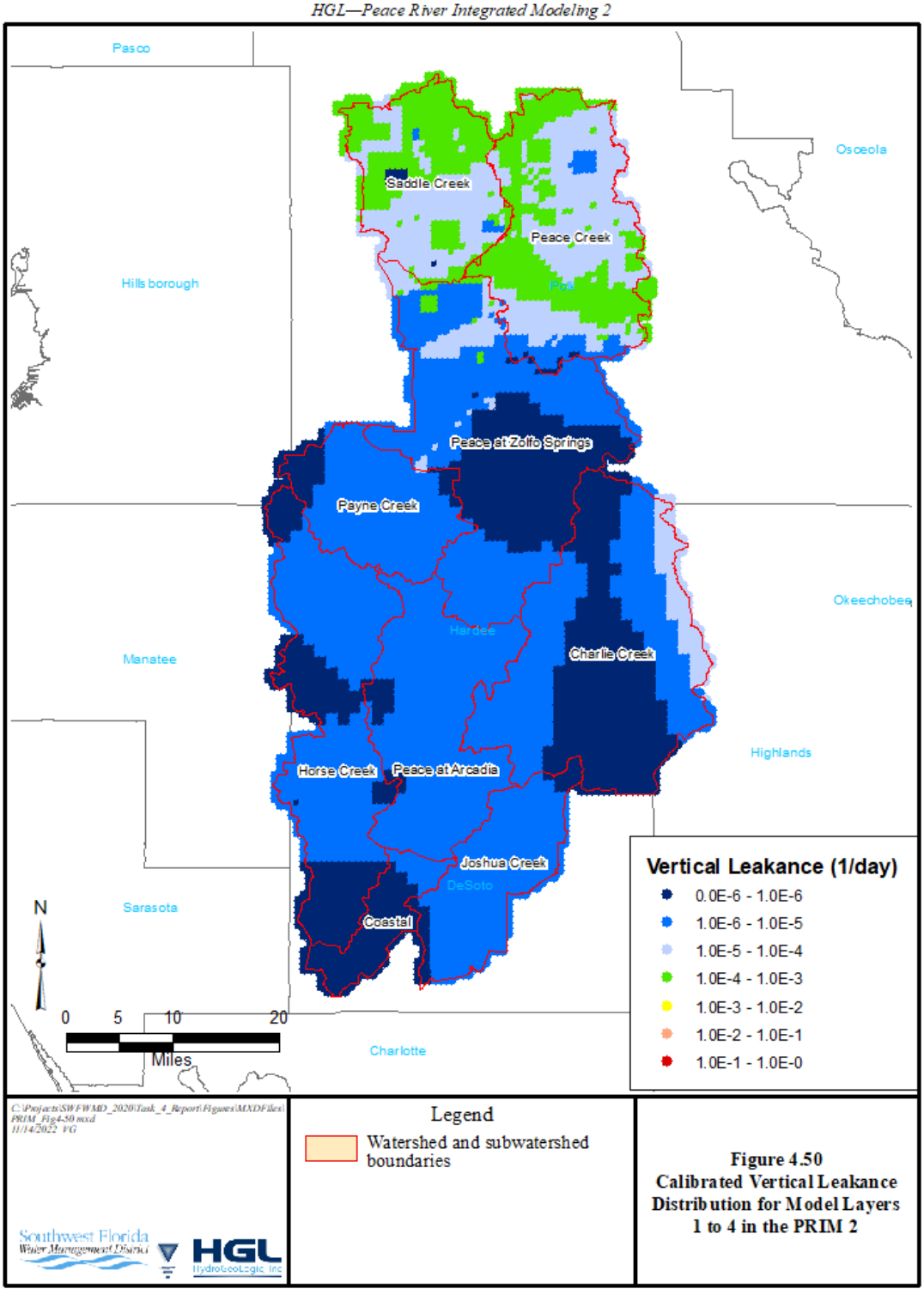

C:\Projects\SWFWMD_2020\Task_4_Report\Figures\MXDFiles\PRIM_Fig4-50.mxd
11/14/2022 VG

Legend

Watershed and subwatershed boundaries

Southwest Florida Water Management District

HGL HydroGeoLogic Inc

Figure 4.50
Calibrated Vertical Leakance Distribution for Model Layers 1 to 4 in the PRIM 2

TABLES

This page was intentionally left blank.

Table 4.1
Primary Calibration Goals

Parameter	Units	Metric [1]	Goal
Streamflows			
Weekly Average Streamflows	cfs	AE, MAE, RMSE	RMSE < 5% AE < 5% for Peace River gages AE < 10% for other gages
Daily Flow Exceedance – 10th Percentile	cfs	MxE, MnE	< ±15%
Daily Flow Exceedance – 50th Percentile	cfs	MxE, MnE	< ±15%
Daily Flow Exceedance – 90th Percentile	cfs	MxE, MnE	< ±15%
Coefficient of Determination for Weekly Flows	-	R^2	$R^2 > 0.6$
Nash Sutcliffe Efficiency	-	E	E > 0.5
Percent Bias	-	PBIAS	PBIAS < ±25%
RMSE (model)/SD (data) (Normalized RMSE)	-	NRMSE	NRMSE < 0.7
Lake Levels			
Lake Levels	ft	AE, MAE, RMSE, MxE, MnE	RMSE < 2 MxE, MnE < ± 5
Lake Coefficient of Determination	-	R^2	$R^2 > 0.7$
Groundwater Levels			
Surficial Aquifer (SA) Heads	ft	AE, MAE, RMSE, MxE, MnE	AE < ±1, MAE < 4 RMSE < 5 MxE, MnE < ± 10 MAE < 2.5 ft for 50% of the wells, MAE < 5 ft for 80% of the wells
SA Coefficient of Determination	-	R^2	$R^2 > 0.5$
SA Nash Sutcliffe Efficiency	-	E	E > 0.5
SA Percent Bias	-	PBIAS	PBIAS < ±25%
Intermediate Aquifer System (IAS) Heads	ft	AE, MAE, RMSE, MxE, MnE	RMSE < 5, MAE < 4 MxE, MnE < ± 10 MAE < 2.5 ft for 50% of the wells, MAE < 5 ft for 80% of the wells
IAS Coefficient of Determination	-	R^2	$R^2 > 0.5$
IAS Nash Sutcliffe Efficiency	-	E	E > 0.5
IAS Percent Bias	-	PBIAS	PBIAS < ±25%
Upper Floridan Aquifer (UFA) Heads	ft	AE, MAE, RMSE, MxE, MnE	RMSE < 5, MAE < 4 MxE, MnE < ± 10 MAE < 2.5 ft for 50% of the wells, MAE < 5 ft for 80% of the wells
UFA Coefficient of Determination	-	R^2	$R^2 > 0.7$
UFA Nash Sutcliffe Efficiency	-	E	E > 0.5
UFA Percent Bias	-	PBIAS	PBIAS < ±25%

[1]See Appendix A for definitions of calibration metrics.

Table 4.2
Calibration Statistics for Selected Streamgages

Site	AE[(1)] (cfs)	%AE (< 5%)	RMSE (cfs)	%RMSE (< 5%)	R^2 (≥ 0.60)	E (≥ 0.70)	Percent Bias <25%	NRMSE (RMSE/ Obs SD) <0.7
Peace River								
Bartow	-22.77	-0.57%	175.74	4.38%	0.78	0.76	-11.64	0.49
Fort Meade	-30.30	-1.24%	171.23	6.99%	0.80	0.77	-13.77	0.48
Zolfo Springs	-21.83	-0.21%	340.64	3.31%	0.82	0.82	-4.00	0.43
Arcadia	110.07	0.51%	752.13	3.47%	0.77	0.76	11.08	0.49
Sub-Basins								
Saddle Creek at P-11	1.11	0.07%	8.74	0.54%	0.99	0.99	0.04	0.00
Peace Creek nr. Wahneta	18.18	1.86%	71.63	7.34%	0.74	0.72	19.98	0.53
Payne Creek nr. Bowling Green	-35.63	-0.77%	171.42	3.72%	0.62	0.33	-26.87	0.82
Charlie Creek nr. Gardner	105.66	1.16%	400.87	4.39%	0.56	0.50	37.79	0.71
Horse Creek near Arcadia	16.25	0.93%	45.69	2.63%	0.69	0.62	43.30	0.61
Joshua Creek nr. Nocatee	34.94	0.46%	196.56	2.58%	0.52	0.51	26.91	0.70

[(1)]Error = observed-simulated

Table 4.3
Observed and Simulated Flow Percentiles for Main Peace River Gages from 2003 to 2018

Gage Name	10th			50th			90th		
	Observed (cfs)	Simulated (cfs)	Error[(1)] (%)	Observed (cfs)	Simulated (cfs)	Error (%)	Observed (cfs)	Simulated (cfs)	Error (%)
Peace River at Bartow	9.1	9.8	7.6%	52.6	62.7	19.4%	552.0	617.9	11.9%
Peace River at Fort Meade	5.7	11.9	108 .7%	70.0	85.9	22.8%	675.0	733.0	8.6%
Peace River at Zolfo Spring	43.1	66.3	53.9%	241.0	282.0	17.0%	1510.0	1529.8	1.3%
Peace River at Arcadia	72.8	83.9	15.3%	401.0	405.0	1.0%	2775.0	2236.8	-19.4%

[(1)]%Error = (observed/simulated)/observed

Table 4.4
Observed and Simulated Flow Percentiles for Tributary Streamgages from 2003 to 2018

Gage Name	10th			50th			90th		
	Observed (cfs)	Simulated (cfs)	Error[1] (%)	Observed (cfs)	Simulated (cfs)	Error (%)	Observed (cfs)	Simulated (cfs)	Error (%)
Saddle Creek at Structure P-11	0.0	0.0	N/A	0.1	3.5	N/A[2]	260.0	260.1	0.0%
Peace Creek near Wahneta	7.0	7.8	11.6%	34.5	28.1	-18.1%	267.0	175.4	-33.2%
Charlie Creek at Gardner	6.6	6.0	-9.7%	62.2	66.8	8.2%	837.4	480.9	-41.9%
Payne Creek at Bowling Green	6.0	10.6	76.7%	50.0	79.9	-10.60%	317.0	466.4	8.52%
Horse Creek near Arcadia	5.1	0.5	-98.2%	42.6	21.9	-71.0%	490.0	356.9	-50.6%
Joshua Creek at Nocatee	14.0	11.5	-7.14%	36.0	34.2	-5.56%	315.0	184.6	-52.41%

[1]%Error = (observed/simulated)/observed
[2] Observed is close to zero

Table 4.5
Summary of Lake Level Calibration Results

Metric (Calibration Goal)	Number of Sites	% of Sites
R^2 (>0.70)		
< 0.50	26	29%
≥0.50	63	71%
≥0.70	29	33%
≥0.90	2	2%
RMSE (< 2 feet)		
< 1	15 (min = 0.49 feet)	17%
< 2	53	60%
< 3	74	83%
< 4	77	87%
< 5	84 (max =12.4 feet)	94%
Average Error		
-1 ≤ × ≤ 1 feet	26	29%
-2 ≤ × ≤ 2 feet	64	72%
-3 ≤ × ≤ 3 feet	76 (min = -7.9 feet; max = + 12.4 feet)	85%

Table 4.6
Summary of Groundwater Calibration Statistics

(a) 2003-2018 Average Head

Metric	Aquifer		
	SA	IAS	UFA
Long-Term Average Heads			
AE[(1)] < ±1 (ft)	0.01	-1.47	0.34
MAE (ft) < 4 (ft)	2.94	2.93	2.69
RMSE < 6 (ft)	4.71	3.97	3.75
Max Error < ± 10 (ft)	21.71	3.23	11.28
Min Error < ± 10 (ft)	-9.82	-9.12	-6.27
AE < 2.5 ft for 50% of the wells	64%	61%	61%
AE < 5 ft for 80% of the wells	86%	82%	81%
R^2 > 0.8, 0.7, 0.6	0.97	0.98	0.97
Nash-Sutcliffe Efficiency > 0.5	0.97	0.98	0.97
Percent Bias < ±25%	-0.01%	2.10%	-0.47%

[(1)]Error = observed-simulated

(b) Heads at Individual Wells

Metric	Aquifer					
	SA		IAS		UFA	
	Number of Wells	Percent of Aquifer	Number of Wells	Percent of Aquifer	Number of Wells	Percent of Aquifer
R^2						
≥0.60	24	57%	21	75%	34	94%
≥0.70	15	36%	17	61%	29	81%
≥0.80	3	7%	10	36%	21	58%
RMSE						
< 2	11	26%	3	11%	3	8%
< 4	30	71%	15	36%	20	56%
< 6	35	83%	21	75%	30	83%
AE[(1)]						
-1 ≤ × ≤ 1 feet	10	24%	7	25%	11	30%
-2 ≤ × ≤ 2 feet	21	50%	14	50%	18	50%
-3 ≤ × ≤ 3 feet	29	69%	19	68%	22	61%
MAE						
MAE < 2.5 ft for 50% of the wells	26	62%	10	36%	12	33%
MAE < 5 ft for 80% of the wells	35	83%	22	79%	29	81%
Nash-Sutcliffe Efficiency						
>0.5	30	71%	22	79%	34	94%
>0.7	15	36%	17	61%	29	81%
>0.9	1	2%	0	0%	6	17%
PBias						
PBias < ±25%	42	100%	28	100%	36	100%

[(1)]Error = observed-simulated

Table 4.7
Annual Water Budgets for the Calibrated PRIM Model

	Inflow (in/yr)					Outflow (in/yr)						Total (in/yr)		
Year	Lateral GW Inflow	NPDES Discharge	Injection	Rainfall	Return Flow	Lateral GW Outflow	SW Outflow	EVT	Lake Hancock Pumping	GW Pumping	Storage Gain	Total In	Total Out	Discrepancy
2003	2.05	0.99	0.99	51.15	1.79	3.70	13.92	40.03	0.00	1.92	-2.34	56.97	57.24	0.48%
2004	2.21	1.22	1.29	59.97	1.78	3.95	17.87	40.68	0.00	1.91	2.61	66.47	67.03	0.85%
2005	2.37	1.40	0.78	66.13	1.40	4.64	21.99	42.66	0.00	1.53	1.63	72.07	72.45	0.52%
2006	2.50	0.44	0.07	44.31	2.24	5.03	5.82	41.31	0.00	2.37	-4.86	49.57	49.67	0.20%
2007	2.06	0.32	0.04	36.62	2.17	4.74	1.61	41.10	0.00	2.30	-8.50	41.21	41.25	0.08%
2008	2.42	0.45	0.04	46.19	1.86	4.52	3.53	39.50	0.00	2.02	1.45	50.97	51.02	0.10%
2009	2.67	0.57	0.04	46.81	2.22	4.68	3.05	39.66	0.00	2.35	2.64	52.31	52.39	0.14%
2010	2.45	0.73	0.16	47.68	2.11	4.05	5.59	42.87	0.00	2.16	-1.47	53.13	53.20	0.12%
2011	2.85	0.49	0.26	46.28	1.84	4.72	4.19	40.53	0.00	1.88	0.49	51.73	51.81	0.17%
2012	2.74	0.53	0.27	44.61	2.24	4.77	4.49	38.42	0.00	2.31	0.41	50.39	50.41	0.04%
2013	2.47	0.89	0.22	46.24	1.93	4.27	7.27	39.39	0.00	1.98	-1.15	51.75	51.76	0.02%
2014	2.59	0.53	0.54	50.60	1.68	4.02	5.04	41.58	0.00	1.73	3.65	55.95	56.02	0.14%
2015	2.47	0.90	0.56	54.64	1.58	4.17	10.07	42.78	0.00	1.67	1.55	60.15	60.24	0.15%
2016	2.48	0.94	0.73	52.46	1.59	4.18	11.22	43.62	0.15	1.67	-2.52	58.19	58.31	0.20%
2017	2.39	0.75	1.11	53.42	1.79	4.69	12.70	40.68	0.04	1.89	0.31	59.46	60.32	1.44%
2018	2.16	2.92	0.93	55.35	1.73	3.94	10.88	42.59	0.19	1.78	3.81	63.09	63.18	0.13%
Average	2.43	0.88	0.50	50.15	1.87	4.38	8.70	41.09	0.02	1.97	-0.14	55.84	56.02	0.32%

This page was intentionally left blank.

5.0 SUMMARY AND DISCUSSION

The Peace River Integrated Model (PRIM) has been updated and recalibrated using long-term data from 2003 to 2018 (16 years) and is now referred to as PRIM 2. Several of its strengths have been detailed in this document including the calibration period of the current version, which is more than three times that of the original (PRIM 1) model, which was calibrated using data from 1998 to 2002. The calibration of PRIM 2 also demonstrates that it is able to reproduce observed high and low patterns of streamflow, lake levels, and groundwater heads quite accurately. Moreover, PRIM 2 also matched groundwater potentiometric elevations successfully.

Streamflow was calibrated using observations from 19 streamgages. Of these gages, four are located along the Peace River, and six are located along sub-basin main tributary streams near the respective confluences between the tributary streams and the Peace River. Discharge or streamflow percentiles, along with other statistical metrics, were used to demonstrate the agreement between observed data and simulation results. Calibration criteria were met at all four gages along the Peace River, while at the six tributary gages most calibration criteria were met. Most stream gages were favorably replicated in terms of magnitude, temporal fluctuation, and flow percentiles.

For the PRIM 1 model, the calibration focused on the 20 lakes in the Saddle Creek (11 lakes) and Peace Creek (9 lakes) sub-basins. These lakes were individually calibrated. For the PRIM 2 model, the calibration focused on 11 Minimum Flows and Levels (MFL) lakes. Five of these 11 lakes were part of the PRIM 1-focused lakes. Most of the MFL lakes met all or most of the calibration criteria. However, the deviation from the observed data was thought to be affected by the resolution of lake storage information (depth-area relation). Moreover, lake elevations were found to be sensitive to leakance changes in the SA, which could also affect streamflows. The current lake properties were a compromise between the calibration of groundwater heads, streamflows, and lakes.

Groundwater head calibration statistics indicate that all aquifers met all calibration criteria, except for average error (AE) in the IAS. Based on the negative AE and the relatively small mean absolute error (MAE), it may be inferred that the simulated potentiometric surface in the IAS is similar to that of the observed; however, the simulated surface is generally lower than the observed. The leakances between the SA and the UFA in the model could not be further adjusted, as the statistics in the SA and the UFA as well as streamflows at gages would be significantly impacted. The deviation in the IAS could also stem from the discretization disparity between PRIM 2 and the ECFTX model. The IAS boundary heads of PRIM 2 were extracted from the ECFTX model, which has one layer representing the IAS, whereas the IAS in PRIM 2 was simulated using two layers. The IAS is considered less known than the SA and the UFA due to its complex hydrogeology. The accuracy of the IAS may be improved in the future with additional information and vertical refinement of the ECFTX model.

This page was intentionally left blank.

6.0 REFERENCES

Barnes, 1967. Roughness Characteristics of Natural Channels. USGS Water-Supply Paper 1849, 213 pages.

Barr, G.L., 1996. Hydrogeology of the Surficial and Intermediate Aquifer Systems in Sarasota and Adjacent Counties. U.S. Geological Survey WRI Report 96-4063.

Basso, R.J., 2002. Hydrostratigraphic Zones within the Eastern Tampa Bay Water Use Caution Area. Southwest Florida Water Management District.

BCI Engineers & Scientists, Inc. (BCI), 2006. Lake Hancock Lake Level Modification Project Minimum Flows and Levels Recovery Conceptual ERP Submittal, Appendix A, Single Event Watershed Model. Southwest Florida Water Management District, Brooksville, Florida.

Beach, M.H., 2006. Southern District Ground-Water Flow Model, Version 2.0. Hydrologic Evaluation Section, Resource Conservation and Development Department, Southwest Florida Water Management District, Brooksville, Florida.

Chow, V.T., 1959. Open-Channel Hydraulics. McGraw Hill Book Company.

Central Florida Water Initiative, 2020. Model Documentation Report East-Central Florida Transient Expanded (ECFTX) Model. Central Florida Water Initiative, February 2020.

Clayton, J.M., 2009. Summary of Well Construction Activities at Three Nested Well Sites around Lake Hancock in West-Central Polk County, Florida. Southwest Florida Water Management District.

Duerr, A.D. and G.M. Enos, 1990. Hydrogeology of the Intermediate Aquifer System and Upper Floridan Aquifer, Hardee and DeSoto Counties, Florida. U.S. Geological Survey Water Resources Investigations Report 90-4104.

Environmental Simulations, Inc., 2004. Development of the District Wide Regulation Model for Southwest Florida Water Management District.

Garlanger, J.E., 2002. Effects of Phosphate Mining and Other Land Uses on Peace River Flows, for the Florida Phosphate Council, January 11.

Geurink, J.S., M. Nachabe, M. Ross, and P. Tara, 2000. Development of Interfacial Boundary Conditions for the Southern District Ground Water Model of the Southwest Florida Water Management District (Draft Final Report). Southwest Florida Water Management District.

HydroGeoLogic, Inc. (HGL), 2007. MODHMS (Version 3.0) – A MODFLOW-Based Hydrologic Modeling System. Documentation and User's Guide, HydroGeoLogic, Inc., Reston, Virginia.

HydroGeoLogic, Inc. (HGL), 2008. Peace River Integrated Modeling Report (PRIM) – Report for Phase III.

HydroGeoLogic, Inc. (HGL), 2009. Report for Phase I – Peace River Integrated Modeling Project (PRIM). Prepared for Southwest Florida Water Management District.

HydroGeoLogic, Inc. (HGL), 2011. Peace River Integrated Modeling Project (PRIM) Final Report Phase IV: Basin-Wide Model. Prepared for Southwest Florida Water Management District.

Knochenmuss, L.A., 2006. Regional evaluation of the hydrogeologic framework, hydraulic properties and chemical characteristics of the intermediate aquifer system underlying southern west-central Florida. Scientific Investigations Report 2006-5013.

Lee, T.M., and A. Swancar, 1997. Influence of evaporation, groundwater, and uncertainty in the hydrologic budget of Lake Lucerne, a seepage lake in Polk County, Florida. U.S. Geological Survey Water-Supply Paper 2439, 61 pages.

Lewelling, B.R., and R.W. Wylie, 1993. Hydrology and Water Quality of Unmined and Reclaimed Basins in Phosphate-Mining Areas, West-Central Florida. U.S. Geological Survey Water Resources Investigations Report 93-4002, 93 pages.

Lewelling, B.R., A.B. Tihansky, and J.L. Kindinger, 1998. Assessment of the Hydraulic Connection Between Groundwater and the Peace River, West-Central Florida. Water Resources Investigations Report 97-4211. U.S. Geological Survey. 102 pages.

Metz, P.A., and B.R. Lewelling, 2010. Hydrologic Conditions that Influence Streamflow Losses in a Karst Region of the Upper Peace River, Polk County, Florida. USGS Scientific Investigations Report 2009-5140.

PBS&J, 2004. Peace Creek Watershed Management Plan – Watershed Evaluation Report.

PBS&J, 2007. Final Report for the Peace River Cumulative Impact Study. Prepared for Florida Department of Environmental Protection, Bureau of Mine Reclamation, and Southwest Florida Water Management District.

Said, A., 2010. Investigation of Leakage and Water Budget of Lake Hancock. Southwest Florida Water Management District.

SDI Environmental Services, Inc. (SDI), 2003. Cumulative Risk of Decreasing Streamflows in the Peace River Basin.

Singhofen, P., and L. Eaglin, 1995. ICPR User's Manual, Version 2.0. Streamline Technologies, Inc.

Southwest Florida Water Management District (SWFWMD), 2000. Aquifer Characteristics within the Southwest Florida Water Management District, Fourth Edition, Report 99-1.

SWFWMD, 2002. Upper Peace River−An Analysis of Minimum Flows and Levels, Draft. August 25.

Spechler, R.M., and S.E. Kroening, 2007. Hydrology of Polk County, Florida, U.S. Geological Survey Report SIR 2006-5320.

This page was intentionally left blank.

APPENDIX A

DEFINITION OF CALIBRATION METRICS

This page was intentionally left blank.

APPENDIX A
DEFINITION OF CALIBRATION METRICS

CALIBRATION METRICS

Calibration criteria were decided after a careful review of the objectives of the current modeling effort and of criteria used in other integrated groundwater/surface water models including the Western Orange and Seminole County Model (HGL, 2006), Marsh Driven Operations Model (HGL, 2006), and the Volusia County Tiger Bay/Bennett Swamp Model (CDM & DHI Water & Environment, Inc. [DHI], 2003).

The following metrics were employed to evaluate calibration and validation of the model:

Root Mean Square Error (RMSE): The mean value of the squared differences between observed and simulated values, calculated as

$$RMSE = \left[\frac{1}{n} \sum_{i=1}^{n} (x_i - s_i)^2 \right]^{0.5}$$

where

x_i = observed value
s_i = simulated value
n = number of observations (targets)

The RMSE is used to measure the discrepancy between modeled and observed values on an individual basis and indicates the overall predictive accuracy of the model. Due to the quadratic term, greater weight is given to larger discrepancies. Smaller values of RMSE indicate better model performance.

Average Error (AE): The mean value of the squared differences between observed and simulated values, calculated as

$$AE = \left[\frac{1}{n} \sum_{i=1}^{n} (x_i - s_i) \right]$$

The AE is used to measure the collective discrepancy between modeled and observed values and indicates the bias in simulated results. A value close to zero indicates no bias and thus reflects better model performance.

Maximum Error (MxE) and Minimum Error (MnE): The greatest positive and negative residuals between observed and simulated values.

$$MxE = Max\left[(x_i - s_i)\right]$$
$$MnE = Min\left[(x_i - s_i)\right]$$

When the MxE and MnE are expressed as a percentage, they are computed as

$$MxE = (Max[(x_i - s_i)]/x_i)100\%$$
$$MnE = (Min[(x_i - s_i)]/x_i)100\%$$

MxE and MnE represent the largest positive and negative residuals and indicate the worst errors, reflecting possible outlier situations in simulation or in the observed data.

Coefficient of Determination/Pearson Product-Moment Correlation Coefficient (R^2) between observed and simulated values, calculated as

$$R^2 = \left[\frac{\sum(x_i - x_m)(s_i - s_m)}{\left(\sum(x_i - x_m)^2 \sum(s_i - s_m)^2\right)^{0.5}}\right]^2$$

where

x_m = mean of observed data
s_m = mean of simulated data

R^2 is the measure of the degree of linear association between simulated and observed values and represents the amount of variability between them. The R^2 value can vary from 0 to 1, with 1 indicating a perfect fit between observed and simulated values.

Standard deviation (σ_x) of the observed values, calculated as

$$\sigma_x = \sqrt{\left[\frac{\sum(x_i - x_m)^2}{N}\right]}$$

where

x_m = mean of observed data

Standard deviation (σ_s) of the simulated values, calculated as

$$\sigma_s = \sqrt{\left[\frac{\sum(s_i - s_m)^2}{N}\right]}$$

where

s_m = mean of simulated data

Standard deviation is a measure of the dispersion/spread of the data set.

Nash-Sutcliffe Efficiency Coefficient (E) between observed and simulated values, calculated as

$$E = 1 - \left[\frac{\sum (x_i - s_i)^2}{\sum (x_i - x_m)^2} \right]$$

Like the R^2 discussed above, E is another indicator of goodness of fit and is one that has been recommended by the American Society of Civil Engineers (ASCE, 1993) for use in hydrologic studies. A value equal to 1 indicates a perfect fit between observed and simulated values, and values equal to zero indicate that the model is predicting no better than using the average of the observed data. Therefore, any positive value above zero suggests that the model has some utility, with higher values indicating better performance. Generally, the R^2 values tend to be higher than E values because an outlying value on a single event will significantly lower E while only slightly affecting R^2. Further, the E value favors high flows while sacrificing low flows and hence is a measure of a good match to the high flows.

10^{th}, 50^{th}, and 90^{th} percentiles of daily flow exceedances, for instance, 10^{th} percentile is daily flow value that is exceeded 10% of the time. Percentile exceedances reflect the model's capability for different flow regimes. The 10^{th} percentile value reflects storm events, the 90^{th} percentile value reflects baseflow, and the 50^{th} percentile (median) reflects the expected flow.

This page was intentionally left blank.

APPENDIX B

STREAMFLOW CALIBRATION RESULTS

This page was intentionally left blank.

APPENDIX B
STREAMFLOW CALIBRATION RESULTS

Streamgage	UID Site ID	Average Error (cfs)	AE % of (Max-Min)	RMSE (cfs)	RMSE % of (Max-Min)	R^{2*}	E**
Saddle Creek at St. Hwy 542 near Lakeland, FL	2294217	22.22	2.69	49.56	6.00	0.73	0.54
Lake Parker Outlet at Lakeland, FL	2294260	4.38	1.56	21.24	7.56	0.50	0.46
Saddle Creek at Structure P-11 near Bartow FL	2294491	48.44	2.99	152.44	9.41	0.35	-0.03
Peace Creek Drainage Canal near Wahneta, FL	2293987	18.18	1.86	71.63	7.34	0.74	0.72
Peace River at Bartow, FL	2294650	-22.77	-0.57	175.74	4.38	0.78	0.76
Peace River near Bartow, FL	2294655	-30.50	-0.75	181.59	4.44	0.78	0.76
Sixmile Creek at Bartow, FL	2294747	9.44	2.73	32.85	9.50	0.07	-0.25
Peace River at Clear Springs near Bartow, FL	2294775	-41.55	-1.41	200.67	6.80	0.68	0.64
Peace River near Homeland, FL	2294781	-39.37	-1.16	176.26	5.18	0.81	0.77
Peace River at Fort Meade, FL	2294898	-30.30	-1.24	171.23	6.99	0.80	0.77
Bowlegs Creek near Fort Meade, FL	2295013	12.12	0.67	58.71	3.24	0.57	0.53
Peace River at Zolfo Springs, FL	2295637	-21.83	-0.21	340.64	3.31	0.82	0.82
Payne Creek near Bowling Green, FL	2295420	-35.63	-0.77	171.42	3.72	0.62	0.33
Charlie Creek near Gardner, FL	2296500	105.66	1.16	400.87	4.39	0.56	0.50
Peace River at Arcadia, FL	2296750	110.07	0.51	752.13	3.47	0.77	0.76
Joshua Creek at Nocatee, FL	2297100	34.94	0.46	196.56	2.58	0.52	0.51
Horse Creek near Myakka Head, FL	2297155	16.25	0.93	45.69	2.63	0.69	0.62
Horse Creek near Arcadia, FL	2297310	50.75	0.68	182.35	2.44	0.79	0.77
Overall		11.25	0.05	251.39	1.16	0.78	0.78

*Coefficient of determination
**Nash Sutcliffe Efficiency

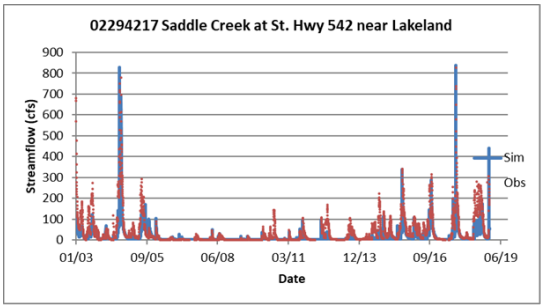
02294217 Saddle Creek at St. Hwy 542 near Lakeland
Streamflow (cfs)
900
800
700
600
500
400
300
200
100
0
01/03
09/05
06/08
03/11
12/13
09/16
06/19
Date
Sim
Obs

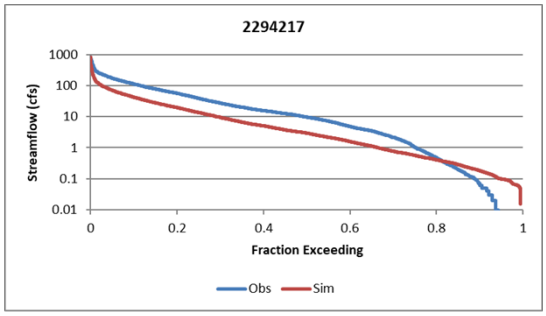
2294217
Streamflow (cfs)
1000
100
10
1
0.1
0.01
0
0.2
0.4
0.6
0.8
1
Fraction Exceeding
Obs
Sim

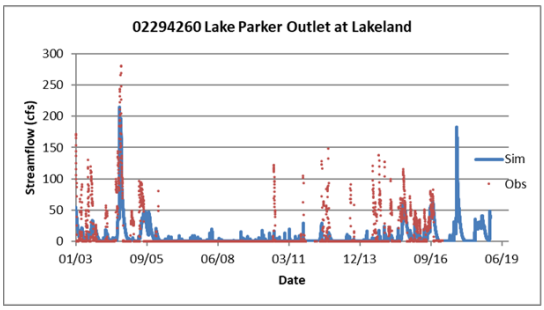
02294260 Lake Parker Outlet at Lakeland
Streamflow (cfs)
300
250
200
150
100
50
0
01/03
09/05
06/08
03/11
12/13
09/16
06/19
Date
Sim
Obs

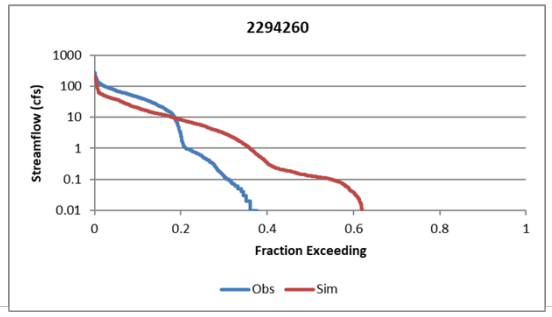
2294260
Streamflow (cfs)
1000
100
10
1
0.1
0.01
0
0.2
0.4
0.6
0.8
1
Fraction Exceeding
Obs
Sim

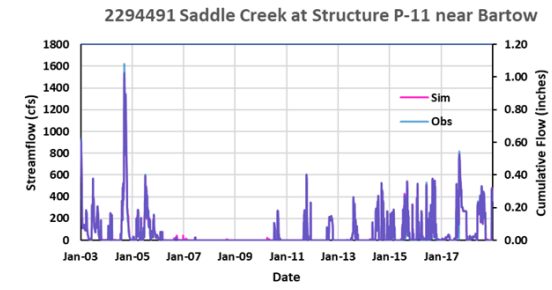
2294491 Saddle Creek at Structure P-11 near Bartow
Streamflow (cfs)
1800
1600
1400
1200
1000
800
600
400
200
0
Cumulative Flow (inches)
1.20
1.00
0.80
0.60
0.40
0.20
0.00
Jan-03
Jan-05
Jan-07
Jan-09
Jan-11
Jan-13
Jan-15
Jan-17
Date
Sim
Obs

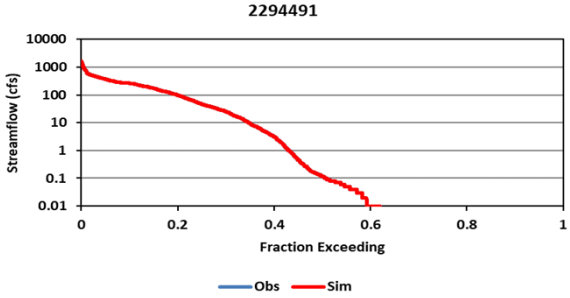
2294491
Streamflow (cfs)
10000
1000
100
10
1
0.1
0.01
0
0.2
0.4
0.6
0.8
1
Fraction Exceeding
Obs
Sim

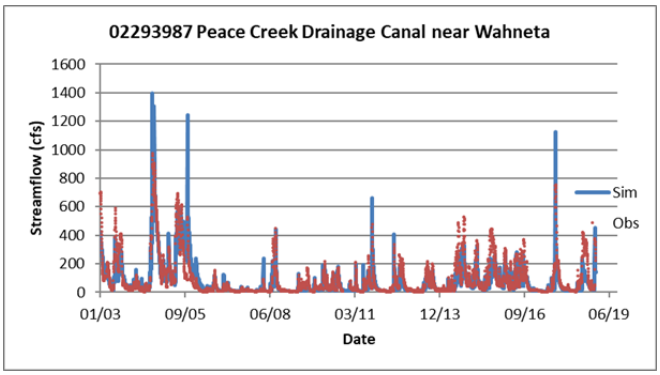
02293987 Peace Creek Drainage Canal near Wahneta
Streamflow (cfs)
1600
1400
1200
1000
800
600
400
200
0
01/03
09/05
06/08
03/11
12/13
09/16
06/19
Date
Sim
Obs

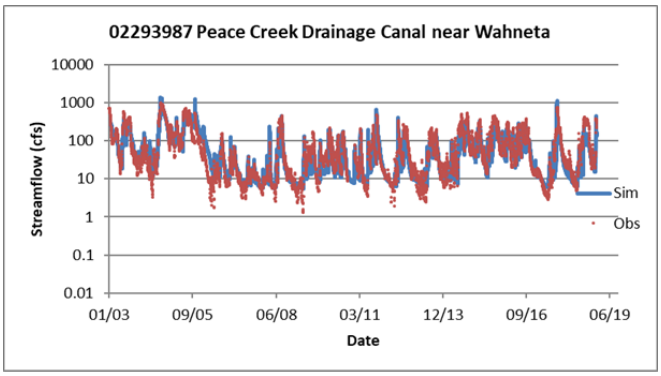
02293987 Peace Creek Drainage Canal near Wahneta
Streamflow (cfs)
10000
1000
100
10
1
0.1
0.01
01/03
09/05
06/08
03/11
12/13
09/16
06/19
Date
Sim
Obs

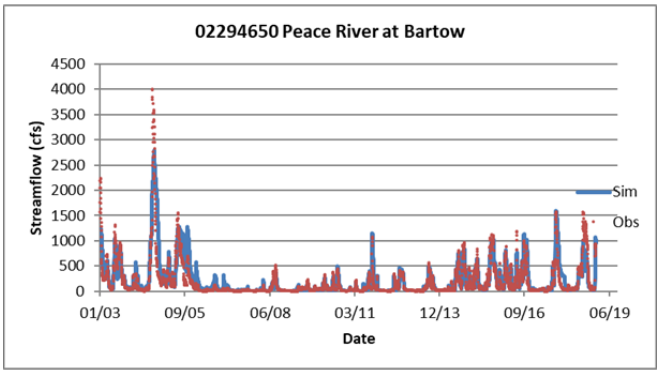
02294650 Peace River at Bartow
Streamflow (cfs)
4500
4000
3500
3000
2500
2000
1500
1000
500
0
01/03
09/05
06/08
03/11
12/13
09/16
06/19
Date
Sim
Obs

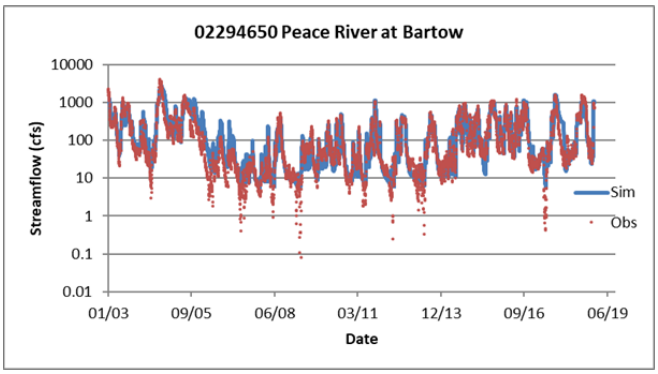
02294650 Peace River at Bartow
Streamflow (cfs)
10000
1000
100
10
1
0.1
0.01
01/03
09/05
06/08
03/11
12/13
09/16
06/19
Date
Sim
Obs

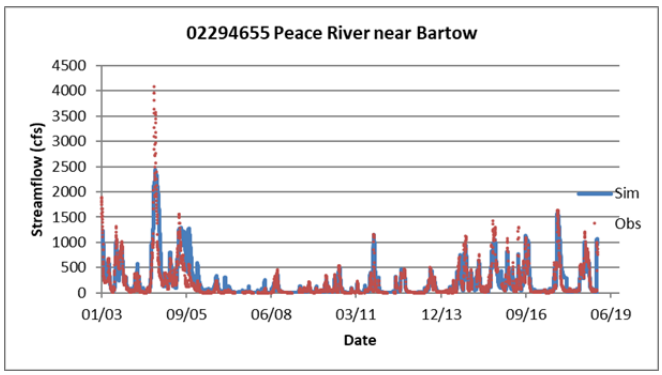
02294655 Peace River near Bartow
Streamflow (cfs)
4500
4000
3500
3000
2500
2000
1500
1000
500
0
01/03
09/05
06/08
03/11
12/13
09/16
06/19
Date
Sim
Obs

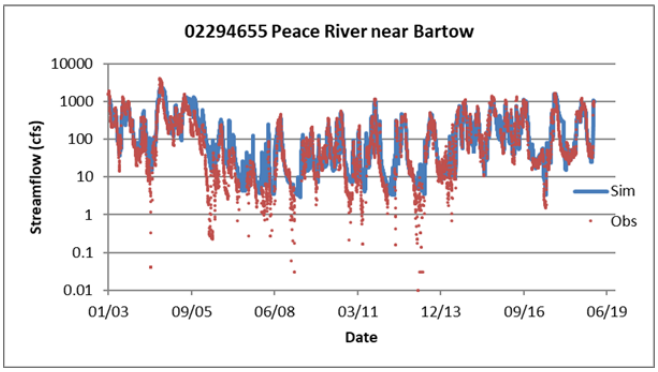
02294655 Peace River near Bartow
Streamflow (cfs)
10000
1000
100
10
1
0.1
0.01
01/03
09/05
06/08
03/11
12/13
09/16
06/19
Date
Sim
Obs

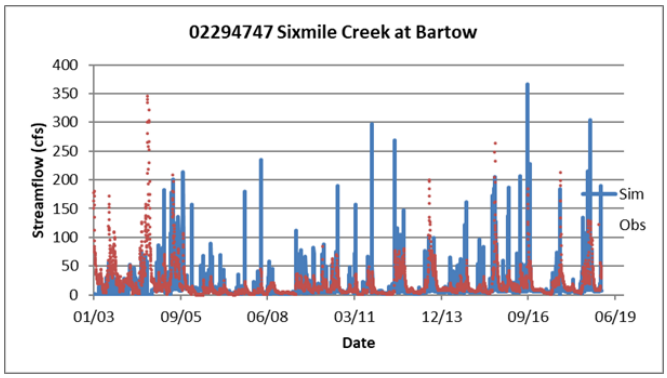
02294747 Sixmile Creek at Bartow
Streamflow (cfs)
400
350
300
250
200
150
100
50
0
01/03
09/05
06/08
03/11
12/13
09/16
06/19
Date
Sim
Obs

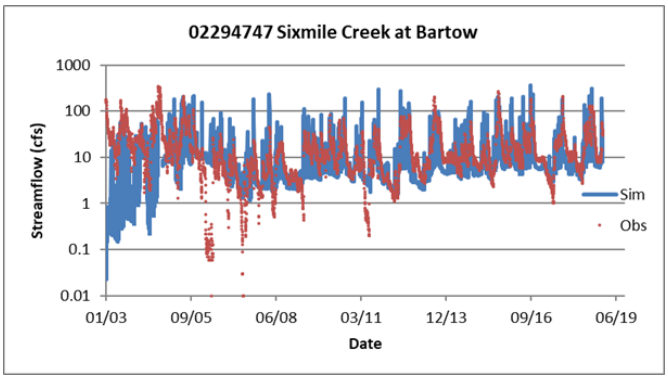
02294747 Sixmile Creek at Bartow
Streamflow (cfs)
1000
100
10
1
0.1
0.01
01/03
09/05
06/08
03/11
12/13
09/16
06/19
Date
Sim
Obs

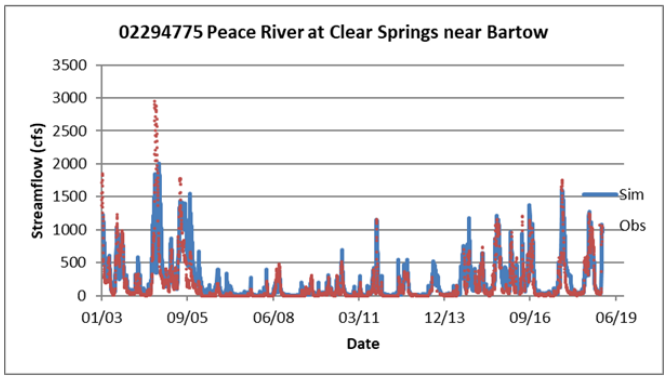
02294775 Peace River at Clear Springs near Bartow
Streamflow (cfs)
3500
3000
2500
2000
1500
1000
500
0
01/03
09/05
06/08
03/11
12/13
09/16
06/19
Date
Sim
Obs

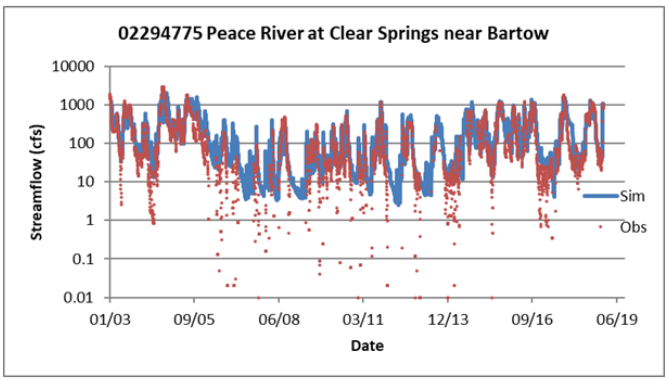
02294775 Peace River at Clear Springs near Bartow
Streamflow (cfs)
10000
1000
100
10
1
0.1
0.01
01/03
09/05
06/08
03/11
12/13
09/16
06/19
Date
Sim
Obs

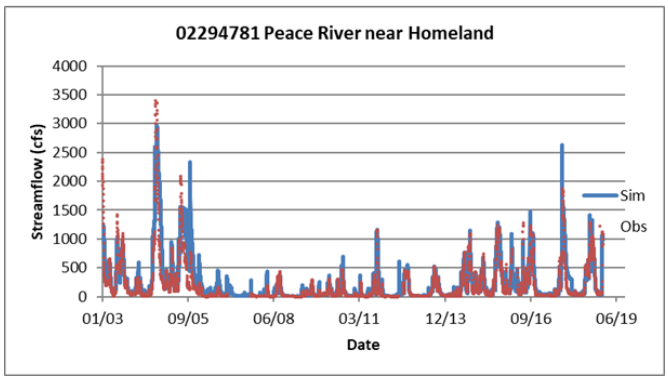
02294781 Peace River near Homeland
Streamflow (cfs)
4000
3500
3000
2500
2000
1500
1000
500
0
01/03
09/05
06/08
03/11
12/13
09/16
06/19
Date
Sim
Obs

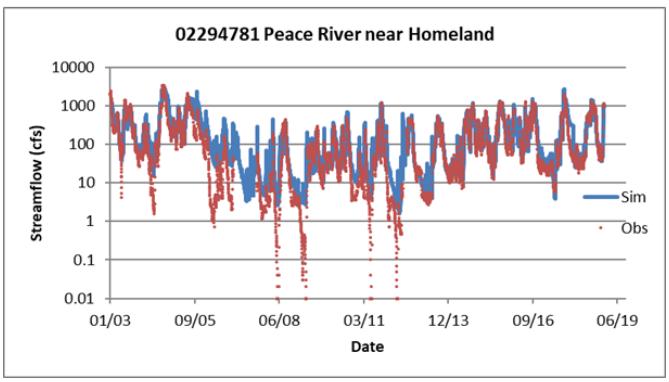
02294781 Peace River near Homeland
Streamflow (cfs)
10000
1000
100
10
1
0.1
0.01
01/03
09/05
06/08
03/11
12/13
09/16
06/19
Date
Sim
Obs

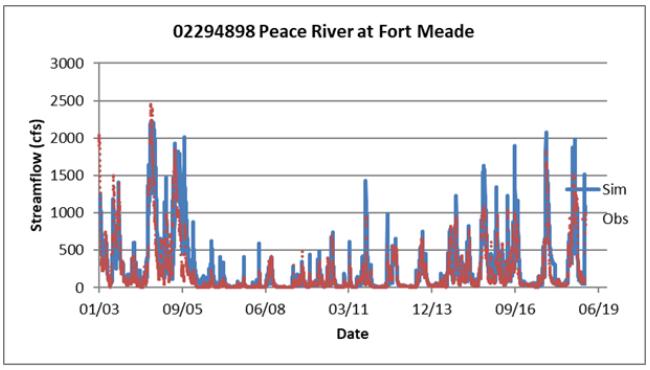
02294898 Peace River at Fort Meade
Streamflow (cfs)
3000
2500
2000
1500
1000
500
0
01/03
09/05
06/08
03/11
12/13
09/16
06/19
Date
Sim
Obs

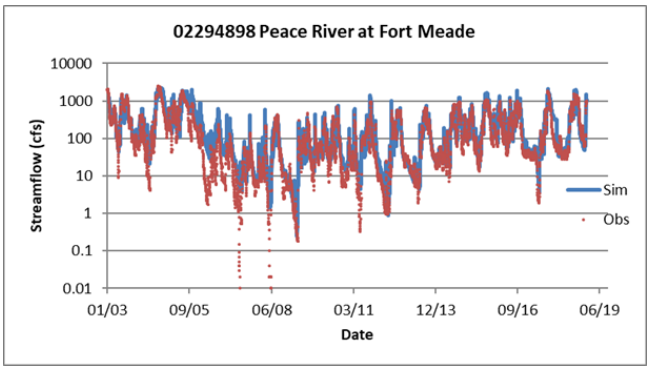
02294898 Peace River at Fort Meade
Streamflow (cfs)
10000
1000
100
10
1
0.1
0.01
01/03
09/05
06/08
03/11
12/13
09/16
06/19
Date
Sim
Obs

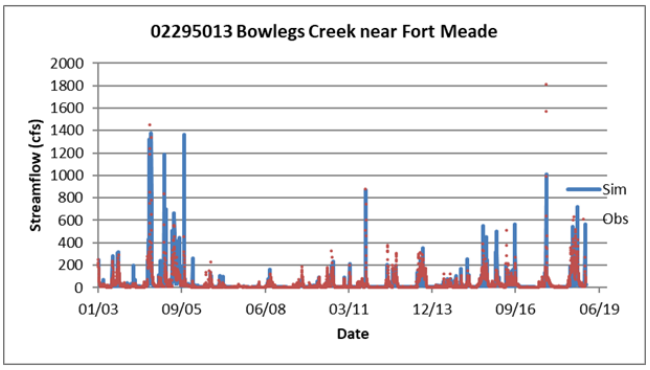
02295013 Bowlegs Creek near Fort Meade
Streamflow (cfs)
2000
1800
1600
1400
1200
1000
800
600
400
200
0
01/03
09/05
06/08
03/11
12/13
09/16
06/19
Date
Sim
Obs

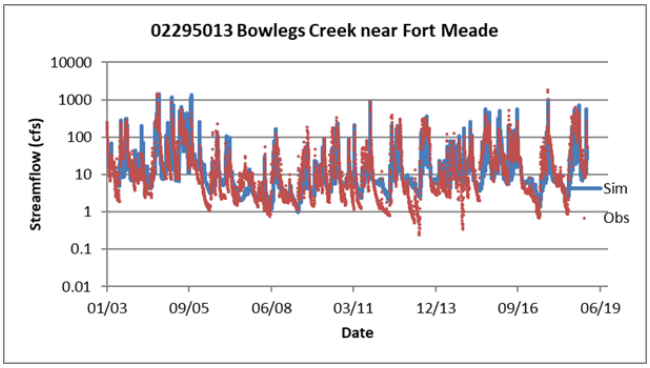
02295013 Bowlegs Creek near Fort Meade
Streamflow (cfs)
10000
1000
100
10
1
0.1
0.01
01/03
09/05
06/08
03/11
12/13
09/16
06/19
Date
Sim
Obs

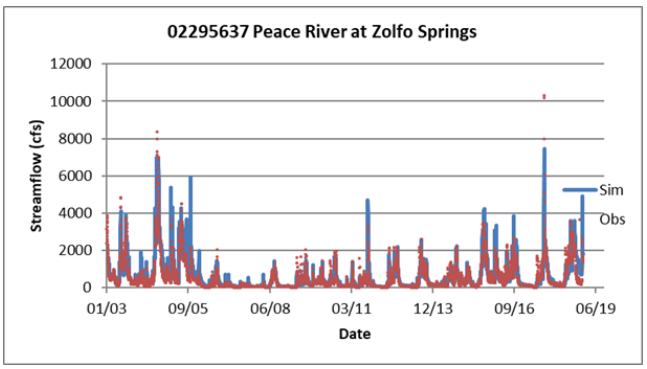
02295637 Peace River at Zolfo Springs
Streamflow (cfs)
12000
10000
8000
6000
4000
2000
0
01/03
09/05
06/08
03/11
12/13
09/16
06/19
Date
Sim
Obs

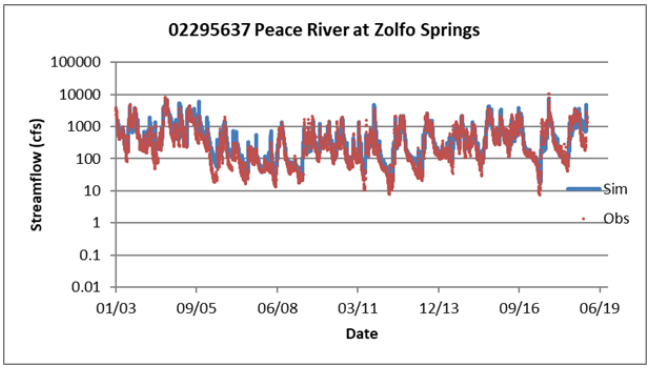
02295637 Peace River at Zolfo Springs
Streamflow (cfs)
100000
10000
1000
100
10
1
0.1
0.01
01/03
09/05
06/08
03/11
12/13
09/16
06/19
Date
Sim
Obs

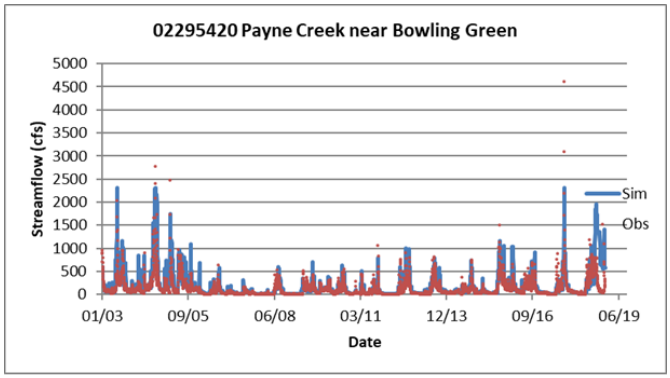
02295420 Payne Creek near Bowling Green
Streamflow (cfs)
5000
4500
4000
3500
3000
2500
2000
1500
1000
500
0
01/03
09/05
06/08
03/11
12/13
09/16
06/19
Date
Sim
Obs

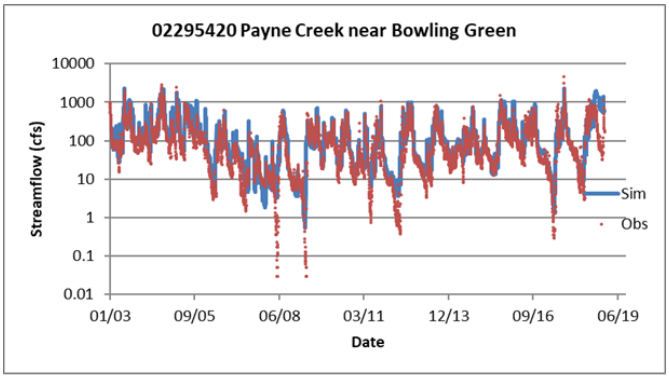
02295420 Payne Creek near Bowling Green
Streamflow (cfs)
10000
1000
100
10
1
0.1
0.01
01/03
09/05
06/08
03/11
12/13
09/16
06/19
Date
Sim
Obs

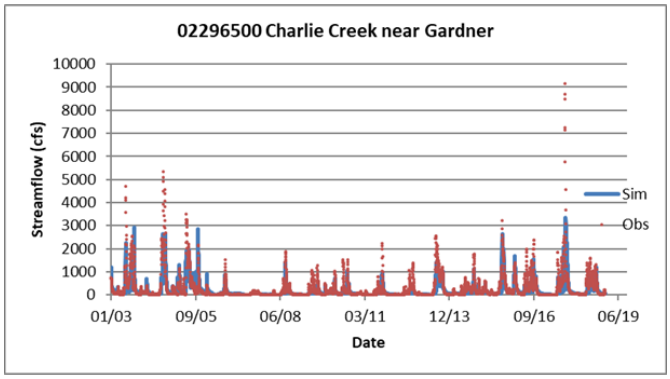
02296500 Charlie Creek near Gardner
Streamflow (cfs)
10000
9000
8000
7000
6000
5000
4000
3000
2000
1000
0
01/03
09/05
06/08
03/11
12/13
09/16
06/19
Date
Sim
Obs

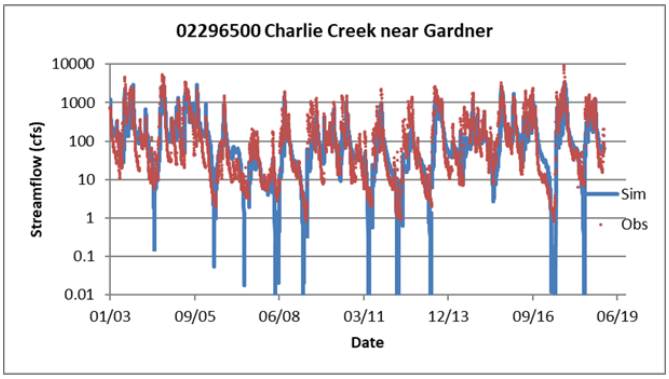
02296500 Charlie Creek near Gardner
Streamflow (cfs)
10000
1000
100
10
1
0.1
0.01
01/03
09/05
06/08
03/11
12/13
09/16
06/19
Date
Sim
Obs

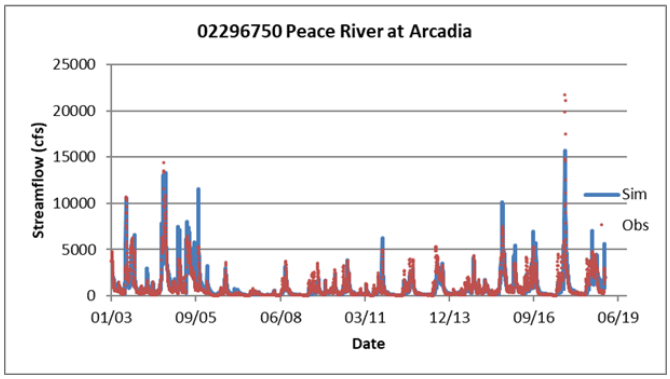
02296750 Peace River at Arcadia
Streamflow (cfs)
25000
20000
15000
10000
5000
0
01/03
09/05
06/08
03/11
12/13
09/16
06/19
Date
Sim
Obs

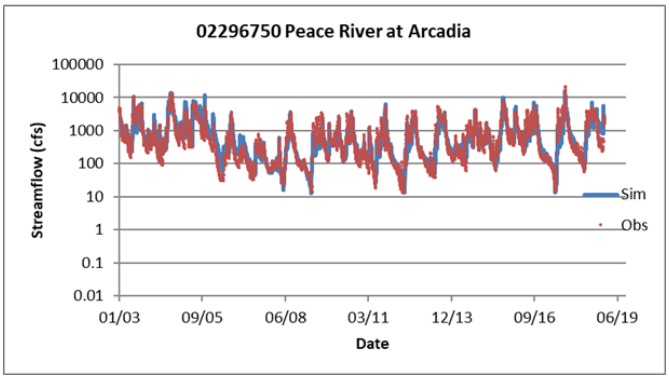
02296750 Peace River at Arcadia
Streamflow (cfs)
100000
10000
1000
100
10
1
0.1
0.01
01/03
09/05
06/08
03/11
12/13
09/16
06/19
Date
Sim
Obs

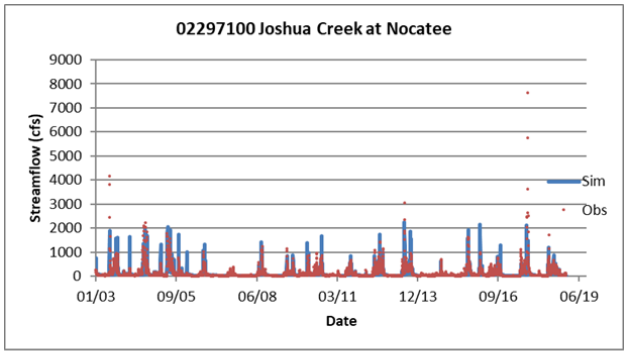
02297100 Joshua Creek at Nocatee
Streamflow (cfs)
9000
8000
7000
6000
5000
4000
3000
2000
1000
0
01/03
09/05
06/08
03/11
12/13
09/16
06/19
Date
Sim
Obs

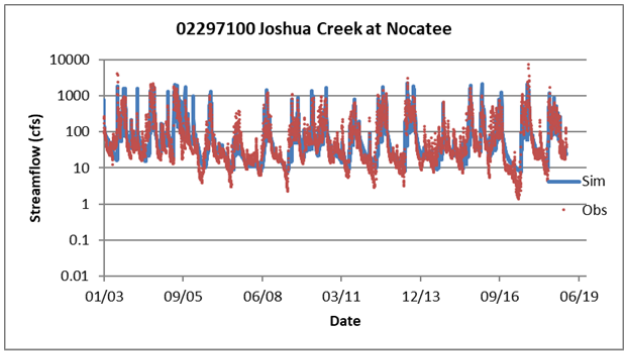
02297100 Joshua Creek at Nocatee
Streamflow (cfs)
10000
1000
100
10
1
0.1
0.01
01/03
09/05
06/08
03/11
12/13
09/16
06/19
Date
Sim
Obs

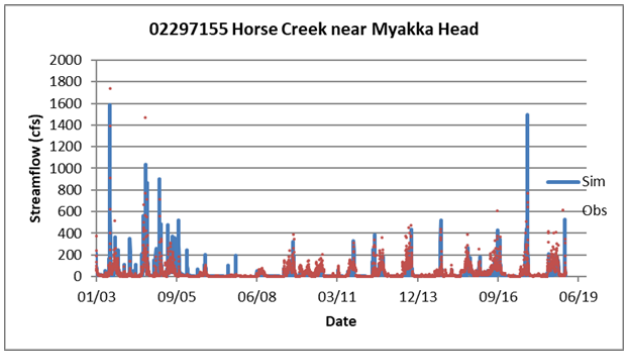
02297155 Horse Creek near Myakka Head
Streamflow (cfs)
2000
1800
1600
1400
1200
1000
800
600
400
200
0
01/03
09/05
06/08
03/11
12/13
09/16
06/19
Date
Sim
Obs

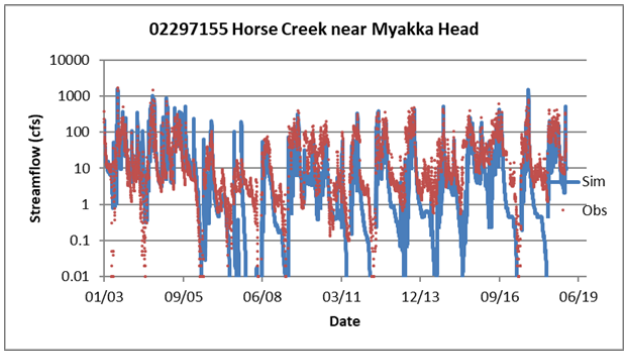
02297155 Horse Creek near Myakka Head
Streamflow (cfs)
10000
1000
100
10
1
0.1
0.01
01/03
09/05
06/08
03/11
12/13
09/16
06/19
Date
Sim
Obs

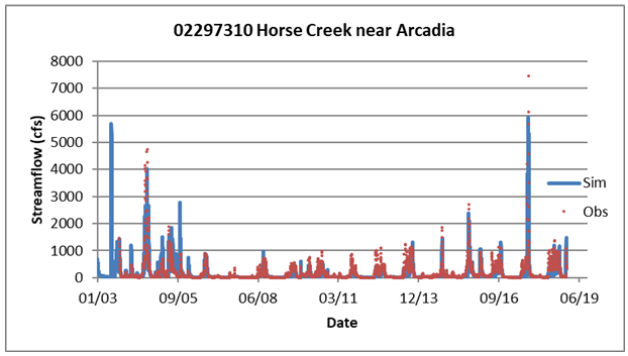
02297310 Horse Creek near Arcadia
Streamflow (cfs)
8000
7000
6000
5000
4000
3000
2000
1000
0
01/03
09/05
06/08
03/11
12/13
09/16
06/19
Date
Sim
Obs

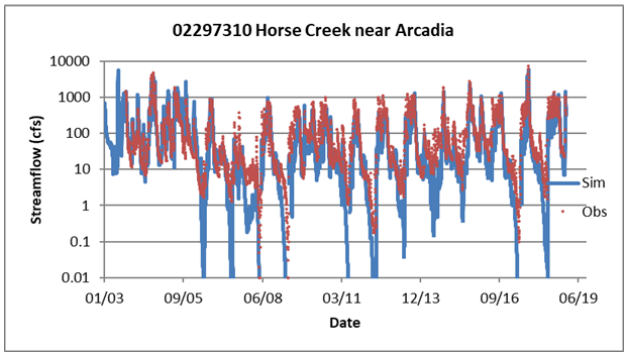
02297310 Horse Creek near Arcadia
Streamflow (cfs)
10000
1000
100
10
1
0.1
0.01
01/03
09/05
06/08
03/11
12/13
09/16
06/19
Date
Sim
Obs

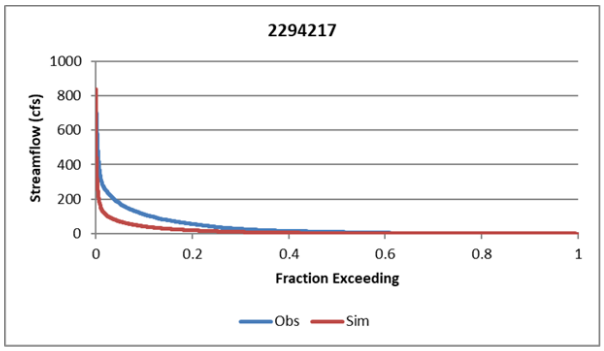
2294217
Streamflow (cfs)
1000
800
600
400
200
0
0
0.2
0.4
0.6
0.8
1
Fraction Exceeding
Obs
Sim

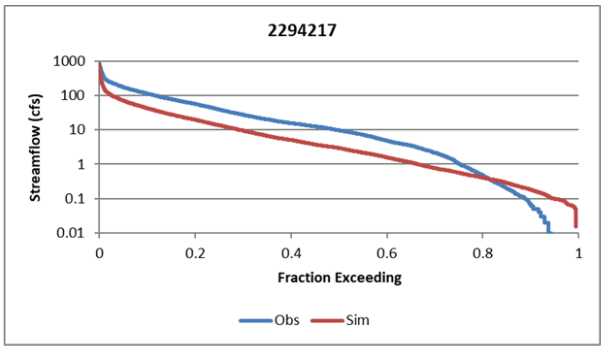
2294217
Streamflow (cfs)
1000
100
10
1
0.1
0.01
0
0.2
0.4
0.6
0.8
1
Fraction Exceeding
Obs
Sim

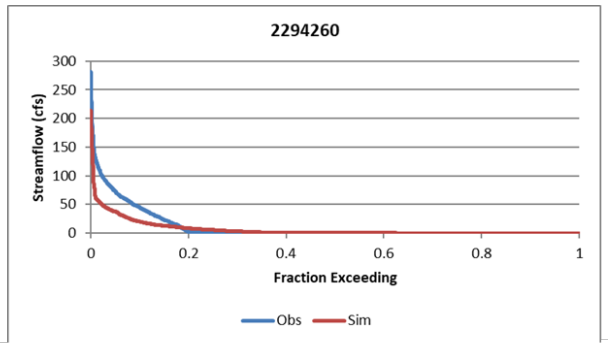
2294260
Streamflow (cfs)
300
250
200
150
100
50
0
0
0.2
0.4
0.6
0.8
1
Fraction Exceeding
Obs
Sim

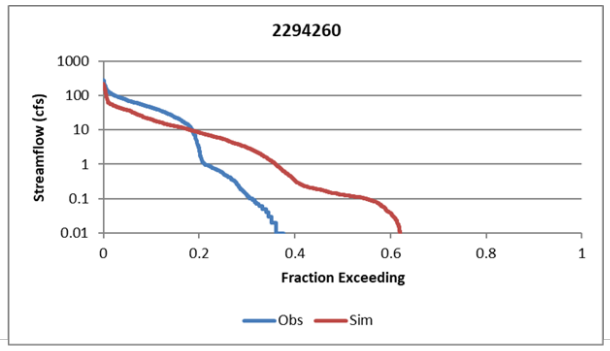
2294260
Streamflow (cfs)
1000
100
10
1
0.1
0.01
0
0.2
0.4
0.6
0.8
1
Fraction Exceeding
Obs
Sim

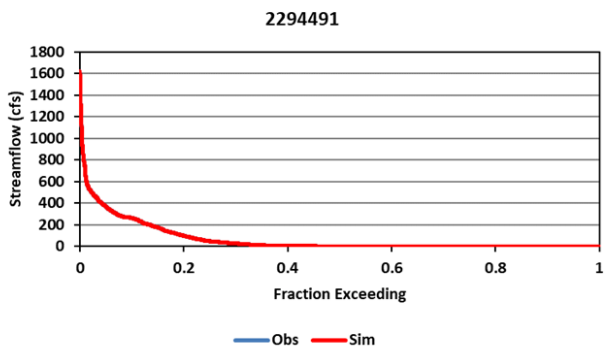
2294491
Streamflow (cfs)
1800
1600
1400
1200
1000
800
600
400
200
0
0
0.2
0.4
0.6
0.8
1
Fraction Exceeding
Obs
Sim

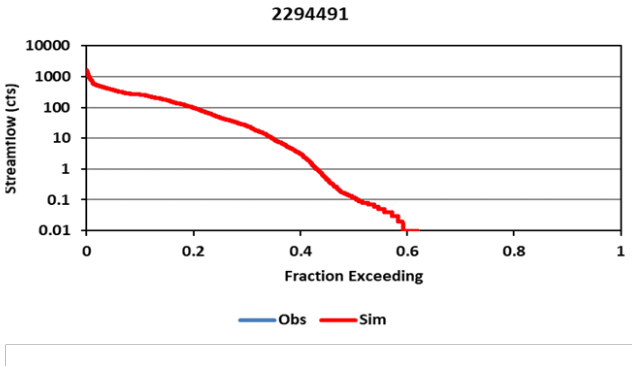
2294491
Streamflow (cfs)
10000
1000
100
10
1
0.1
0.01
0
0.2
0.4
0.6
0.8
1
Fraction Exceeding
Obs
Sim

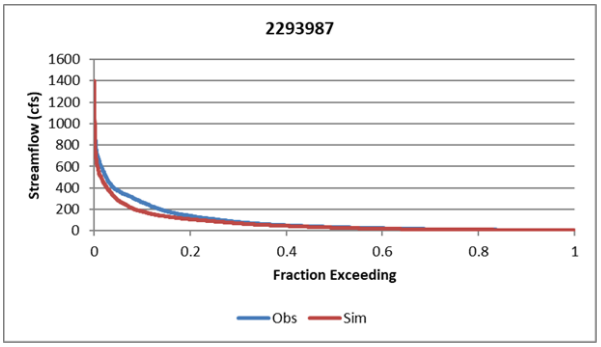
2293987
Streamflow (cfs)
1600
1400
1200
1000
800
600
400
200
0
0
0.2
0.4
0.6
0.8
1
Fraction Exceeding
Obs
Sim

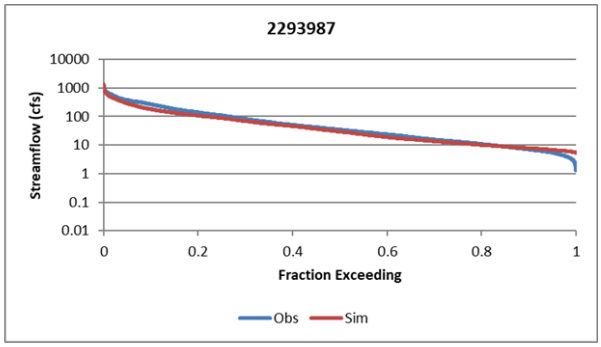
2293987
Streamflow (cfs)
10000
1000
100
10
1
0.1
0.01
0
0.2
0.4
0.6
0.8
1
Fraction Exceeding
Obs
Sim

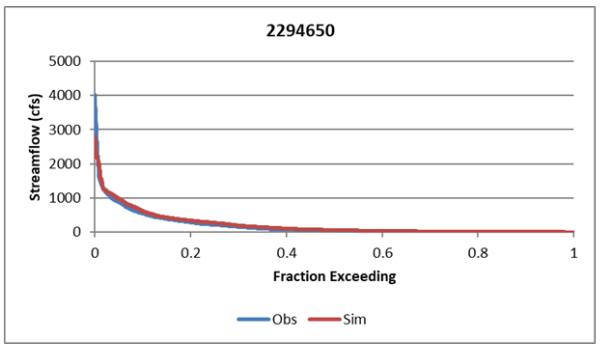
2294650
Streamflow (cfs)
5000
4000
3000
2000
1000
0
0
0.2
0.4
0.6
0.8
1
Fraction Exceeding
Obs
Sim

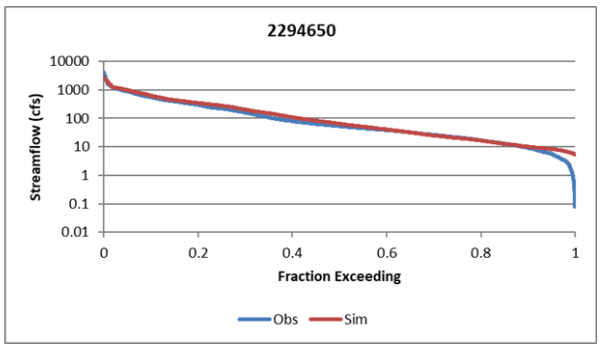
2294650
Streamflow (cfs)
10000
1000
100
10
1
0.1
0.01
0
0.2
0.4
0.6
0.8
1
Fraction Exceeding
Obs
Sim

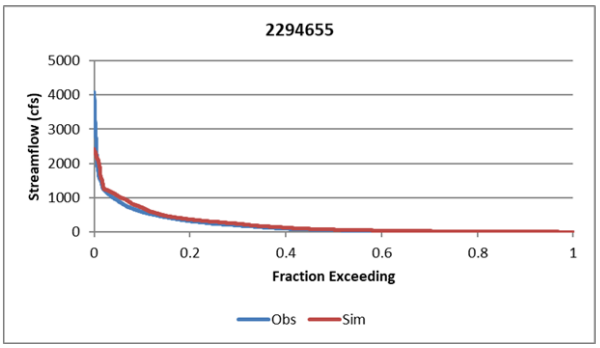
2294655
Streamflow (cfs)
5000
4000
3000
2000
1000
0
0
0.2
0.4
0.6
0.8
1
Fraction Exceeding
Obs
Sim

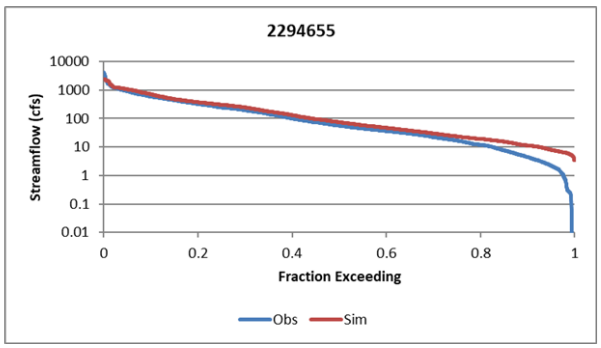
2294655
Streamflow (cfs)
10000
1000
100
10
1
0.1
0.01
0
0.2
0.4
0.6
0.8
1
Fraction Exceeding
Obs
Sim

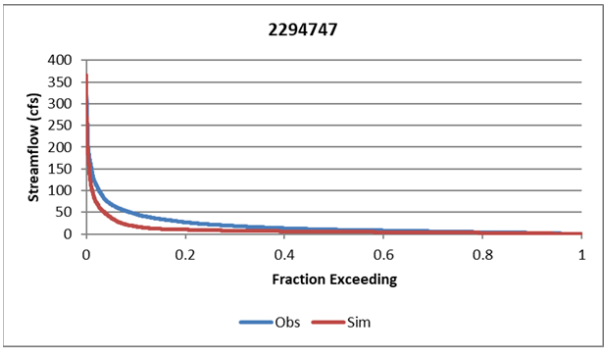
2294747
Streamflow (cfs)
400
350
300
250
200
150
100
50
0
0
0.2
0.4
0.6
0.8
1
Fraction Exceeding
Obs
Sim

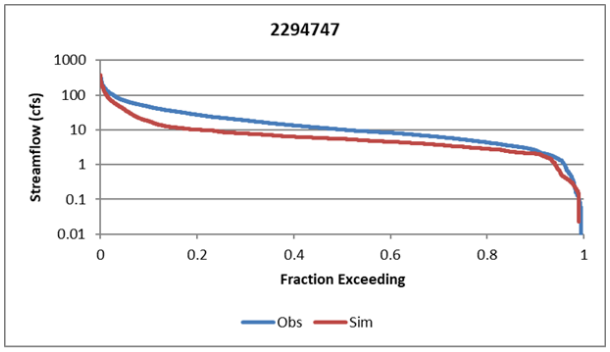
2294747
Streamflow (cfs)
1000
100
10
1
0.1
0.01
0
0.2
0.4
0.6
0.8
1
Fraction Exceeding
Obs
Sim

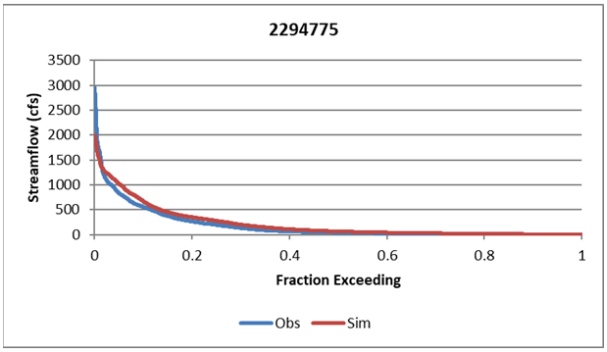
2294775
Streamflow (cfs)
3500
3000
2500
2000
1500
1000
500
0
0
0.2
0.4
0.6
0.8
1
Fraction Exceeding
Obs
Sim

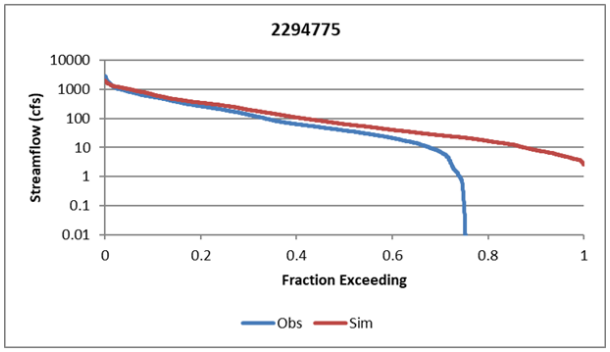
2294775
Streamflow (cfs)
10000
1000
100
10
1
0.1
0.01
0
0.2
0.4
0.6
0.8
1
Fraction Exceeding
Obs
Sim

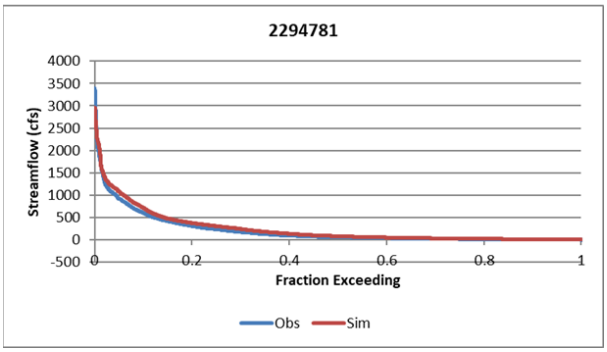
2294781
Streamflow (cfs)
4000
3500
3000
2500
2000
1500
1000
500
0
-500
0
0.2
0.4
0.6
0.8
1
Fraction Exceeding
Obs
Sim

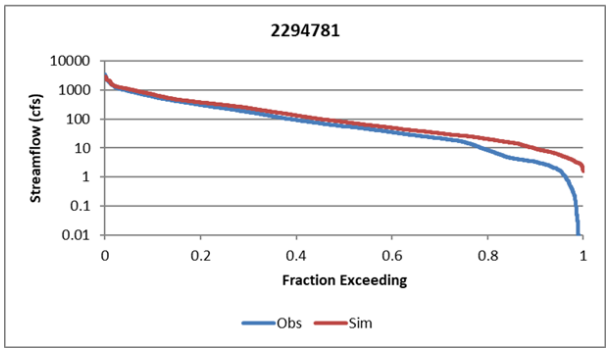
2294781
Streamflow (cfs)
10000
1000
100
10
1
0.1
0.01
0
0.2
0.4
0.6
0.8
1
Fraction Exceeding
Obs
Sim

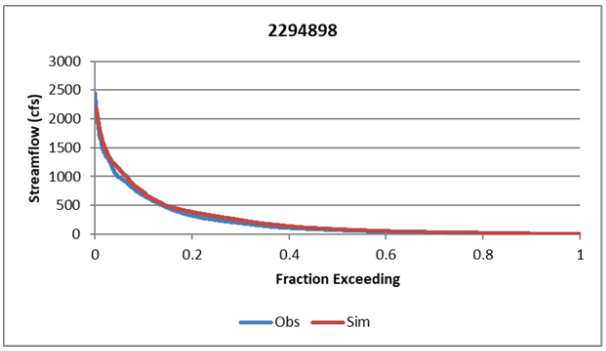
2294898
Streamflow (cfs)
3000
2500
2000
1500
1000
500
0
0
0.2
0.4
0.6
0.8
1
Fraction Exceeding
Obs
Sim

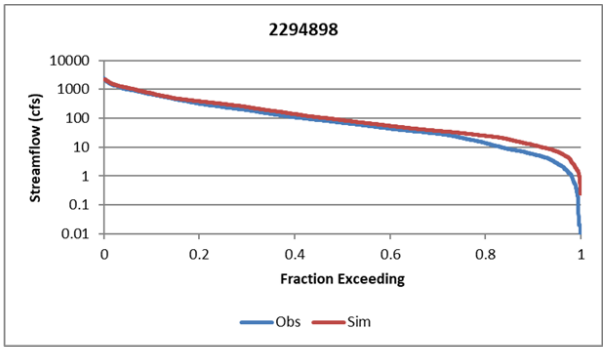
2294898
Streamflow (cfs)
10000
1000
100
10
1
0.1
0.01
0
0.2
0.4
0.6
0.8
1
Fraction Exceeding
Obs
Sim

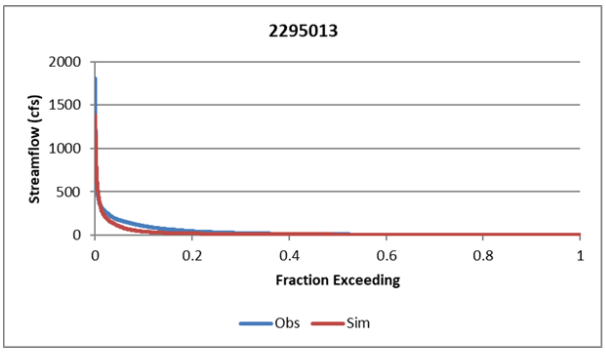
2295013
Streamflow (cfs)
2000
1500
1000
500
0
0
0.2
0.4
0.6
0.8
1
Fraction Exceeding
Obs
Sim

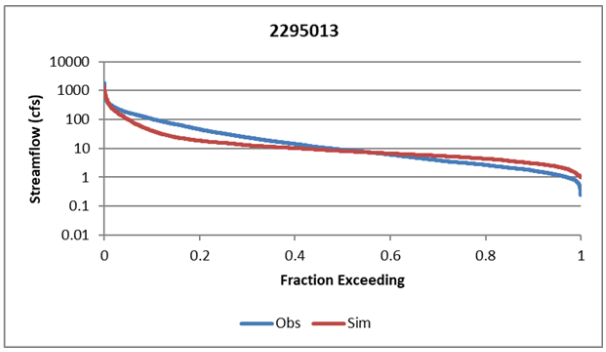
2295013
Streamflow (cfs)
10000
1000
100
10
1
0.1
0.01
0
0.2
0.4
0.6
0.8
1
Fraction Exceeding
Obs
Sim

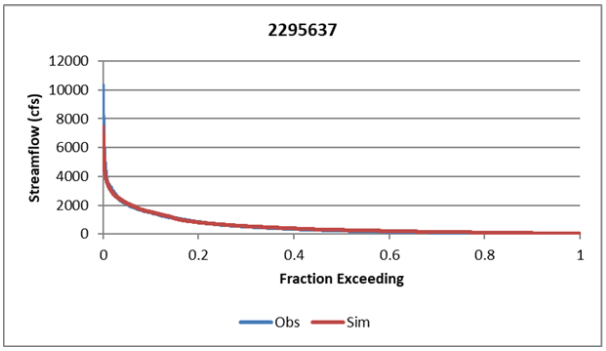
2295637
Streamflow (cfs)
12000
10000
8000
6000
4000
2000
0
0
0.2
0.4
0.6
0.8
1
Fraction Exceeding
Obs
Sim

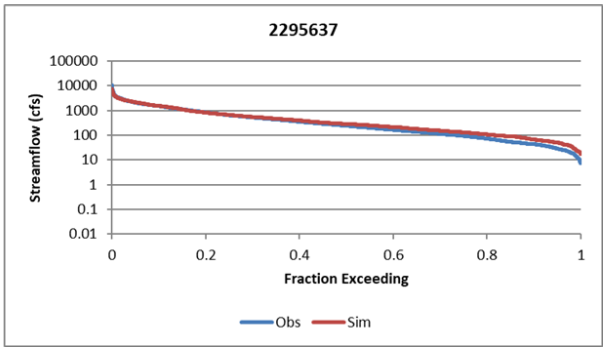
2295637
Streamflow (cfs)
100000
10000
1000
100
10
1
0.1
0.01
0
0.2
0.4
0.6
0.8
1
Fraction Exceeding
Obs
Sim

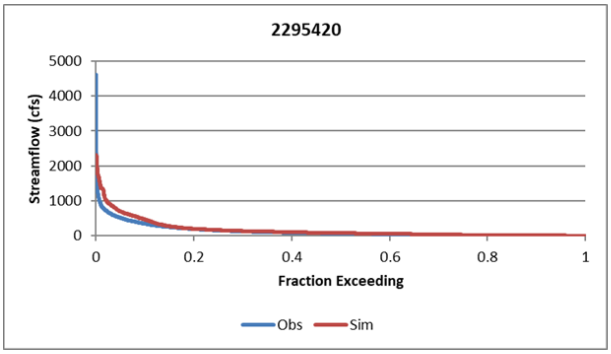
2295420
Streamflow (cfs)
5000
4000
3000
2000
1000
0
0
0.2
0.4
0.6
0.8
1
Fraction Exceeding
Obs
Sim

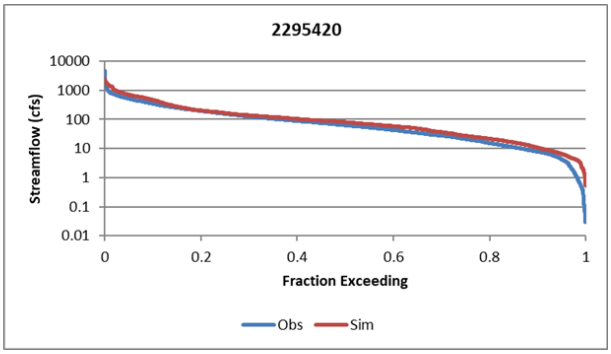
2295420
Streamflow (cfs)
10000
1000
100
10
1
0.1
0.01
0
0.2
0.4
0.6
0.8
1
Fraction Exceeding
Obs
Sim

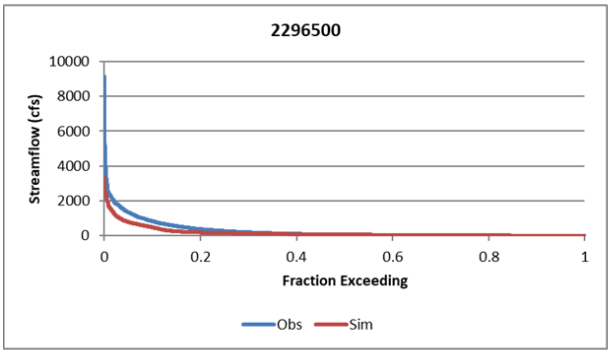
2296500
Streamflow (cfs)
10000
8000
6000
4000
2000
0
0
0.2
0.4
0.6
0.8
1
Fraction Exceeding
Obs
Sim

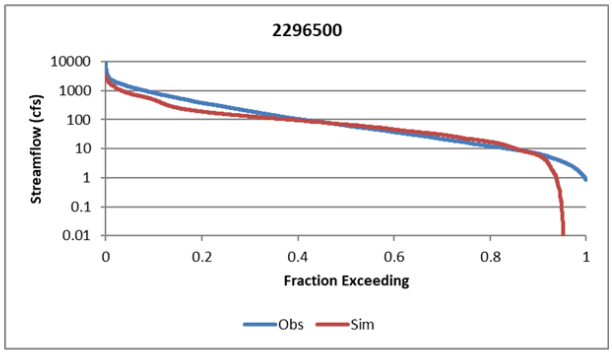
2296500
Streamflow (cfs)
10000
1000
100
10
1
0.1
0.01
0
0.2
0.4
0.6
0.8
1
Fraction Exceeding
Obs
Sim

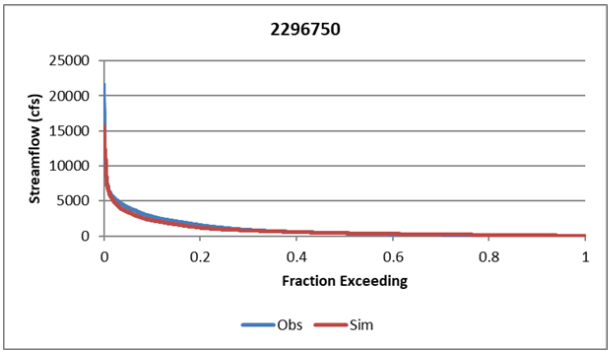
2296750
Streamflow (cfs)
25000
20000
15000
10000
5000
0
0
0.2
0.4
0.6
0.8
1
Fraction Exceeding
Obs
Sim

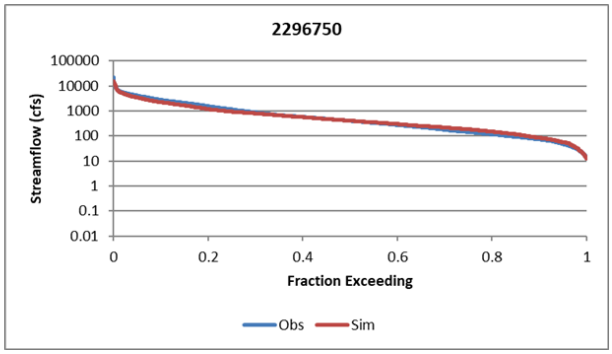
2296750
Streamflow (cfs)
100000
10000
1000
100
10
1
0.1
0.01
0
0.2
0.4
0.6
0.8
1
Fraction Exceeding
Obs
Sim

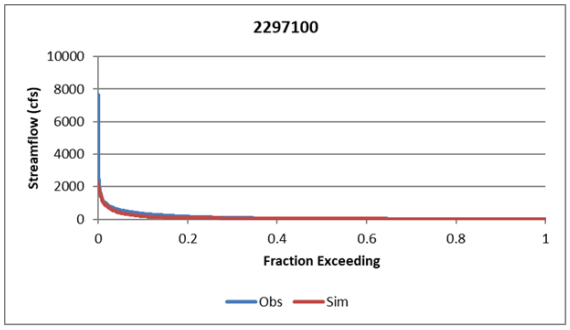
2297100
Streamflow (cfs)
10000
8000
6000
4000
2000
0
0
0.2
0.4
0.6
0.8
1
Fraction Exceeding
Obs
Sim

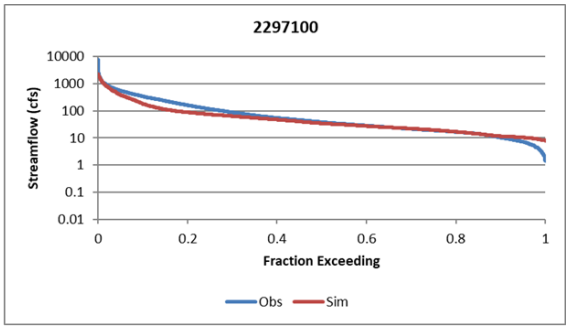
2297100
Streamflow (cfs)
10000
1000
100
10
1
0.1
0.01
0
0.2
0.4
0.6
0.8
1
Fraction Exceeding
Obs
Sim

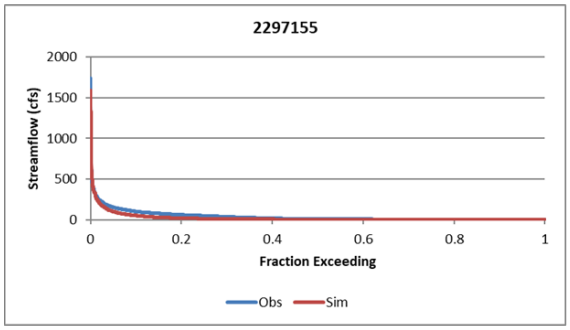
2297155
Streamflow (cfs)
2000
1500
1000
500
0
0
0.2
0.4
0.6
0.8
1
Fraction Exceeding
Obs
Sim

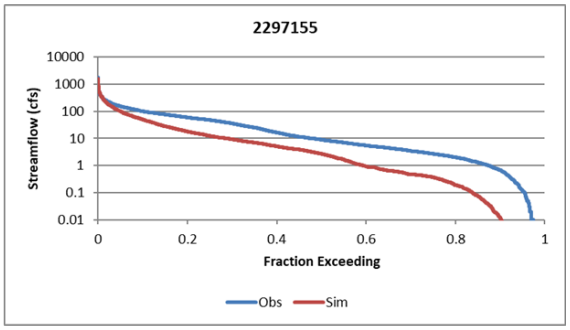
2297155
Streamflow (cfs)
10000
1000
100
10
1
0.1
0.01
0
0.2
0.4
0.6
0.8
1
Fraction Exceeding
Obs
Sim

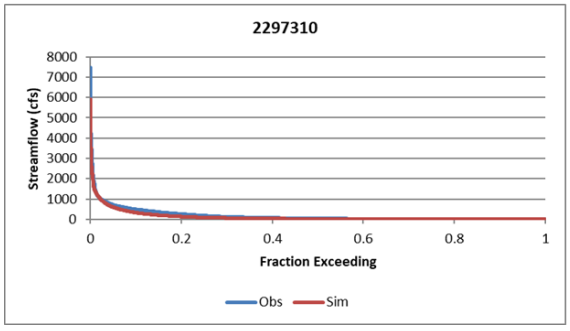
2297310
Streamflow (cfs)
8000
7000
6000
5000
4000
3000
2000
1000
0
0
0.2
0.4
0.6
0.8
1
Fraction Exceeding
Obs
Sim

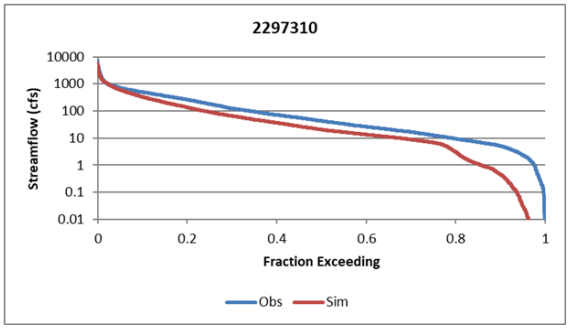
2297310
Streamflow (cfs)
10000
1000
100
10
1
0.1
0.01
0
0.2
0.4
0.6
0.8
1
Fraction Exceeding
Obs
Sim

This page was intentionally left blank.

APPENDIX C

LAKE LEVEL CALIBRATION STATISTICS AND LAKE LEVEL PLOTS

This page was intentionally left blank.

APPENDIX C
LAKE LEVEL CALIBRATION STATISTICS AND LAKE LEVEL PLOTS

Lake Observation Name	Average Error (feet)	RMSE (feet)	R^2
Lake Sanitary (Mariana)	-2.47	2.68	0.20
Lake George (Polk)	-0.22	0.75	0.55
Lake Gibson Northeast	1.57	1.61	0.49
Lake Camp	-1.36	1.88	0.62
Lake Eva (nr Lake Alfred)	-7.90	7.93	0.49
Lake Griffin (Polk)	-1.77	2.02	0.74
Gum Lake	-1.95	2.13	0.56
Lake Ariana	-1.37	1.89	0.23
Lake Arietta (USGS)	-0.18	1.76	0.08
Lake Eva (Haines City)	12.39	12.42	0.71
Blue Lake South	1.95	2.29	0.75
Tractor Lake	-6.28	6.53	0.44
Lake Altamaha	-1.46	2.00	0.75
Lake Parker nr Lake Wales	1.51	1.72	0.56
Lake Hancock	0.63	1.14	0.26
Lake Whistler	-1.24	1.41	0.22
Lake Myrtle I	0.41	1.05	0.56
Reeves Lake	-1.72	2.19	0.63
Lake GROSS	2.05	2.20	0.75
Lake Hart	-1.68	2.30	0.77
River Lake	-1.35	2.88	0.25
Lake Mcleod	2.54	2.88	0.68
Lake Shipp	1.03	1.23	0.64
Eagle Lake	-2.05	3.01	0.09
Millsite Lake	0.09	1.15	0.52
Grassy Lake I	1.28	1.96	0.35
Banana Lake at Boat Ramp	1.06	1.18	0.67
Surveyors Lake	1.29	1.46	0.53
Polecat Lake	-0.48	1.67	0.37
Gator Lake	1.22	1.43	0.55
Lake Walker	-1.82	1.97	0.91
Lake Garfield	0.42	0.87	0.55
Lake Hamilton North	1.35	1.54	0.66
Lake Howard	1.04	1.24	0.64
Lake Silver	-2.27	2.83	0.88
Lake Ida (Winter Haven)	-0.05	1.15	0.73
Lake Pansy (Polk)	0.33	0.83	0.65
Sears Lake	-1.55	2.11	0.56
Spirit Lake	-2.58	2.96	0.65
Thomas Lake I	-0.34	1.42	0.76
Lake Deer	0.33	0.82	0.19
Blue Lake nr Auburndale	0.23	0.82	0.32
Lake Lena Canal at P-1 Structure	-1.74	2.16	0.14

Lake Observation Name	Average Error (feet)	RMSE (feet)	R^2
Lake Bentley	1.25	1.43	0.22
Lake Holloway	1.52	1.59	0.53
Crystal Lake (Lakeland)	5.80	6.33	0.04
Lake Bonny	1.31	1.91	0.69
Lake Parker	0.32	0.99	0.68
Lake Haines	0.41	0.70	0.76
Lake Alfred	-3.50	4.71	0.23
Lake Swoope	-1.58	2.58	0.87
Mountain Lake	3.49	4.27	0.86
Lake Myrtle (Ashton) North	0.32	0.54	0.73
Dinner Lake (Lake Wales)	0.91	1.43	0.86
Lake Starr	4.75	4.97	0.78
Mabel Lake	4.62	4.99	0.51
Lake Venus	-1.03	1.56	0.81
Lake Lee	1.28	1.63	0.75
Lake Ruby	0.49	0.82	0.26
Lake Bess	0.60	0.89	0.31
Lake Fox	0.82	0.89	0.64
Lake Annie (Polk)	2.51	2.77	0.69
Lake Dexter	0.83	1.06	0.26
Lake Menzie	6.38	6.76	0.34
Lake Dell	2.90	3.05	0.56
Lake Gordon	1.87	2.50	0.64
Lake Effie	1.15	1.20	0.63
Lake Cooper (Worth)	-1.01	1.08	0.35
Twin Lake (East)	2.30	2.65	0.74
Lake Weader	0.51	0.72	0.23
Twin Lake (West)	3.34	3.52	0.74
Lake Daisy	1.16	1.18	0.85
Ned Lake	1.53	1.56	0.58
Lake Florence	0.19	0.75	0.53
Lake Otis	-1.54	1.76	0.82
Lake Mariam	-3.52	4.76	0.07
Lake Link	-2.06	2.50	0.85
Lake Maude	-1.23	1.89	0.68
Lake Martha	-1.11	2.02	0.58
Lake Elbert	-2.25	2.64	0.61
Lake Idyl	0.32	0.49	0.55
Lake Smart	1.24	1.75	0.76
Lake Buckeye	1.18	1.24	0.75
Lake Conine	0.78	1.23	0.86
Lake Echo	-2.45	2.89	0.57
Lake Rochelle	0.79	1.27	0.84
Lake Sanitary Sw	-4.37	4.38	0.48
Lake Silver 2	-3.98	4.08	0.93
Lake Smart (Scada)	0.47	0.87	0.82

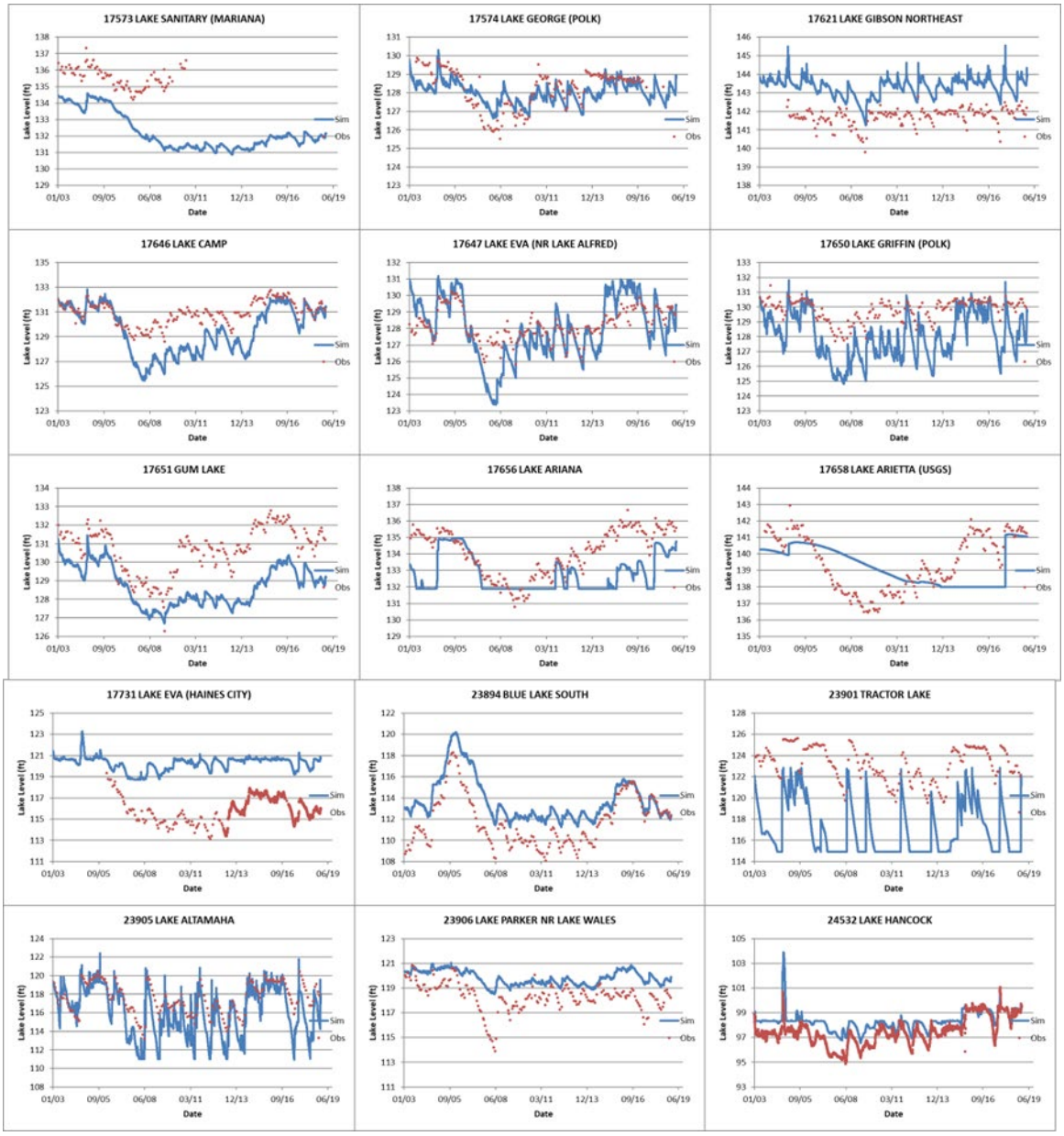
17573 LAKE SANITARY (MARIANA)
17574 LAKE GEORGE (POLK)
17621 LAKE GIBSON NORTHEAST
17646 LAKE CAMP
17647 LAKE EVA (NR LAKE ALFRED)
17650 LAKE GRIFFIN (POLK)
17651 GUM LAKE
17656 LAKE ARIANA
17658 LAKE ARIETTA (USGS)
17731 LAKE EVA (HAINES CITY)
23894 BLUE LAKE SOUTH
23901 TRACTOR LAKE
23905 LAKE ALTAMAHA
23906 LAKE PARKER NR LAKE WALES
24532 LAKE HANCOCK
Lake Level (ft)
Date
Sim
Obs

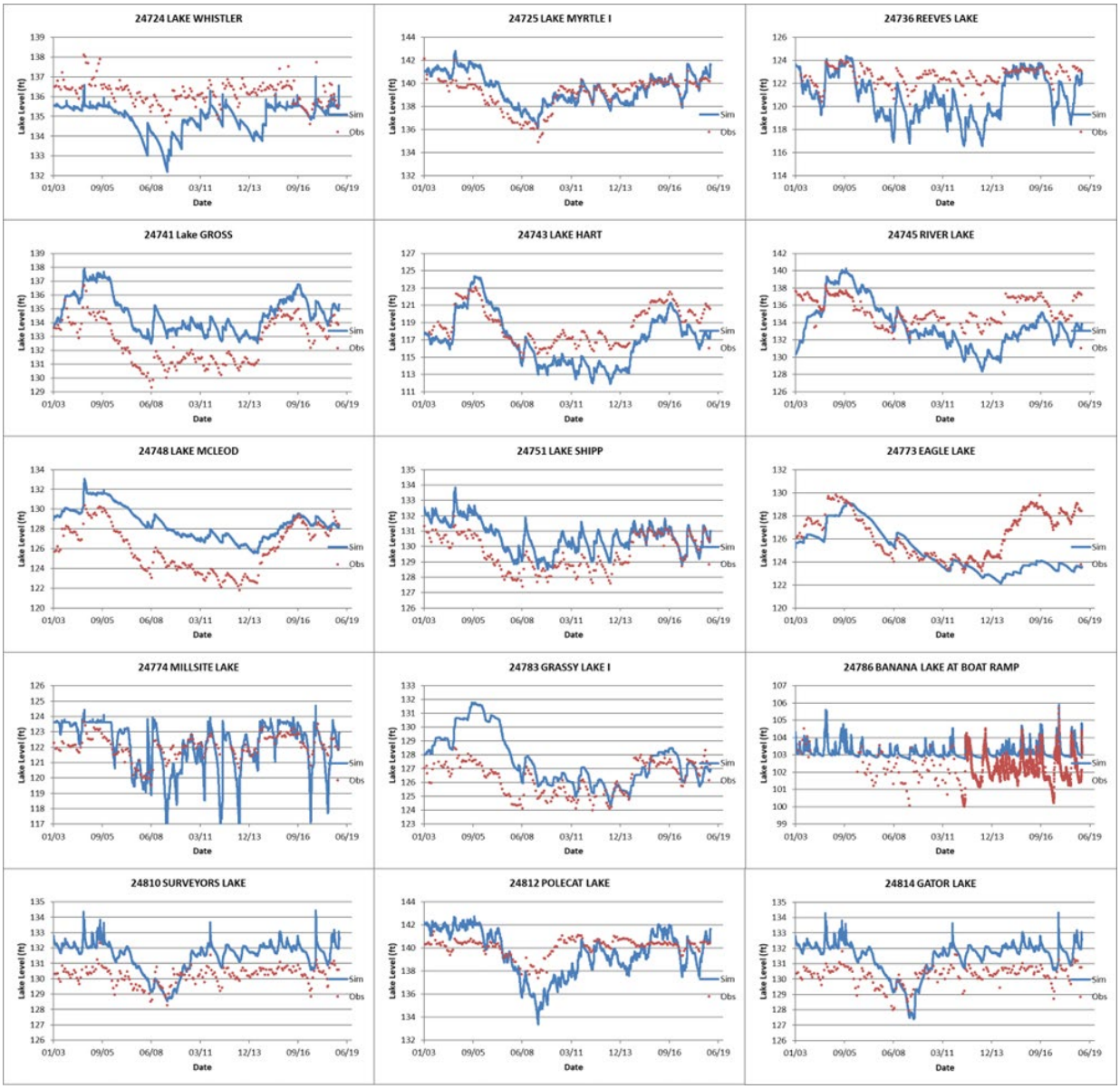
24724 LAKE WHISTLER
24725 LAKE MYRTLE I
24736 REEVES LAKE
24741 Lake GROSS
24743 LAKE HART
24745 RIVER LAKE
24748 LAKE MCLEOD
24751 LAKE SHIPP
24773 EAGLE LAKE
24774 MILLSITE LAKE
24783 GRASSY LAKE I
24786 BANANA LAKE AT BOAT RAMP
24810 SURVEYORS LAKE
24812 POLECAT LAKE
24814 GATOR LAKE
Lake Level (ft)
Date
Sim
Obs

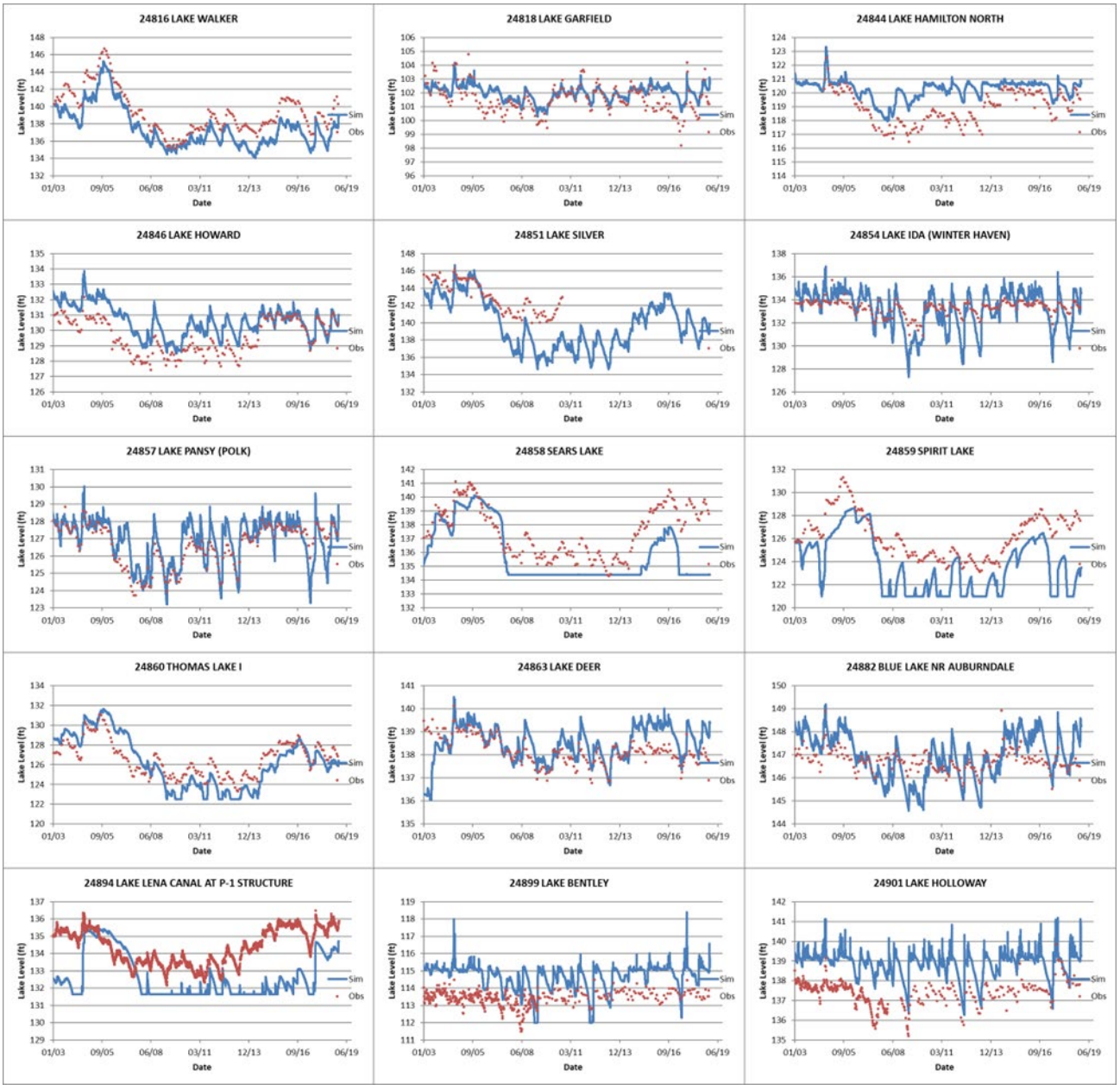
24816 LAKE WALKER
24818 LAKE GARFIELD
24844 LAKE HAMILTON NORTH
24846 LAKE HOWARD
24851 LAKE SILVER
24854 LAKE IDA (WINTER HAVEN)
24857 LAKE PANSY (POLK)
24858 SEARS LAKE
24859 SPIRIT LAKE
24860 THOMAS LAKE I
24863 LAKE DEER
24882 BLUE LAKE NR AUBURNDALE
24894 LAKE LENA CANAL AT P-1 STRUCTURE
24899 LAKE BENTLEY
24901 LAKE HOLLOWAY
Lake Level (ft)
Date
01/03
09/05
06/08
03/11
12/13
09/16
06/19
Sim
Obs

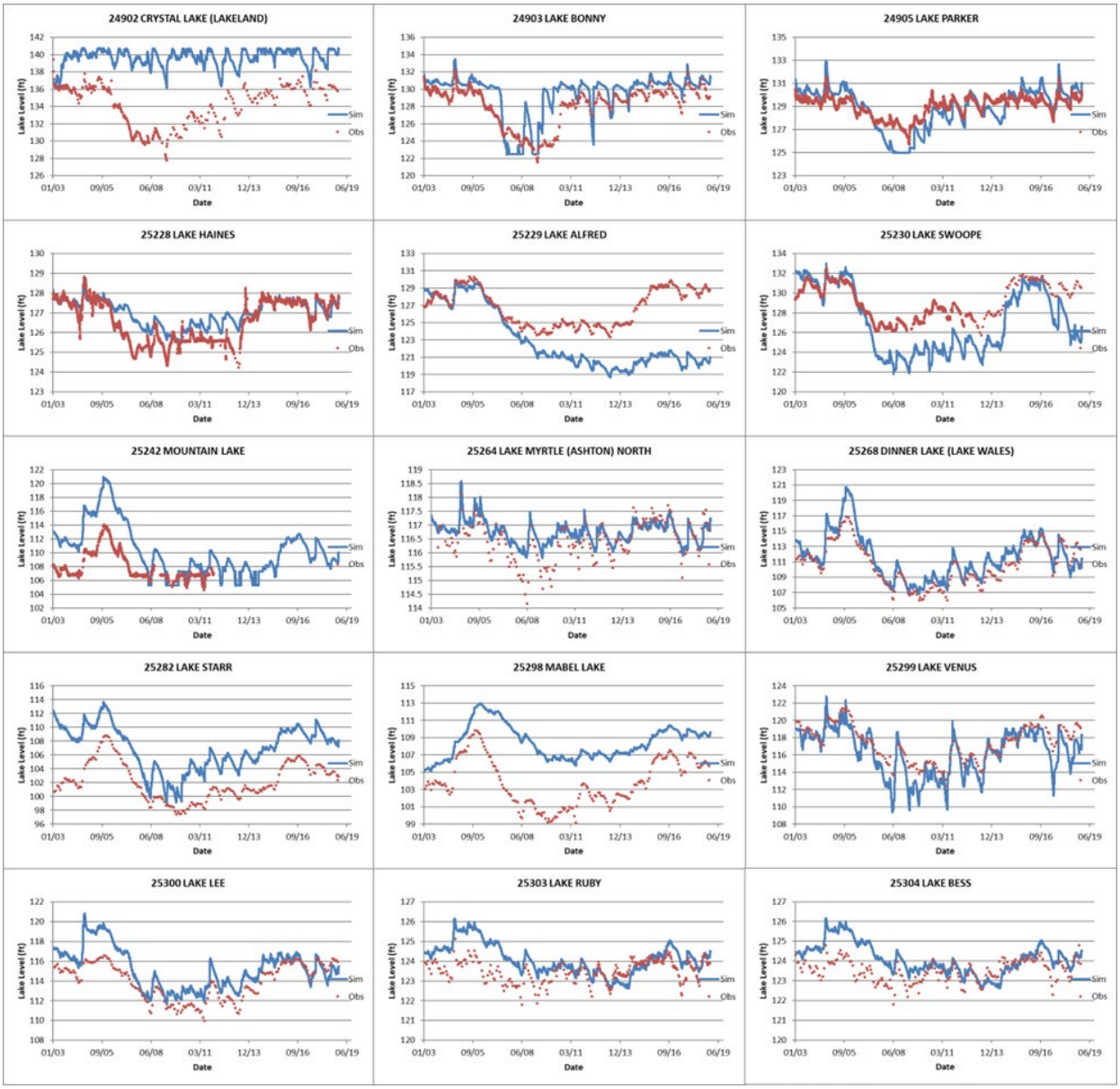
24902 CRYSTAL LAKE (LAKELAND)
24903 LAKE BONNY
24905 LAKE PARKER
25228 LAKE HAINES
25229 LAKE ALFRED
25230 LAKE SWOOPE
25242 MOUNTAIN LAKE
25264 LAKE MYRTLE (ASHTON) NORTH
25268 DINNER LAKE (LAKE WALES)
25282 LAKE STARR
25298 MABEL LAKE
25299 LAKE VENUS
25300 LAKE LEE
25303 LAKE RUBY
25304 LAKE BESS
Lake Level (ft)
Date
Sim
Obs
01/03
09/05
06/08
03/11
12/13
09/16
06/19

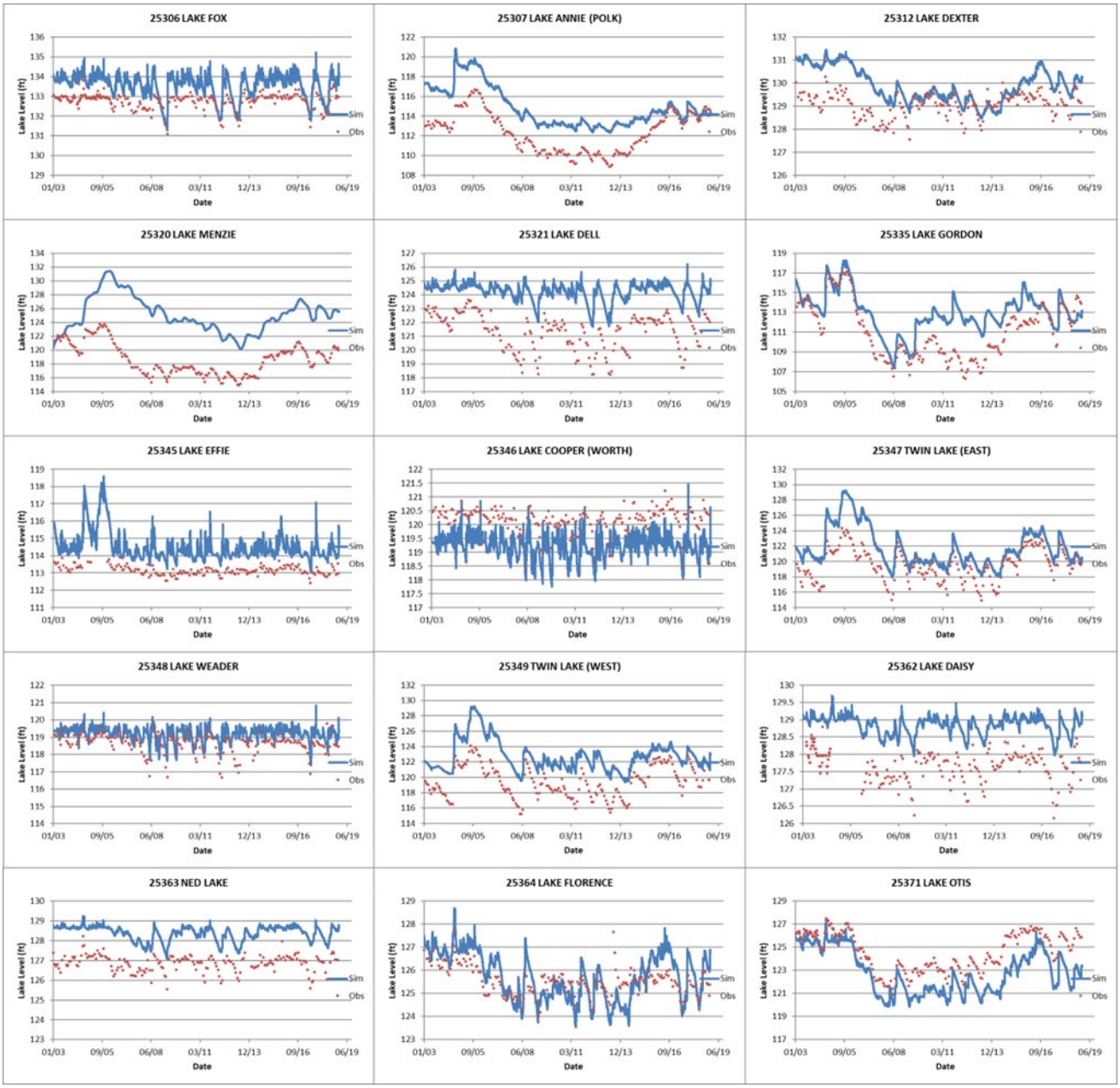
25306 LAKE FOX
25307 LAKE ANNIE (POLK)
25312 LAKE DEXTER
25320 LAKE MENZIE
25321 LAKE DELL
25335 LAKE GORDON
25345 LAKE EFFIE
25346 LAKE COOPER (WORTH)
25347 TWIN LAKE (EAST)
25348 LAKE WEADER
25349 TWIN LAKE (WEST)
25362 LAKE DAISY
25363 NED LAKE
25364 LAKE FLORENCE
25371 LAKE OTIS
Lake Level (ft)
Date
01/03
09/05
06/08
03/11
12/13
09/16
06/19
Sim
Obs

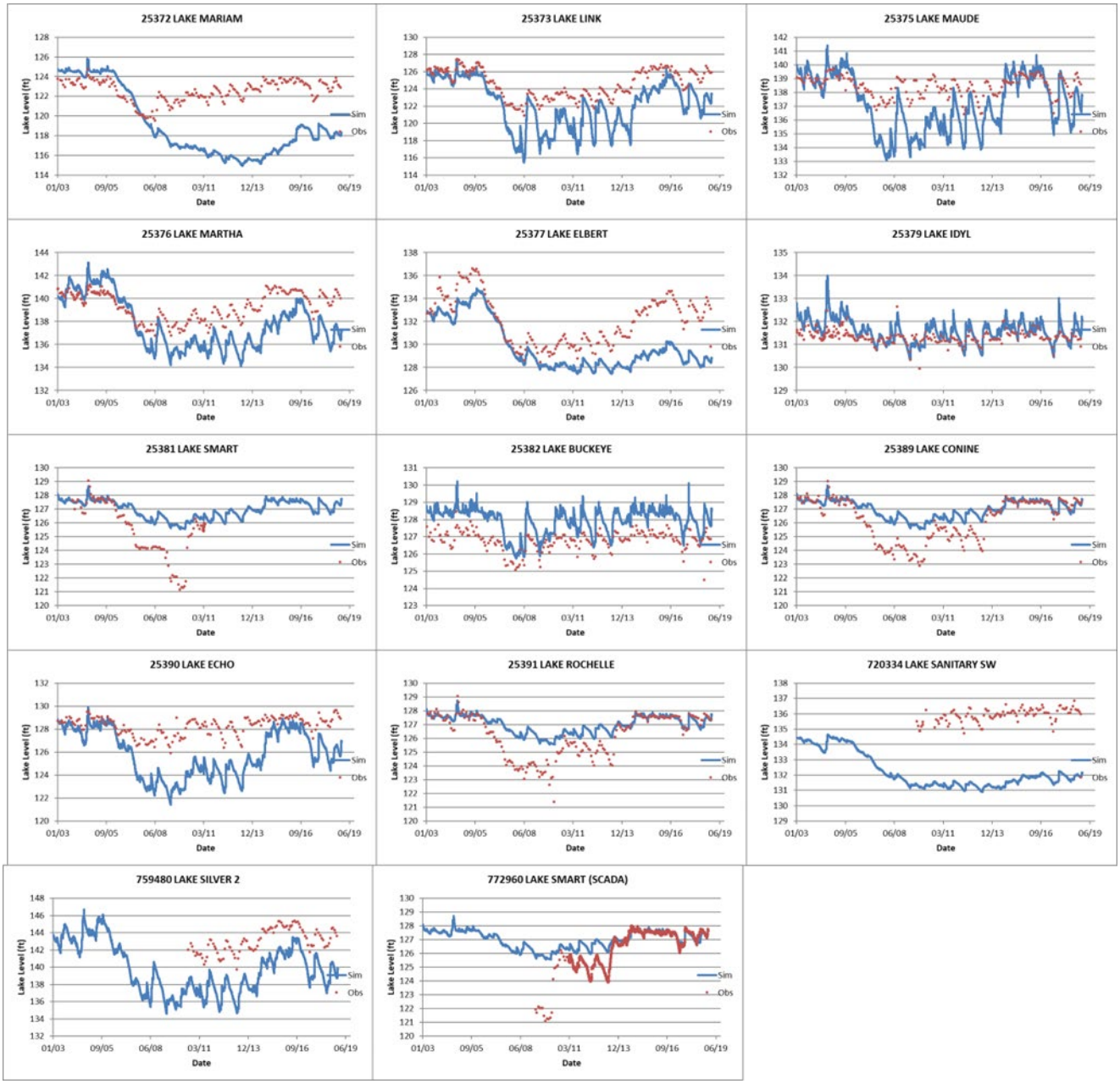
25372 LAKE MARIAM
25373 LAKE LINK
25375 LAKE MAUDE
25376 LAKE MARTHA
25377 LAKE ELBERT
25379 LAKE IDYL
25381 LAKE SMART
25382 LAKE BUCKEYE
25389 LAKE CONINE
25390 LAKE ECHO
25391 LAKE ROCHELLE
720334 LAKE SANITARY SW
759480 LAKE SILVER 2
772960 LAKE SMART (SCADA)
Lake Level (ft)
Date
Sim
Obs
01/03
09/05
06/08
03/11
12/13
09/16
06/19

APPENDIX D

GROUNDWATER CALIBRATION RESULTS

This page was intentionally left blank.

APPENDIX D
GROUNDWATER CALIBRATION RESULTS

Site Name	Aquifer	Average Error (feet)	MAE (feet)	RMSE (feet)	Max Error (feet)	Min Error (feet)	R^2	E	PBias (%)
ROMP 40 Surf Aq Monitor	SA	-0.42	1.24	1.50	2.04	-4.34	0.64	-1.80	-0.31
ROMP 31 Surf Aq Monitor	SA	1.81	1.86	2.02	4.31	-1.58	0.91	0.48	2.54
ROMP 43 Surf Aq Monitor Repl	SA	2.17	2.20	2.44	6.29	-1.16	0.72	-0.39	2.37
ROMP 43 U Arca Aq Monitor	SA	4.94	4.94	5.20	10.68	1.07	0.79	-1.77	5.58
ROMP 30 Surf Aq Monitor	SA	0.85	1.24	1.41	2.63	-2.66	0.53	-1.51	1.36
ROMP 17 Surf Aq Monitor	SA	1.80	1.84	2.00	4.05	-2.53	0.61	-1.01	9.90
ROMP 16 Surf Aq Monitor	SA	1.26	1.50	1.71	3.63	-3.49	0.58	-0.19	2.10
ROMP 26 Surf Aq Monitor	SA	-0.53	1.12	1.35	3.54	-3.51	0.62	0.29	-0.78
ROMP 35 Surf Aq Monitor	SA	-1.37	1.67	2.11	2.16	-6.34	0.17	-2.34	-2.28
ROMP 41 Surf Aq Monitor	SA	-0.45	0.92	1.11	2.03	-3.42	0.73	0.56	-0.38
Tenoroc Road Int nr Lakeland	SA	-3.81	3.81	3.91	-1.79	-6.87	0.90	-2.46	-3.20
Ridge WRAP P-3 Surf	SA	-2.10	2.32	2.90	2.50	-8.31	0.57	0.03	-1.58
ROMP 58 Surf Aq Monitor	SA	-1.30	1.59	1.89	2.51	-5.36	0.81	0.41	-1.05
ROMP 57 Surf Aq Monitor Repl	SA	-3.37	3.38	3.63	0.16	-6.39	0.66	-3.87	-2.87
Ridge WRAP P-2 Surf	SA	0.03	1.65	2.02	6.50	-3.93	0.55	0.55	0.02
Oak Hill Pump House Surf	SA	11.47	11.47	11.70	17.98	4.65	0.70	-10.58	13.36
LW3P Surf Aq Monitor	SA	2.44	5.56	6.62	13.18	-9.53	0.54	-7.96	2.86
PRIM PNC01 Fort Green Road Surf Aq Monitor	SA	-2.20	2.65	3.26	3.05	-9.31	0.28	-6.05	-1.71
PRIM PC07 Lake Buffum Road Surf Aq Monitor	SA	0.86	1.45	1.63	3.11	-3.66	0.67	0.03	0.67
PRIM SC03 Crystal Lake Elem Surf Aq Monitor	SA	-8.81	8.81	8.93	-5.82	-15.35	0.38	-27.01	-6.11
PRIM PC04 Chain of Lakes Elem Surf Aq Monitor	SA	-2.32	2.32	2.65	0.20	-6.53	0.77	-0.07	-1.80
PRIM SC07A Valleyview Elem Surf Aq Monitor	SA	4.91	5.26	6.06	10.92	-3.20	0.44	-6.13	3.94
PRIM SC02 Lena Vista Elem Surf Aq Monitor	SA	-9.84	9.84	9.93	-6.11	-13.24	0.58	-26.32	-6.85
PRIM PC05 FDOT Compound Surf Aq Monitor	SA	-7.36	7.36	7.48	-3.82	-10.80	0.80	-5.76	-7.27
PRIM SC01 Tenoroc Surf Aq Monitor	SA	1.63	1.95	2.32	5.59	-3.17	0.73	0.20	1.51
PRIM PNC02 Hardee Lakes Park Surf Aq Monitor	SA	-0.38	1.67	1.92	3.84	-3.83	0.75	0.02	-0.33
PRIM PNC03B Pyatt Park Surf Aq Monitor	SA	-7.37	7.37	7.52	-4.88	-12.31	0.45	-13.11	-6.82
PRIM PC01 Water Tower Surf Aq Monitor	SA	-2.19	2.22	2.61	1.59	-7.76	0.70	-0.19	-1.71

Site Name	Aquifer	Average Error (feet)	MAE (feet)	RMSE (feet)	Max Error (feet)	Min Error (feet)	R^2	E	PBias (%)
PRIM PC02 Water Systems Plant Surf Aq Monitor	SA	-4.70	4.70	4.81	-2.26	-8.07	0.75	-5.76	-3.26
PRIM SC05 Polk Utilities Surf Aq Monitor	SA	-0.59	2.01	2.43	3.03	-7.74	0.41	-1.01	-0.50
Lake Hancock NW Surf Aq Monitor	SA	-2.51	3.38	4.01	3.47	-9.75	0.39	-4.54	-2.46
Lake Hancock E Surf Aq Monitor	SA	3.02	3.10	3.35	5.44	-2.35	0.74	-0.68	2.88
PRIM PC03A Calvary Baptist Church Surf Aq Monitor	SA	-0.67	1.08	1.44	1.86	-4.55	0.61	0.49	-0.53
PRIM BC02 Flywheelers Surf Aq Monitor	SA	1.80	1.99	2.23	4.11	-3.52	0.33	-0.96	1.38
PRIM BC01 Greenwood Surf Aq Monitor	SA	1.73	1.76	2.02	4.13	-2.32	0.42	-1.19	1.35
PRIM LCC01 Moseley Surf Aq Monitor	SA	0.44	1.45	1.76	3.59	-4.37	0.48	-0.77	0.77
PRIM CC03 Davidson Surf Aq Monitor	SA	1.32	1.60	1.90	4.46	-2.52	0.63	-0.33	1.48
Lake Hancock NE Surf Aq Monitor	SA	-4.21	4.92	5.85	2.38	-12.13	0.17	-17.28	-3.73
ROMP 29 Surf Aq Monitor	SA	-4.30	4.30	4.67	0.06	-8.99	0.70	-6.75	-5.17
PRIM CC01 Crews Surf Aq Monitor	SA	-2.09	2.10	2.19	0.45	-4.37	0.72	-6.58	-2.35
PRIM PNC04 Mosaic Surf Aq Monitor	SA	-1.47	2.07	2.39	3.18	-5.66	0.64	-1.01	-1.34
ROMP 42 Surf Aq Monitor	SA	1.88	2.40	2.70	4.98	-3.55	0.47	-0.94	1.34
ROMP 40 U Arca Aq Monitor	IAS	-4.56	4.56	4.74	-0.89	-9.06	0.16	-16.57	-3.62
ROMP 31 L Arca Aq Monitor	IAS	-0.67	3.34	4.16	13.76	-8.23	0.87	0.71	-1.51
ROMP 43 L Arca Aq Monitor	IAS	-0.98	1.83	2.34	14.01	-9.99	0.87	0.83	-1.31
ROMP 30 L Arca Aq Monitor	IAS	-0.97	2.61	3.17	9.53	-6.12	0.89	0.78	-2.05
ROMP 30 U Arca Aq Monitor	IAS	0.35	2.23	2.91	10.39	-5.92	0.89	0.79	0.73
ROMP 17 L Arca Aq Monitor	IAS	2.63	2.67	3.08	11.04	-1.82	0.67	-0.34	6.71
ROMP 17 U Arca Aq Monitor	IAS	1.23	1.38	1.63	7.00	-1.88	0.78	0.49	3.80
ROMP 16 Htrn As Monitor	IAS	0.30	0.88	1.20	8.97	-3.69	0.80	0.79	0.65
ROMP 16 L Arca Aq Monitor	IAS	1.02	1.38	1.83	13.53	-3.68	0.71	0.58	2.25
Arcadia 2 Int	IAS	1.41	1.66	3.08	21.79	-1.92	0.41	0.24	3.29
ROMP 26 U Arca Aq Monitor	IAS	2.16	2.21	2.78	15.13	-4.05	0.86	0.63	5.12
ROMP 26 L Arca Aq Monitor	IAS	1.66	1.81	2.43	14.80	-4.81	0.86	0.73	3.95
ROMP 35 L Arca Aq Monitor	IAS	2.98	3.05	3.81	12.90	-1.57	0.82	0.47	9.31
ROMP 35 U Arca Aq Monitor	IAS	-9.18	9.18	9.27	-4.46	-12.60	0.76	-16.43	-18.26
Fort Green Springs Int	IAS	-5.59	6.16	7.18	12.48	-17.49	0.67	0.16	-8.24
ROMP 45 L Arca Aq Monitor (was Htrn As)	IAS	-0.49	2.85	3.45	10.79	-7.33	0.82	0.72	-0.67

Site Name	Aquifer	Average Error (feet)	MAE (feet)	RMSE (feet)	Max Error (feet)	Min Error (feet)	R^2	E	PBias (%)
ROMP 45 Pcrv Perm Unit Monitor (was Surf Aq)	IAS	-1.04	1.97	2.35	4.12	-6.17	0.81	0.06	-1.04
Homeland DEP 4 Int	IAS	2.49	4.66	6.42	21.18	-8.08	0.36	0.16	3.46
ROMP 59 U Arca Aq Monitor 2	IAS	-1.24	2.59	2.97	4.74	-5.71	0.66	0.53	-1.47
ROMP 59 U Arca Aq Monitor 1	IAS	-2.06	3.64	4.34	6.19	-9.28	0.41	0.21	-2.37
LW1P U Arca Aq Monitor	IAS	-8.64	8.64	8.89	-1.87	-16.19	0.47	-9.86	-9.77
ROMP 57 U Arca Aq Monitor	IAS	-3.95	3.95	4.12	-1.13	-6.42	0.74	-4.53	-3.47
ROMP 41 L Arca Aq Monitor	IAS	-6.27	6.81	7.59	13.51	-13.40	0.84	-0.15	-9.25
Clear Springs 6-In Htrn	IAS	-4.09	6.02	6.41	11.96	-13.72	0.61	0.22	-4.98
LW4P U Arca Aq Monitor	IAS	-8.28	8.95	9.68	8.69	-18.60	0.38	-1.34	-10.27
LW3P Htrn CU Monitor	IAS	0.70	4.73	5.50	10.42	-10.27	0.57	-4.71	0.82
LW3P L Arca Aq Monitor	IAS	3.13	3.79	5.26	17.72	-15.03	0.73	0.55	4.13
ROMP 42 U Arca Aq Monitor	IAS	-1.56	1.83	2.24	5.18	-6.18	0.71	0.26	-1.29
ROMP 40 U Arca Aq Monitor	IAS	-4.56	4.56	4.74	-0.89	-9.06	0.16	-16.57	-3.62
ROMP 31 L Arca Aq Monitor	IAS	-0.67	3.34	4.16	13.76	-8.23	0.87	0.71	-1.51
ROMP 40 U Fldn Aq Monitor	UFA	-0.63	3.03	3.77	15.09	-10.76	0.84	0.83	-1.66
ROMP 31 U Fldn Aq Monitor	UFA	0.14	3.27	4.17	15.50	-7.91	0.87	0.73	0.34
ROMP 43 U Fldn Aq (Swnn) Monitor	UFA	-1.38	1.99	2.54	13.29	-10.38	0.87	0.80	-1.83
ROMP 43 U Fldn Aq (Avpk) Monitor	UFA	-1.31	1.94	2.49	13.63	-10.44	0.87	0.81	-1.74
ROMP 30 U Fldn Aq Monitor	UFA	0.10	3.35	4.33	15.42	-8.47	0.88	0.74	0.23
ROMP 17 U Fldn Aq (Noca-Swnn) Monitor	UFA	-1.67	1.90	2.22	8.90	-5.70	0.72	0.33	-3.82
ROMP 17 U Fldn Aq (Swnn) Monitor	UFA	-1.88	2.06	2.36	8.39	-6.09	0.72	0.19	-4.28
ROMP 17 U Fldn Aq (Avpk) Monitor	UFA	-1.44	1.70	2.01	9.32	-6.26	0.73	0.42	-3.29
ROMP 16 U Fldn Aq Monitor	UFA	-0.03	1.07	1.45	13.15	-5.21	0.69	0.64	-0.06
ROMP 26 U Fldn Aq Monitor	UFA	0.49	1.27	1.80	14.22	-5.88	0.85	0.84	1.16
Fish Lake Deep nr Lakeland	UFA	-5.53	5.53	5.81	-2.03	-10.03	0.66	-7.60	-4.93
ROMP 45 U Fldn Aq (Swnn) Monitor	UFA	-0.31	2.74	3.39	13.42	-9.02	0.85	0.79	-0.45
ROMP 45 U Fldn Aq (Avpk) Monitor	UFA	-1.66	2.89	3.48	11.55	-10.75	0.85	0.77	-2.38
ROMP 59 U Fldn Aq Interface Monitor	UFA	-1.13	1.78	2.14	9.86	-4.77	0.95	0.89	-1.55
Sanlon Ranch Fldn	UFA	2.09	2.64	2.90	5.57	-4.82	0.71	0.38	2.33
ROMP 70 U Fldn Aq Monitor	UFA	-0.52	3.44	3.83	9.49	-8.43	0.67	0.13	-0.55
Cargill FA-1 Fldn	UFA	-3.91	4.51	5.22	10.10	-12.58	0.83	0.52	-5.77

Site Name	Aquifer	Average Error (feet)	MAE (feet)	RMSE (feet)	Max Error (feet)	Min Error (feet)	R^2	E	PBias (%)
Smith Deep	UFA	2.33	2.89	3.57	8.42	-6.39	0.83	0.71	3.44
LW1P U Fldn Aq Monitor	UFA	3.55	3.71	4.86	19.11	-2.39	0.84	0.30	4.72
LAKE ALFRED DEEP AT LAKE ALFRED	UFA	-3.27	3.50	4.88	4.38	-10.20	0.21	-0.44	-2.66
ROMP 58 U Fldn Aq Monitor	UFA	-2.14	2.38	2.84	6.15	-8.75	0.70	0.30	-2.11
ROMP 57 U Fldn Aq Monitor	UFA	-0.46	1.17	1.55	6.00	-5.67	0.74	0.71	-0.44
ROMP 73 U Fldn Aq Monitor	UFA	1.81	1.86	2.17	6.80	-2.09	0.78	0.27	1.58
ROMP 41 U Fldn Aq (Avpk) Monitor	UFA	-6.33	6.61	7.28	8.90	-12.52	0.86	-0.10	-9.33
ROMP 41 U Fldn Aq (Swnn) Monitor	UFA	-6.24	6.67	7.39	10.16	-12.86	0.85	-0.09	-9.22
Homeland DEP 9 Fldn	UFA	0.06	2.67	3.30	13.55	-7.13	0.89	0.81	0.09
LW4P U Fldn Aq Monitor	UFA	0.42	3.82	5.02	17.07	-9.98	0.64	0.52	0.59
LW3P U Fldn Aq Monitor	UFA	3.34	3.68	5.12	17.55	-3.22	0.77	0.55	4.47
Lake Hancock NW U Fldn Aq Monitor	UFA	9.94	9.94	10.23	17.13	4.18	0.91	-2.62	12.03
Lake Hancock E U Fldn Aq Monitor	UFA	2.86	2.86	3.25	11.37	-0.13	0.92	0.31	3.06
Lake Hancock S U Fldn Aq Monitor	UFA	8.27	8.27	8.88	20.06	2.59	0.88	-0.89	11.15
Lake Hancock NE U Fldn Aq Monitor	UFA	4.99	4.99	5.09	8.78	3.01	0.93	-1.30	5.16
ROMP 29 U Fldn Aq Monitor	UFA	7.74	7.74	8.39	19.73	2.02	0.72	-1.30	12.78
ROMP 42 U Fldn Aq (Swnn) Monitor	UFA	-4.11	4.11	4.33	0.92	-7.76	0.93	0.27	-5.11
ROMP 42 U Fldn Aq (Avpk) Monitor	UFA	-3.31	3.34	3.60	1.69	-7.18	0.92	0.47	-4.18

APPENDIX E

SUBBASIN WATER BUDGETS

This page was intentionally left blank.

APPENDIX E
SUBBASIN WATER BUDGETS

Table E.1
Annual Water Budgets for the Saddle Creek Subbasin

ANNUALIZED BUDGETS FOR SADDLE CREEK IN in/yr													
	Rainfall	NPDES + Return Flow	SW Inflow	Lateral GW Inflow	Total In	Total Out	EVT	GW Pumping	Lateral GW Outflow	SW Outflow	CHF Storage Gain	OLF Storage Gain	GW Storage Gain
2003	48.86	13.37	0.17	4.93	**67.34**	**67.92**	38.33	2.68	13.68	17.68	-1.05	-0.57	-2.83
2004	63.40	16.96	0.35	5.14	**85.85**	**87.40**	39.10	2.83	13.11	29.19	0.43	0.08	2.66
2005	61.37	11.17	0.29	5.22	**78.05**	**78.96**	40.78	2.82	12.84	20.53	0.13	0.06	1.80
2006	46.68	3.64	0.16	5.63	**56.11**	**56.29**	40.85	3.28	14.37	3.90	-0.44	-0.27	-5.40
2007	37.05	2.90	0.11	6.09	**46.15**	**46.19**	41.43	2.89	14.06	0.64	-0.95	-0.95	-10.95
2008	44.40	2.65	0.41	6.99	**54.45**	**54.53**	38.78	2.69	12.99	0.62	0.02	0.44	-1.01
2009	45.92	2.83	0.20	6.56	**55.51**	**55.53**	38.12	2.92	12.81	0.14	-0.03	-0.11	1.69
2010	49.52	4.12	0.24	5.84	**59.73**	**59.75**	41.59	2.80	11.85	2.82	0.15	0.17	0.38
2011	51.58	5.12	0.30	6.44	**63.44**	**63.62**	39.74	2.68	12.51	4.87	0.24	0.38	3.21
2012	44.83	5.53	0.22	6.18	**56.76**	**56.76**	37.59	2.95	12.02	4.08	-0.03	0.07	0.09
2013	42.97	4.76	0.17	5.25	**53.15**	**53.15**	38.04	2.78	11.21	2.95	-0.16	-0.27	-1.41
2014	55.78	7.92	0.24	5.30	**69.24**	**69.43**	40.81	2.34	9.88	9.12	0.42	0.43	6.43
2015	57.19	8.44	0.29	4.73	**70.65**	**70.85**	41.32	2.62	11.11	13.52	0.21	0.01	2.06
2016	55.55	10.38	0.31	4.62	**70.86**	**69.57**	42.02	2.78	11.06	15.52	-0.06	-0.07	-1.67
2017	52.42	14.47	0.30	5.29	**72.48**	**72.21**	39.76	2.82	12.76	17.11	0.23	0.01	-0.47
2018	61.72	12.35	0.25	5.49	**79.80**	**77.72**	41.99	2.73	12.96	14.07	0.77	0.34	4.86
Average	51.20	7.91	0.25	5.61	**64.97**	**64.99**	40.01	2.79	12.45	9.80	-0.01	-0.02	-0.04

Table E.2
Annual Water Budgets for the Peace Creek Subbasin

ANNUALIZED BUDGETS FOR PEACE CREEK IN in/yr													
	Rainfall	NPDES + Return Flow	SW Inflow	Lateral GW Inflow	Total In	Total Out	EVT	GW Pumping	Lateral GW Outflow	SW Outflow	CHF Storage Gain	OLF Storage Gain	GW Storage Gain
2003	47.75	3.51	0.11	2.01	**53.38**	**53.73**	39.70	3.32	8.00	7.61	-1.43	-1.11	-2.35
2004	63.31	3.39	0.34	2.13	**69.17**	**70.65**	39.79	3.21	8.41	13.18	1.47	0.53	4.06
2005	69.99	3.22	0.44	2.08	**75.73**	**76.04**	43.60	2.99	9.32	16.35	0.98	0.20	2.60
2006	42.23	4.24	0.08	2.38	**48.94**	**49.15**	40.05	4.06	9.87	3.12	-2.05	-1.03	-4.86
2007	35.96	4.12	0.03	2.35	**42.47**	**42.72**	38.98	3.93	10.19	1.01	-2.39	-1.64	-7.36
2008	50.05	3.75	0.08	2.52	**56.41**	**56.58**	37.59	3.60	9.60	2.57	0.56	0.49	2.16
2009	45.36	3.97	0.04	2.48	**51.85**	**52.01**	37.66	3.81	9.87	1.23	-0.63	-0.70	0.78
2010	48.10	3.80	0.07	2.20	**54.18**	**54.20**	40.39	3.60	8.91	2.24	0.26	-0.05	-1.14
2011	51.61	3.46	0.14	2.35	**57.56**	**57.58**	38.88	3.25	9.24	3.28	0.66	0.14	2.13
2012	43.87	4.04	0.08	2.49	**50.48**	**50.39**	37.29	3.86	9.52	2.04	-0.54	-0.43	-1.36
2013	45.01	3.56	0.05	2.16	**50.78**	**50.68**	37.61	3.41	8.61	2.04	-0.21	-0.31	-0.47
2014	57.27	3.35	0.09	2.14	**62.85**	**62.75**	41.36	3.14	8.10	4.27	1.09	0.67	4.13
2015	55.48	3.35	0.22	2.20	**61.25**	**61.14**	42.27	3.13	8.44	5.66	0.44	0.37	0.85
2016	52.83	3.34	0.19	2.20	**58.56**	**58.47**	42.04	3.10	8.29	5.37	-0.01	0.43	-0.74
2017	46.72	3.53	0.16	2.38	**52.79**	**53.02**	39.58	3.27	8.88	3.46	-0.31	-0.24	-1.64
2018	53.59	3.54	0.24	2.33	**59.69**	**59.70**	40.80	3.32	8.94	3.09	0.53	0.27	2.74
Average	50.57	3.63	0.15	2.28	**56.63**	**56.80**	39.85	3.44	9.01	4.78	-0.10	-0.15	-0.03

Table E.3
Annual Water Budgets for the Payne Creek Subbasin

ANNUALIZED BUDGETS FOR PAYNE CREEK IN in/yr													
	Rainfall	NPDES + Return Flow	SW Inflow	Lateral GW Inflow	Total In	Total Out	EVT	GW Pumping	Lateral GW Outflow	SW Outflow	CHF Storage Gain	OLF Storage Gain	GW Storage Gain
2003	54.64	11.54	1.46	10.81	**78.45**	**78.51**	37.10	1.76	10.33	29.19	-0.10	-0.28	0.51
2004	62.22	16.44	2.03	12.22	**92.91**	**93.27**	38.88	1.62	11.67	39.89	0.01	0.08	1.12
2005	62.68	17.29	2.10	11.90	**93.97**	**94.18**	40.55	1.44	11.64	39.58	0.01	0.10	0.85
2006	42.93	5.11	0.38	9.57	**58.00**	**58.07**	40.85	1.96	10.73	9.66	-0.02	-0.10	-5.00
2007	35.28	3.84	0.04	8.51	**47.66**	**47.73**	40.08	1.82	10.62	4.60	-0.02	-0.12	-9.24
2008	41.40	5.61	0.15	9.31	**56.47**	**56.52**	37.77	1.70	10.38	7.15	0.00	-0.03	-0.45
2009	49.52	6.03	0.26	8.96	**64.76**	**64.80**	39.73	1.79	10.06	8.90	0.04	0.04	4.25
2010	43.89	7.83	0.32	10.32	**62.36**	**62.39**	42.57	1.20	10.44	11.93	-0.03	-0.06	-3.66
2011	43.87	5.17	0.31	10.41	**59.76**	**59.79**	40.07	1.05	10.99	7.89	0.00	-0.01	-0.18
2012	47.54	6.79	0.70	9.46	**64.49**	**64.52**	36.70	1.91	10.81	14.07	0.01	-0.01	1.04
2013	42.07	10.68	0.51	9.32	**62.58**	**62.62**	38.87	1.59	9.77	14.95	0.01	-0.03	-2.53
2014	47.71	6.43	0.39	10.08	**64.61**	**64.63**	39.94	1.47	9.79	10.57	-0.01	0.03	2.84
2015	55.50	10.60	0.81	10.48	**77.39**	**77.47**	40.14	1.33	10.31	21.62	0.01	0.11	3.95
2016	48.57	9.16	1.09	11.28	**70.10**	**70.15**	42.85	1.01	11.10	19.80	-0.01	-0.10	-4.49
2017	49.60	8.61	1.03	9.70	**68.93**	**69.15**	39.11	1.12	11.15	18.36	0.00	0.01	-0.61
2018	56.21	40.84	0.75	9.28	**107.09**	**107.63**	41.24	1.11	9.23	49.93	0.13	0.51	5.47
Average	48.98	10.75	0.77	10.10	**70.60**	**70.71**	39.78	1.49	10.56	19.26	0.00	0.01	-0.38

Table E.4
Annual Water Budgets for the Horse Creek Subbasin

ANNUALIZED BUDGETS FOR HORSE CREEK IN in/yr													
	Rainfall	NPDES + Return Flow	SW Inflow	Lateral GW Inflow	Total In	Total Out	EVT	GW Pumping	Lateral GW Outflow	SW Outflow	CHF Storage Gain	OLF Storage Gain	GW Storage Gain
2003	55.53	0.81	1.10	7.06	**64.51**	**64.49**	40.95	0.87	8.09	17.30	-0.38	-0.41	-1.94
2004	61.02	0.89	2.04	8.88	**72.83**	**72.80**	41.81	1.04	9.89	20.34	0.08	-0.03	-0.34
2005	66.41	0.61	2.06	9.69	**78.77**	**78.71**	42.80	0.81	10.81	24.30	-0.11	0.09	0.02
2006	46.01	1.10	0.42	10.03	**57.55**	**57.52**	41.40	1.17	11.23	7.17	-0.13	-0.22	-3.10
2007	36.23	1.12	0.01	8.89	**46.25**	**46.25**	40.32	1.14	10.28	0.69	-0.04	-0.13	-6.01
2008	47.58	0.84	0.38	9.05	**57.84**	**57.84**	39.69	0.86	10.33	4.81	0.02	-0.02	2.14
2009	46.06	1.06	0.04	10.89	**58.06**	**58.06**	39.62	1.09	12.06	2.81	0.08	0.03	2.39
2010	47.03	1.00	0.22	8.62	**56.88**	**56.86**	43.42	1.03	9.60	5.03	-0.05	0.00	-2.17
2011	42.67	0.84	0.22	8.03	**51.76**	**51.75**	40.22	0.86	9.13	2.70	-0.02	-0.03	-1.12
2012	43.30	1.11	0.26	9.08	**53.74**	**53.72**	37.20	1.11	10.12	3.92	0.03	0.08	1.26
2013	46.02	1.07	0.38	9.66	**57.14**	**57.12**	39.39	1.09	10.46	7.67	-0.04	-0.01	-1.45
2014	47.74	0.74	0.19	10.08	**58.75**	**58.73**	40.77	0.77	10.98	3.59	0.10	0.06	2.46
2015	53.13	0.79	0.89	8.95	**63.75**	**63.73**	42.50	0.84	9.77	9.74	0.02	0.10	0.76
2016	50.35	0.71	0.81	9.23	**61.10**	**61.07**	43.64	0.78	10.14	10.12	-0.12	-0.11	-3.39
2017	52.14	0.90	1.83	10.74	**65.61**	**65.61**	39.63	0.94	11.88	12.33	0.03	0.01	0.79
2018	57.23	0.77	0.67	8.39	**67.05**	**67.04**	42.01	0.83	8.91	10.65	0.27	0.17	4.20
Average	49.90	0.90	0.72	9.20	**60.72**	**60.71**	40.96	0.95	10.23	8.95	-0.02	-0.03	-0.34

Table E.5
Annual Water Budgets for the Charlie Creek Subbasin

ANNUALIZED BUDGETS FOR CHARLIE CREEK IN in/yr													
	Rainfall	NPDES + Return Flow	SW Inflow	Lateral GW Inflow	Total In	Total Out	EVT	GW Pumping	Lateral GW Outflow	SW Outflow	CHF Storage Gain	OLF Storage Gain	GW Storage Gain
2003	50.85	1.38	0.57	2.13	**54.94**	**54.90**	42.12	1.39	2.75	11.84	-0.10	-0.54	-2.57
2004	55.09	1.52	0.73	2.32	**59.66**	**59.93**	41.50	1.55	2.70	12.86	0.00	0.04	1.28
2005	64.99	0.99	1.00	1.92	**68.90**	**68.93**	43.56	1.02	2.98	19.86	0.00	0.90	0.62
2006	41.33	1.81	0.16	2.46	**45.76**	**45.69**	41.48	1.86	2.91	4.48	-0.02	-1.02	-4.00
2007	36.93	1.70	0.00	2.25	**40.89**	**40.81**	41.75	1.73	2.54	0.89	-0.02	-0.04	-6.04
2008	47.12	1.40	0.10	2.14	**50.76**	**50.71**	40.60	1.41	2.58	3.04	0.01	0.03	3.04
2009	46.19	1.85	0.07	2.35	**50.46**	**50.39**	40.97	1.87	2.51	2.26	0.01	0.01	2.76
2010	46.68	1.84	0.21	2.22	**50.95**	**50.89**	43.96	1.89	2.46	4.43	-0.01	-0.01	-1.83
2011	43.68	1.40	0.16	2.04	**47.28**	**47.22**	40.95	1.44	2.49	2.91	0.00	0.00	-0.57
2012	42.84	1.74	0.07	2.33	**46.98**	**46.90**	39.81	1.80	2.43	1.64	0.00	0.00	1.22
2013	49.40	1.58	0.40	2.28	**53.65**	**53.61**	40.56	1.61	2.57	8.88	0.00	0.02	-0.04
2014	50.70	1.40	0.16	2.26	**54.52**	**54.47**	43.24	1.42	2.60	4.40	0.01	0.07	2.72
2015	53.75	1.17	0.45	2.32	**57.70**	**57.67**	44.94	1.20	2.86	8.54	0.00	-0.01	0.15
2016	53.54	1.28	0.48	2.33	**57.62**	**57.58**	45.43	1.30	2.97	10.69	-0.01	-0.05	-2.74
2017	58.49	1.53	1.91	2.53	**64.46**	**68.37**	42.04	1.57	2.98	19.84	0.01	0.05	1.87
2018	50.23	1.49	0.23	2.48	**54.44**	**54.36**	43.98	1.52	2.70	6.17	0.00	-0.03	0.02
Average	49.49	1.50	0.42	2.27	**53.69**	**53.90**	42.31	1.54	2.69	7.67	-0.01	-0.04	-0.26

Table E.6
Annual Water Budgets for the Joshua Creek Subbasin

ANNUALIZED BUDGETS FOR JOSHUA CREEK IN in/yr													
	Rainfall	NPDES + Return Flow	SW Inflow	Lateral GW Inflow	Total In	Total Out	EVT	GW Pumping	Lateral GW Outflow	SW Outflow	CHF Storage Gain	OLF Storage Gain	GW Storage Gain
2003	55.45	2.31	0.58	8.59	**66.92**	**66.86**	42.67	2.26	8.78	15.40	-0.05	-0.46	-1.72
2004	60.03	2.20	0.72	6.53	**69.48**	**69.41**	43.05	2.08	6.97	17.69	-0.01	-0.11	-0.27
2005	69.82	1.72	1.04	13.02	**85.59**	**85.49**	44.87	1.73	13.58	24.97	0.01	0.13	0.22
2006	48.94	3.14	0.21	12.81	**65.10**	**65.08**	42.21	3.04	12.40	9.12	-0.01	-0.16	-1.52
2007	38.04	2.89	0.02	9.21	**50.16**	**50.16**	40.84	2.84	8.93	2.26	-0.01	-0.09	-4.61
2008	49.70	2.14	0.14	12.74	**64.72**	**64.72**	41.14	2.16	12.98	6.98	0.01	0.02	1.44
2009	47.31	2.84	0.11	11.68	**61.94**	**61.93**	39.66	2.79	11.35	5.48	0.01	0.00	2.65
2010	54.38	2.77	0.30	14.25	**71.70**	**71.67**	45.87	2.69	14.23	10.47	0.00	0.03	-1.61
2011	49.29	2.36	0.18	20.70	**72.53**	**72.52**	42.32	2.26	21.00	6.59	0.00	0.02	0.33
2012	50.69	2.90	0.19	17.56	**71.34**	**71.33**	40.83	2.75	17.32	10.19	0.00	-0.02	0.26
2013	52.72	2.34	0.53	12.95	**68.53**	**68.49**	39.83	2.24	13.10	14.83	0.00	-0.03	-1.47
2014	48.07	1.76	0.15	14.14	**64.13**	**64.10**	42.57	1.78	14.39	3.43	0.01	0.04	1.87
2015	53.86	1.40	0.40	12.43	**68.10**	**68.04**	44.20	1.42	13.20	9.19	0.00	0.03	0.00
2016	54.84	1.62	0.50	13.77	**70.73**	**70.68**	44.93	1.61	14.40	12.26	-0.01	-0.08	-2.42
2017	61.11	2.33	0.91	9.00	**73.35**	**73.29**	39.65	2.27	9.08	20.72	0.01	0.05	1.52
2018	54.74	2.08	0.24	7.10	**64.16**	**64.13**	43.74	2.06	7.10	10.34	0.00	-0.02	0.90
Average	53.06	2.30	0.39	12.28	**68.03**	**68.00**	42.40	2.25	12.42	11.24	0.00	-0.04	-0.28

APPENDIX F

FLOW AT OR NEAR THE P-11 STRUCTURE

This page was intentionally left blank.

APPENDIX F
FLOW AT OR NEAR THE P-11 STRUCTURE

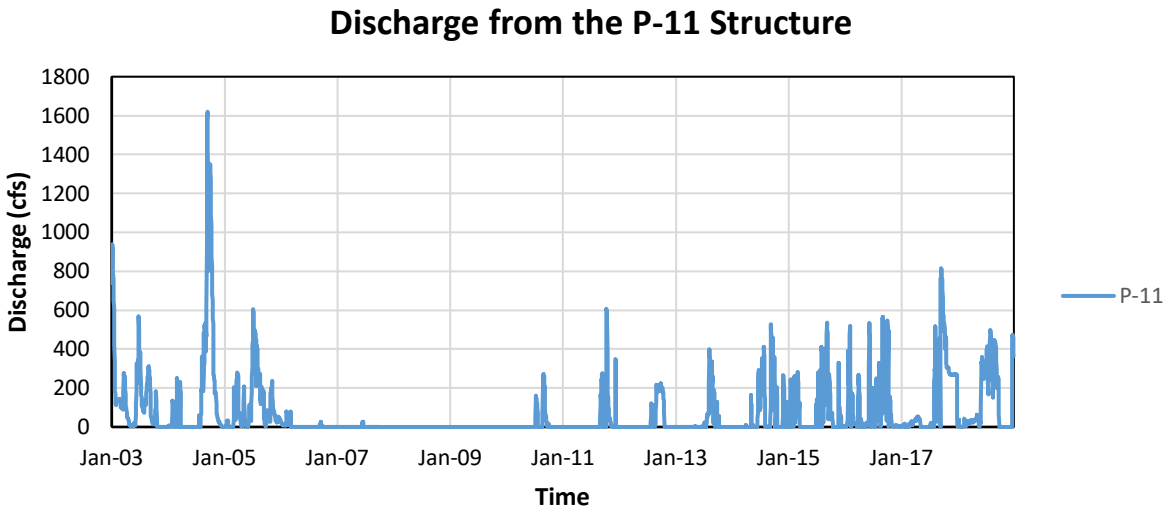

Figure F.1 Discharge from P-11

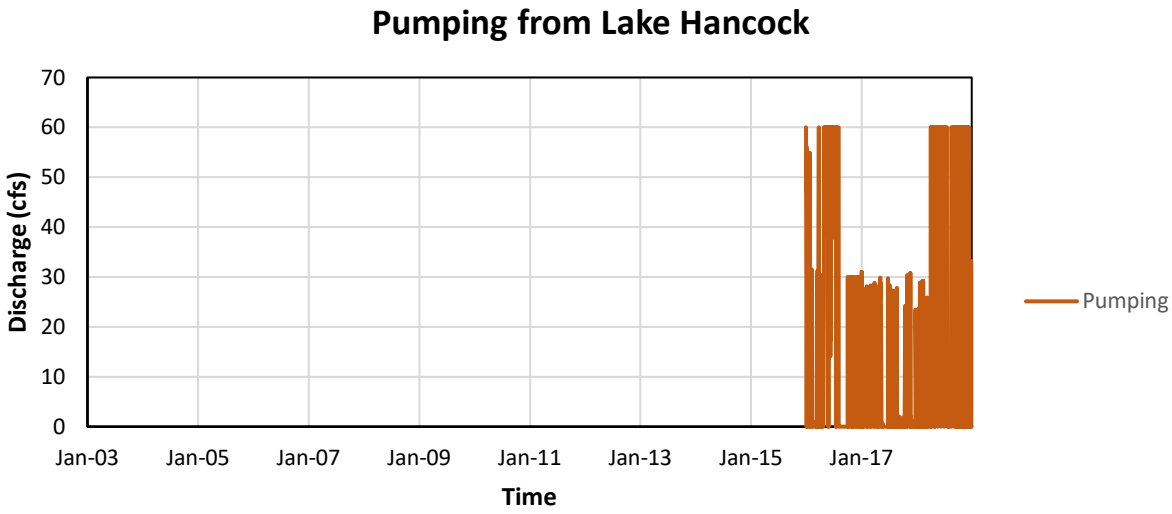

Figure F.2 Pumping from Lake Hancock

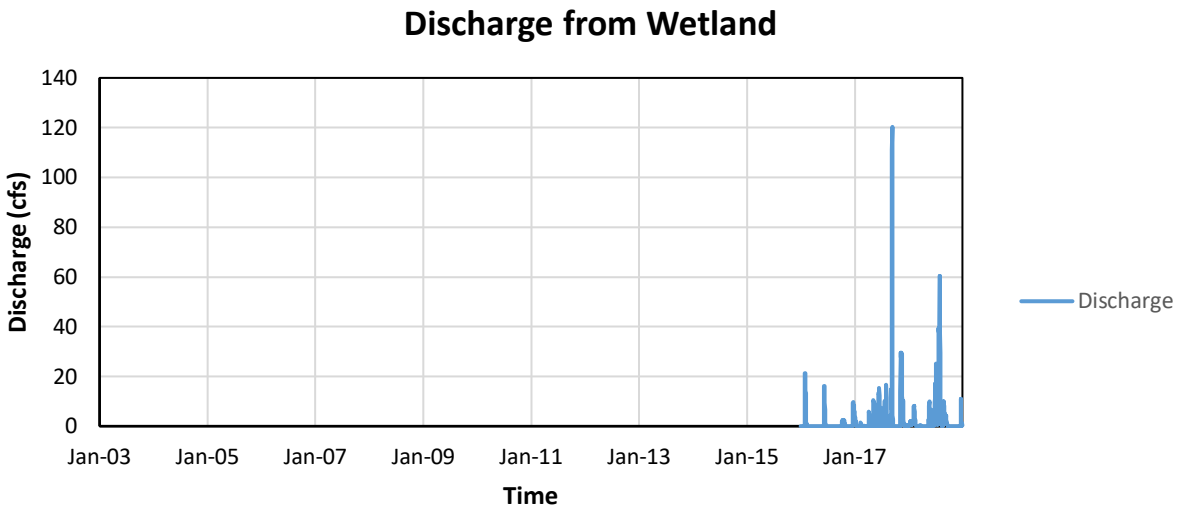

Figure F.3 Flow at the Wetland Downstream from P-11